

**LAKE ALMANOR COLD-WATER FEASIBILITY STUDY:  
HYDRAULIC MODEL**

Robert Ettema, Marian Muste, A. Jacob Odgaard, and Yong Lai



IIHR Technical Report No. 438

IIHR – Hydroscience & Engineering  
College of Engineering  
The University of Iowa  
Iowa City, Iowa 52242

July 2004

## ABSTRACT

The principal objective of this study was to determine the feasibility of modifying Prattville Intake to selectively release colder water from Lake Almanor during summer. The study entailed extensive tests conducted using a unique hydraulic model of Prattville Intake and a large portion of Lake Almanor surrounding the Intake. The model had the capability to simulate the stratified water-temperature condition that typically develops in the lake during summer months. To accomplish that simulation required that the hydraulic model be vertically distorted, whereby its vertical-length scale was smaller than its horizontal-length scale (herein, modeling scale is the ratio prototype-value/model-value). To address the influence of vertical distortion on the model's results, and to aid validation of hydraulic-model results, auxiliary laboratory modeling was conducted using a pair of testboxes that replicated, in somewhat simplified form, vertically distorted and undistorted geometry of Prattville Intake and its surrounding bathymetry. Moreover, hydraulic modeling was aided by means of comprehensive computational modeling using a set of numerical models of Lake Almanor and of the hydraulic model.

Tests with the hydraulic model, aided by the supplemental modeling, led to the recommendation that a large floating curtain be placed around Prattville Intake. Additionally it is recommended that modest bathymetry changes be made in front of the Intake. Those changes entail removing a portion of the submerged levees flanking a submerged channel crossing the bed of Lake Almanor. The curtain, together with levee removal, would enable Prattville Intake to withdraw substantially colder water from Lake Almanor than the Intake presently can withdraw. Further work with the hydraulic model led to the conceptual design of a removable bottom sill placed around Prattville Intake for the purpose of conserving cold water during late spring and early summer.

## ACKNOWLEDGEMENTS

The writers gratefully acknowledge the guidance and technical advice provided by Scott Tu and Todd Johnson of Pacific Gas and Electric (PG&E), and by Pat Ryan and Fred Locher of Bechtel, PG&E's engineering consultants for the present project. They together came up with the challenging notion of using a vertically distorted hydraulic model, together with a set of numerical models, to investigate the feasibility of modifying Prattville Intake to release colder water during summer.

Thanks also are due the members of the Ecological Resources Committee, associated with the Rock Creek and Crest License (FERC License no. 1962) under which PG&E operates Prattville Intake. Their constructive responses to the meeting presentations of the modeling study described in the present report were helpful in completing the study.

Additionally, the writers gratefully acknowledge the hydraulic-modeling assistance given by students Ahmed Lachhab and Ozan Abaci, and by IIHR technician Chris Buren. They each played substantial roles in conducting the tests with the hydraulic model. The writers thank Ping Zeng who helped in running one of the numerical models for the study. Moreover, thanks are due to IIHR Director V.C. Patel who was instrumental in the initial setting up of the study's numerical modeling component. The excellent support work provided collectively by IIHR staff Mark Wilson, Paul Below, Mike Kundert, as well as Darian De Jong and his workshop colleagues, is appreciatively acknowledged.

## EXECUTIVE SUMMARY

### Introduction

This report presents the findings of a study conducted by IIHR-Hydroscience and Engineering to determine the feasibility of modifying an existing water-intake structure for the purpose of facilitating the increased release of cold water from a thermally stratified lake. The intake, Prattville Intake, is located in Lake Almanor, a storage reservoir in northern California. Figure 1 indicates the Intake's location in Lake Almanor.

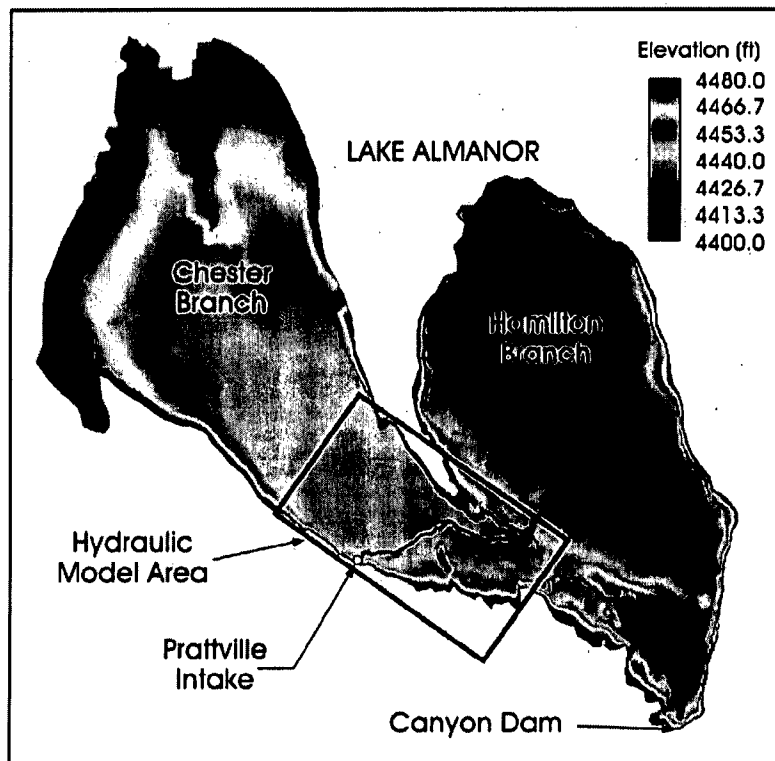


Figure 1. Bathymetry map of Lake Almanor, showing the location of Prattville Intake and the area modeled.

The modifications were investigated to determine whether the Intake could be operated to release colder water during summer months (mid-June to mid-September). Pacific Gas and Electric, the owner and operator of Prattville Intake, was required to investigate the feasibility of releasing colder water from Lake Almanor during summer so as to enhance

habitat conditions for trout and other fish species in the North Fork of the Feather River downstream from Lake Almanor. The Intake's existing configuration results in the summer-time release of water whose temperature environmental interests consider too warm for trout habitat. Prattville Intake, operated at its normal outflow rates, presently withdraws water from over the full depth of water, and is therefore unable to selectively withdraw cold-water from the lake.

The study required the use of a unique hydraulic model that encompassed a large area of Lake Almanor, as delineated in Figure 1. No prior hydraulic model of comparable size and complexity had been used for studying the management of cold-water release from a thermally stratified reservoir or lake. A key consideration that made the model feasible was the availability at IIHR of large volumes of water (cold, temperate, and warm) for combination in establishing water temperature profiles closely similar to those prevailing in Lake Almanor.

### **Modification Alternatives**

The following modification alternatives were tested to assess their capability to enable Prattville Intake to release colder water during summer:

- a large, skimming curtain placed around Prattville Intake;
- a long pipe fitted with a hooded inlet. The pipe would extend from a cofferdam built around Prattville Intake, effectively moving the Intake further into the lake; and,
- a short pipe fitted with a hooded inlet. The pipe would extend from a cofferdam built around Prattville Intake.

Also tested in conjunction with these alternatives were excavation adjustments to the lake bathymetry in the vicinity of Prattville Intake.

A further modification was aimed at blocking, and thereby conserving cold water, during late spring and early summer:

- a removable bottom sill. In concept, the sill could be formed using curtain fabric suspended from the same structure used to support the skimming curtain.

Though this modification presently is not needed for operating Prattville Intake, information on the modification's performance was considered useful for possible future reference.

### **Hydraulic Model**

The hydraulic model encompassed a 3.1-mile by 1.9-mile area of Lake Almanor surrounding Prattville Intake, as indicated in Figure 1. The area extended from Prattville intake out to the region linking the Chester and the Hamilton Branches of Lake Almanor and out across from the intake to Almanor Peninsula. A bathymetric feature of the modeled area is a submerged channel called the incised channel. The incised channel connects the Intake with the Hamilton Branch, the main source of cold water, and is thought to be of importance in the operation of a modified Intake. A large area also was needed to ensure that the model had sufficient volumes of warm water and cold water to maintain the temperature profile of water in the model, and thereby enable outflow from the model Intake to attain a steady temperature.

The model also had to be adequately deep so that it would simulate the flow field at Prattville Intake as well as the prospective flow of colder water moving over the lakebed near the Intake and along the incised channel from the lake's Hamilton Branch. It was anticipated that the modifications would cause cold water to be drawn as a density current along the lakebed and in the incised channel toward the Intake. The model therefore had to simulate the frictional and temperature aspects of the density current flow toward the Intake.

After considering the constraints, including issues such as the Reynolds number of the flow approaching the Intake, a horizontal-length scale of  $X_r = 220$  ( $\equiv$  prototype horizontal length/model horizontal length) and a vertical scale of  $Y_r = 40$  were selected. This combination of length scales was judged to be a practicable compromise between the needs to encompass a large portion of the lake, have adequate model flow depth, and adequately simulate the flow field along the incised channel and near the Intake. Figure 2 is an overview of the hydraulic model.

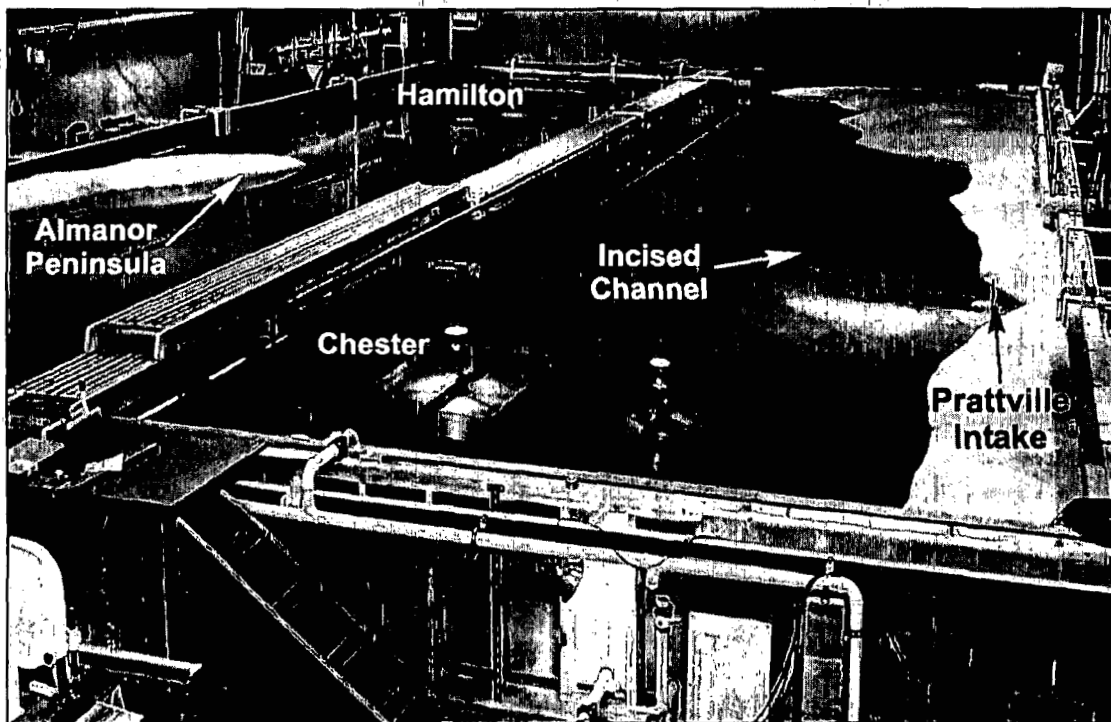


Figure 2. View of the hydraulic model. Prattville Intake is on the right.

### **Calibration, Validation, Verification**

An innovative calibration, validation, and verification procedure was needed to ensure the validity of results obtained from the vertically distorted hydraulic model. The processes relied on laboratory tests using a pair of testbox simulations of the Intake and the lake bathymetry in its immediate vicinity. Additionally, extensive use was made of numerical modeling to support the results from the testboxes.

The testboxes provided key calibration information for setting the discharge scale for the hydraulic model, and thereby ensuring that the model Intake would develop essentially the same flow-field features as occurs at Prattville Intake. The testboxes comprised simplified, vertically distorted and undistorted representations of Prattville Intake placed amidst simplified forms of the lake bathymetry near Prattville Intake. Work with each testbox entailed measuring the variation of outflow temperatures  $T_{out}$  over a range of outflow discharge,  $Q$ , normalized with the normal operating discharge,  $Q_0$ , for a given water-temperature profile (e.g., typical of Lake Almanor in July).

Figure 3 illustrates conceptually the relationships between  $T_{out}$  and  $Q/Q_0$  obtained from the distorted and the undistorted testboxes. The offset between the data curves obtained from the two testboxes represents the value of the discharge-calibration coefficient,  $\alpha$ , needed to interpret the results from the hydraulic model, and apply those results to Prattville Intake; the same offset is expected to occur between the vertically distorted hydraulic model of Prattville Intake and an undistorted version of the hydraulic model.

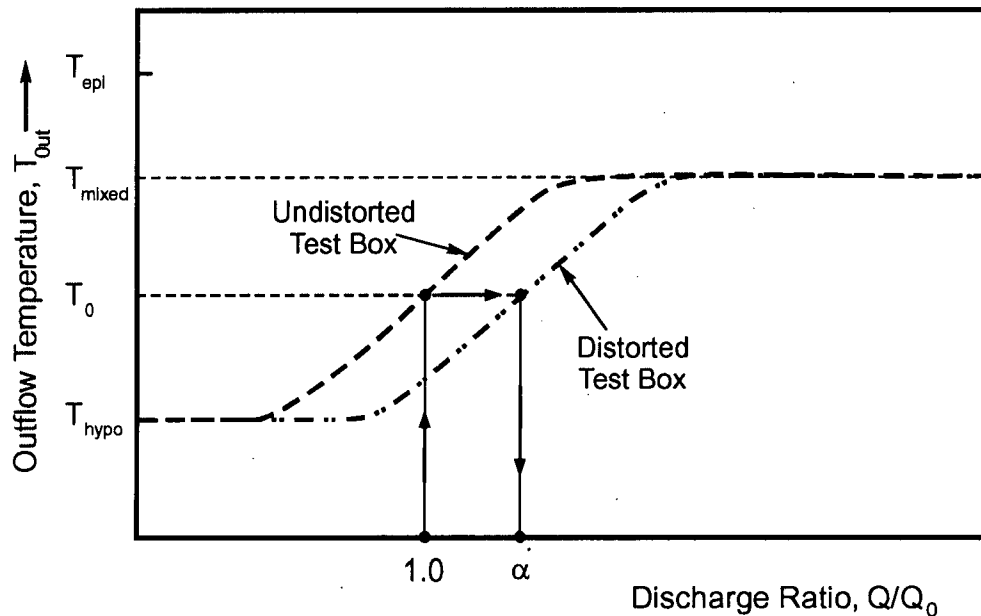


Figure 3. Conceptual relationship between outflow temperature and discharge ratio in the distorted and undistorted testboxes, indicating the discharge-calibration factor  $\alpha$ .

The value of  $\alpha = 1.7$  was determined from the data curves from the undistorted and the distorted testboxes. That value was obtained for two forms of the testboxes, and it was validated using data obtained from tests with two other temperature profiles and water-surface elevations of the lake (June and August). Additional calibration information was provided from numerical models used to simulate the testboxes. Subsequently, field data relating outflow temperature to outflow rate from Prattville Intake verified the value determined for  $\alpha$ . Consequently, the model Intake operated at the discharge ratio  $Q/Q_0 = 1.7$  produced the same value of  $T_{out}$  as actually measured for Prattville Intake when  $Q/Q_0 = 1.0$ . It was found that the factor  $\alpha$  applied to the full range of model discharges used in testing ( $0.25 \leq Q/Q_0 \leq 2.75$ ).

### **Numerical Models**

Several numerical models were used for simulating the evolution of thermal stratification in Lake Almanor as well as simulating the flow and temperature field in the vicinity of the Prattville Intake. The models were based on IIHR's three-dimensional-flow code, U2RANS, and are described in detail in a separate report.

In particular, the numerical models were used as support to interpret the performance curves obtained from the vertically distorted hydraulic model of Prattville Intake when in its existing condition, and when the Intake was fitted with the most promising modification. The numerical models were extended to simulate flow and temperature conditions in an equivalent, undistorted hydraulic model, thereby extending the results from the vertically distorted hydraulic model, and addressing the likely effects of vertical distortion on the data obtained from the hydraulic model. The results from the numerical models of the actual hydraulic model were in good agreement with the results obtained from the hydraulic model. However, the extended numerical modeling met some difficulties with the computational mesh used, and in the large amount of time needed to complete simulations of the undistorted version of the hydraulic model. Further work, beyond the resources of the present study, would be needed to overcome those difficulties.

## Hydraulic-Model Tests

The hydraulic model was used to carry out a series of baseline-performance tests that simulated the outflow performance of Prattville Intake in its existing configuration. It was used for a series of screening tests to ascertain the capabilities of each of the three proposed modifications to reduce the outflow temperature of water released from the Intake. The outflow performance of the most promising modification, or set of modifications, then was extensively tested and documented. A series of validation tests was done with the undistorted testbox to confirm that the selected modification set performed appropriately in undistorted form, and to help in scaling the results from the distorted hydraulic model to prototype values.

Tests with the hydraulic model showed that the greatest decreases in outflow temperature,  $T_{out}$  were obtained when a large floating, skimming curtain was placed around Prattville Intake. Additionally, the tests showed that a further reduction in  $T_{out}$  could be achieved by removing a portion of the submerged levees flanking the incised channel in the bed of Lake Almanor. Figure 4 depicts the model of Prattville Intake with the curtain in place and the levees removed.

The data indicate that the curtain together with levee removal would enable Prattville Intake to release water 4.5°C to 5.2°C colder during July and August than the Intake presently can release during those months. The corresponding peak outflow temperatures would be in the range of 17°C to 18°C during July and August, for the water-temperature profiles used in this study.

There exist comparable skimming curtains placed in reservoirs or lakes. The U.S. Bureau of Reclamation, notably, uses curtains in several of its reservoirs. The curtain could be built from special-purpose fabric, as used already for the existing curtains.

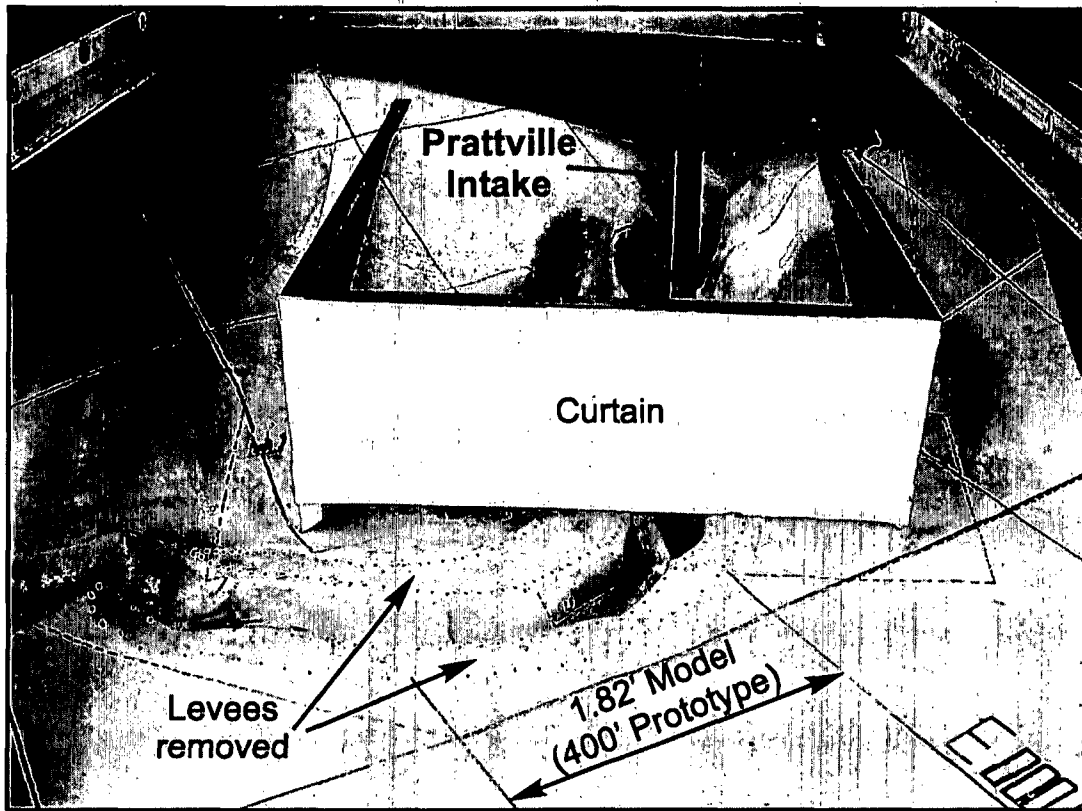


Figure 4. Prattville Intake surrounded by the recommended skimming curtain, and the levees removed in front of the curtain.

The temperature-reducing effect of a skimming curtain and removal of the levees is illustrated conceptually in Figure 5, which shows the relationship between  $T_{out}$  and  $Q/Q_0$  obtained with existing configuration of Prattville Intake, and when a curtain was positioned around the Intake, and the levees removed. For small outflows (nominally,  $0.25 \approx Q/Q_0$ ), the Intake, with or without the curtain, withdraws essentially cold water from the hypomnion (bottom layer) at a representative temperature of  $T_{hypo}$ . The curtain then has negligible effect on  $T_{out}$  at this flow rate.

For  $Q/Q_0$  values approaching and somewhat exceeding the Intake's usual operating range of flows ( $Q/Q_0 = 1$ ), the curtain blocks warm water from approaching the Intake. As the value of  $Q/Q_0$  exceeds the Intake's usual outflow range, the effect of the curtain diminishes. Based on an extrapolation of the trends shown by the data curves from the

hydraulic model,  $Q/Q_0$  would be approximately 10 or greater before the curtain had no influence on outflow temperature. At that limit, the flow is fully mixed as it passes beneath the curtain. Then, the outflow temperature, though lower than the representative temperature of the epilimnion  $T_{epi}$  (upper layer), would be the same as obtained for the present configuration of Prattville Intake operated at such large values of  $Q/Q_0$ .

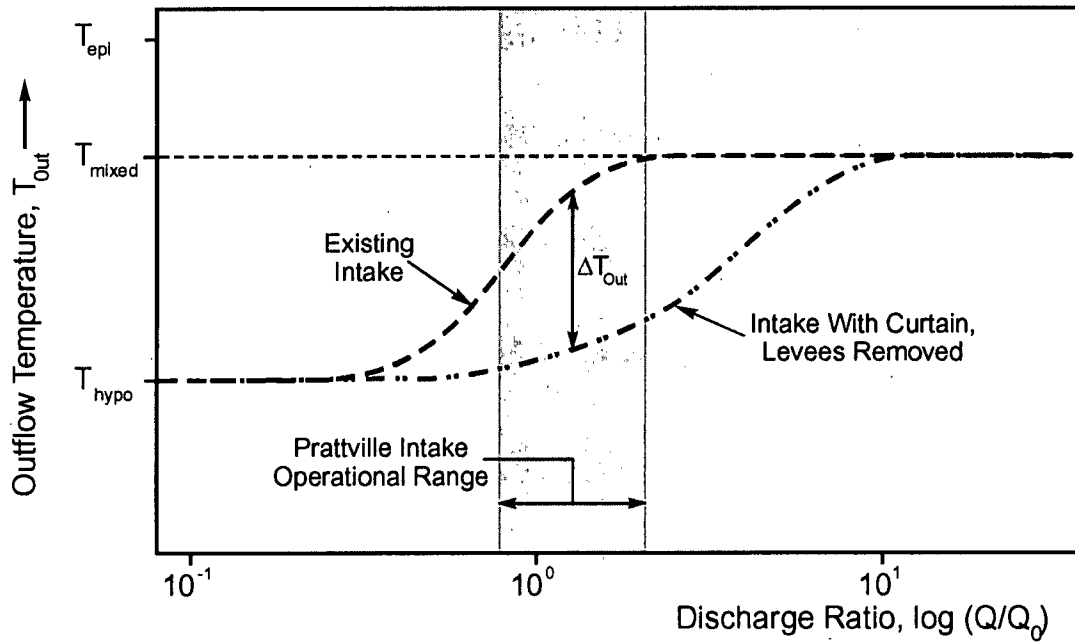


Figure 5. Conceptual illustration of the effect of the skimming curtain on the temperature of outflow released from Prattville Intake.

The two modifications involving a pipe extension from a cofferdam built around Prattville Intake proved to be less effective in releasing cold water than was the modification combination of curtain and levee removal. During the simulated August water-temperature condition of the lake, the long pipe, with a hooded inlet, reduced outflow temperature by about  $3.5^{\circ}\text{C}$  when the Intake released its normal discharge. The short pipe, with a hooded inlet, reduced outflow temperature by about  $3.0^{\circ}\text{C}$  for the same outflow and simulated condition of the lake.

Further work with the hydraulic model led to the conceptual design of a removable bottom sill placed around Prattville Intake for the purpose of conserving cold water during late spring and early summer. The sill could be built from the same fabric as would be used for the curtain, and likely could be incorporated into the overall design of the structure also used to support the curtain. Sill performance in conserving cold water was slightly better when the levees were removed, as the levees mildly diminished the sill's capability to block cold water. The sill raised outflow temperatures by about 2°C for the water-temperature conditions typical of Lake Almanor during June. This performance indicates a commensurate conservation of colder water for possible release during summer. Figure 6 shows the model of Prattville Intake with the modeled sill.

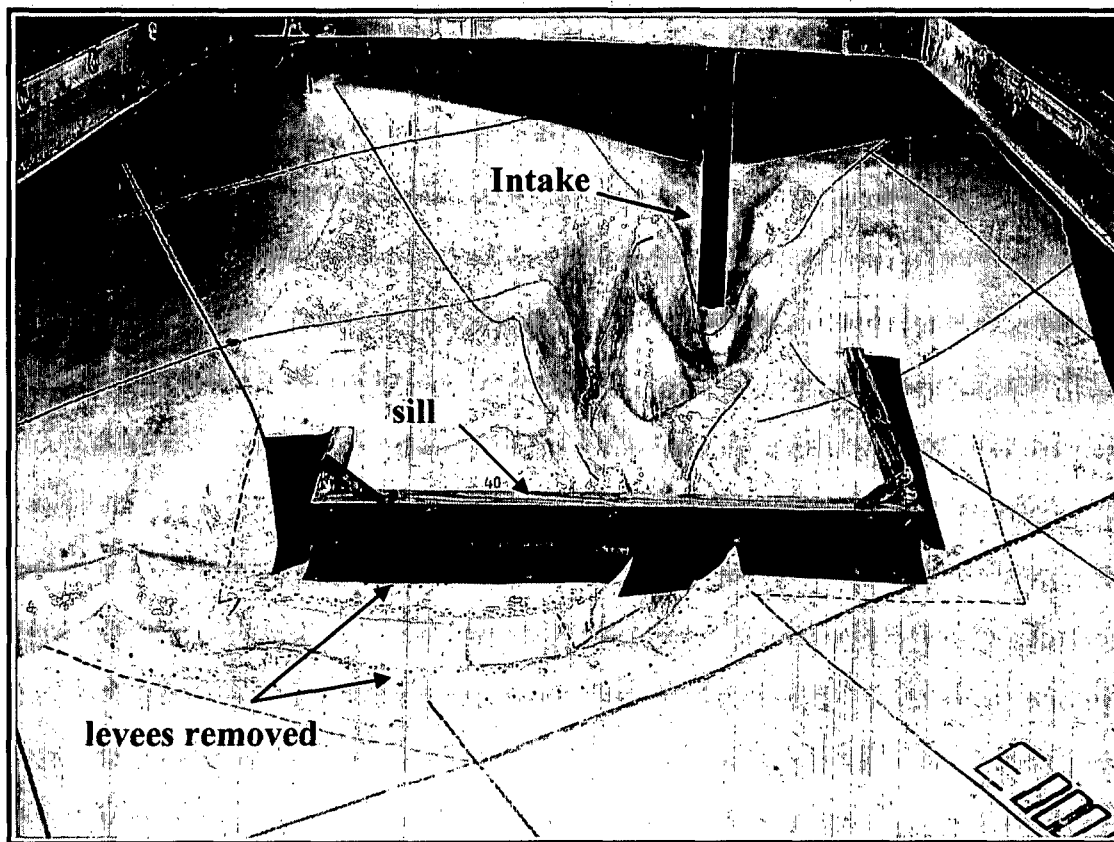


Figure 6. Prattville Intake surrounded by a sill for conserving the colder water.

## Performance Validation

Table 1 summarizes the principal results obtained from the testing with the hydraulic model. The results are presented as a listing of outflow temperature  $T_{out}$  and decrease in outflow temperature  $\Delta T_{out}$  produced by the model Intake fitted with the modifications.

Table 1. Outflow temperatures,  $T_{out}$ , and temperature reductions,  $\Delta T_{out}$ , when the hydraulic model was operated at  $Q/Q_O = 1.7$  (i.e., equivalent to normal outflow of 1,600cfs from Prattville Intake). The lake's water-surface elevations are indicated also.

Intake Configuration	June (EL. 4491.5ft)		July (EL. 4489.0ft)		August (EL. 4482.5ft)	
	$T_{out}$ (°C)	$\Delta T_{out}$ (°C)	$T_{out}$ (°C)	$\Delta T_{out}$ (°C)	$T_{out}$ (°C)	$\Delta T_{out}$ (°C)
Existing configuration	16.5	-	19.1	-	21.2	-
Intake modified to release colder water						
Curtain added	12.2	4.3	14.7	4.4	17.6	3.6
Curtain added and levees removed	12.0	4.5	13.1	5.8	16.0	5.2
Long pipe with hooded inlet, and levees removed	-	-	-	-	17.4	3.8
Short pipe with hooded inlet, and levees removed	-	-	-	-	19.1	2.1
Levees removed, no curtain	15.8	-0.7	-	-	-	-
Intake modified to conserve colder water						
Existing configuration, sill added	18.3	-1.8 (16.5 - 18.3)	-	-	-	-
sill, when levees removed	17.8	-2.0 (15.8 - 17.8)	-	-	-	-

Note: the highlighted row is modification set giving greatest reduction in outflow temperature.

The results from the performance-screening tests reveal a set of practicable modifications that hold promise for enabling Prattville Intake to release colder water than it currently releases during summer months. The recommended modifications comprise a skimming curtain whose bottom elevation is at EL. 4445ft, plus removal of the levees flanking a length of the incised channel in the immediate vicinity of the curtain. To confirm and document the performance of this set of modifications, and to check its sensitivity to curtain bottom elevation, a series of additional tests was conducted using the hydraulic model aimed at delineating a margin of uncertainty.

Additionally, performance-validation tests were carried out using the testboxes and the numerical models. Those validation tests served as an essential check to confirm the results from the vertically distorted hydraulic model, as well as to help in establishing the correct scaling of hydraulic-model results to the performance of Prattville Intake. The validation tests confirmed the temperature-reducing performance of a curtain identified from tests in the hydraulic model.

## **Recommendations**

Tests with hydraulic model, aided by supplemental modeling with the testboxes and the numerical models, led to the following recommendations:

1. For Prattville Intake to release colder water during summer, a set of modifications should be considered:
  - (a). installation of a skimming curtain of length 2,600ft, whose bottom elevation is at EL. 4445ft, and whose face is approximately 900ft offshore from the front of Prattville Intake; and,
  - (b). removal of the levees flanking the incised channel immediately in front of Prattville Intake.

In accordance with the data highlighted in Table 1, these modifications are expected to reduce outflow temperatures by about 4.5 to 5.2°C for the lake

conditions prescribed for July and August. The modifications are illustrated in Figure 4.

2. If cold water must be conserved during late spring, a submerged sill could be installed. The recommended crest elevation of the sill is EL. 4460ft. With the levees removed, the sill would raise outflow temperature by about 1.5°C to 2.0°C during late spring and early summer.



## TABLE OF CONTENTS

ABSTRACT.....	i
ACKNOWLEDGEMENTS.....	ii
EXECUTIVE SUMMARY .....	iii
TABLE OF CONTENTS.....	xvi
LIST OF FIGURES .....	xx
LIST OF TABLES.....	
1. INTRODUCTION AND SCOPE .....	1-1
1.1 Introduction.....	1-1
1.2 Scope and Objectives.....	1-2
1.3 Approach.....	1-4
1.4 Numerical Models.....	1-7
1.5 Outline of Report .....	1-8
Figure .....	1-12
2. PROBLEM DESCRIPTION AND BACKGROUND.....	2-1
2.1 Introduction .....	2-1
2.2 Prattville Intake .....	2-1
2.3 Problem Description.....	2-1
2.4 Physical Setting of Prattville Intake .....	2-3
2.4.1 Bathymetry.....	2-3
2.4.2 Water Sources .....	2-4
2.4.3 Climate.....	2-5
2.4.4 Thermal Stratification .....	2-6
2.5 Prior Studies .....	2-7
2.5.1 Skimming Curtains .....	2-8
2.5.2 Hooded-Pipe Outlet .....	2-11
2.5.3 Comments .....	2-11
Figures .....	2-14

3. MODEL DESIGN AND OPERATION .....	3-1
3.1 Introduction .....	3-1
3.2 Area Encompassed by Model.....	3-1
3.3 Selection of Length Scales .....	3-2
3.4 Model Construction.....	3-7
3.4.1 Bathymetry.....	3-8
3.4.2 Temperature-Control System.....	3-11
3.4.3 Water Flow Control and Distribution System .....	3-12
3.5 Procedure for Temperature Profiles .....	3-13
3.6 Instrumentation.....	3-16
3.7 Model Operation.....	3-19
Figures .....	3-21
4. MODEL CALIBRATION, VALIDATION, VERIFICATION .....	4-1
4.1 Introduction .....	4-1
4.2 General Calibration Activities.....	4-2
4.3 Water-Temperature Stratification.....	4-4
4.4 Outflow Discharge – Testbox Experiments .....	4-5
4.4.1 Discharge Scale for 2D Flows .....	4-6
4.4.2 Testboxes .....	4-8
4.4.3 Calibration, Validation, Verification Sequence: Existing Intake Configuration .....	4-9
4.5 Testbox Validation of Intake Modification.....	4-11
4.6 Numerical Model of Testboxes .....	4-13
Figures.....	4-14
5. PROGRAM OF HYDRAULIC MODELING TESTS .....	5-1
5.1 Introduction .....	5-1
5.2 Modifications Tested.....	5-2
5.3 Calibration, Validation, Verification Tests .....	5-2
5.-4 Baseline Performance Tests .....	5-2

5.5	Modification Screening Tests.....	5-3
5.6	Performance Documentation Tests .....	5-3
	Figures.....	5-10
6.	TESTBOX RESULTS: EXISTING INTAKE CONFIGURATION.....	6-1
6.1	Introduction .....	6-1
6.2	Outflow Adjustment Factor.....	6-2
6.3	Normalization of Data .....	6-5
6.4	Calibration Tests: Testboxes .....	6-6
6.5	Validation Results: Testboxes .....	6-9
6.6	Validation Results: Numerical Model.....	6-11
6.7	Comparison with Field Data.....	6-11
6.8	Comments.....	6-12
	Figures.....	6-14
7.	RESULTS FROM HYDRAULIC MODEL .....	7-1
7.1	Introduction .....	7-1
7.2	Baseline Performance Tests: Prattville Intake.....	7-2
7.2.1	Temperature Field.....	7-3
7.2.2	Variation of Outflow Temperature with Outflow Discharge.....	7-3
7.2.3	Flow Field .....	7-6
7.3	Screening Tests: Modifications to Reduce Outflow Temperature .....	7-8
7.4	Screening Tests: Skimming Curtain.....	7-9
7.4.1	Curtain Geometry.....	7-9
7.4.2	Effect of Curtain No. 4 on Outflow Temperatures .....	7-11
7.4.3	Flow Field at Curtain No. 4 .....	7-12
7.5	Screening Test: Curtain, Levees Removed .....	7-15
7.5.1	Influence on Outflow Temperature.....	7-16
7.5.2	Flow Field When Levees Removed.....	7-17
7.6	Screening Test: Curtain, Levees Removed, Further Excavation.....	7-18
7.7	Screening Tests: Short-pipe with Hooded Inlet .....	7-19

7.7.1	Influence on Outflow Temperature.....	7/20
7.7.2	Flow Field.....	7-21
7.8	Screening Tests: Long-pipe with Hooded Inlet.....	7-21
7.8.1	Influence on Outflow Temperatures.....	7-22
7.8.2	Flow Field Generated by Long-pipe with Hooded Inlet.....	7-22
7.9	Screening Tests: Bottom Sill to Conserve Colder Water.....	7-24
7.9.1	Influence on Outflow Temperature.....	7-24
7.9.2	Flow Field.....	7-25
7.10	Screening Tests: Summary of Results.....	7-26
	Figures.....	7-27
8.	PERFORMANCE DOCUMENTATION AND VALIDATION.....	8-1
8.1	Introduction.....	8-1
8.2	Performance-Documentation Tests.....	8-2
8.3	Validation Tests with Testboxes.....	8-3
8.4	Validation Tests with Numerical Model.....	8-5
8.5	Discussion.....	8-6
	Figures.....	8-9
9.	CONCLUSIONS AND RECOMMENDATIONS.....	9-1
9.1	Summary.....	9-1
9.2	Conclusions.....	9-3
9.3	Recommendations.....	9-7
	REFERENCES.....	
	APPENDICES	
A.	CONSTRUCTION DRAWINGS.....	A-1
B.	LISTING OF VIDEO CLIPS.....	B-1

## LISTS OF FIGURES

<u>Figure</u>	<u>Page</u>
2-1 Location of Lake Almanor and the North Fork of the Feather River .....	2-14
2-2 Lake Almanor and the Butt Valley Powerhouse facilities.....	2-15
2-3 Layout and dimensions of the Prattville Intake .....	2-16
2-4 Bathymetry of Lake Almanor .....	2-17
2-5 Water temperature profiles measured in Lake Almanor.....	2-18
2-6 Average profiles of water temperature in Lake Almanor for June, July, and August 2000.....	2-21
3-1 Area of Lake Almanor encompassed by model.....	3-21
3-2 Location of the testboxes in the hydraulic model .....	3-22
3-3 View of hydraulic model .....	3-23
3-4 Sources of bathymetry information .....	3-24
3-5 Supplemental bathymetry information obtained in field survey.....	3-25
3-6 Survey sections for contouring the incised channel.....	3-26
3-7 Bathymetry templates selected for constructing the area near the Intake.....	3-27
3-8 Model bed topography near Prattville Intake. Grid on bottom represents a 400 ft by 400 ft prototype grid.....	3-28
3-9 Layout of the water lines in the hydraulic model .....	3-29
3-10 Cross section through the hydraulic model.....	3-30
3-11 Typical ssequence for attaining prescribed water temperature profiles in the model .....	3-31
3-12 Development of June condition temperature profile .....	3-32
3-13 Temperature monitoring during water feeding.....	3-33
3-14 Samples of water stratifications attained in the model .....	3-36
3-15 Layout of measurement system .....	3-37
3-16 View of fully instrumented model .....	3-38
3-17 Thermistor chain arrangement .....	3-39
3-18 Interface for thermistor-chain temperatures.....	3-40
3-19 Interface for monitoring outflow temperature .....	3-41

3-20	Temperature profiles at the binning and end of a series of tests.....	3-42
3-21	Filling the hydraulic model.....	3-43
4-1	Views of the test tank.....	4-14
4-2	Example of thermistor calibration curve.....	4-15
4-3	Temperature variation over time for a uniform body of water placed in the test tank.....	4-15
4-4	Temperature variation over time for two layers of water fed in the test tank...	4-16
4-5	Layout and dimensions of the undistorted and distorted Bay testboxes .....	4-17
4-6	Photographs of the distorted and undistorted Bay testboxes .....	4-18
4-7	A perspective sketch of the undistorted Open testbox.....	4-19
4-8	Layout and dimensions of the undistorted Open testbox.....	4-20
4-9	Photograph of the undistorted Open testbox.....	4-21
4-10	Layout and dimensions of the distorted Open testbox.....	4-22
4-11	Photograph of the distorted Open testbox.....	4-23
5-1	Simulated skimming Curtain No. 4 .....	5-10
5-2	Short pipe with hooded inlet.....	5-11
5-3	Long pipe with hooded inlet .....	5-11
5-4	Levees removed from the incised channel near the Intake. Levee location is indicated by dashed lines.....	5-12
5-5	Channel excavated in the confluence area near Prattville Intake .....	5-13
5-6	A view of the model bottom sill. The levees are removed .....	5-14
6-1	General relationship between the outflow temperature $T_{out}$ and discharge ratio $Q/Q_0$ for the distorted and undistorted testboxes .....	6-14
6-2	Results from Bay testboxes; July condition.....	6-15
6-3	Results from Open testboxes; July condition.....	6-16
6-4	Normalized results from Bay testboxes; July condition .....	6-17
6-5	Normalized results from the Open testboxes; July condition.....	6-18
6-6	Results from Bay testboxes; August condition (no curtain) .....	6-19
6-7	Results from Open testboxes; August condition (no curtain).....	6-20
6-8	Results from Bay testboxes; June condition (no curtain) .....	6-21

6-9	Variation of outflow temperature, $T_{out}$ , with $Q/Q_0$ for the Bay testboxes subject to June, July, and August conditions .....	6-22
6-10	Comparison of result from the distorted Open testbox and from the undistorted Open testbox; August condition.....	6-23
6-11	Comparison of results obtained from the testboxes and from the simulations of the testboxes; June condition (no curtain) .....	6-24
6-12	Comparison of results from the undistorted Open testbox with field data from Prattville Intake .....	6-25
7-1	Variation of outflow temperature from Prattville Intake for June, July and August. Also shown are field data from Prattville Intake .....	7-27
7-2	The field data, adjusted with discharge calibration factor, $\alpha = 1.7$ , align with results from the hydraulic model .....	7-28
7-3	Normalized outflow temperature obtained with the hydraulic model for June, July and August .....	7-29
7-4	Oscillation of outflow temperature after a change in Intake outflow discharge.....	7-30
7-5	Visualization of flow to Prattville Intake.....	7-31
7-6	Layouts of the curtains tested. Curtain No. 4 was selected for further testing .....	7-33
7-7	Layout and dimensions of Curtain No. 4 .....	7-34
7-8	Elevation views of Curtain No. 4 (prototype dimensions) .....	7-35
7-9	Opening area between the curtain lip and lakebed for Curtain No. 4.....	7-36
7-10	View of Curtain No. 4.....	7-37
7-11	Effect of Curtain No. 4 on outflow temperature .....	7-38
7-12	Comparison of Curtain No. 4 effects on outflow temperatures for June, July, and August conditions .....	7-41
7-13	Conceptual trends showing the reduction in outflow temperature when the intake is fitted with a curtain .....	7-42
7-14	Visualization of flow to Prattville Intake fitted with Curtain No. 4 .....	7-43
7-15	Variation of water temperature profiles inside the curtain .....	7-45

7-16	Variation of outflow temperature until steady temperature at $T_{out} = 17.4^{\circ}\text{C}$ is obtained .....	7-46
7-17	Curtain No. 4 with levees removed.....	7-47
7-18	View of Curtain No. 4 with levees removed.....	7-48
7-19	Reduction in outflow temperature produced by Curtain No. 4 with levees removed .....	7-49
7-20	Outflow temperature obtained with Curtain No. 4 and levees removed.....	7-52
7-21	Visualization of the flow approaching and passing Curtain No. 4 when levees are removed.....	7-53
7-22	Flow along the incised channel approx 15ft (3,300 ft prototype) upstream from the Intake .....	7-55
7-23	Visualization of the flow approaching and passing Curtain No. 4 without levees, operating without thermal stratification in the lake.....	7-56
7-24	Excavation near the Intake.....	7-57
7-25	Comparison of the performances of Curtain No. 4 (with and without levees) with additional excavation in the confluence area .....	7-58
7-26	Short pipe with hooded inlet (SPHI).....	7-59
7-27	Elevation view of the cross-section through the hood and the incised channel (prototype dimensions) for the modeled SPHI.....	7-60
7-28	View of the SPHI in the model .....	7-60
7-29	Effect of the short-pipe with hooded inlet without levees on outflow temperature; August condition.....	7-61
7-30	Visualization of the flow approaching the SPHI. The arrows indicate flow paths produced by the short pipe with hooded inlet .....	7-62
7-31	Location of the long pipe with hooded inlet (LPHI) relative to Prattville Intake .....	7-63
7-32	Elevation view of the cross-section through the hood and the incised channel (prototype dimensions) for the modeled LPHI.....	7-64
7-33	View of the LPHI in the model.....	7-64
7-34	Comparison of the performances of the LPHI with levees not removed and Curtain No. 4 for August condition.....	7-65

7-35	Comparison of the performances of LPHI with levees removed and Curtain No. 4 (with and without levees); August condition .....	7-66
7-36	Visualization of the flow approaching the LPHI. Arrows indicating flow paths produced by the long pipe with hooded inlet (LPHI) .....	7-67
7-37	Layout of the bottom sill. The sill crest is at 4450 ft .....	7-68
7-38	View of the sill with levees (a) and without levees (b).....	7-69
7-39	Comparison of the outflow performance produced by a sill at either of two crest elevations: levees in place, June condition .....	7-70
7-40	Comparison of the outflow performance produced by a sill at either of two crest elevations with levees removed; June condition.....	7-71
8-1	Validation of the hydraulic model results with field data. The field data are adjusted by factor $\alpha = 1.7$ applied to $Q/Q_0$ .....	8-9
8-2	Sensitivity of Curtain No. 4 with variation of lip elevation (tests conducted for August condition).....	8-10
8-3	Performance curves with margins of uncertainty: (a) June condition .....	8-11
8-4	Performance of the Bay testboxes fitted with skimming walls.....	8-14
8-5	Perspective view of the undistorted Open testbox with curtain.....	8-16
8-6	Layout and dimensions of the curtain placed around the undistorted Open testbox .....	8-17
8-7	View of the undistorted Open testbox with curtain .....	8-18
8-8	Layout and dimensions of Curtain No. 4 placed around the distorted Open testbox .....	8-19
8-9	View of the distorted Open testbox with Curtain No. 4 .....	8-20
8-10	Performance of the Open testboxes fitted with curtains .....	8-21
8-11	Comparison of numerical-model and hydraulic-model results for vertically distorted representation of Prattville Intake .....	8-23
8-12	Comparison between the field data and the results of numerical simulation for a virtual undistorted Prattville Intake for August condition.....	8-24

## LIST OF TABLES

<u>Table</u>	<u>Page</u>
1-1. Modeling phases and tasks.....	1-11
2-1. Reference profiles of water temperature in Lake Almanor during June, July, and August. Also given is the elevation of the water surface for each month.....	2-13
3-1. Major physical dimensions of the Lake Almanor and the hydraulic model ( $X_r = 220$ , $Y_r = 40$ ).....	3-7
3-2. Sources of bathymetry data used in constructing the hydraulic model .....	3-10
5-1. List of the tests conducted with the Hydraulic Model and the Testboxes .....	5-5
7-1. Summary of data from screening tests with skimming curtains; for the August condition of Lake Almanor and $Q/Q_0 = 1.7$ in the model (the equivalent outflow from Prattville Intake is 1,600cfs) .....	7-10
7-2. Summary of data from tests with Curtain No. 4 with $Q/Q_{Om} = 1.7$ in the model (the equivalent outflow from Prattville Intake is 1,600cfs) .....	7-11
7-3. Summary of data from tests with Curtain No. 4 with levees removed, for model discharge set at $Q/Q_0 = 1.7$ (the equivalent outflow from Prattville Intake is 1,600cfs).....	7-16
7-4. Summary of screening-performance data (to reduce $T_{out}$ ) for the August condition of Lake Almanor, and $Q/Q_0 = 1.7$ in the model (the equivalent outflow from Prattville Intake is 1,600cfs).....	7-26
9-1. Summary of hydraulic-model data on outflow temperatures, $T_{out}$ , and temperature reductions, $\Delta T_{out}$ , obtained when $Q/Q_0 = 1.7$ in the model (an equivalent outflow of 1,600cfs from Prattville Intake). Also indicated is the water-surface elevation for each month .....	9-7

# 1. INTRODUCTION AND SCOPE

## 1.1 Introduction

This report presents the results from a hydraulic-model study conducted to determine the feasibility of modifying Prattville Intake, a water-intake structure located in Lake Almanor, California. Modifications to the Intake needed to be investigated so that, during summer months, the Intake could be operated to release colder water than it presently can release. One or more modifications were proposed for enabling the Intake to withdraw colder water from the lower levels of the lake during summer. Also considered in the investigation was a modification that could enable the Intake to be operated so as to conserve the lake's limited supply of cold water during spring months, and thereby increasing the amount of colder water available for subsequent release during summer.

Lake Almanor is a storage reservoir along the North Fork of the Feather River. Prattville Intake is located on the lake's southwest shoreline, as is illustrated in Figure 1-1. The present operation of Prattville Intake results in the summertime release of water whose temperature environmental interests consider too warm for trout in the North Fork of the Feather River downstream from Lake Almanor. Accordingly, Pacific Gas and Electric (PG&E), the owner and operator of Prattville Intake and the dam retaining Lake Almanor, together with the Ecological Resource Committee (established under the Rock Creek and Cresta operating license for Prattville Intake [FERC 1962]) collaboratively decided to initiate an investigation as to the feasibility of reducing the temperature of water released from the reservoir during summer (mid-June to mid-September).

The study entailed the use of a hydraulic model that was unique insofar that no prior hydraulic model of comparable size, encompassed area, and complexity had been undertaken for studying water movement in, and managed release from, a thermally stratified body of water. A further challenging feature of the model is that the model had to be vertically distorted in order to tackle the problems posed in simulating a large extent of thermally stratified Lake Almanor, as well as replicating the key details of the flow

field in the vicinity of Prattville Intake. To meet the requirements for replicating a large area of the lake, and for having an adequate water depth to satisfy criteria for modeling stratified flow to the intake, the model's vertical-length scale had to be smaller than the model's horizontal scale. The difference in horizontal and vertical scales results in what is referred to as a vertically distorted model. Herein, the convention used for model scale is prototype value divided by model value.

As with many comprehensive modeling efforts, the present study had its uncertainties and its intriguing results. The uncertainties primarily concerned the use of a vertically distorted hydraulic model, which meant there had to be judicious care in model operation and in the interpretation of data and observations obtained from the hydraulic model. That care was accomplished in part by means of auxiliary laboratory experiments used to calibrate the hydraulic model and to help confirm results obtained from it. Additionally, a set of three-dimensional computational fluid dynamics (CFD) numerical models was used to assess the uncertainties as well as to help support and interpret the results from the hydraulic model. In describing the conduct and findings of the hydraulic model, the present report describes the concerted development and use of all the models. The intriguing results concern not only the density-driven water-movement processes observed in the model. They also concern the calibration relationship determined for setting outflow discharge from the vertically distorted hydraulic model. The relationship is an essential consideration for interpreting results from the hydraulic model, and for extending those results to predict the performance of Prattville Intake.

## **1.2 Scope and Objectives**

The scope of the project entailed the conduct of extensive simulation tests using a complicated hydraulic model to evaluate the capabilities of several conceptual design modifications to Prattville Intake that could enable the Intake to release colder water during summer. The use of a hydraulic model was supported by means of auxiliary laboratory experiments as well as a set of numerical models.

The project's specific objectives are as follow:

1. Establish the baseline outflow-performance of Prattville Intake in its existing configuration. This objective entailed obtaining a set of curves relating outflow temperature and outflow rate from Prattville Intake for a range of water stratification conditions (water-temperature profiles and water-surface elevations) in Lake Almanor. To achieve this objective entailed conducting extensive calibration tests aimed at ensuring accurate interpretation of the performance data produced from the hydraulic model. (*Calibration Tests, and then Baseline Performance Tests*);
2. Ascertain the comparable outflow-performance curves produced by Prattville Intake in conjunction with two general modifications intended to facilitate the Intake's release of colder water: a skimming curtain surrounding the intake; and, a hooded-inlet pipe fitted to a caisson structure at the Intake. (*Modification Screening Tests - A*);
3. Ascertain the comparable outflow-performance curves produced by Prattville Intake in conjunction with modifications intended to facilitate Intake operation to conserve colder water: a bottom sill surrounding the Intake. (*Modification Screening Tests - B*); and,
4. If indeed the Intake modifications show strong promise of meeting the requirements, then document and validate the design layout of the recommended modifications. (*Performance Documentation Tests*).

The design and performance information associated with the project's scope and objectives would enable PG&E to determine the feasibility of modifying the overall configuration of Prattville Intake to better manage cold water release from Lake Almanor.

### 1.3 Approach

The approach taken comprised a phased sequence of tasks aimed at meeting the project's objectives. The project's success required the concerted use of the hydraulic model and the set of numerical models, which were based on the Computational Fluid Dynamics (CFD) for modeling three-dimensional flow. The code was developed at IIHR and is an Unsteady and Unstructured Reynolds Averaged Navier-Stokes (U<sup>2</sup>RANS) solver. The project entailed the series of tasks structured as in Table 1-1 and as briefly explained below.

Table 1-1 shows the relationships between the tasks and the phased implementation of the hydraulic model, the auxiliary laboratory experiments, and numerical models. The auxiliary laboratory experiments herein are called the "testbox" experiments. The tasks directly associated with the hydraulic model and the testbox experiments are designated as Tasks H1-8, and those directly associated with the numerical model are designated as Tasks N1-8.

Objectives 1 through 4 were pursued primarily by means of tests conducted with the hydraulic model. It was used to gain insights into the flow and thermal conditions at Prattville Intake, and to ascertain the performance of design concepts enabling Prattville Intake to release colder water during summer.

The series of testbox experiments were carried out using a companion pair of testboxes that respectively comprised a vertically distorted and an undistorted, approximate replication of Prattville Intake. One testbox was built at the same set of horizontal and vertical scales as used for Prattville Intake in the hydraulic model; that testbox replicated, in simplified form, the distorted geometry of the model of Prattville Intake and the lake bathymetry around it. The other testbox was built at a single length scale equivalent to the vertical scale of the hydraulic model; that testbox replicated, in simplified form, an undistorted version of the model of Prattville Intake and the lake bathymetry around it.

The pair of testboxes simulated, to selected levels of geometric detail, the water-flow and water-temperature conditions in the immediate vicinity of Prattville Intake. The testboxes, though, were not meant to be exact geometric replications of Prattville Intake; e.g., they do not replicate the Intake's tower structure or the tower's offset from the shoreline. Nevertheless, the testboxes were found to produce curves of outflow temperature versus outflow discharge that were comparable to the curves obtained from the hydraulic model, and so enabled the influence of vertical distortion to be assessed and taken into account in analyses of results obtained from the vertically distorted hydraulic model.

The performance curves (outflow temperature versus outflow discharge) obtained from the testbox pair provided the following information needed for operating the vertically distorted hydraulic model and verifying results obtained from the hydraulic model:

1. A calibration factor for setting the model-scale rate of outflow from the Prattville Intake in the hydraulic model. The factor was needed to adjust the model's performance so that it replicated the performance of Prattville Intake; i.e., the relationship between outflow temperature and outflow rate. Tests to determine the factor were conducted prior to the bulk of the tests with the hydraulic model; and,
2. Data and observations validating the performance curves of the most promising design modification that would facilitate the release of colder water through Prattville Intake during summer months. The validation needed to ensure that essentially the same results would result from an equivalent undistorted hydraulic model of Prattville Intake. Tests to validate the performance of the design modification were conducted after completion of the bulk of the tests with the hydraulic model.

The testbox experiments were conducted using an area at one end of the large basin formed by the hydraulic model. The testboxes were suitably distant from the model of Prattville Intake so that their presence did not influence the flow field in the vicinity of the model Intake. The experiments used the same bodies of water as used in simulating the performance of Prattville Intake.

A set of numerical models were used to address the following issues:

1. Provide support for the performance curves obtained for existing Prattville Intake, and subsequent modification, with the vertically distorted hydraulic model;
2. Extend to an equivalent, virtual, undistorted hydraulic model the results from the vertically distorted hydraulic model;
3. Further extend the results from the hydraulic model to the full-scale conditions existing at Prattville Intake; and,
4. Serve as a means for further investigation into aspects of the performance of Prattville Intake, possibly with additional modification concepts, once the hydraulic model was dismantled.

Table 1-1 lists the modeling phases and tasks completed with the hydraulic model. The general features of the computer code used for the numerical models are described in Section 1-4.

Field data were available for validating the hydraulic model and the numerical models. The data, provided by PG&E, largely comprised temperature profiles at a set of locations

throughout Lake Almanor. Also they included a series of data relating temperature of outflow water released from Prattville Intake and rate of water-outflow from the intake during August 1994, and during June, July and August 2000. Those data were used to verify the accuracy of the modeling results.

#### **1.4 Numerical Models**

A number of 3-dimensional-flow (3D) numerical models were used to simulate the flow and thermal conditions associated with the intake. The 3D models were needed because the flow field developed by Prattville Intake is markedly three-dimensional, as also would be the flow fields developed by the modifications considered for the Intake. The following CFD models were prepared and used:

1. A model of entire Lake Almanor simulated using full-scale dimensions;
2. A model simulating one pair of testboxes;
3. A model simulating a large portion of the hydraulic model; and,
4. A model simulating a virtual undistorted version of the same portion of the hydraulic model as modeled for item 3.

The models simulating a large portion of the hydraulic model simulated the performance of Prattville Intake in its existing configuration, plus the condition when the Intake was fitted with a curtain.

This report concisely presents the main results from the numerical models used to simulate the hydraulic model (items 2 and 3 above). A more comprehensive description of the numerical models is given in an IIHR report that accompanies this report (Lai et al. 2004).

IIHR's 3D flow code, U2RANS, was used as computational source code for the numerical models simulating flow and thermal conditions in Lake Almanor with Prattville Intake operating. The models were used for simulating the evolution of the thermal stratification in Lake Almanor as well as describing the flow and temperature field in the vicinity of the Prattville Intake. The models consisted of computational grids of the site, the input files for specified scenarios, and the U2RANS CFD code, which solves the complete 3D-flow equations. Unlike other 3D numerical codes used in hydraulic engineering, U2RANS does not make the hydrostatic assumption for pressure in the vertical direction. It uses a prism-based flexible mesh system (versus structured hexahedron based grids used by most 3D codes), and incorporates comprehensive water-surface heat exchange models.

The use of U2RANS for hydrodynamic simulation is well verified for numerical accuracy, and is validated for use in numerous research and engineering projects involving isothermal flow fields in the vicinity of water intakes and other hydraulic structures. It is a general-purpose code for modeling fluid flow, heat transfer, and multi-species transport. The code has been specifically developed to solve fluid mechanics and heat-transfer problems in hydraulic engineering such as for flows in rivers and reservoirs, components of hydropower dams, as well as around and through various hydraulic structures (e.g., water intakes and pump sumps). In recent years it has been used successfully for simulating thermal-effluent discharges released into rivers. U2RANS uses advanced, unstructured CFD technology, unifies multi-block structured mesh (quad or hex) and unstructured mesh (quad, triangle, tet, hex, wedge, pyramid, or hybrid elements) into a single platform, and combines 2D and 3D solvers in a common framework. The code is configured to run both on Unix workstations or Pentium-based PCs with Windows or NT operating systems.

## **1.5 Outline of Report**

Chapter 2 of this report briefly describes the site conditions at Prattville Intake and the main physical features of Lake Almanor. It then outlines the background concerns leading to the investigation of the feasibility of modifying the operation of Prattville

Intake so that it could release colder water during summer. Chapter 2 also provides a synopsis of prior modeling studies similar in nature to the present study.

The layout, selection of scales, and the design of the hydraulic model are described in Chapter 3. The critical task of calibrating model-scale values of outflow discharge for the hydraulic-model is described in Chapter 4. Chapter 5 presents the program of tests conducted with the testboxes and the hydraulic model. The calibration results from the testboxes are given in Chapter 6.

Chapter 7, which sets forth the baseline conditions associated with the performance of Prattville Intake in its present configuration, describes the findings of screening tests conducted to identify the modifications most likely to enable the intake to release colder water during the summer months, as well as to retain colder water during spring months. The results of the performance-documentation tests and performance validation tests carried out to define and confirm the most promising design modifications are given in Chapter 8. The performance validation tests were done using the testboxes and the numerical model.

Lai et al. (2004) describe the computational code used for the numerical modeling conducted in support of the hydraulic modeling. The results from numerical modeling are interspersed at pertinent places in Chapters 6 through 8. Those results were used to augment and support the findings from the hydraulic model.

At the outset of the report it is useful to state that tests with the hydraulic model showed that a set of modifications was found to be effective in reducing the temperature of the outflow from Prattville Intake. The set comprised a skimming curtain and some minor bathymetry changes that together enabled Intake operation to release significantly colder water (temperature reductions of around 5°C), and a sill that enabled Intake operation to conserve colder water. Chapter 9 gives the principal conclusions and recommendations

drawn from the hydraulic modeling, together with supporting information gained from the testboxes and the numerical models.

This report is accompanied by an edited set of digital video recordings that show the main features of the hydraulic modeling. In particular, the video recordings show important features of the flow field developed in the hydraulic model of Prattville Intake, for the Intake in its existing configuration and when the Intake was fitted with the modifications tested.

Note that, throughout the report, modeling scale ratio is defined as scale ratio (designated using subscript  $r$ ) = prototype dimension/model dimension (as per ASCE 2000). For example, a horizontal-length scale  $X_r = 220$  means that the horizontal lengths in the model are  $1/220^{\text{th}}$  of corresponding prototype lengths.

Table 1-1. Modeling phases and tasks.

HYDRAULIC MODEL (H)	NUMERICAL MODEL (N)
<i>Phase 1. Model Specification</i>	
Task H1. Model specification & design	Task N1. Model specification & design
<i>Phase 2. Model Construction</i>	
Task H2. Model fabrication	Task N2. Model development
<i>Phase 3. Calibration &amp; Validation</i>	
Task H3. Calibration  Conduct of testbox experiments to determine a flow-adjustment factor and the range of flow rates needed for operating the hydraulic model.	Task N3. Calibration and validation  Calibration of the numerical model using field data taken from Lake Almanor during year 2000. Validation of model using data taken in year 2001. The model simulated the entire lake.
<i>Phase 4. Baseline Tests</i>	
Task H4. Performance testing of the existing design of Prattville Intake subject to prescribed lake conditions for June, July, and August (lake level and temperature characteristics; varied rates of water outflow through the intake).	Task N4. Simulation of flow, temperature field, and outflow temperature in vertically distorted hydraulic model under existing Intake conditions.
<i>Phase 5. Screening Tests of Possible Modifications</i>	
Task H5. Screening tests to ascertain the performance of possible modifications to Prattville Intake. The tests mainly used the August condition (lake level and temperature characteristics). The modifications were for – <ol style="list-style-type: none"> <li>1. releasing colder water during June, July and August; and,</li> <li>2. storage of colder water during other months.</li> </ol> This task entailed testbox experiments to confirm the performance of the most promising modification	Task N5: Simulation of flow, temperature field, and outflow temperature with the most promising intake modification <ol style="list-style-type: none"> <li>1. in the vertically distorted hydraulic model; and,</li> <li>2. in an equivalent, virtual, undistorted hydraulic model</li> </ol>
<i>Phase 6. Performance-documentation &amp; -demonstration Testing of Modifications</i>	
Task H6. Performance-documentation and -demonstration of the most promising modifications for <ol style="list-style-type: none"> <li>1. releasing colder water during June, July and August</li> <li>2. storage of colder water during other months.</li> </ol>	Task N6. Numerical modeling focused on simulating the performance of a large portion of the hydraulic model for the condition of Prattville Intake with, then without, a skimming curtain. The simulations were done for the distorted hydraulic model, and an undistorted version of the hydraulic model.
Task H7. Report preparation	Task N7. Report preparation
Task H8. Dismantling of model	Task N8. Documentation of CFD model and transfer to PG&E.



Figure 1-1. A view of Prattville Intake and Lake Almanor.

## **2. PROBLEM DESCRIPTION AND BACKGROUND**

### **2.1 Introduction**

This chapter briefly introduces the site location of Prattville Intake then describes the problem addressed by the present project. Information also is given regarding the physical setting, bathymetry, climate, and water sources of Lake Almanor and thereby Prattville Intake. Additionally, the chapter provides a brief synopsis of the prior studies concerning the management of cold-water withdrawal from lakes, reservoirs, and rivers.

### **2.2 Prattville Intake**

Prattville Intake is located on the southwest shore of Lake Almanor, Plumas County, in northern California. The geographic location of Lake Almanor is indicated in Figure 2-1. The Intake is owned and operated by PG&E, and is part of PG&E's "North Fork Feather River Project." The Intake diverts water from Lake Almanor to Butt Valley Powerhouse and Reservoir through a conduit known as the Prattville tunnel and penstock. Water then flows from Butt Valley Reservoir downstream through a series of hydroelectric facilities. Figure 2-2 is a layout schematic of part of PG&E's system of hydropower facilities immediately downstream of Prattville Intake.

Figure 2-3 shows the layout and structural features of Prattville Intake. Lake water enters the Intake through an inlet near the bottom of the Intake structure. The invert elevation of the Intake's inlet is at EL. 4410ft. The top of the inlet is at EL. 4427ft. Water entering the Intake passes through a 13ft-diameter penstock to PG&E's Butt Valley Powerhouse. Water then flows through Butt Valley Reservoir, then passes through further penstocks to PG&E's Caribou Powerhouses, which discharge into Belden Reservoir, and subsequently enter the North Fork of the Feather River (Figure 2-2).

### **2.3 Problem Description**

The California Department of Fish and Game, and PG&E, have studied water temperature trends in the North Fork Feather River, and found that water temperatures

often exceed the levels desirable for trout habitat during summer. In an extensive study commissioned by PG&E, Woodward-Clyde Consultants (1986) concluded that the water-temperature requirements for trout habitat could be met if water released through Prattville Intake could be lowered by about 3 to 4°C during the summer months of June, July, and August. To reduce water temperatures would require modifying the Intake so that it could selectively withdraw water from the lower temperature stratum, or hypolimnion, of Lake Almanor.

Several conceptual modifications were identified as potentially enabling Prattville Intake to be operated so as to release colder water during summer. Each modification concept, however, required testing to determine whether indeed the concept is effective and practicable. The following concepts were selected as holding good promise technically for enabling colder water to be released through the Intake:

1. A skimming curtain placed around the Intake;
2. A pipe extending a short distance to the lakebed in fairly close proximity to the Intake; and,
3. A somewhat longer pipe connecting Prattville Intake to the a submerged channel already formed in the bed of Lake Almanor.

As the deepest region of Lake Almanor is more than three miles from Prattville Intake, the concept of using a very long pipe to connect the Intake directly to the lake's deepest and coldest region was deemed overly expensive and therefore infeasible.

The concepts of a skimming curtain (sometimes called a temperature-control curtain), and a pipe extension to a nearby region of the lakebed, were considered worth investigating for their technical feasibility. That investigation required the use of a hydraulic model and of a set of numerical models, as is explained in Chapter 1. An initial hydraulic modeling effort (Vermeyen, 1995) had been conducted but proved

inconclusive, mainly because the model did not encompass a sufficiently large portion of the lake around Prattville Intake. It was concluded, however, that a further hydraulic model would be needed, and that model would need to encompass a region extending several miles in length and width over the lake, so that modeling could be conducted with an adequately large volumes of water, and for adequately long durations. Moreover, the model would need to be built at appropriately large size to enable the levels of simulation and measurement accuracy needed. The required model is without precedent, and some experts considered such a hydraulic model to be infeasible.

To be feasible, the model would need to be limited in area so that it would fit in the floor space of a hydraulics laboratory, which in turn meant that the model would have to be vertically distorted; i.e., its vertical-length scale larger than its horizontal-length scale (herein scale  $\equiv$  prototype value/model value). The technical trade-off for that arrangement of hydraulic model would be the potential complications incurred with interpreting the effects of vertical distortion.

## **2.4 Physical Setting of Prattville Intake**

The physical setting described here comprises Lake Almanor's bathymetry, weather conditions, and water sources, and the design features of Prattville Intake.

### 2.4.1 Bathymetry

Lake Almanor is retained by Canyon Dam, an earth-fill dam 135ft high and 1,400ft wide. The lake forms two main lobes or branches, the Chester Branch and the Hamilton Branch. Prattville Intake is located close to the southwest shore of the lake's Chester Branch. The bathymetry of Lake Almanor is shown in Figure 2-4. The maximum water depth in the Chester Branch near the Intake is about 50ft. The lake is deepest near Canyon Dam, its overall maximum depths attaining about 80ft there. On average, the Hamilton Branch is considerably deeper than is the Chester Branch.

The two branches of Lake Almanor are connected at a narrow region locally called the "Narrows." A peninsula extends into the lake at the Narrows, and acts to partially isolate the Chester and Hamilton Branches.

A feature of the lakebed of the lake's Chester Branch is the presence of a submerged channel that runs from Prattville Intake to the Narrows. The channel is referred to in the present report as the "incised channel." It averages a depth of about 13ft below the lakebed of the Chester Branch and is on average about 90ft wide. The incised channel was constructed in the 1920s, before Lake Almanor was formed. The channel's original purpose was to convey cold water, diverted from springs in an area of what now is the lakebed of the Hamilton Branch, all the way across the Chester Branch to a small former intake that once served the early hydropower system of which Prattville Intake is now part.

The lakebed of the Chester Branch of Lake Almanor also features the now-submerged, braided channels of the North Fork of the Feather River and tributary streams. Precise information on the channels (their depths, widths, and alignments) was not available for the present project. In contrast to the braided channels in the Chester Branch, the Hamilton Branch has a flat bottom, intersected by a single winding channel that conveyed the outflow from springs (the Big Springs) and Hamilton Creek across a flat plain to the vicinity of the present location of Canyon Dam.

#### 2.4.2 Water Sources

The major surface-water inflow to Lake Almanor is the North Fork Feather River at Chester. It has an annual average flow of approximately 380cfs. Other inflows to the lake include stream flow into the Hamilton Branch, which receives an annual average flow of 80cfs, and the Hamilton Branch Powerhouse, which releases an annual average flow of 110cfs into the lake. A number of minor tributaries and various groundwater springs also contribute significant flows into the lake.

The groundwater springs are a substantial source of coldwater inflows, and have a major impact on the thermal regime. According to PG&E, the coldwater inflows are estimated at about 375 to 450cfs, which is a significant part of the lake's inflow during late summer. The manner in which the cold water enters the lake is not well defined. Initially for the project, it was assumed that cold water mainly enters the lake from one, possibly, two sources:

1. The primary source is spring water from springs called Big Springs, located near the eastern shoreline of the Hamilton Branch; and,
2. Much lesser sources include a series of springs in the Chester Branch and near the eastern shore of the Hamilton Branch.

PG&E usually stores water in Lake Almanor during winter and spring, and releases water from the lake during summer and autumn. When the lake is at its normal water-surface level of El. 44494ft it stores about 1,142,000 acre-ft of water.

The outflows from the lake include the Prattville outlet (the Intake) and the Canyon Dam outlet. The releases from Prattville Intake represent the major part of outflow from the lake. The Intake releases water at a normal operating discharge of 1,600cfs, but may release water up to a flow rate of 2,200cfs. Flow releases from Canyon Dam typically amount to only about 35cfs, and are withdrawn through a near-bottom outlet.

### 2.4.3 Climate

Lake Almanor experiences a wide variation in weather conditions throughout the year. Over the period extending from mid-1948 through to early 2003, air temperatures have attained average monthly maxima of about 24°C, 30°C, and 29°C (74 °F, 86°F, and 84°F) for the regions warmest months, June, July, and August, respectively. For the same period of years, the average monthly minimum temperatures are 6°C, 8°C, and 8°C (43°F, 47°F, and 47°F) in June, July, and August, respectively. The region's coolest months are December, January, and February, which have average monthly maximum temperatures

of about 3°C, 4°C, and 6°C (38°F, 39°F, and 43°F), respectively. For the same months, the average monthly minimum temperatures are -5°C, -6°C, and -5°C (23°F, 22°F, and 23°F), respectively. The annual average maximum and minimum temperatures for the Lake Almanor region are about 16°C, and 0.5°C (61°F and 33°F), respectively.

The summer months of June, July and August are the driest months for the region. The average total amounts of rainfall for those months are 0.76in, 0.19in, and 0.30in, respectively. January is the wettest month, receiving 7.48in of rainfall and 33.2in of snow. These climate data are provided by the Western Regional Climate Center ([www.wrcc.dri.edu](http://www.wrcc.dri.edu)).

#### 2.4.4 Thermal Stratification

Climate conditions cause seasonal heating and cooling cycles of water in Lake Almanor. Typically, warming causes the lake to become thermally stratified during the summer (mid-June through mid-September). The sets of water-temperature profiles presented in Figures 2-5a-c were measured on June 22, July 20, and August 17 of 2000. The profiles were measured at 7 to 8 locations in Lake Almanor (LA verticals 1, 2, B-G). They show how the lake's water warms over its depth, and how the lake establishes a warm upper layer (epilimnion) and relatively cold bottom layer (hypolimnion). The two layers are connected by a thermocline region, over which water temperature varies steeply with water depth. As indicated in Chapter 3, several of the profiles (LA-2, LA D, and LA-C) are located close to the area encompassed by the hydraulic model.

Also indicated are temperature profiles determined using a one-dimensional numerical model, MITEMP. This model was used to determine seasonal variations of water temperature in Lake Almanor, and to assess the availability of cold water available in the lake. Work with the model led to a preliminary conclusion that use of a skimmer curtain could enable Prattville Intake to release colder water such that water temperatures downstream of Lake Almanor would be lowered by about 2°C (Woodward-Clyde Consultants 1986).

The average profiles of water temperature versus water depth estimated for June, July, and August shown in Figure 2-6. Table 2-1 is a tabulation of these average temperature profiles. The hydraulic modeling and auxiliary modeling (testbox and numerical) carried out for the present study are based on these profiles. The profiles given in Figure 2-6a-c and Table 2-1 are taken as being representative of water conditions in Lake Almanor during June, July, and August.

Water temperatures of outflow released from Prattville Intake were measured on June 22, July 19, and August 17 of 2000. Additionally outflow temperatures were measured during August 1 through 5 of 1994.

## **2.5 Prior Studies**

The technical literature documenting the design considerations and use of skimming curtains is not extensive. Nor is there extensive literature on submerged intakes somewhat similar in design to the pipe concept contemplated as a modification to Prattville Intake. In several respects, it is clear from the existing literature that the design of curtains and submerged intakes must necessarily be tailored to the local circumstances of site bathymetry, thermal conditions, and flow requirements. Consequently, much of the literature on curtains and submerged intakes involves descriptions of model studies conducted to develop and confirm design performance.

Early studies on the selective withdrawal of water in thermally stratified reservoirs, cooling ponds, and lakes practically began with the development of large thermal power plants. Among the studies of relevance to the present study are the studies by Harleman et al. (1958), Harleman and Elder (1965), Ryan and Harleman (1973), and Jirka (1979). Harleman and Elder (1965), for example, conducted experiments aimed at designing skimming walls as a means for selective withdrawal. Jirka (1979) presented an analysis of the flow and thermal field associated with the use of a two-dimensional wall selectively withdrawing water from a stratified body of water. A number of studies have hydraulically modeled thermal stratification of water in rivers and canals (e.g., Stolzenbach and Harleman 1967), and an extensive literature exists on thermal plumes in

various water bodies (e.g., Wilkinson 1991). A review of these studies is not given here, though the study by Stolzenbach and Harleman is considered a little further.

The study by Stolzenbach and Harleman is pertinent for the present study insofar that it provides a useful discussion of the similitude considerations associated with modeling the withdrawal of colder water from a two-layer stratification in a river. Additionally, their study investigated the performance of skimmer walls in facilitating the withdrawal of colder water from the river. The comparatively shallow depth of the river (about 21ft) at the site under investigation required the use of a hydraulic model whose horizontal and vertical scales were  $X_r = 120$ , and  $Y_r = 40$ ; subscript  $r$  denotes scale ratio. The model proved successful in providing the engineering information needed to resolve questions regarding the performance of the skimming walls. The essential similitude guidelines proposed by Stolzenbach and Harleman (and assessed by Ryan and Harleman 1973) are considered subsequently in Chapter 3, when discussing the selection of length scales for the present study.

### 2.5.1 Skimming Curtains

The U. S. Bureau of Reclamation has used curtains to facilitate the selective withdrawal of cold water from two of its reservoirs used for hydropower generation and water diversion for irrigation. The curtains resulted in the release of colder water to meet water-temperature requirements for fish habitat downstream of the reservoirs. Several conference papers by Bureau researchers describe the Bureau's experience (Vermeyen 1997, Vermeyen and Johnson 1993, Johnson and Vermeyen 1993, Johnson et al. 1993). The Bureau has installed three curtains in the following Bureau reservoirs: Lewiston Lake in northern California, and Whiskey Town Reservoir, also in northern California. The Bureau reports that the curtains are effective in reducing the temperature of outflow water (Vermeyen, 1995). The curtains have reduced water temperatures in the downstream reaches by 2 to 3°C. In each case, a hydraulic model was used in designing the curtain. The models were geometrically undistorted (having the same horizontal and length scales), and involved replication of a prevailing thermal condition of the water body in which the curtain would be placed.

The models were useful for their intended purpose, though a couple of concerns needed to be taken into account with their use:

1. The small scales for length (e.g.,  $X_r = Y_r = 120$  for Lewiston Lake, and  $X_r = Y_r = 72$  for Whiskeytown Reservoir) used incurred values of Reynolds numbers in the laminar and transitional ranges (especially for  $X_r = Y_r = 120$ ), such that the models may not have fully replicated turbulent mixing and flow entrainment; and,
2. The comparatively small quantities of water used may not have enabled flow conditions to attain adequate equilibrium in outflow temperature.

Though these concerns somewhat limited the capability of the hydraulic models to yield reliable quantitative model information on curtain performance, the models were useful aids for design. Indeed they were significant achievements in hydraulic modeling; in particular, scant few prior models of hydraulic structures had simulated the temperature profile of a reservoir.

The present project was preceded by a hydraulic model study conducted by the Bureau (Vermeyen, 1995). That study was based on the use of an undistorted hydraulic model built at a length scale of  $X_r = Y_r = 40$ . The model encompassed a 1,400ft by 800ft area of Lake Almanor's bathymetry surrounding Prattville Intake. However, the model suffered from several shortcomings, especially in limited area modeled and in the manner used to provide water to the model. The stratified thermal structure of water in the model was established by using cold water slowly discharged beneath a layer of warm water in the model. This approach proved problematic, and limited volume of water did not facilitate the establishment of a steady-state condition in the model.

The Bureau tested several modifications that might enable Prattville Intake to selectively withdraw cold water from Lake Almanor: i.e., a short skimming curtain, a pipe with a hooded inlet, and excavation of an approach channel. For most of the tests, the pipe with

a hooded inlet was found most effective at reducing outflow temperature and minimizing the amount of warmer water mixing with the colder water. As would be expected, each of the modifications performed better for outflow of 800cfs rather than the normal operating outflow of 1,600cfs. Testing of curtain performance would have been rather difficult for the model because time is needed for an equilibrium temperature distribution to be attained in the volume of water behind the curtain before the outflow temperature attains an equilibrium temperature. Though the model was helpful in assessing the potential feasibility of increasing cold-water release through Prattville Intake, the results from the model were inconclusive.

There presently are no published (or widely acknowledged) criteria for the design of skimming curtains for use in the selective withdrawal of water from a lake or a reservoir. Those criteria remain to be evaluated by way of a model study, hydraulic or numerical. There exists, however, a broad variety of submerged-inlet designs. Submerged, offshore water inlets are used quite commonly for withdrawing water from coastal waters. For example, they are used to meet the diverse water needs of thermal power stations, oil refineries, and urban communities located near coastal areas. Many different intake designs are used in practice (Chen et al. 2003). Some designs have multiple inlets, and others have just one inlet.

To the best of the writers' knowledge, no bottom-founded, submerged inlet has been designed for use in the selective withdrawal of colder water from a lake or reservoir. There are, to be sure, intake towers built with multiple openings over a range of water depths. Such intake towers are fairly common for reservoirs. However, the writers are unaware of existing, single opening inlet placed on the bottom or bed of a reservoir or lake with the purpose of withdrawing the colder water from the lower elevations of water in the reservoir or lake. Where such bottom inlets are used, they primarily are placed at sufficient depth so that they have adequate submergence for suitable hydraulic performance. An additional consideration for the operation of bottom water inlets in water bodies prone to frazil-ice formation is that they do not entrain, and get blocked by,

frazil ice. A further consideration is the unwanted entrainment of fish larvae. This concern is a major design consideration for intakes in some lakes.

### 2.5.2 Hooded-Pipe Outlet

Presently there are no published guidelines on the design of the hood to be placed over a submerged inlet to a pipe, as considered for the present project. The criteria for hood dimensions and clearance above a pipe inlet remain to be evaluated by way of a model study, hydraulic or numerical.

Goldring (1989), though, conducted experiments on circular submerged inlets fitted with hoods, and without hoods, for the purpose of selectively withdrawing colder water from the hypolimnion of a stratified (two layer) water body subject to a cross-flow. His experiments led to equations for use in predicting the drawdown of the upper layer (epilimnion) as the flow rate increased into the inlet. In his effort to normalize and interpret his data, he used the following normalization of outflow-water temperature drawn through the inlet:

$$\frac{T_M - T_2}{T_1 - T_2} = T_N \quad (2-1)$$

in which  $T_M$  = the temperature of outflow water,  $T_1$  = temperature of the epilimnion (upper layer) water, and  $T_2$  = temperature of the hypolimnion (bottom layer) water. Though the present project did not use Goldring's equations for incipient drawdown of the epilimnion, it used a similar normalizing expression as Eq. (2-1) to assist interpretation of results from the hydraulic model.

### 2.5.3 Comments

The site location of Prattville Intake, the disposition of the principal source of cold water in Lake Almanor, and the overall bathymetry of Lake Almanor, are features complicating the present study, and that were not faced by prior studies of intake withdrawal from

stratified reservoirs or lakes. Especially difficult for the present study is the comparative shallowness of water depths in the vicinity of the Intake combined with the large distance between the Intake and Lake Almanor's Hamilton Branch, the principal source of cold water. For a hydraulic model to accommodate these features adequately requires that the model be built at differing vertical and horizontal scales; in other words, the hydraulic model must be vertically distorted. The effects of vertical distortion on model performance have been considered by a few prior studies of flow in thermally stratified water bodies, notably the studies by Stolzenbach and Harleman (1967) and Ryan and Harleman (1973). Two more recent studies involved vertically distorted hydraulic models for investigating aspects of selective withdrawal (Nystrom 1981, Zeng et al. 2001), but they do not provide significant new insight into the effects on model results of vertical distortion.

Chapter 3 further discusses the need for the present study to use a vertically distorted hydraulic model. That need entails ensuring that water flow in the model behaves essentially the same as in Lake Almanor.

Table 2-1. Reference profiles of water temperature in Lake Almanor during June, July, and August. Also given is the elevation of the water surface for each month.

June 22, 2000 (EL. 4491.5ft)		July 20, 2000 (EL. 4489.0ft)		August 17, 2000 (EL. 4482.5ft)	
Elevation (ft)	Temp (°C)	Elevation (ft)	Temp (°C)	Elevation (ft)	Temp (°C)
4401.25	8.75	4401.25	9.59	4401.25	10.20
4406.17	8.75	4406.17	9.59	4406.17	10.20
4411.09	8.82	4411.09	9.61	4411.09	10.25
4416.01	9.00	4416.01	9.86	4416.01	10.54
4420.93	9.43	4420.93	10.61	4420.93	11.39
4426.18	9.50	4426.18	10.81	4426.18	11.92
4431.10	9.57	4431.10	10.94	4431.10	12.23
4436.02	9.83	4436.02	11.33	4436.02	12.81
4440.94	10.28	4440.94	12.01	4440.94	13.95
4445.87	11.08	4445.87	13.32	4445.87	16.05
4451.12	12.43	4451.12	15.44	4451.12	19.24
4456.04	14.25	4456.04	18.21	4456.04	22.79
4460.96	16.22	4460.96	21.15	4460.96	23.16
4465.88	18.24	4465.88	21.67	4465.88	23.16
4470.80	20.12	4470.80	21.67	4470.80	23.16
4476.05	20.94	4476.05	21.67	4476.05	23.16
4480.97	20.94	4480.97	21.67	4480.97	23.16
4485.89	20.94	4485.89	21.67	4485.89	23.16
4490.81	20.94	4489.17	21.67	4486.22	23.16
4491.47	20.94				

Note: Outflow temperatures measured on June 22, July 19, and August 17 of 2000.

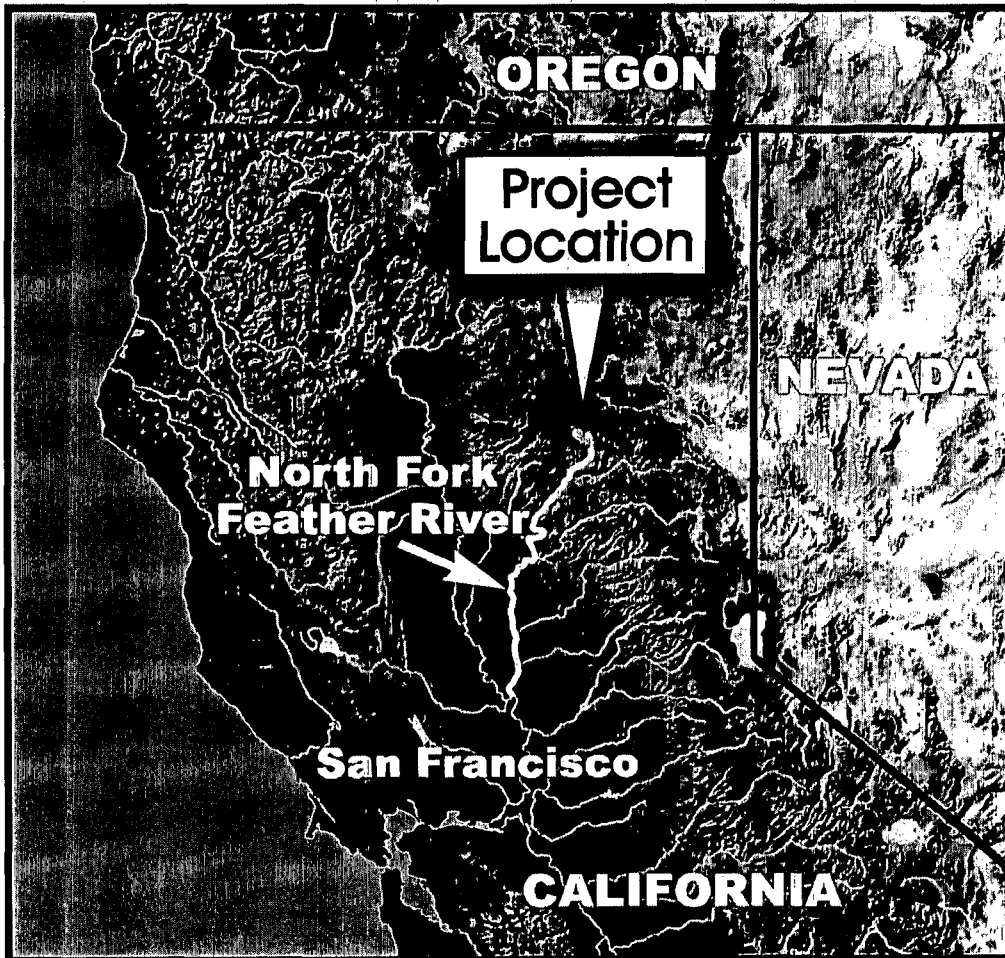


Figure 2-1. Location of Lake Almanor and the North Fork of the Feather River.

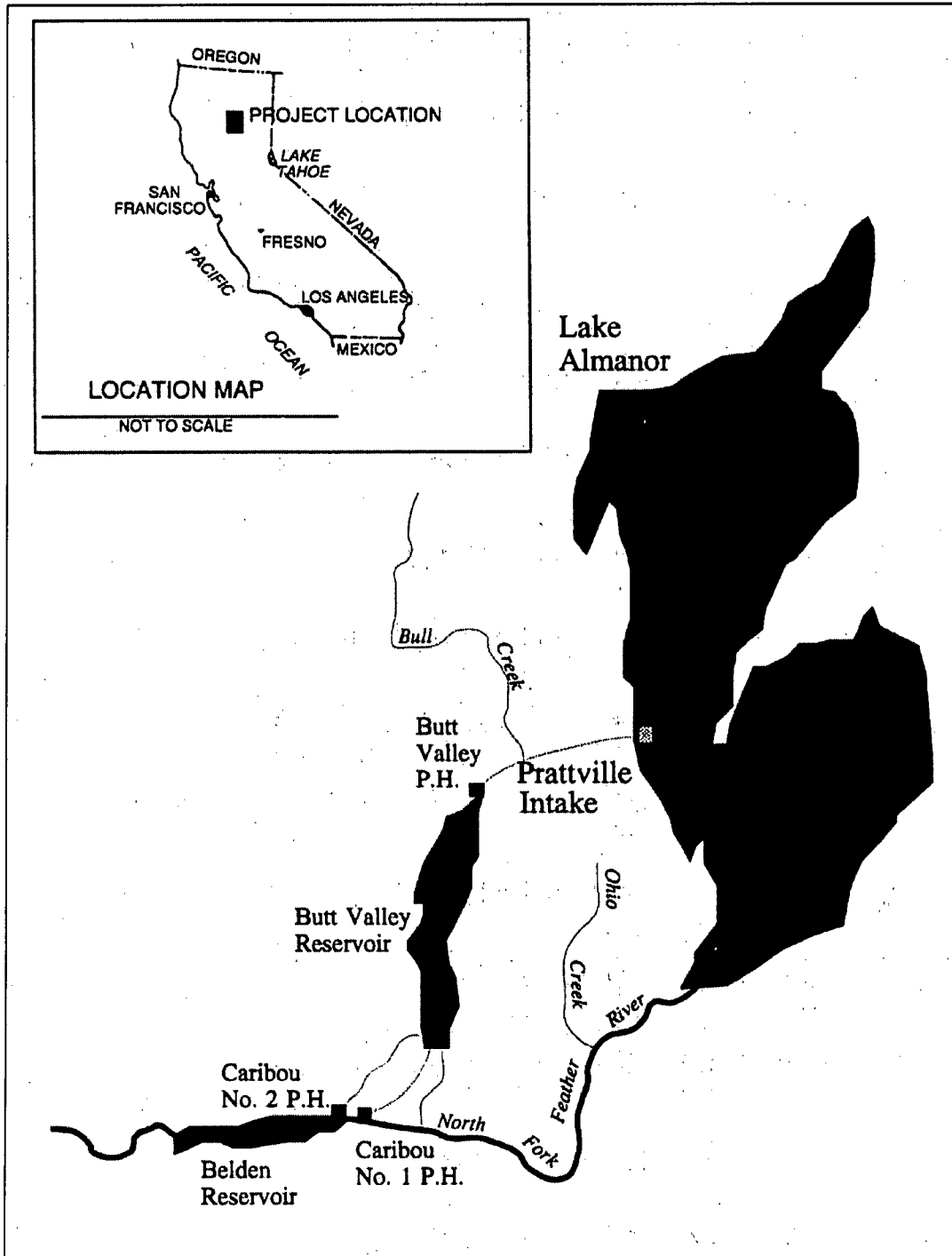


Figure 2-2. Lake Almanor and the Butte Valley Powerhouse facilities.



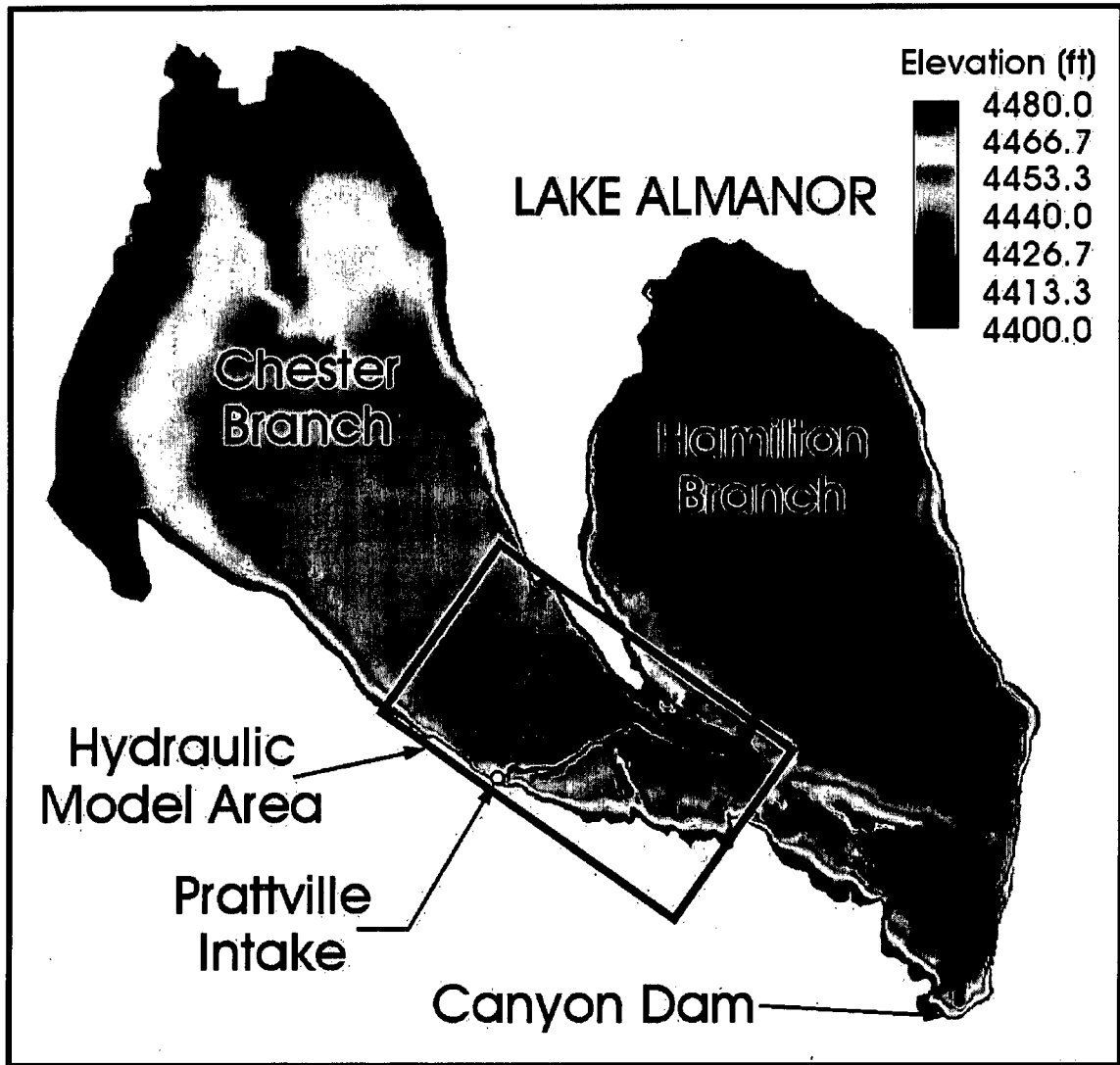


Figure 2-4. Bathymetry of Lake Almanor.

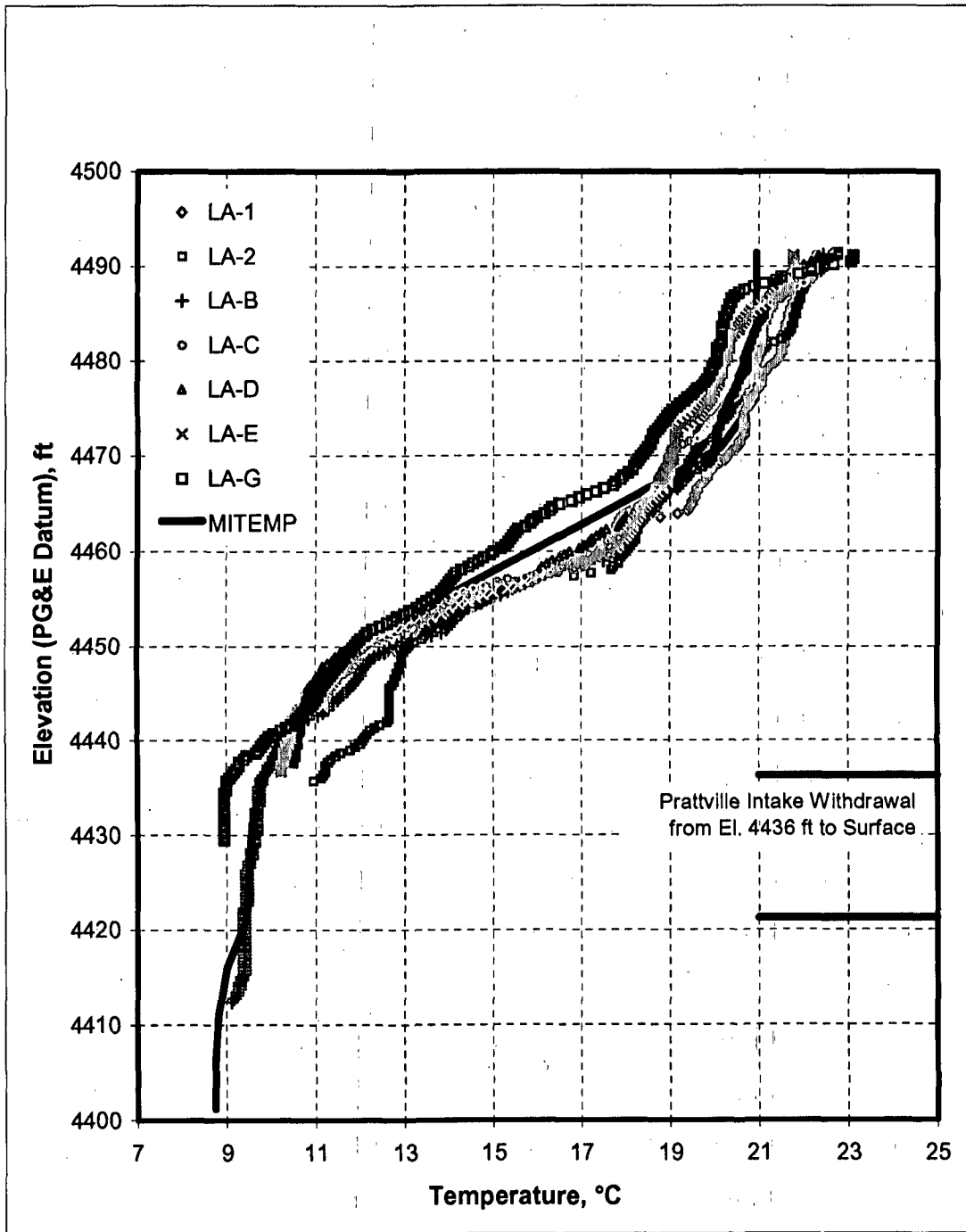


Figure 2-5. Water temperature profiles measured in Lake Almanor: (a) on June 20, 2000 (data provided by PG&E).

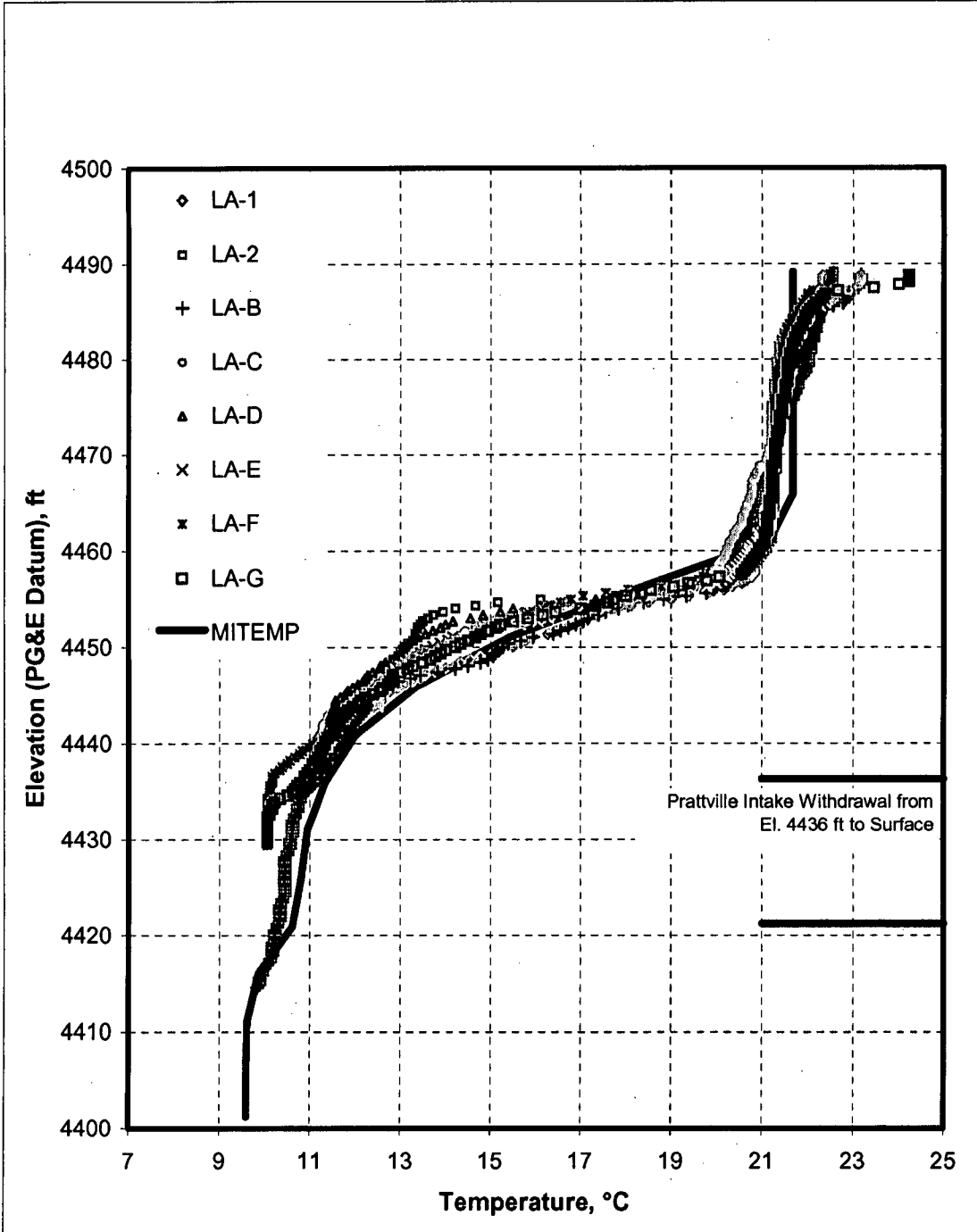


Figure 2-5 continued. Water temperature profiles measured in Lake Almanor: (b) on July 22, 2000 (data Provided by PG&E).

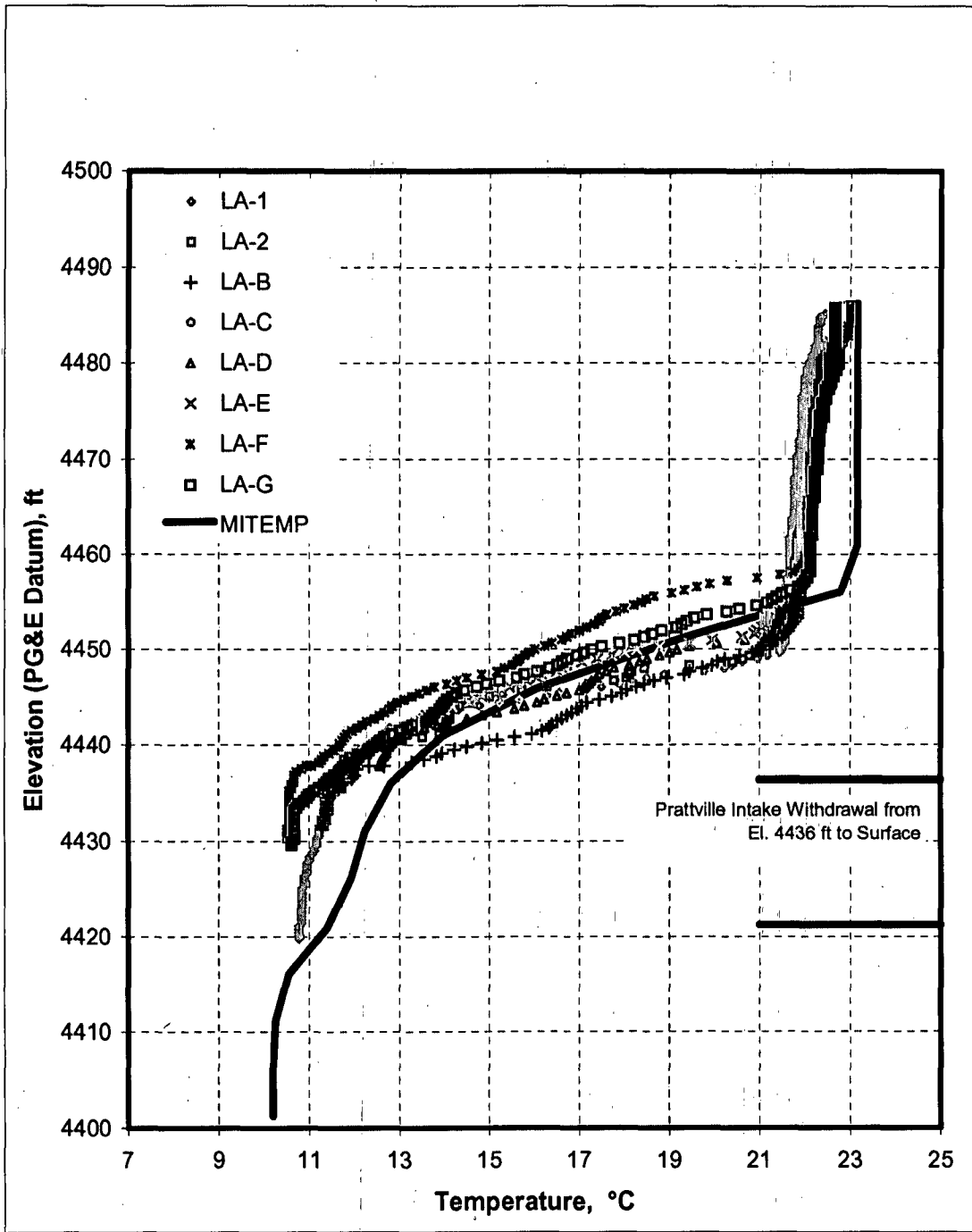


Figure 2-5 continued. Water temperature profiles measured in Lake Almanor: (c) on August 17, 2000 (data provided by PG&E).

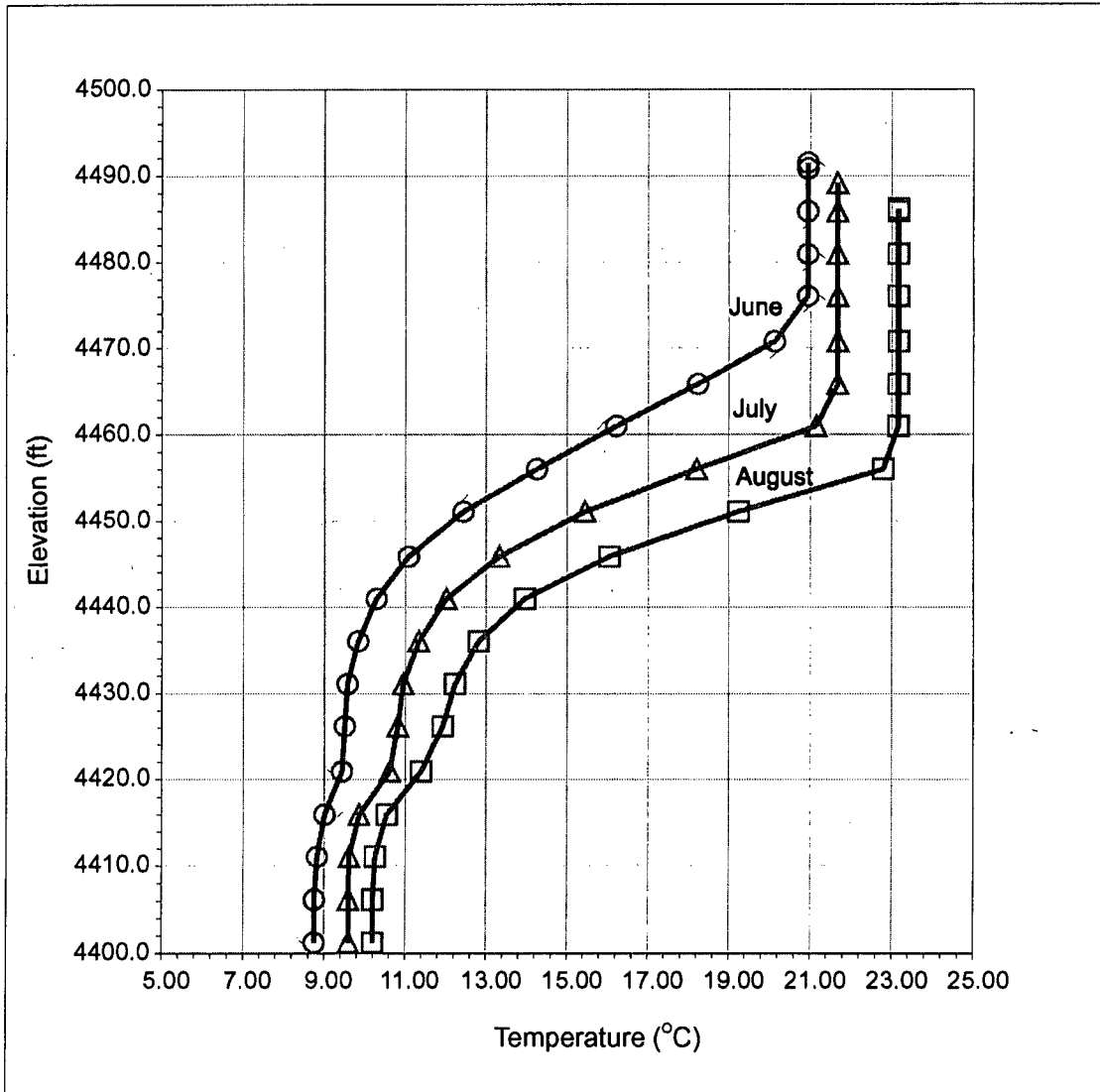


Figure 2-6. Average profiles of water temperature in Lake Almanor for June, July, and August 2000.

### **3. MODEL DESIGN AND OPERATION**

#### **3.1 Introduction**

The modeling approach required the use of a vertically distorted hydraulic model that could contain a body of water whose vertical profiles of water temperature practically would be identical to those measured in Lake Almanor. In this manner, the model could be used to simulate the same normalized density differences,  $\Delta\rho/\rho_0$ , as prevail in the lake, and thereby the same overall patterns of water flow. To be feasible, this approach required the use of a complicated and unusual hydraulic model. The present chapter describes the considerations involved in the design, construction, calibration, and operation of that model.

The water-temperature profiles and water-surface elevations prescribed for simulation in the hydraulic model are those shown in Figure 2-6 and listed in Table 2-1. They were assumed to be representative of Lake Almanor during June, July, and August.

#### **3.2 Area Encompassed by Model**

The model encompassed an area delineated by a 3.1-mile by 1.9-mile perimeter of Lake Almanor, as indicated in Figure 3-1. The area extended from Prattville intake out to the so called "narrows" region that links the Chester and the Hamilton Branches of Lake Almanor, and out across from the intake to the Almanor Peninsula.

It was necessary to have this area of coverage for several reasons:

1. To ensure that the model had a sufficient volume of water, especially cold water, to enable flow conditions to attain a steady state for the flow conditions investigated;
2. Commensurate with item 1 above, to include the full length of the incised channel (Figure 2-4) that runs from the Hamilton Branch of Lake Almanor to Prattville Intake. Cold-water springs in the Hamilton Branch are assumed to be the

principal source of cold water entering the lake during summer. The incised channel connects the intake with the Hamilton Branch, and is thought to be of importance in modifying the intake so that it releases colder water from the lake; and,

3. To keep the model's boundaries adequately distant from the Intake so that they do not affect the Intake's outflow performance.

In order for IIHR's Model Annex to encompass the prescribed area of the lake, and provide sufficient flow depth to enable acceptably detailed definition of water-temperature and -velocity profiles, the hydraulic model was required to be geometrically distorted, such that the horizontal-length scale was larger than the vertical-length scale.

The prescribed area extends toward the locations where vertical profiles of water temperature were measured in Lake Almanor. Those temperature profiles were needed in preparing the hydraulic model for testing.

### **3.3 Selection of Length Scales**

The considerations of the area to be encompassed led to selection of a horizontal-length scale of  $X_r = 220$ . In addition to encompassing a sufficiently large area, the hydraulic model had to be adequately deep to simulate the flow field at Prattville Intake, as well as simulate the prospective flow of colder water moving along the incised channel from the Hamilton Branch of Lake Almanor to Prattville Intake.

Flow into the Intake's entrance had to be fully turbulent. Accordingly, the vertical scale of the model had to be smaller than the horizontal scale. Also, a smaller vertical scale was need so that the vertical profiles of water temperature in the lake could be simulated and measured with sufficient detail. Close simulation of the temperature profile is important for determining the relationship between outflow temperature and outflow discharge, as well as for determining the elevations of the components of the proposed

modifications (e.g., bottom elevation of skimming curtain, or hood elevation of a hooded inlet).

Furthermore, it was envisioned at the outset of modeling that increased flow along the incised channel between Prattville Intake and the Hamilton Branch could be a significant feature in the performance of a design modification to Prattville Intake. This consideration, as well as ensuring that water movement was appropriately simulated in all significant regions of the model, required that the hydraulic model be vertically distorted; i.e., that its vertical scale be less than its horizontal scale.

An important dimensionless parameter for use in simulating flow in the lake is densimetric Froude number; i.e.,

$$F_D = \frac{U}{\sqrt{g(\Delta\rho/\rho_0)Y}} \quad (3-1)$$

in which  $U$  is a characteristic velocity,  $Y$  is a representative flow depth,  $g$  is gravity acceleration,  $\rho_0$  is the density of the ambient water, and  $\Delta\rho$  is the density difference owing to temperature stratification over the water column.  $F_D$  expresses a ratio of inertia force and gravity force acting on a flow. It is also the square root of a dimensionless parameter called the Richardson number, which in turn is an approximation of the gradient Richardson number, which expresses the ratio of the stabilizing density gradient to disturbing shear gradient acting across a stratified flow.

Dynamic similitude of flows with significant density-difference effects typically requires  $F_D$  to be equal in the model and at full scale, or at least to be close in value; i.e.,

$$F_{Dr} = 1 \quad (3-2)$$

in which subscript  $r$  denotes scale ratio.

It should be noted, though, that the values of  $F_D$  are small in Lake Almanor, except at locations influenced by the Intake (and its potential modifications). Based on the temperature profiles in the lake, values of  $\Delta\rho/\rho_0$  range up to about  $2 \times 10^{-3}$ . Additionally, for the magnitude of outflow discharges, and the cross-sectional areas of the incised channel, velocities within Lake Almanor are very small, becoming perceptible only for water near the Intake.

If the normalized density difference,  $\Delta\rho/\rho_0$ , is held constant between model and prototype, Eq. (3-2) reduces to

$$U_r = \sqrt{Y_r} \quad (3-3)$$

The model's design and operation will take into account the influence of water viscosity and boundary roughness on water motion and mixing. Those considerations customarily are expressed in terms of Reynolds number and a flow-resistance coefficient, such as the Darcy-Weisbach coefficient  $f$ . The relative magnitudes of inertia and viscous forces acting on a flow can be related using flow Reynolds number;

$$Re = \frac{UL}{\nu} \quad (3-4)$$

in which  $L$  is a characteristic length (such as flow depth,  $Y$ ) associated with the flow field, and  $\nu$  is the kinematic viscosity of water; the value of  $\nu$  varies with water temperature. It is usually not possible to expressly have the same value of Reynolds number ( $Re$ ) at model and full scales, and simultaneously satisfy Eq. (3-3). Nevertheless, to ensure similarity of flow field and flow movement, it is necessary that the values of  $Re$  and resistance coefficient  $f$  in the model be such that the overall flow condition be maintained.

The possibility of flow along the incised channel was an important flow feature to be investigated in the study. Though the magnitude of flow along the incised channel was

unclear at the outset of the study, it was possible to estimate the value of  $Re$  for that flow in rather approximate terms. Based on tests with the hydraulic model,  $Re$  is estimated as being in the range of about  $5 \times 10^4$ . This estimate is based on a prototype nominal flow depth ( $L = Y$ ) of 10ft; a depth-average velocity of flow assessed from observations in the hydraulic model, to be about  $5 \times 10^{-2}$ ft/sec; and, a kinematic viscosity of about  $10^{-5}$ ft<sup>2</sup>/s for water in the channel. For that magnitude of  $Re$ , flow in the incised channel is in the transitional condition, between turbulent and laminar flow. In this region, and for laminar flow,  $f$  is sensitive to  $Re$ , and increases quickly as  $Re$  decreases; the Stokes equation gives

$$f = \frac{64}{Re} \quad (3-5)$$

For flow in the transition region between laminar and turbulent condition, flow resistance (and  $f$ ) also is sensitive to boundary roughness.

To ensure that flow resistance of the incised channel in the hydraulic model is not excessive, but is comparable to that of the actual channel, it is important that the model-scale value of  $Re$  be kept as large as practicable, such that the model value of  $f$  be close in value to that of the actual channel. This constraint leads to the need for a vertical-length scale smaller than 220. Also, it leads to the need for a smooth boundary for the model of the incised channel.

Stolzenbach and Harleman (1967) propose two similitude relationships of use in bracketing practical values of vertical-length scale once a horizontal-length scale has been selected; or in delineating an allowable vertical distortion  $G = X_r/Y_r$ . The relationships stem from similitude considerations of frictional effects (at bottom boundary as well as at the interface between a density current and the water above) and temperature changes in a model of water flow in a thermally stratified water body. The Darcy-Weisbach equation for headloss ( $h_f$ ) owing to friction,

$$h_i = f \frac{L U^2}{4R 2g} \quad (3-6)$$

generally relates vertical distortion to the scale ratio for friction-factor,

$$G = X_r / Y_r = f_r^{-1} \quad (3-7)$$

in a model operated in terms of Froude number similitude, and for which the velocity scale  $U_r = Y_r^{0.5} \approx R_r^{0.5}$ , the hydraulic-radius scale.

In terms of similitude in temperature change, and stability of density current, Stolzenbach and Harleman propose

$$G = X_r^{1/3} \quad (3-8)$$

For  $X_r = 220$ , Eq. (3-8) gives  $G = 6.0$ . For the range of Reynolds numbers associated with flow in the incised channel, and for trial-and-error assumed values of  $Y_r$ , the scale ratio for  $f$  potentially could be in the approximate range  $f_r \approx 0.10$  to  $0.25$ . The small value for  $f_r$  is estimated using Eq. (3-5), whereas the larger value is assessed as a reasonable upper bound for  $f_r$ . In accordance with Eq. (3-7),  $G$  should be 10.0 to 4.0.

For the present hydraulic model a vertical scale of  $Y_r = 40$  was selected, giving a geometric distortion factor  $G = 5.5$ . This value of  $Y_r$  was judged to be a practicable compromise between the needs to adequately model flow depth for flow stability and measurement, as well as the constraints on area to be encompassed and on availability of cold water. The value is within the range used by prior studies involving hydraulic models of thermal processes in large water bodies; e.g., Stolzenbach and Harleman (1967) used  $G = 3$ ; Nystrom (1981) used  $G = 5$  ( $X_r/Y_r = 200/40$ ); Zeng et al. (2002) used  $G = 10$  ( $X_r/Y_r = 1200/120$ ).

The comprehensive approach described in Section 1.3 was developed to address the concern about possible reduction in the quality of the results from the model. That approach involved the use of two testboxes that were located at one corner of the hydraulic model as indicated in Figure 3-2.

### 3.4 Model Construction

The model comprised an enclosed, watertight, and thermally insulated concrete-block box that contained the modeled area indicated in Figures 3-1 and 3-2. The set of photographs contained in Appendix A illustrates the several stages of hydraulic-model construction, and illustrate how the model was constructed. The photographs give useful insights into the model's complexity, and the care taken in constructing the model so that thermal conditions could be controlled. A broad overview of the constructed model is given by Figure 3-3.

Table 3-1 relates elevations and areas in the lake and the model. As mentioned subsequently, the elevations and overall dimensions used for the hydraulic model are based on data provided by PG&E.

Table 3-1. Major physical dimensions of the Lake Almanor and the hydraulic model  
( $X_r = 220$ ,  $Y_r = 40$ )

Characteristics	Prototype Dimensions*	Model Dimensions
Elevation	<ul style="list-style-type: none"> <li>• Water depth near Prattville Intake = 82ft; EL. 4500.2ft (normal max) – EL. 4418.2ft.</li> <li>• EL. 4500.2ft (normal max). The invert of the Intake is at EL. 4410ft; depth = 90.2ft</li> <li>• Max. prototype depth <math>\approx</math> 95 to 100ft. (including margin for extreme events)</li> </ul>	Max depth is 2.5ft
Surface area	6 square miles (3.12 miles $\times$ 1.9 miles)	3,375ft <sup>2</sup> (75ft $\times$ 45ft)

\* Elevations are relative to PG&E datum. PG&E and USGS data are related using the equation:  
USGS elevation (ft) = PG&E elevation (ft) + 10.2 ft

### 3.4.1 Bathymetry

The bathymetry of the modeled area was constructed using a bed of gravel and sand, covered with a smooth concrete cap, 1.5in thick. The model conformed to the lake bathymetry data shown in Figure 3.4, and as provided by the data sources listed in Table 3-2. Figure 3-5 gives additional bathymetry data for the region immediately around the Intake. Those data, obtained in the summer of 2002, were needed to aid in forming the lake bathymetry around the Intake.

The bathymetry data were transcribed to bathymetry templates that were used for constructing the model. Detailed attention was given to the bathymetry details along the incised channel and near the Intake, as indicated in Figures 3-6 and 3-7, respectively.

The components of the model of Prattville Intake were built from Plexiglas, fiberglass and metal. The external dimensions of the model intake, the entrance opening of the intake, and the immediate vicinity of the intake were built at the same horizontal and vertical scales as used for the entire model: i.e.,  $X_r = 220$  and  $Y_r = 40$ . The intake's trashrack and other appurtenances were not replicated in the model.

Plywood templates and steel rods were used to set the bathymetry elevations and form the bathymetry contours in the model (see Appendix A). Regions of substantial changes in bathymetry were formed with the aid of plywood templates. Such regions included the incised channel between Prattville Intake and the lake's Hamilton Branch, and the replicated shoreline of the lake. The space between the templates was filled with compacted gravel and sand. For the remaining area of the model, steel rods were used to benchmark bathymetry elevations. The rods were positioned in a variable grid arrangement (from  $1 \times 1 \text{ ft}^2$  to  $4 \times 4 \text{ ft}^2$ , in model dimensions) depending on the local slope of the model.

The following data provided by PG&E were used in establishing the model's bathymetry:

- Figure7\_plus.dwg (cross-sections along the Hamilton incised channel)

- Figure10.dwg (cross-sections along the Hamilton incised channel)
- 1927Contour\_a.dwg (to establish the  $1 \times 1\text{ft}^2$  to  $4 \times 4\text{ft}^2$  grid elevations)
- The near-intake data collected by PG&E in summer 2002

Precise bathymetry measurements of the submerged braided channels on the bed of the Chester branch were unavailable for use in model construction. According to PG&E, soundings previously conducted in that area (Fleenor, 2002) were insufficient for defining features of the braided channels. Further, it was decided that there was no need to replicate the braided channels, as their amplitudes (in depth and width) would be negligibly small in the model.

The focal point of the model was the Prattville intake (see Figure 3-8). The area around it was carefully replicated using as dense a spacing as was allowed by the size of the model scale templates. To aid flow visualization, the near-field area was overlaid with the local coordinate grid that related the Intake location to east-north orientation, and that helped in estimating length dimensions around the Intake (Figure 3-8).

The configuration of water-supply lines throughout the hydraulic model is illustrated in Figure 3-9, which also indicates something of the complexity of the model's construction. A further view through the model is provided by Figure 3-10, which reveals the composite nature of the model bed and sidewalls. Figure 3-10 shows how the cold-water filling lines were placed in the model. The channel-cooling lines placed along the incised channel were never used, though were included in the model for use if needed.

Table 3-2. Sources of bathymetry data used in constructing the hydraulic model.

Area	Data Source
Big Spring Area (2001)	Big_Spring.dwg AutoCAD plan view drawing with layers showing; March 2001 Bathythermograph locations at Big Spring Cove Bathymetry transect approximate locations for lines labeled 5, 10 and 15 Big_spring.xyz ASCII
Prattville Intake Area (1992, 2000, 2002)	'Bathymetry_Prattville.tiff' (1992) - Underwater Resource Inc. Figure7.dwg Elevation contour map showing Prattville Intake channel (2000) Figure7a.dwg Same as Figure7 with Prattville Intake included (2000) Figure7_plus.dwg Same as Figure7 plus each elevation data point printed (2000) Intake 1-5.xyz ASCII csv files with data displayed in Figure7_plus.dwg Figure10.dwg Elevation contour map showing old riverbed leading to Prattville Intake area (2000) csv file with XY and depth data for bathymetry transects 5, 10, and 15 Additional survey in the near intake area (summer, 2002)
Canal 1-4.xyz	ASCII csv files with data used for contouring figure10 1. data for lines 57-40 2. data for lines 39-25 3. data for lines 24-8 4. data for lines 7-4
Lake Almanor (1927)	1927Contour_a.dwg Digitized contours from 1927 map showing transect locations for figure 10 and east section of lake bathymetry transect location and printed data EASTLAKE.xyz
Lake Almanor and Butt Valley Reservoir (1985)	Reconnaissance bathymetric surveys conducted with Raytheon DE-719B portable survey echo sounder (data reported in Woodward-Clyde Consultants 1985)

### 3.4.2 Temperature-Control System

Two temperature-control, or heat-exchange, concerns had to be considered in operating the model:

1. Heat gain through the model's bed and sidewalls; and,
2. Heat loss or gain between air above the model and water contained in the model.

Because the model needed to maintain water at prescribed temperature distributions for several hours, the model's bed and sidewalls were insulated thermally to practically eliminate heating of the lower layer (hypolimnion) of water in the model. Insulation was provided by means of polystyrene foam sheets placed as indicated in Figure 3-10.

The large range of air temperatures that potentially could occur in IIHR's Model Annex building over the duration of the project posed a concern for maintaining the temperature profile in the epilimnion. Though the building is heated during winter, air temperatures in the building potentially could range from about 30°C in Summer to about 7 to 8°C during winter. Such a large range could affect the temperature of water in the epilimnion. Initially, it was thought that a light framework supporting plastic sheets (a form of thermo-dome) would be needed to enclose the air above model so as to protect the model free surface against thermal losses to ambient (evaporation and thermal conductivity). Additionally, it was thought that air-conditioning and heating would be needed to control the ambient air such that the epilimnion remain in thermal equilibrium (same temperature) throughout model operation. However, early tests with the model showed that water temperatures held sufficiently steady such that an insulation dome was not necessary. Only during tests conducted on unusually hot days did the upper layer of water warm to temperatures above those specified for the epilimnion.

In planning the procedure for model operation, it was recognized that the model's bed and bed sub-structure would have to be cooled down to the lower layer temperature of the water column; otherwise, the bed would add heat to the water layer. Moreover, there was a concern that the model's bed may warm during model operation, and thereby adversely

affect the temperature distribution of the modeled water body. Therefore, two sets of chiller pipes were embedded in the concrete cap of the model's bed, as illustrated in Figures 3-9 and 3-10; Figure A-9 of Appendix A also shows the arrangement of chiller pipes. The chiller configuration comprised several separate cooling coils fed with cold water drawn from the refrigerated ice tank. One configuration was placed along the bed of the incised channel. The second configurations comprised a loop placed in the region of the Chester branch. A series of valves and thermometers placed in each circuit enabled control and monitoring of chilled water flow in each circuit.

#### 3.4.3 Water Flow Control and Distribution System

Water inflow to the model was controlled using a system of inlet pipes and distribution manifolds. The system facilitated controlled inflow of water at several temperatures. It was more elaborate than in actuality proved necessary for operating the model.

Warm water entered through a manifold formed around three sides of the model (Figure 3-9). The inlet pipes were fitted with orifice meters calibrated to deliver the prescribed discharges, and were fitted with valves to provide the requisite inflow distributions during model operation. Each manifold comprised two inlet pipes whose openings could be adjusted to produce desired distributions of inflow (including local flow direction) over pre-determined depths of flow.

Cold water entered the model through an arrangement of ten riser pipes (pop-ups) placed in the floor of the mode (Figure 3-10). The riser pipes also served to replenish the cold water in the model during operation of the model. During early tests with the model it was found that only eight far-field risers along the model's central axis needed to be used.

Because the sources of cold water entering Lake Almanor were not well defined at the time the model was built, it was thought prudent to include a system of perforated pipes placed along the centerline of the incised channel. If necessary, the pipes could feed cold water into the incised channel. However, before commencement of testing with the model, it had been ascertained that cold water predominantly originated from springs

located in the Hamilton Branch, and that it would not be necessary to feed cold water through the bed of the incised channel. Consequently, this facility of the model was not used.

### **3.5 Procedure for Temperature Profiles**

A key aspect of the model's success was the ability to establish the requisite profiles of water temperature such that the model simulated the water-temperature stratification of water in Lake Almanor during summer. Considerable trial-and-error testing was needed to develop the process for producing the temperature profiles associated with the temperature stratification occurring in the lake during June, July, and August.

Water inflow to the model was supplied in batches, each at its pre-determined temperature. Three sources of water were used to obtain the most complex stratification scenarios. The source of cold water used for the model was the 4,600ft<sup>3</sup> ice basin in IIHR's refrigerated laboratory, which adjoins IIHR's Model Annex Building. The availability of this volume of cold water was a critical factor enabling the hydraulic model to simulate the temperature profiles. A buffer-water reservoir was provided by the large 19,760ft<sup>3</sup> underground reservoir located beneath the Model Annex. A supply of warm water was provided from a 64,150ft<sup>3</sup> reservoir located beneath IIHR's East Annex. Water in that reservoir was heated using two 500,000 BTU/hr gas-fired water heaters.

The chief considerations in establishing the temperature profiles were as follow:

1. Slow feeding to avoid shear formation, water mixing, and layer breakup;
2. Pre-establishment of the proper temperature for each water source in order to account for temperature modifications during transport of the water to the model and feeding of the layers; and,
3. Acquiring an understanding or feel for the model's response to water feeding, heat exchanges between air and the model's water surface, and between water and

the model's boundaries, and the temporal durability of the temperature gradient established in the model.

One of the procedures for establishing a desired water-temperature profile in the model is described below, and is illustrated by the sequence of sketches in Figure 3-11:

1. Dry bed. To achieve repeatability of profiles, each experiment had to begin from the same initial condition (Figure 3-11a). All procedures started with the model empty (dry bed) and at ambient air temperature;
2. Cold-water feeding. Cold water (water temperature at about 1°C) was discharged slowly into the gravel bed beneath the model's concrete cap (Figure 3-11b);
3. Bed cooling and excess water removal, followed by a waiting time to chill the bed (Figure 3-11c). The cooling time differed from temperature profiles, and had to be adjusted in response to seasonal variations in ambient temperature conditions;
4. Buffer-layer feeding of water temperature at 16°C to 18°C (Figure 3-11d). The feeding could be done quickly, as there was no other layer present in the model;
5. Warm-layer feeding of water temperature at 25°C to 27°C (Figure 3-11e). From this instant on, the feeding of water occurred at very low velocity, with repeated inspection of the flow appearance and close monitoring of the temperature in the layer. Injection of the layer is made through the pop-ups, distributed along the centerline of the model; and,
6. Final cold-water feeding (Figure 3-11f). The cold water used to establish the hypolimnion was discharged slowly into the model, in a carefully monitored manner to achieve the desired temperature profile.

The water-filling procedures for the three months involved the three source of water, though mixed in differing amounts.

The target water-temperature profile in the model was obtained using water feeding, a procedure that differed for each temperature profile sought; i.e., for June, July, and August. The manner of feeding the water layers into the model was developed during preliminary experiments in both the model and a special purpose test tank. The exact thickness of each water stratum fed into the model, overall rate of inflow, and the procedures to enable the introduction of water into the model all had to be worked out during numerous trial-and-error iterations that led to precise feeding recipes as illustrated in Figure 3-12 for the temperature profiles prescribed for June condition.

The temporal evolution of the temperature during the feeding of water to attain the August profile is shown in Figures 3-13a-c. After obtaining the water-temperature profile in the model, small adjustments of inflow and outflow were made, as were adjustments to the cooling system and cold-water inflow to maintain the profile. Due to the model's large volume, it was found that there was no need to add warm water in the model. The drop in the water level during typical experiments with the Prattville intake did not exceed 1ft in prototype dimension. Most of the cold water fed in the model could be supplied through the incised channel crossing diagonally the model, then dispersed laterally over the model bed.

The stability of the water-temperature profile in the hydraulic model during each series of tests meant that additional water-tuning efforts operations were not needed during testing. The profiles remained stable up to 4 hours of testing, and the bed did not warm during the experiments (Figure 3-13). Figures 3-14a,b show examples of temperature profiles obtained in the model in simulating the July and August conditions of Lake Almanor. The profiles are shown in the format displayed by the data-acquisition interface (Labview) used for each test series.

### 3.6 Instrumentation

The model was instrumented for extensive monitoring of flow and temperature variables. Inflows, outflows, temperature at inlets/outlets, and temperature distributions in the model were measured and recorded continuously during model operation. The measurements were taken at locations where they could be compared with water temperatures in the numerical model and Lake Almanor. Extensive flow visualization was undertaken of water movement in the vicinity of the Prattville intake and along the Hamilton Branch incised channel. The layout of the measurement system deployed in the model is indicated in Figure 3-15. A broad overview of the fully instrumented model ready for testing is given by Figure 3-16.

The following items of instrumentation were used to control water flows and temperature and to document qualitatively and quantitatively flow characteristics in the model:

1. Water discharge: Water discharges were measured using precision orifice plates or Venturi contractions fitted to the flow-supply pipes to the model and fitted to the withdrawal pipe used in the simulated Intake. The orifice-plate and Venturi meters were connected to precision manometers for measurement of headloss associated with flow through the meters, whence direct calculation of discharge. The resolution of the differential manometer scale was  $10^{-3}$ ft, resulting in a typical flow measurement precision of 0.02cfs, or 3.4% of  $Q_0$ .
2. Water depth: Water levels, and overall depths, were measured using point gauges mounted on instrument beams placed over the model. The resolution of the point gauge scales is  $10^{-3}$ ft in the model, corresponding to about 0.5inch in the lake;
3. Temperature: The following arrangements were used:
  - (a). Eight, analog, precision thermistors mounted on a vertical support comprised a thermistor chain (see Figure 3-17). The thermistors assembled in the chains (for a maximum water depth of 1.5ft in the model) were positioned at variable

elevations depending on the elevation and gradient of the thermocline for a specific month. Temperature profiles were collected using an automated data acquisition system which sampled each thermistor at pre-established (variable) sampling rates. Prior to the measurements the thermistors were calibrated using multiple temperature readings with high precision thermometers. Periodic checking of the calibration curves were made during the course of the experiments to ensure data quality. The thermistors were connected to digitizing boards connected to the data acquisition computer. The thermistor chains were located at benchmark positions related directly to positions in the numerical model and Lake Almanor, as shown in Figure 3-15:

- (b). The analog thermistors were positioned at selected sites of the inflows and outflow sections of the model, as well as in the water-supply lines. These thermistors played an important role in establishing the stratification in the model and controlling the dynamics of the model during operation.
  - (c). A temperature profiler (single thermistor positioned on a vertical traverse) was positioned in the vicinity of the intake. The thermistor enabled fast and flexible procedures for temperature-data acquisition across the flow region surrounding the model of Prattville Intake.
  - (d). Digital thermometers (with sampling time 1 to 2secs) were available for monitoring purposes outside the area of coverage of the thermistor chains.
4. Velocity measurements: Velocity measurements were taken simultaneously with the temperature measurements from the specialized platforms set in the vicinity of the Prattville intake (see Figure 3-15). Given the near-zero velocities dominant in the model (excepting within 3 ft away from the Prattville intake), the only reliable measurement methods were time-lapse photography and Large-Scale Particle Image Velocimetry (LSPIV). These image-based techniques have been extensively used by IIHR for qualitative and quantitative visualization in

modeling studies (Muste et al., 2000). However, it was found that their use was not particularly needed for the present study.

Time-lapse photography and stop-watch timing were used to determine the velocity magnitude in the incised channel. LSPIV measurements could have been used as a quick means for obtaining whole-field measurements of flow around the intake and its erstwhile modifications, or to determine velocities in the water column. Only tentative use of LSPIV was made for this purpose;

5. Flow visualization: Flow visualization was one of the key experimental procedures used to characterize the flow characteristics in the original model and to assess the effect of the tested selective withdrawal structures. Different dye colors were consistently used for visualizing the upper water layers (red dye) and bottom water layer (blue dye). The visualization tests were recorded using two video recording units. A series of clips are provided along with the final project report to document the tested flow situations. Typically flow visualization entailed two steps:

- (a). soluble dye was dispensed through a wand to obtain overviews of flow paths and flow patterns in the model. Dye also was used to ascertain the progress of potential density-related currents as well as flow dispersion and mixing of water introduced at different temperatures into the model.

- (b). video camera records were made of flow paths and patterns revealed with dye. One video camera was mounted about 15ft above the model, and encompassed the intake vicinity in its field of view (see Figure 3-15). An underwater video camera was used to view and record diagnostic views of flow patterns, especially near flow-modification structures.

### **3.7 Model Operation**

Model operation entailed a sequence of steps that were prepared over several days prior to the test day. The large capacity of the cold and warm water sources necessitated two to three days recovery and conditioning time after the refilling of the reservoirs following the completion of each experiment. Consequently, no more than two experiments per week were possible. Once the sources of water reached the desired temperatures, the model was verified for initial conditions prescribed for the water-filling process (dry bed, proper environmental temperature, etc.), for readiness of the data acquisition system (thermistor positioning varied for the temperature profiles simulated), and for placement of the design modifications to be tested. Each test sequence for a test occasion was designed to ensure that the water-temperature profile and water surface elevation in the model did not depart considerably ( $\pm 5\%$ ) from the prescribed condition.

The time for model preparation ranged between eight to ten hours depending on the temperature profile to be simulated. When preparing for a test, log files were kept of all the relevant parameters necessary to obtain the targeted water condition (temperature of the water inflows, water surface elevation, bed temperature at three locations, environmental humidity and temperature).

A central element of the data-acquisition system was data-acquisition software developed by IIHR especially for collecting temperature data. The interface associated with the software is presented in Figures 3-18 through 3-20. The hardware and software of the assembly sampled each thermistor, applied the individual calibration equation, and stored the temperature measurements in a data file. The log temperature file covered both the preparation and operation time intervals of the model. Temperature profiles were collected at variable sampling rates; i.e., from 1 second to 1 minute with typical rates of 10 seconds. The in-house developed virtual instrument is based on LabView (LabView, 1996). The data-acquisition application has the five interfaces shown in Figures 3-18 through 3-20):

1. Information (specifications about the electronic components and their connection with the software);
2. Setup (information about the auxiliary files needed to be loaded for each specific modeling scenario);
3. Thermistor-chain temperatures (numeric, real-time display of the acquired temperature at all the 56 thermistors. Figure 3-18 shows the format;
4. Outlet temperature (graphic real-time display of the temperature at the three model outlets: Prattville intake, distorted and undistorted testboxes) – Figure 3-19; and,
5. Temperature-profiles graph (graphic real-time display of the reference temperature profile for the modeled scenario along with the temperature profiles at the six locations in the model). Figure 3-20 shows the format.

A pair of model photos showing the model at the beginning and the end of the water-feeding sequence is illustrated in Figures 3-21a,b. The data-acquisition hardware and software facilitated convenient control of the temperature both during model feeding and during the measurements. The model was considerably stable thermally and hydraulically, allowing operation within acceptable modeling specifications for as long as 3 to 4 hours. The steadiness of water flow conditions in the model, and outflow from it, during each test was assessed by monitoring the data-acquisition interface (Figures 3-19 and 3-10). Typically outflow temperature was tracked for over at least a 5-minute period before the outflow temperature was recorded. Any measurements or change of the tested structures during the experiments were made with great care to avoid disturbing the thermal stratification established in the model.

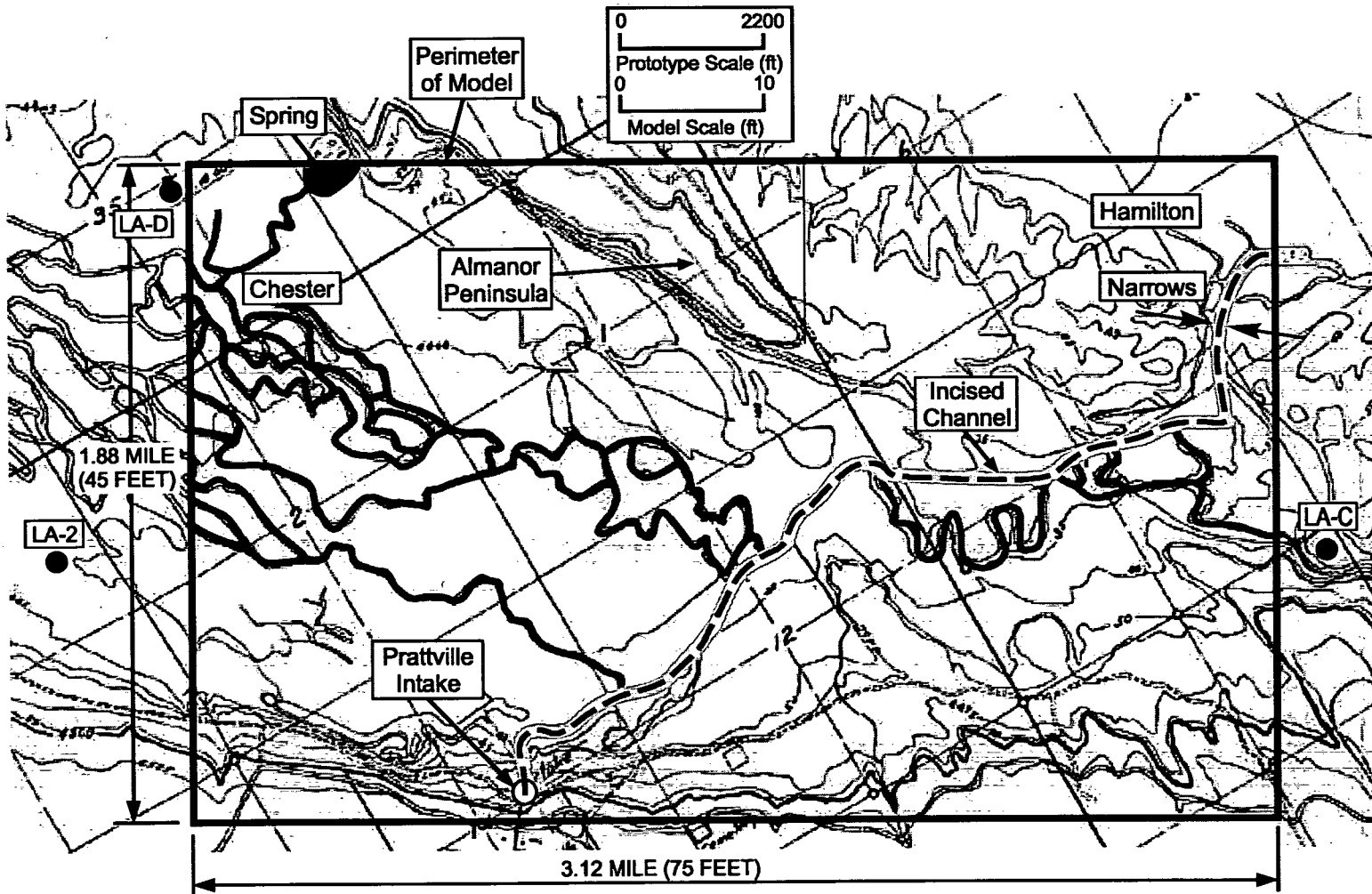


Figure 3-1. Area of Lake Almanor encompassed by model.

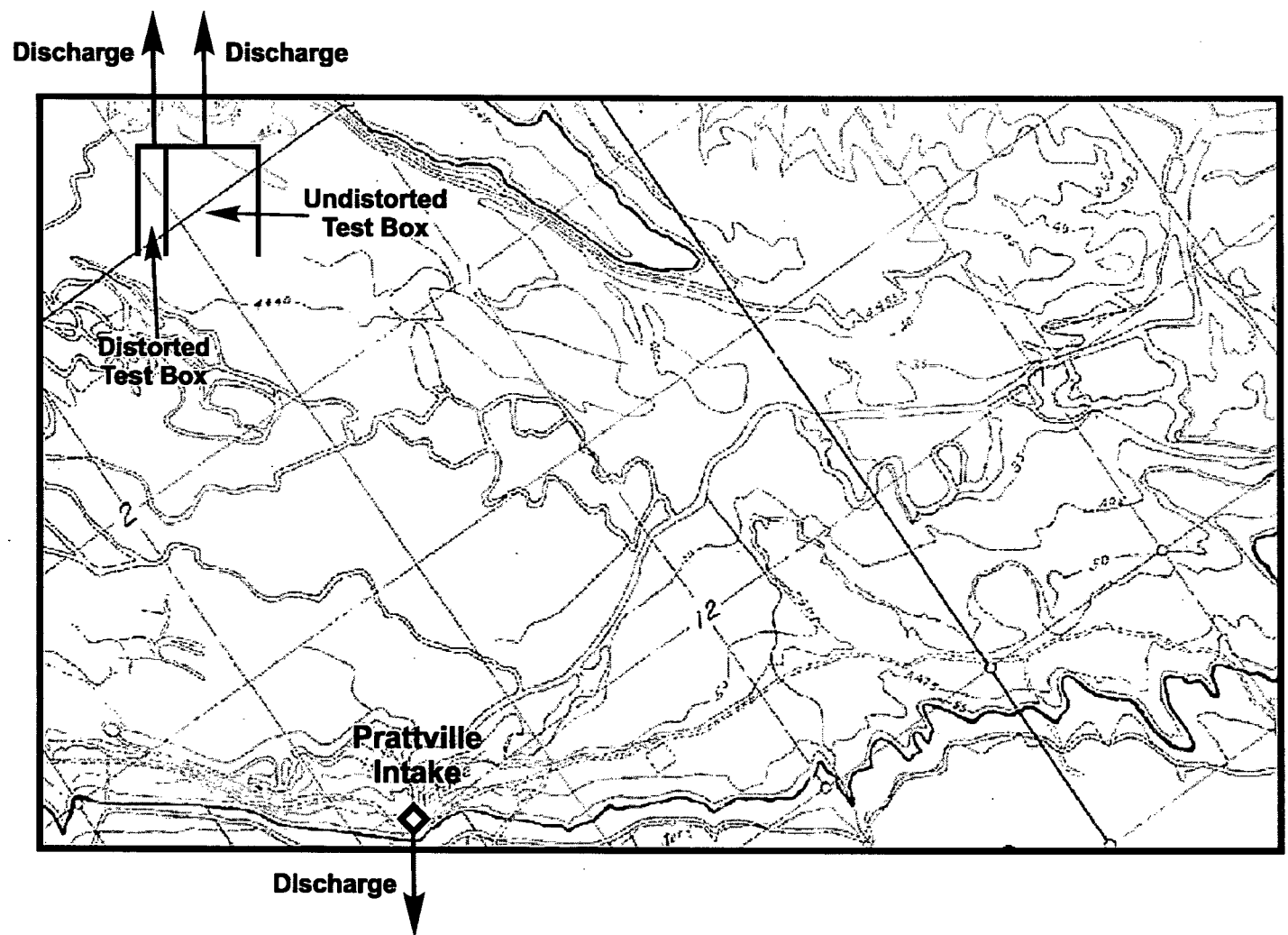


Figure 3-2. Location of the testboxes in the hydraulic model.

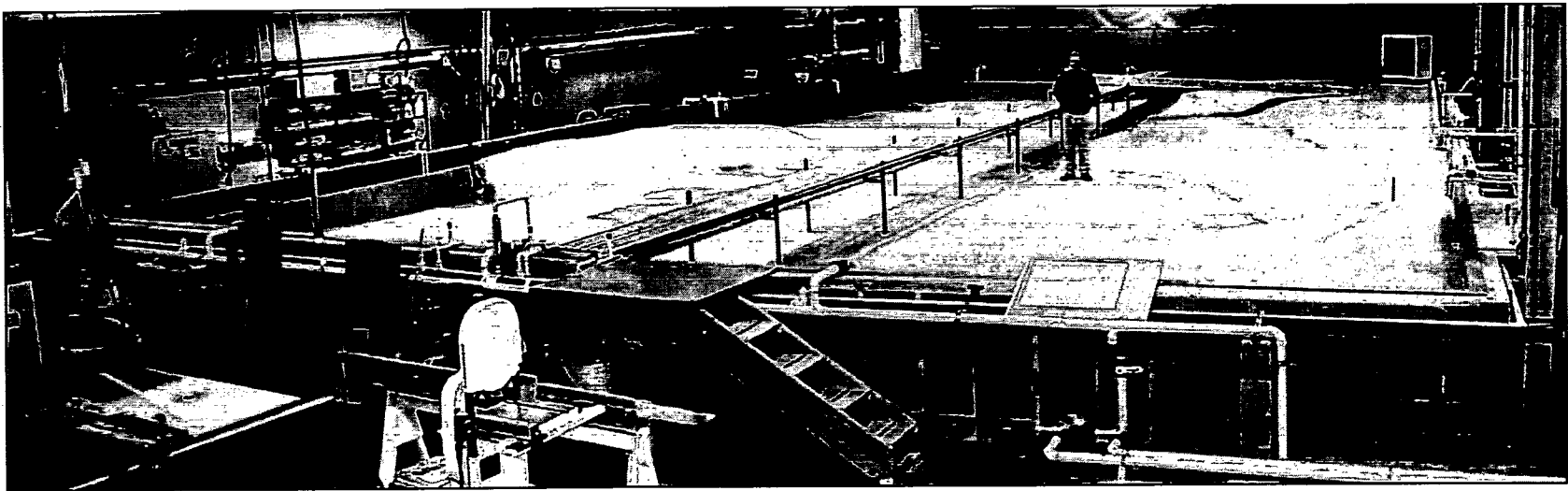


Figure 3-3. View of hydraulic model.

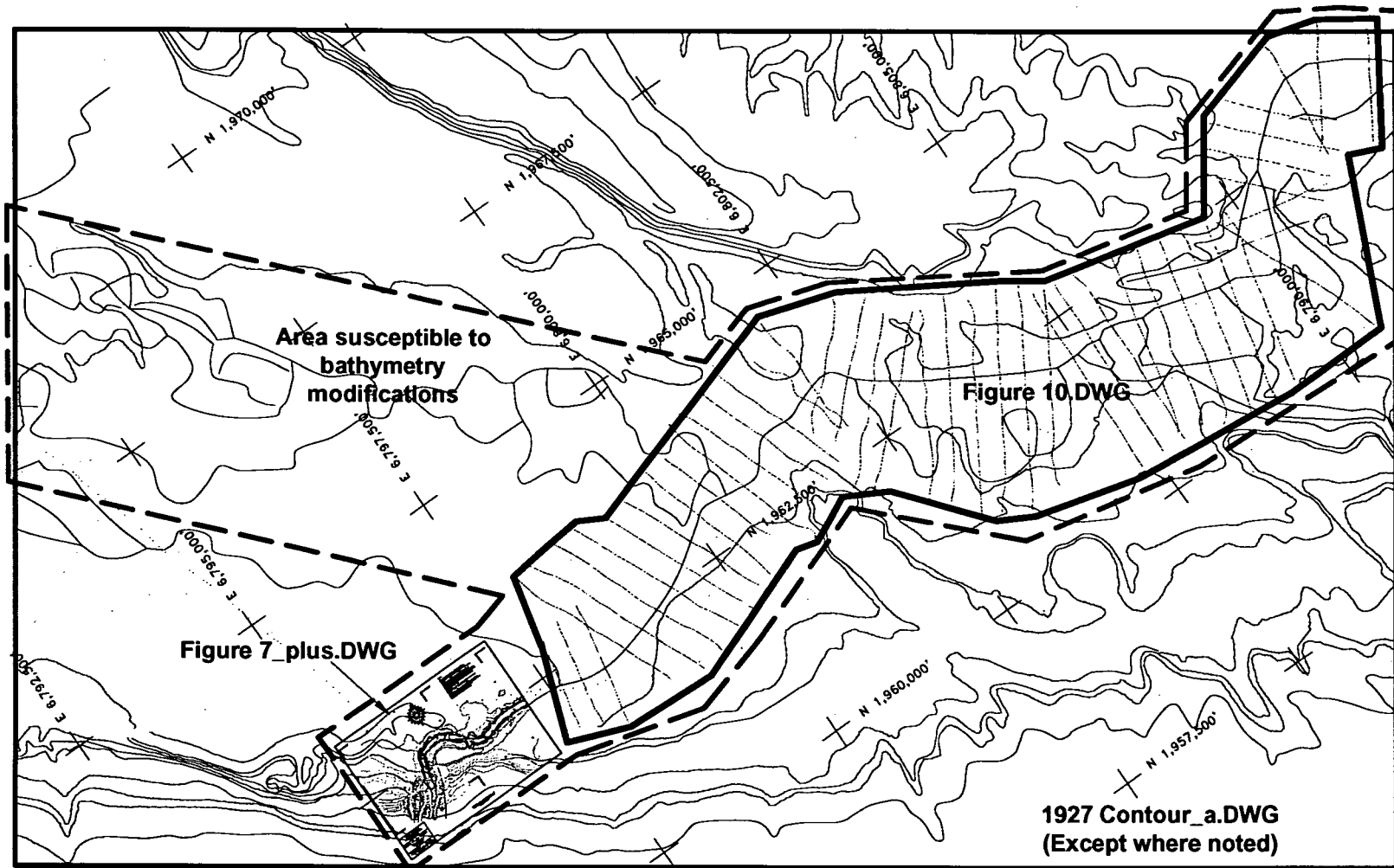


Figure 3-4. Sources of bathymetry information.

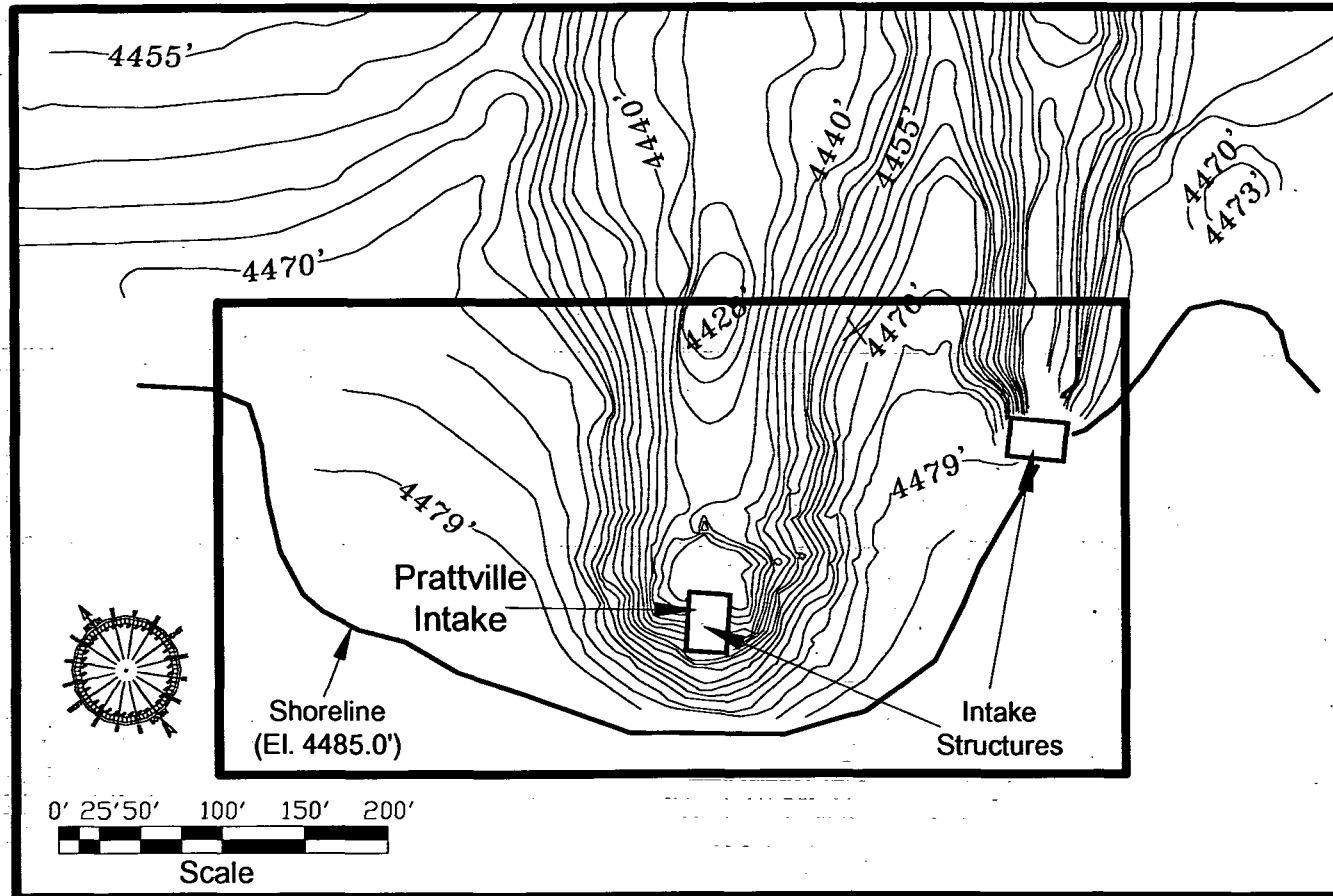


Figure 3-5. Supplemental bathymetry information obtained in filed survey, July 15, 2002 (data provided by PG&E).

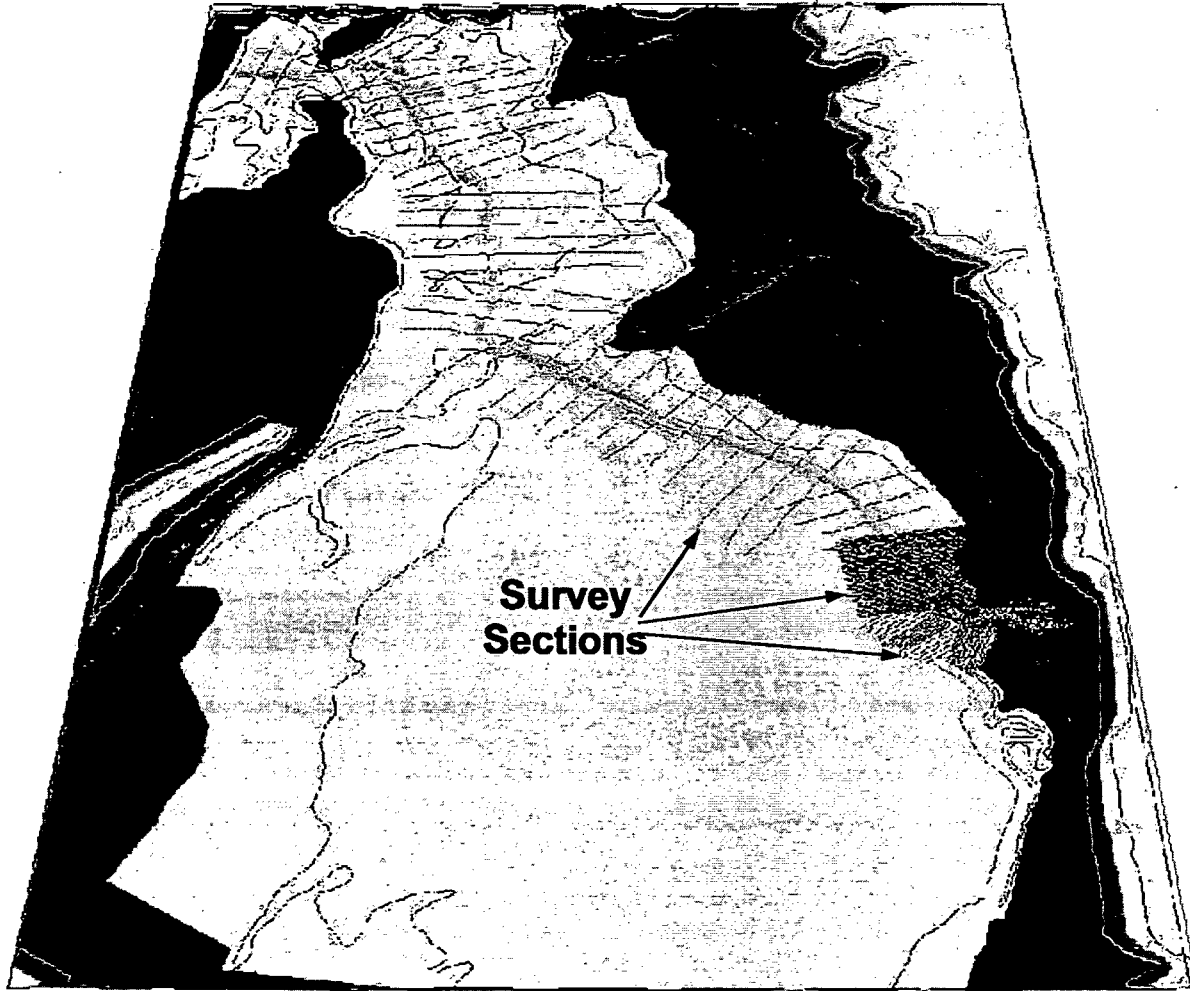


Figure 3-6. Survey sections for contouring the incised channel.

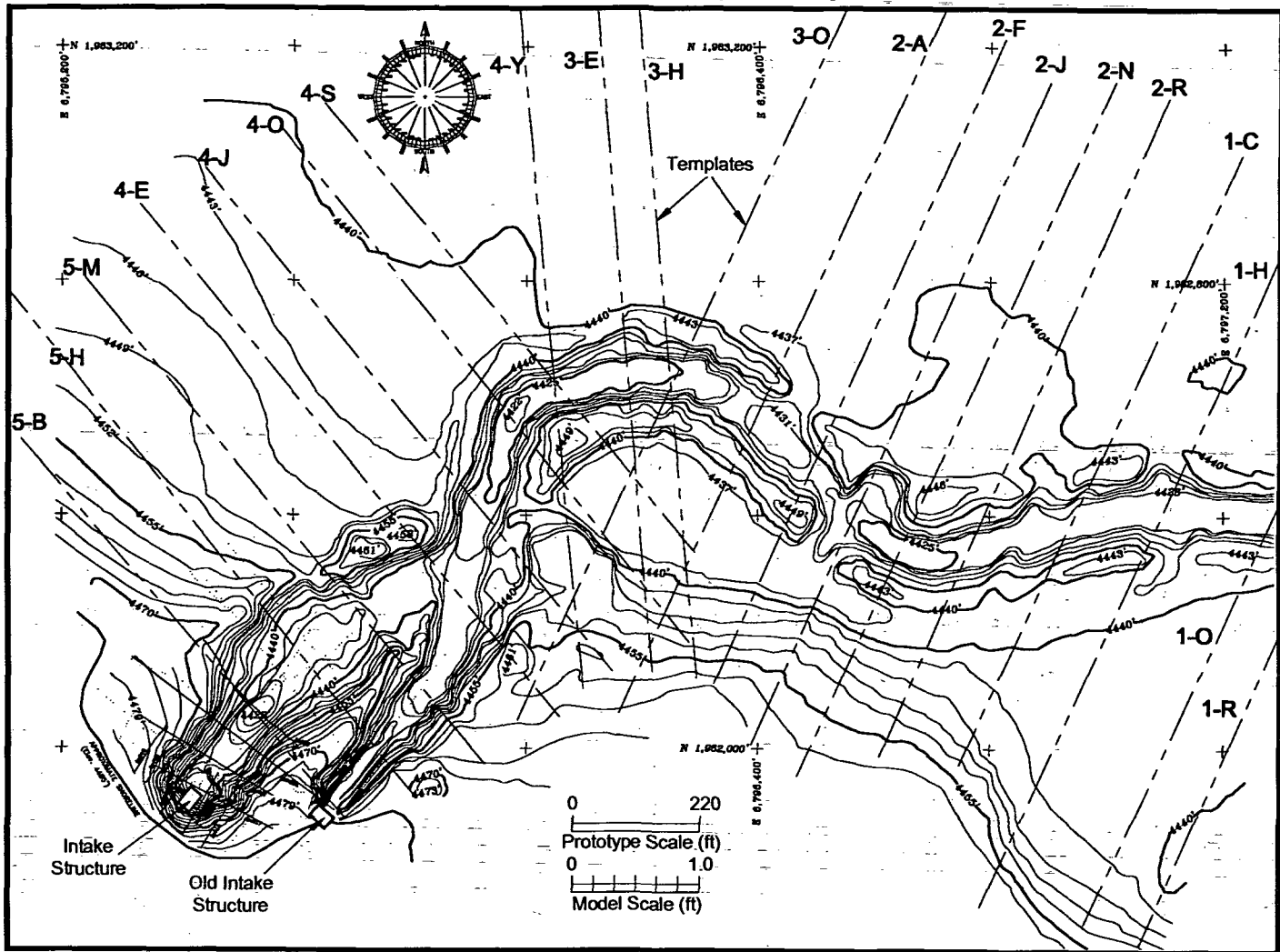


Figure 3-7. Bathymetry templates selected for constructing the area near the Intake.

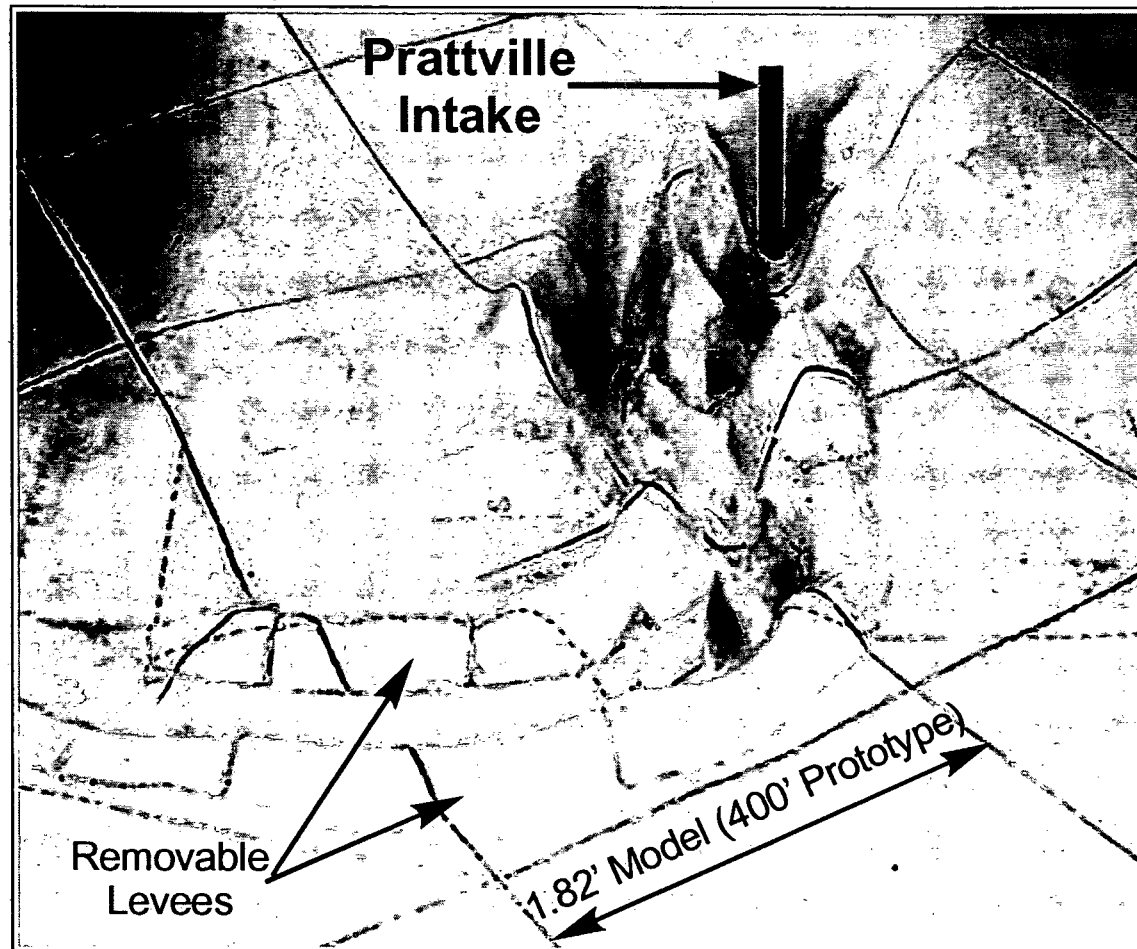


Figure 3-8. Model bed topography near Prattville Intake. Grid on bottom represents a 400 ft by 400 ft prototype grid.

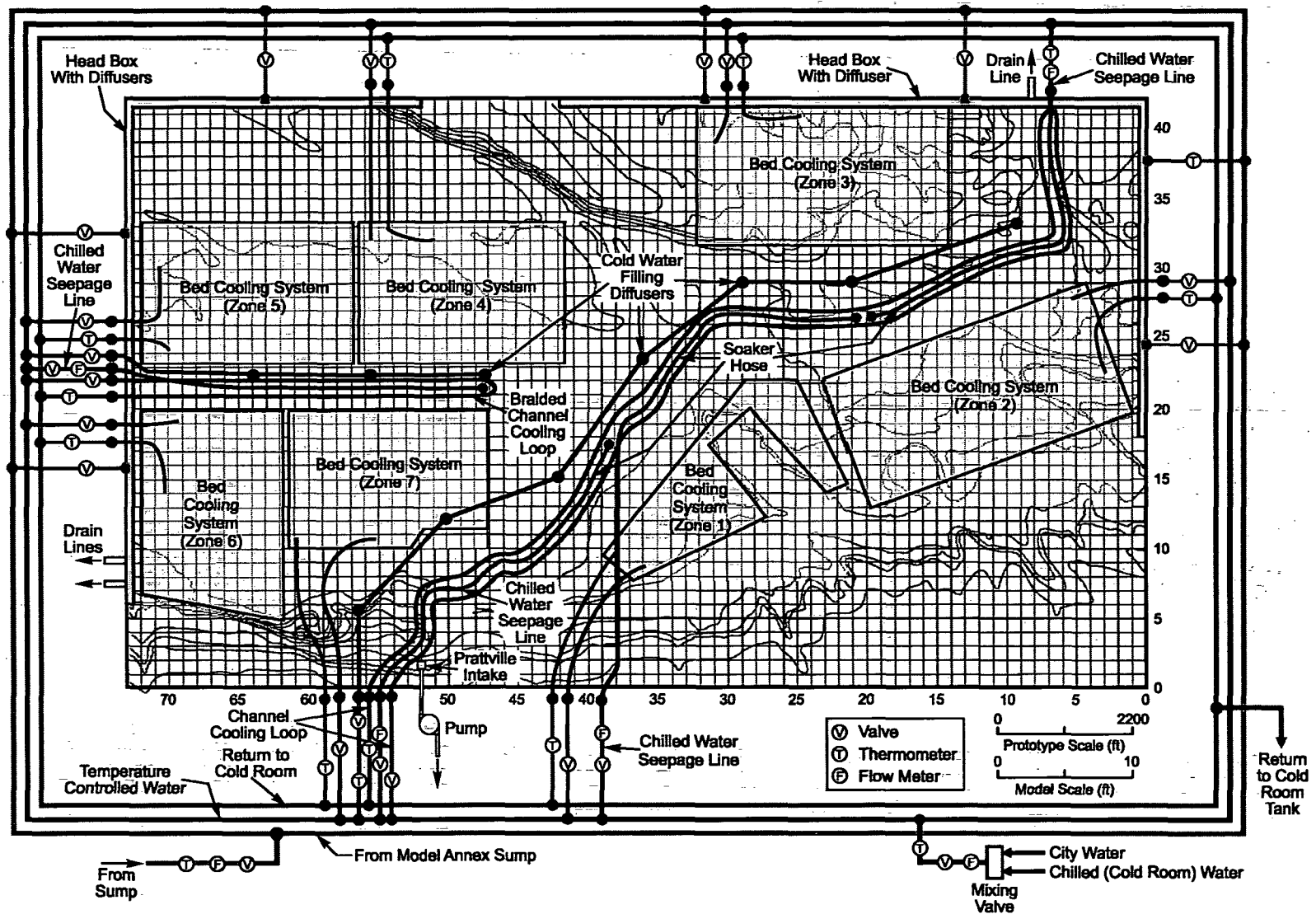


Figure 3-9. Layout of the water lines in the hydraulic model.

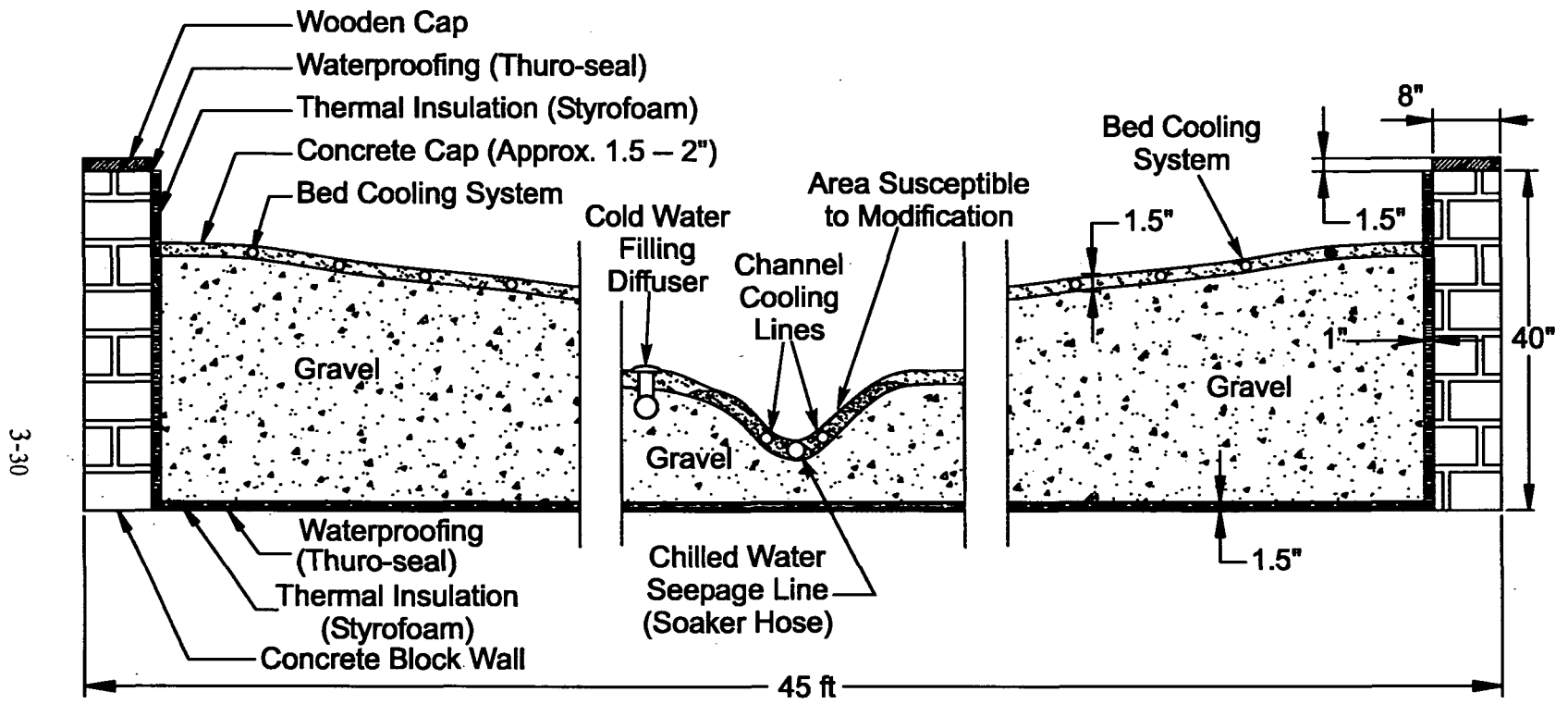


Figure 3-10. Cross section through the hydraulic model.

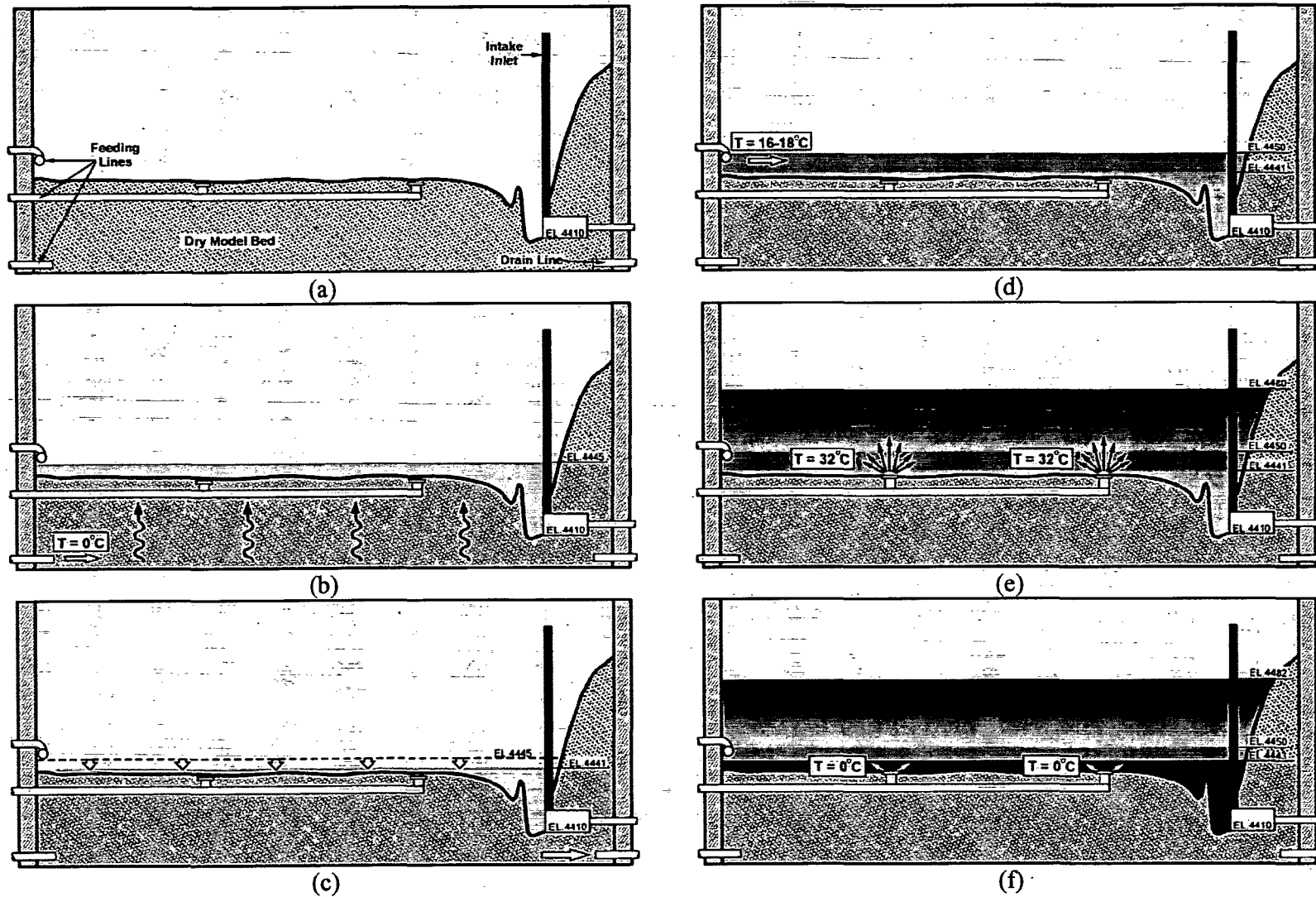


Figure 3-11. Typical sequence for attaining prescribed water temperature profiles in the model: (a) dry bed; (b) cold-water feeding for bed cooling; (c) removal of excess water; (d) buffer-layer feeding; (e) warm-layer feeding; (f) final cold-layer feeding.

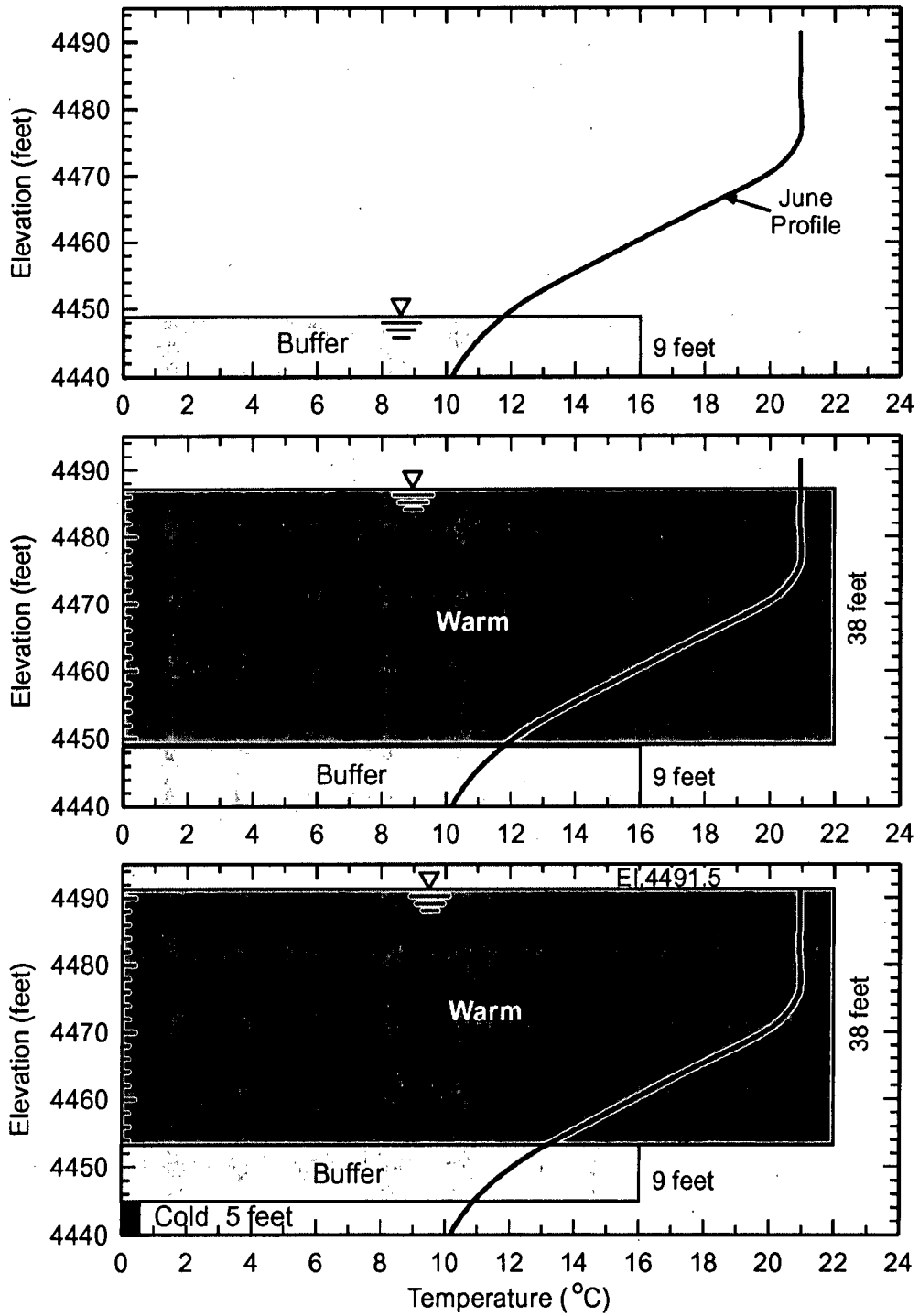
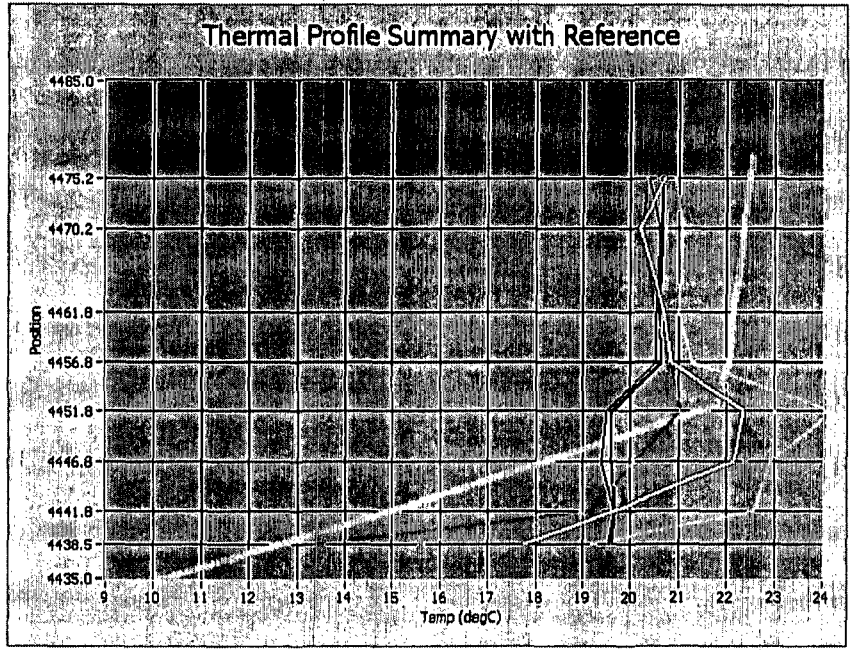
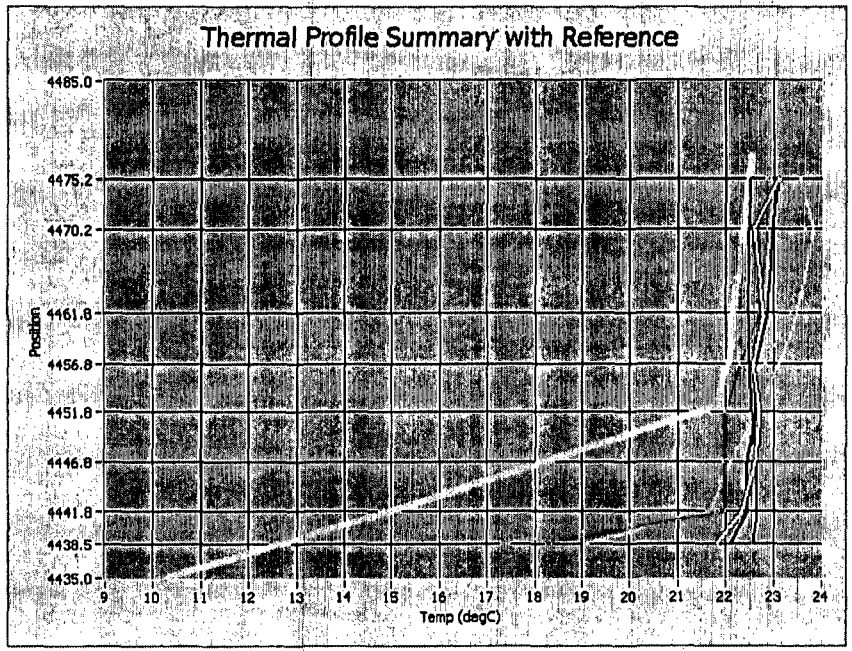


Figure 3.12. Development of June condition temperature profile.

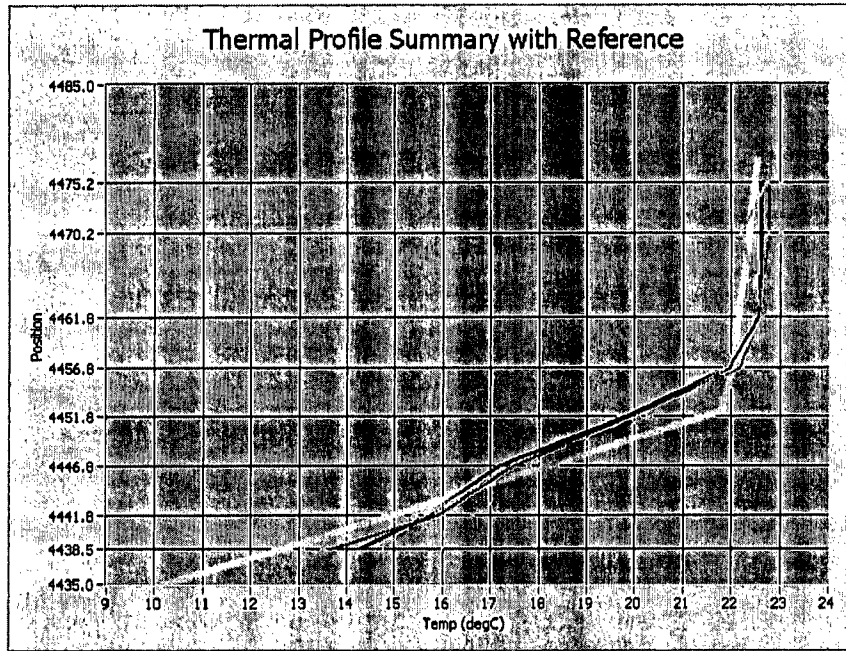


(a)



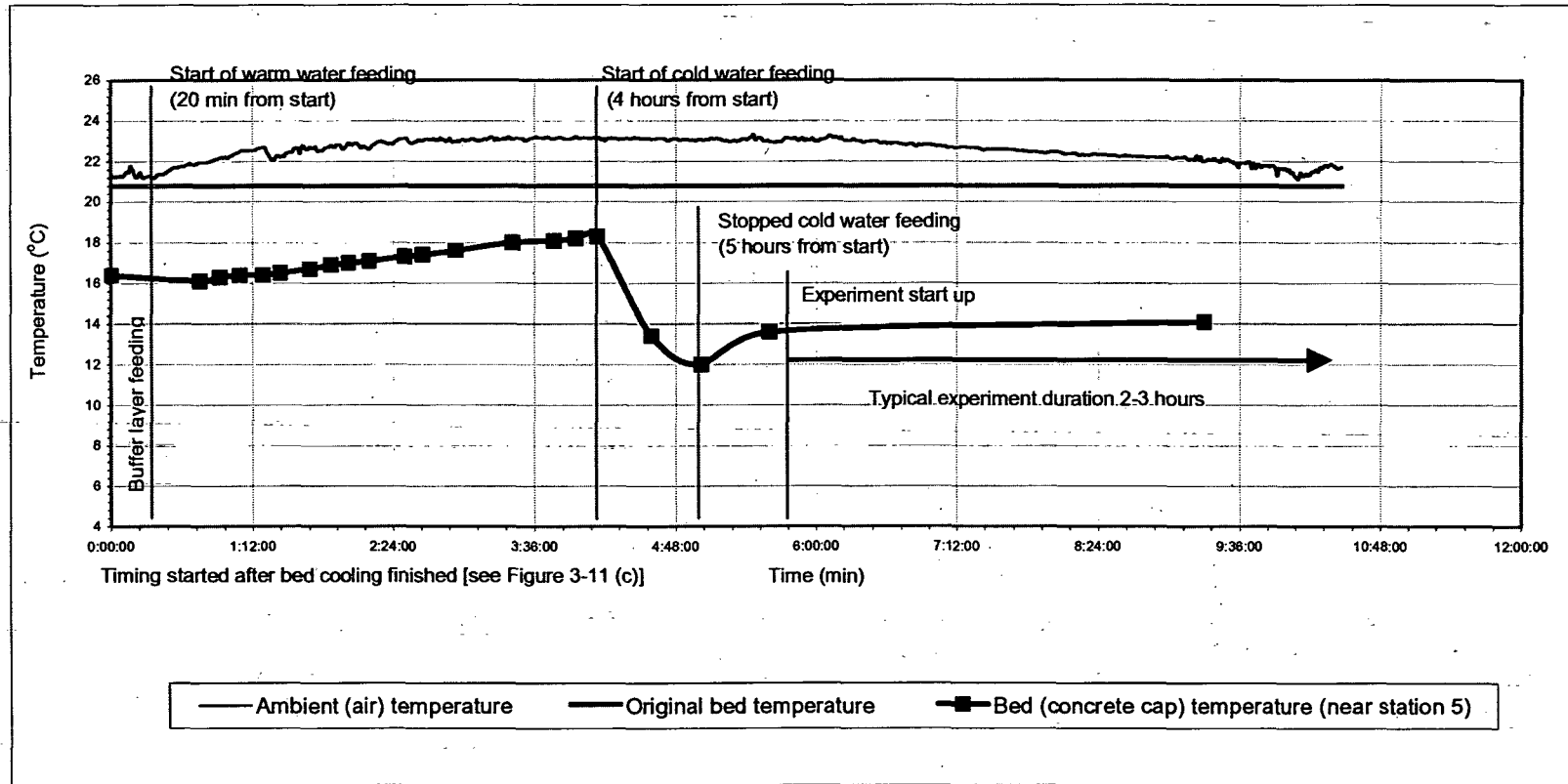
(b)

Figure 3-13. Temperature monitoring during water feeding: (a) buffer-layer feeding; (b) at the end of the warm-water feeding.



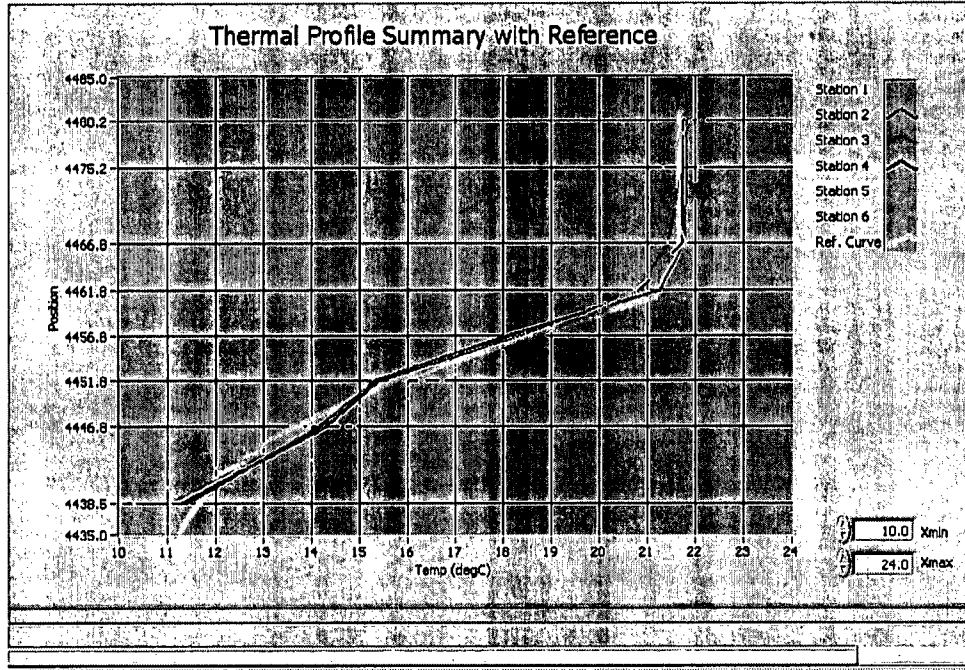
(c)

Figure 3-13 continued. (c) At the end of cold-water feeding (final profile).

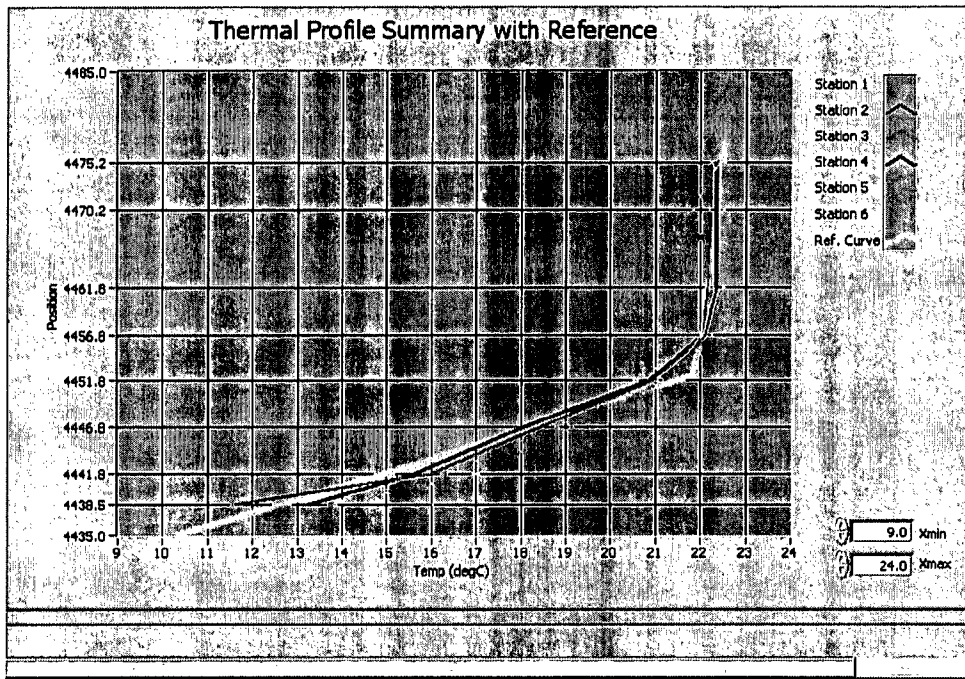


(d)

Figure 3-13 continued. (d) Temperature variation of bed (concrete cap) during model feeding and operation. Also shown is the ambient air temperature variation.



(a)



(b)

Figure 3-14. Samples of water stratifications attained in the model (orange profile is the field reference data): (a) July; (b) August.

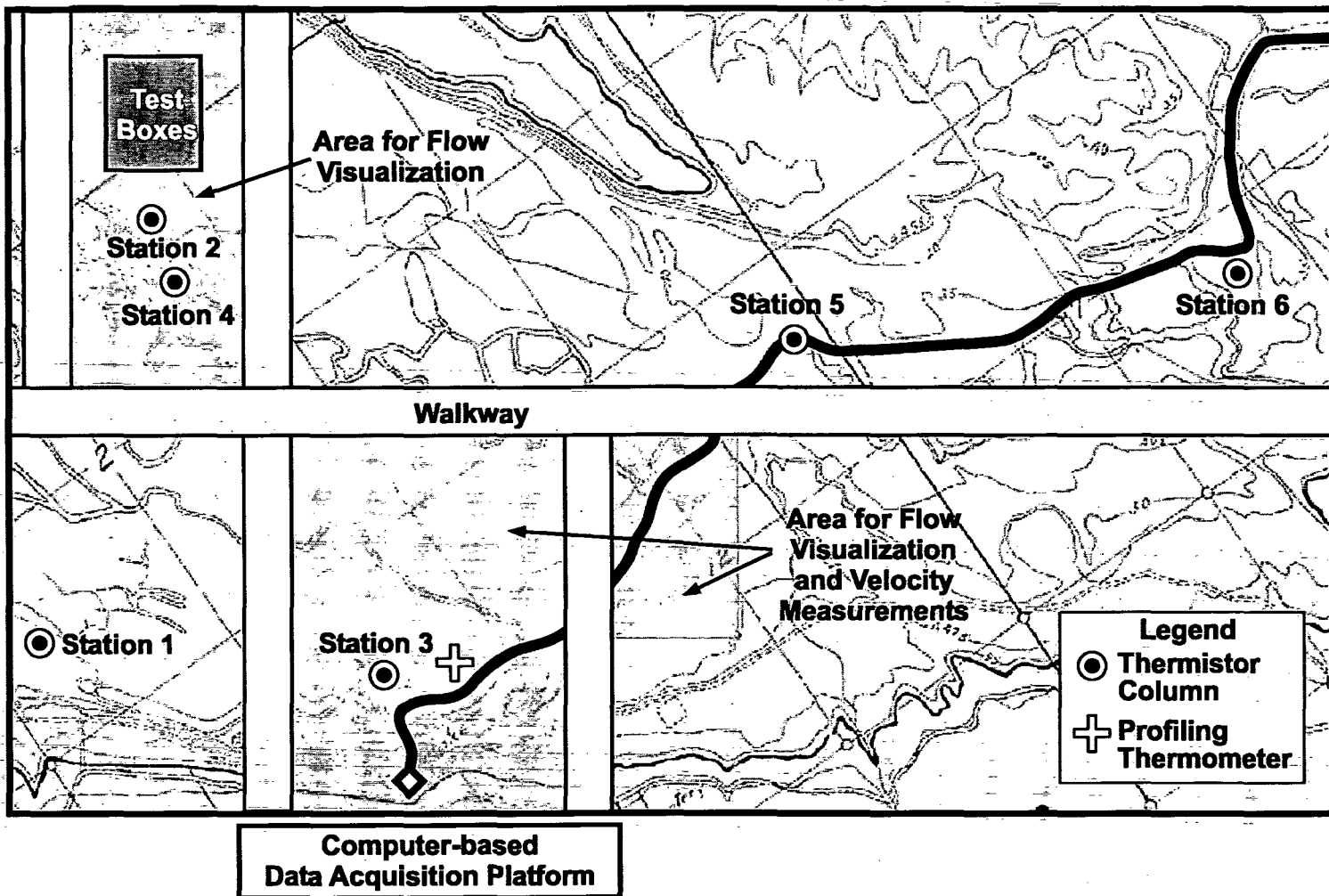
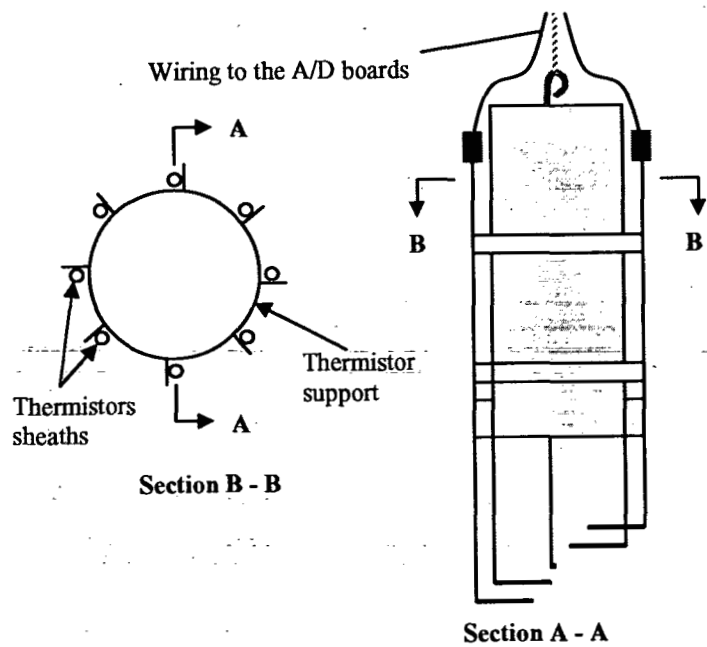


Figure 3-15. Layout of measurement system.

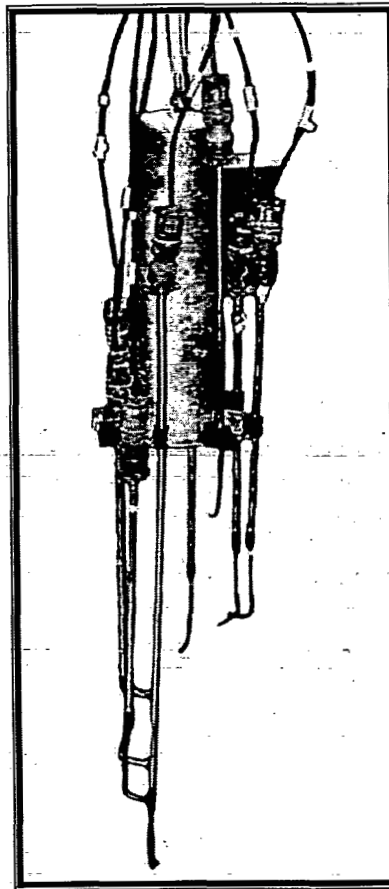


(b)

Figure 3-16. View of fully instrumented model.



(a)



(b)

Figure 3-17. Thermistor chain arrangement: (a) schematic; (b) photograph.

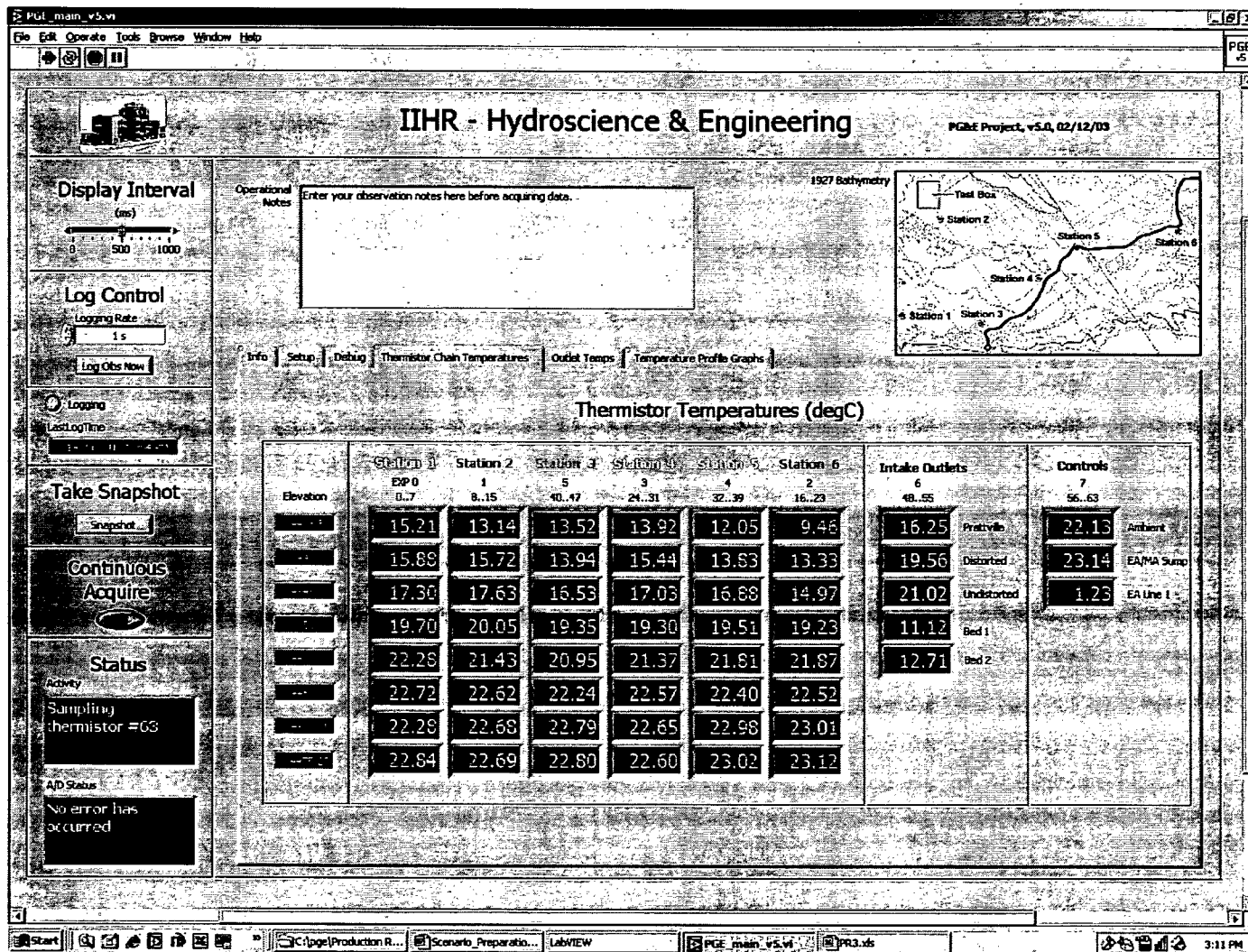


Figure 3-18. Interface for thermistor-chain temperatures.

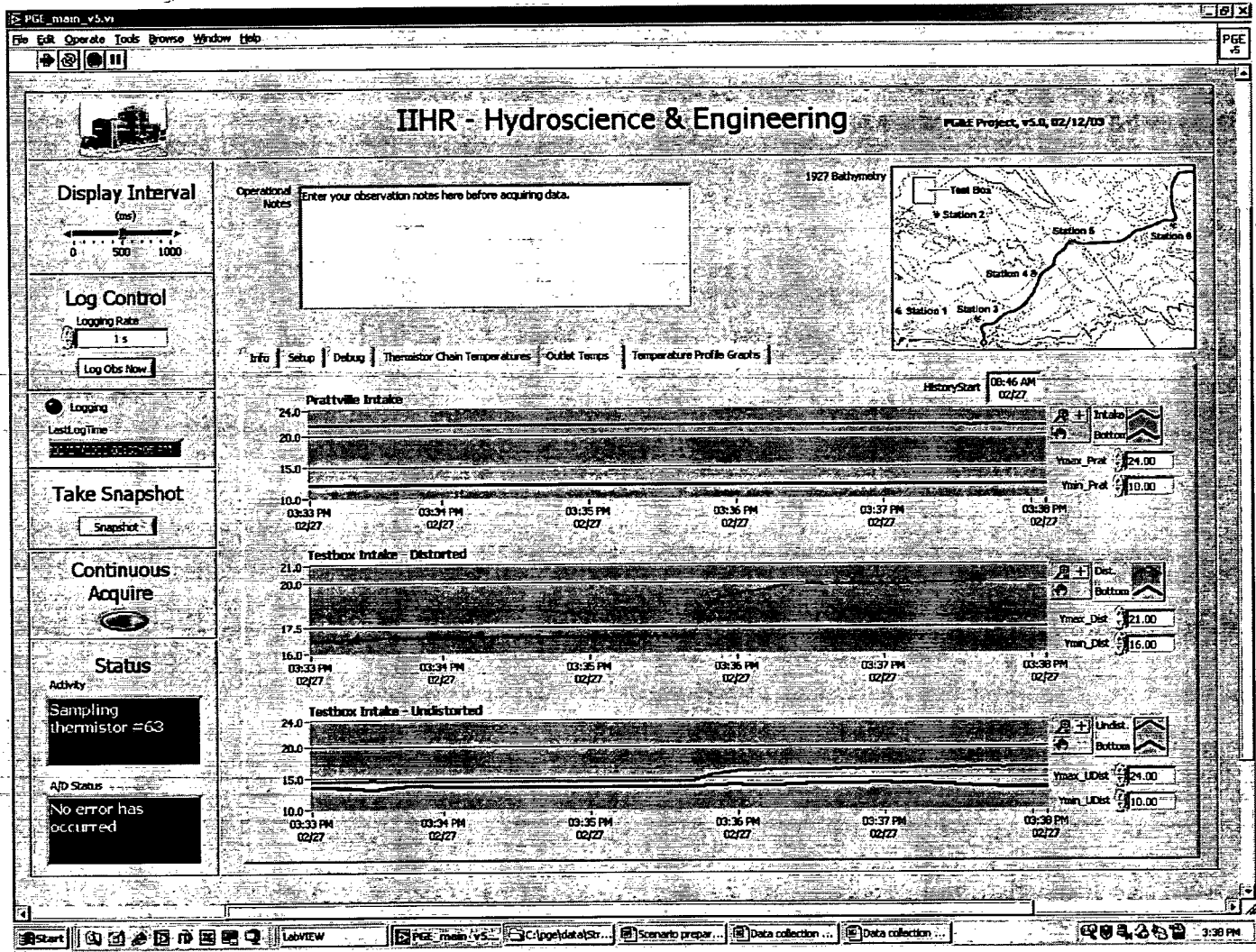
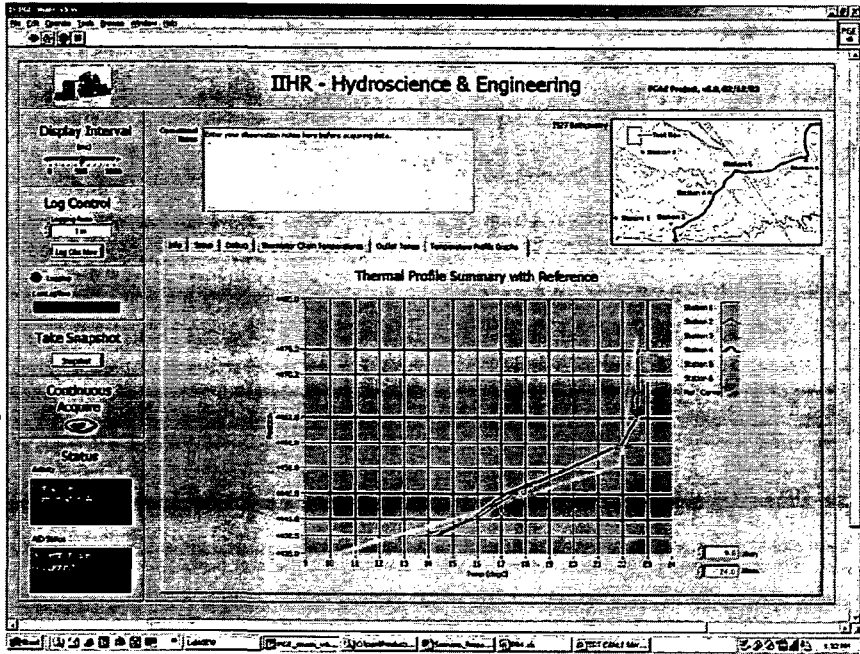
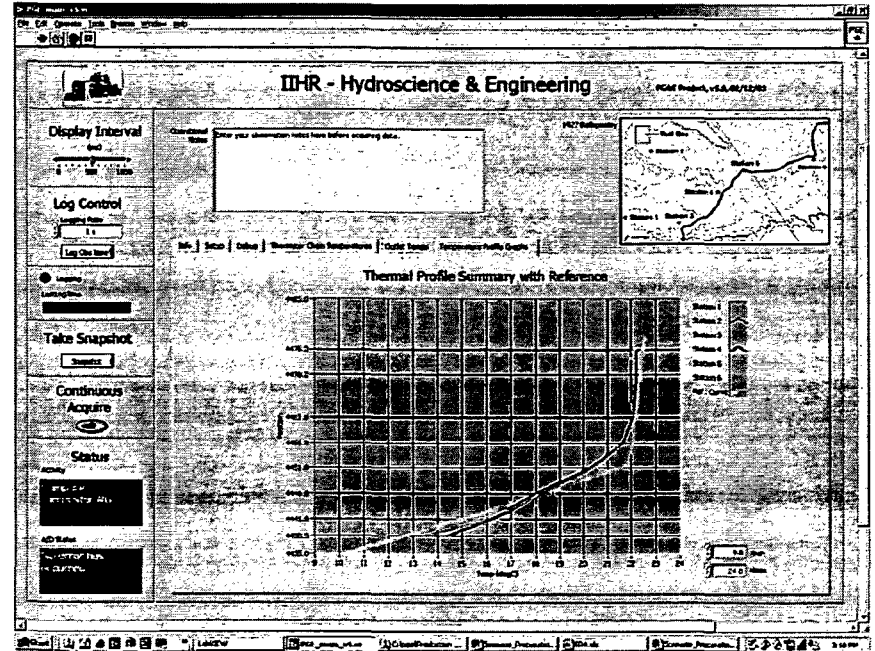


Figure 3-19. Interface for monitoring outflow temperature.

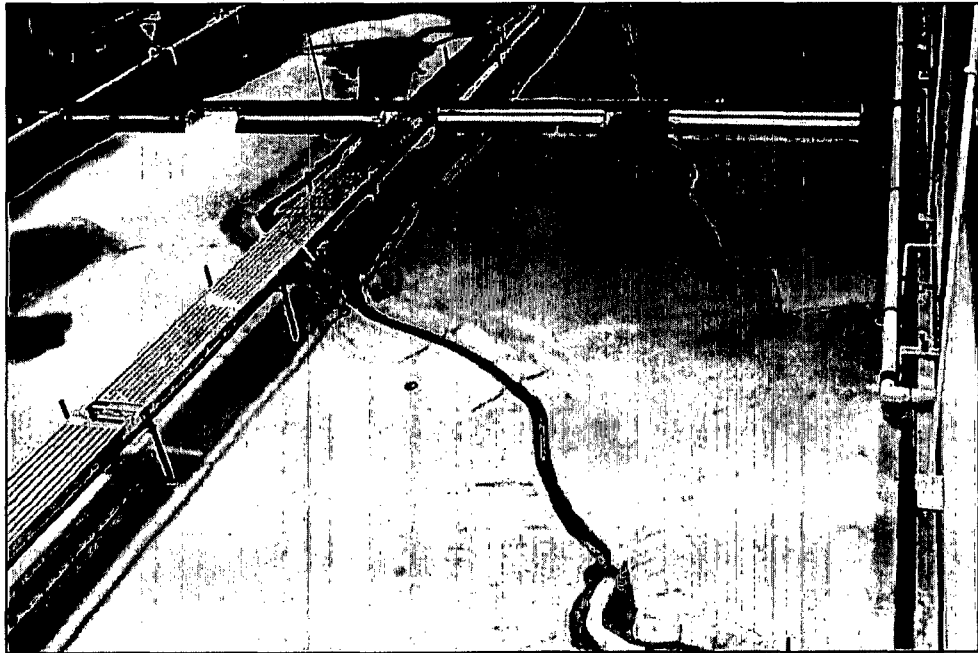


(a)

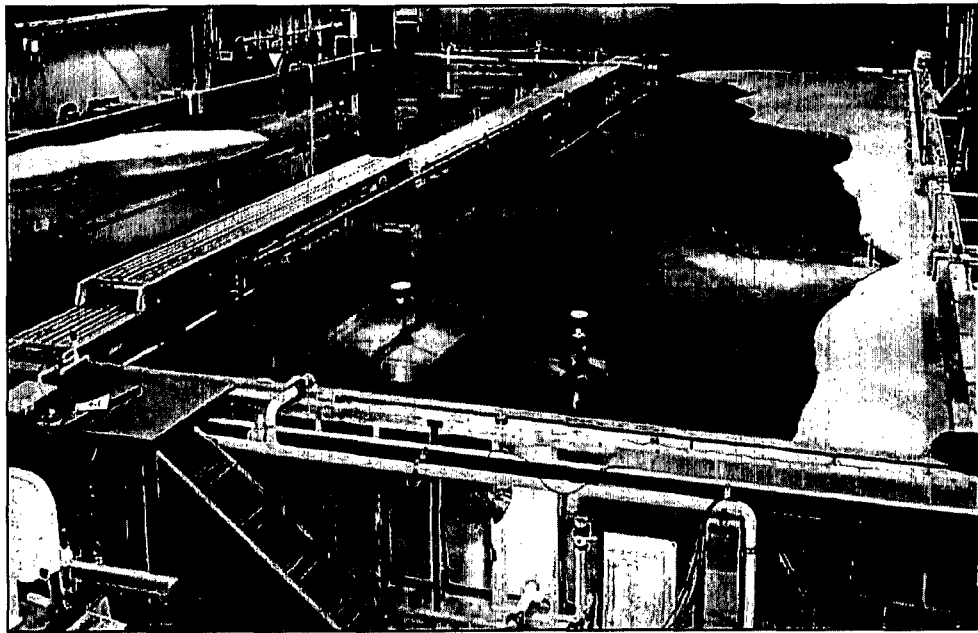


(b)

Figure 3-20. Temperature profiles at the beginning (a) and end (b) of a series of tests.



(a)



(b)

Figure 3-21. Filling the hydraulic model: (a) initial feeding of water in the model; (b) the model ready for testing.

## **4. MODEL CALIBRATION, VALIDATION, VERIFICATION**

### **4.1 Introduction**

This chapter describes the steps taken to calibrate, validate, and verify the hydraulic model's capacity to simulate the water conditions prevailing in the vicinity of Prattville Intake during the summer months of June, July, and August. As introduced at the beginning of this report, use of the hydraulic model entailed a major effort aimed at determining the appropriate scaling of outflow discharge released from Prattville Intake simulated in the hydraulic model. That effort was carried out by way of comprehensive laboratory experiments involving an experimental arrangement herein termed testboxes. They were configured, with two levels of simplification, as vertically distorted and corresponding undistorted replications of Prattville Intake. The calibration effort also involved the use of a numerical model that simulates the testboxes.

The laboratory testboxes are described in Sections 4.4 and 4.5, and the numerical model of the testboxes is described in Section 4.6. The results of the calibration effort are given and discussed in Chapter 6.

The testboxes were used further to substantiate, or validate, the capability of the most promising design modification that would enable Prattville Intake to release colder outflow water. The present chapter also describes the use of the testboxes for that purpose, the results of which are given in Chapter 8.

In this report, as elsewhere generally, calibration refers to a method of adjustment or analysis of an instrument or setting so that the instrument or setting relate directly to a correct measurement value. Calibration also refers to the overall adjustment of the procedure followed in getting the hydraulic model to simulate the representative conditions of water stratification and movement in Lake Almanor. Validation is the step confirming the consistency of the adjustment method, or analysis, and its result. Verification is the step checking that a measurement, or simulation value, indeed

accurately concurs with the value associated with equivalent conditions observed for a prototype or in the field.

## **4.2 General Calibration Activities**

General calibration activities associated with the vertically distorted hydraulic model entailed calibration of instrumentation for measurement, and adjustments of procedures for establishing the thermal and flow conditions in the model.

The following series of calibration tests were conducted with the model:

1. Verify the proper operation of all model components to ensure proper modeling of flow circulation and temperature distribution;
2. Calibrate the thermistors;
3. Establish the heat-exchange characteristics between upper layer and air, between the colder and warm water strata, and between the bed and lower stratum;
4. Evaluate the thermal losses through model boundaries;
5. Develop the combinations of water quantities, bulk temperatures, and rates of feeding needed to establish the vertical profiles of water temperature representing lake conditions during June, July and August; and,
6. Establish the discharge scale for operating the model of Prattville Intake such that replicates the outflow performance of Prattville Intake itself.

The main calibration effort entailed attaining the test water-temperature profiles prescribed for the June, July, and August conditions of Lake Almanor, and for setting the outflow rates from the model. These calibration efforts required two auxiliary studies that used the following equipment:

1. A test tank to develop the procedure, and relative water quantities, for establishing the requisite temperature profiles in the hydraulic model; and,
2. A pair of testboxes for determining an outflow calibration factor for taking into account the effect of vertical distortion on the temperature of outflow water released through the hydraulic model of Prattville Intake. The pair comprised, in simplified form, a vertically distorted and an undistorted replication of the Intake and the lake bathymetry in the region of the Intake. Two configurations of testbox were used. Section 4.4 describes the testbox work.

The test tank for developing the water-mixing procedure was built prior to construction of the hydraulic model. The tank was rigged with the same insulation material and water feeding systems as those planned for the hydraulic model. The configuration and dimensions of the tank are provided in Figure 4-1. Work with the tank confirmed the efficacy of the water-feed system, and facilitated evaluation of the various heat transfer processes attendant to modeling thermally stratified water in the hydraulic model. For example, the work led to the selection of the so-called pop-up risers for feeding cold water into the hydraulic model. It also ensured the feasibility of simulating the water-temperature distributions prescribed for June, July, and August. The insulation material to be used for the hydraulic model was assessed to ascertain its heat exchange characteristics, and to evaluate the duration over which the temperature profiles could be maintained under the ambient temperature conditions (air and floor) prevailing in the laboratory building that would house the hydraulic model.

Throughout the calibration phase of work, calibration results were communicated to PG&E for discussion, and to ensure PG&E's concurrence with the acceptability of test procedures and anticipated results.

### **4.3 Water-Temperature Stratification**

A key task was producing the same stratification conditions in the hydraulic model as are taken to be representative of water in Lake Almanor during June, July, and August. The calibration activities aimed at establishing the requisite water-temperature profiles in the model entailed the following procedures:

1. Calibration of thermistors. Calibration relationships were established directly by relating thermistor signals to measurements from high-resolution thermometers taken over a range of temperature encompassing those expected in the hydraulic model operation; i.e., 0 to 30°C. The thermistors were calibrated individually, using data points obtained from a water bath whose temperature was adjustable. Thermometer accuracy is 0.1°C, as documented by the National Institute of Standards and Technology. A sample calibration curve is provided in Figure 4-2;
2. Preliminary tests were conducted, using the test tank containing water of a uniform bulk temperature, to verify the heat-exchange rates between water and air at the free surface; and between water and the insulated walls and bottom of the testbox (Figure 4-3);
3. Preliminary tests were conducted using the test tank to determine effective ways to feed and combine, with minimum mixing, water of differing temperatures so as to establish the requisite water-temperature profiles for the June, July and August water conditions in Lake Almanor (Figure 4-4);
4. Once the hydraulic model was constructed and experience gained with the water-feed procedure, water-temperature profiles were measured at benchmark locations in the hydraulic model. The temperature profiles measured in the model were compared with the profiles measured in the lake;
5. Subsequent to filling, by way of a pre-determined batch combination of feed-water temperatures and volumes, the hydraulic model was left to settle and attain

thermal stability. The period required to attain stability was monitored through continuous measurement of temperature distribution at the benchmark locations. Due care was taken to discharge the several batches of feed-water so as to cause minimum mixing; and,

6. Water-temperature profiles were measured at the benchmark locations in the hydraulic model and were then compared with the field profiles supplemented with temperature profiles provided by the numerical model of Lake Almanor. The initial profiles differed slightly from those measured in the lake. Consequently, the batch combinations of feed-water temperatures and volumes were iteratively adjusted until the water-temperature profiles in the model conformed to those measured in the lake.

#### **4.4 Outflow Discharge – Testbox Experiments**

Vertically distorted hydraulic models are used commonly for modeling flow situations where the flow can be approximated as being two-dimensional (2D), with flow direction being predominantly parallel to the linear average slope of the model bed, such as for flow in a river channel. For such situations, a discharge scale can be determined directly in terms of horizontal- and vertical-length scales, as shown subsequently. However, vertically distorted models are used rarely in situations requiring simulation of the full three-dimensional features of flow, as required for the present model of Prattville Intake. The concern is that vertical distortion changes the flow field so as to alter flow patterns, and thereby flow mixing and entrainment. Those changes affect the simulation of thermocline depression and disruption, and therefore flow mixing, in the vicinity of Prattville Intake. Therefore, the use of a vertically distorted model for the present study required an additional effort aimed at determining how to use the results obtained from the hydraulic model when predicting the performance of Prattville Intake at full scale.

Accordingly, a sequence of calibration, validation, and verification steps was taken to determine the appropriate range of model flows to be used in the hydraulic model. This approach meant assessing an adjustment factor, or range of factors, to be applied to the

discharge scale customarily associated with a vertically distorted hydraulic model operated in accordance with Froude-number similitude. Application of the discharge-scale factor, or range of factors, would make sure that the hydraulic model was calibrated to reproduce the overall flow conditions leading to the relationships between outflow temperature and discharge measured for Prattville Intake.

Obtaining the adjustment factor required carrying out series of laboratory experiments using a pair of testboxes serving as distorted and undistorted replications of Prattville Intake. Also a numerical model was used to support the testbox experiments.

#### 4.4.1 Discharge Scale for 2D Flows

For vertically distorted models used to simulate approximately 2D flow, flow discharge usually is scaled in accordance with the relationship

$$Q_r = V_r A_r = V_r X_r Y_r = Y_r^{1/2} X_r Y_r = X_r Y_r^{3/2} \quad (4-1)$$

where  $X_r$ ,  $Y_r$ ,  $V_r$ , and  $Q_r$  are scale ratios of horizontal distance, vertical length, velocity, and discharge, respectively. The velocity scale estimated from Eq. (3-3) is  $V_r = Y_r^{1/2}$  when scale ratio for modified gravity,  $(\Delta\rho/\rho)_r = 1$ . Eq. (4-1) gives  $Q_r = 5.57 \times 10^4$  for the distorted testbox and for the hydraulic model. This discharge scale converts a prototype, normal operating discharge of  $Q_0 = 1,600$  cfs to a model-scale discharge of  $Q_{0m} = 2.87 \times 10^{-2}$  cfs; the subscript  $m$  denotes model-scale value. The discharge scale is appropriate for the far-field of flow approach to the Intake, as that flow largely moves parallel to the bed of Lake Almanor.

In the near-field vicinity of the intake, Eq. (4-1) may not lead to adequate similitude of flow mixing. Indeed, by virtue of vertical distortion, the model does not accurately simulate the near-field mixing behavior of flow approaching the intake. Flow in the near-field is markedly three-dimensional, marked by numerous eddies and by eddy shedding, and dives toward the intake. Vertical components of flow velocities in the vertical plane are under-scaled using Eq. (4-1).

For a geometrically undistorted hydraulic model ( $Y_r = X_r$ ) operated using Froude-number similitude, the discharge scale usually is

$$Q_r = V_r A_r = V_r Y_r^2 = Y_r^{5/2} \quad (4-2)$$

When  $Y_r = 40$ ,  $Q_r = 1.01 \times 10^4$ .

The discharge scale needed for operating the model lies in the range  $1.01 \times 10^4 \leq Q_r < 5.57 \times 10^4$ . The appropriate value of  $Q_r$  has to be determined by way of calibration and validation testing, the results of which must be verified with field measurements. Such testing usually also provides diagnostic insight as to the basis for  $Q_r$ , and leads to a calibration factor,  $\alpha$ , as in the equation

$$(Q_{0m})_{cal} = \alpha(Q_{0m}) = \alpha(Q_{0p} / Q_r) \quad (4-3)$$

in which  $(Q_{0m})_{cal}$  is the calibrated, model-scale discharge required for simulating the performance of the prototype Intake releasing its design discharge  $Q_{0p} = Q_0 = 1,600\text{cfs}$ . To determine  $\alpha$  for the hydraulic model used in the current project, a series of laboratory experiments were conducted using the test set up herein called the testboxes. They are described below. Subsequently, Section 5.1 further discusses the considerations influencing the flow conditions investigated using the hydraulic model.

It is unclear at this point whether  $\alpha$  has a single value for all tests done with the hydraulic model, or whether it has several values in accordance with different geometries of intake, temperature profiles in the model water body, or outflow discharges. This issue is further discussed in Sections 6.7 and Section 8.5 of the report. An intriguing finding of the study is that a tentative, theoretical value for  $\alpha$  likely can be calculated. Explanation of that finding is left until Section 8.5, which shows that that the theoretical value agrees with the results from tests with the testboxes.

#### 4.4.2 Testboxes

The two testboxes were built with the same vertical scale,  $Y_r$ , but differed in horizontal scale,  $X_r$ :

- A distorted testbox ( $X_r = 220, Y_r = 40$ )
- An undistorted testbox ( $X_r = 40, Y_r = 40$ )

The testboxes approximately replicated the shoreline and lakebed bathymetry around Prattville intake. They were built so as to be adaptable to two idealized geometric layouts:

1. Bay testboxes; testboxes with vertical sidewalls extending the full depth of water so as to form two box-like bays; and,
2. Open testboxes; testboxes opened by having their vertical sidewalls lowered and shortened so as to extend over only part of the water depth, similar in elevation and extent to the submerged ridges flanking Prattville Intake.

The testboxes were built in a region of the basin that comprised a large portion of the hydraulic model that was well away from the model of Prattville Intake, and where the lakebed was fairly flat. Each testbox was fitted with a compound channel, which can be covered, and a recess at the end of the channel. The deeper part of the approach channel was set at elevation EL. 4420ft.

The vertically distorted testbox, essentially covered the overall plan-area of the near-field region around Prattville Intake as simulated in the hydraulic model. The undistorted testbox covered the same features but with undistorted length scales; i.e., the undistorted testbox was 5.5 times wider and longer ( $G = X_r/Y_r = 220/40 = 5.5$ ) than was the distorted testbox. The vertical scale and therefore water depths were the same for both testboxes.

For each testbox, the bottom elevation of the intake invert was the same as the elevation of the invert of Prattville Intake (EL. 4410ft). Additionally, the approach flow to the intake was along a compound channel that approximately replicated a short length of the incised channel immediately in front of Prattville Intake.

The Bay testboxes with full-depth sidewalls are a simplified geometric representation of Prattville Intake and the lake bathymetry surrounding the intake. The approach flow entering each testbox approached the intake opening at the end of the testbox in a more-or-less two-dimensional uniaxial manner, and then converged radially toward the intake opening. The layout used for the undistorted and the distorted Bay testboxes are given in Figure 4-5. Views of the testboxes are provided in Figure 4-6.

The Open testboxes with submerged sidewalls simulated the overall lake bathymetry around Prattville Intake more closely by enabling flow to be drawn radially toward the intake opening, with water increasingly being drawn over the submerged sidewalls when the rate of outflow increases. Figure 4-7 is a perspective sketch of the undistorted testbox, and gives the elevations of the submerged sidewalls flanking the testbox inlet. The submerged sidewalls generally conform to the overall profiles of the submerged ridges that flank Prattville Intake. The layout and overall dimensions of the undistorted testbox are given in Figure 4-8, while Figure 4-9 is a photograph of the undistorted testbox. The layout and dimensions of the distorted Open testbox are given in Figure 4-10. Figure 4-11 is a photograph of the distorted Open testbox. Also indicated in Figures 4-8 and 4-10 are the layout and dimensions of the skimming curtains used with the open testboxes to corroborate the results obtained from the hydraulic model tests with the skimming curtain (elaborated in Chapter 8).

#### 4.4.3 Calibration, Validation, Verification Sequence: Existing Intake Configuration

The following sequence of tests and comparisons was used in determining the value (or value range) for the discharge adjustment factor,  $\alpha$ , determined for the existing configuration of Prattville Intake.

1. Calibration: testbox performance curves obtained for the July, 2000 temperature profile;
2. Validation: Several validation comparisons were made –
  - (i). with performance curves obtained for the August and June, 2000 water-temperature profiles and lake levels; and,
  - (ii). with testbox performance curves obtained from the numerical model simulating an approximate July, 2000 temperature profile and lake level replicated at the testboxes in the hydraulic-model basin;
3. Verification: comparison with field measurements of outflow temperature obtained for Prattville Intake operating under the August, July and June 2000 temperature profiles and lake levels. The comparison is made with the open testboxes, as they most closely resemble Prattville Intake, although they are not fully similar geometrically.

This sequence of tests is an early part of the overall program of tests outlined in Chapter 5.

The Bay testboxes were tested for the August, June, and July conditions for Lake Almanor. The Open testboxes with submerged sidewalls, were tested for the August and July conditions; because the values of calibration coefficient,  $\alpha$ , were found to be consistent between the boxes, it was felt that the June condition need not be tested with the Open testboxes.

Each testbox was operated for a range of discharges:

1. Distorted testbox (simulating flow rates of 0.25 to 6 times the design intake discharge,  $Q_0$ ); and,

2. Undistorted testbox (simulating flow rates of 0.25 to 2.5 times the design intake discharge,  $Q_0$ ).

In most test runs, the tests began with a discharge of 0.25 to 0.5 times the design discharge,  $Q_0$  scaled in accordance with Eq. (4-1); i.e.,  $Q_{0m} = 2.87 \times 10^{-2}$  cfs. The tests then increased the outflow discharge so as to obtain a minimum of three, usually five, data points to define a performance curve. The calibration tests were repeated at least twice, on different days each with a different body of water. The comparatively large volume of water needed for running the undistorted testbox limited the number of tests completed with each body of water.

The field data used for verifying the discharge factor were provided by PG&E, who had run a set of dynamic field tests with Prattville Intake in August 1 through 5, 1994 to determine the sensitivity of outflow temperature to rate of outflow released from the intake. Another set of field measurements was available for June 22, July 19, and August 17, 2000. The validation check involved plotting the field data in the same format as the performance curves used for evaluating the data from the hydraulic model; i.e.,  $T_{out}$  versus  $Q/Q_0$ .

#### **4.5 Testbox Validation of Intake Modification**

Besides their use in calibrating the outflow rates to be used in the hydraulic model, the testboxes were used to confirm the hydraulic model's veracity in simulating the performance of a skimming curtain as an effective means for reducing the temperature of outflow water released from Prattville Intake. As discussed subsequently in Chapter 7, tests with the hydraulic model show that a skimming curtain, together with some bathymetric adjustment (levee removal), comprise the modification holding best promise for reducing the temperature of outflow water released through Prattville Intake during June, July, and August.

In essence, this use of the testboxes is an extension of textbox use in calibrating outflows for the hydraulic model; verification of curtain performance relies basically on the

satisfactory simulation of the flow field in the vicinity of the curtain. Accordingly, the further validation tests with the testboxes sought to obtain the following validation information:

1. the discharge-calibration factor,  $\alpha$ , for operating the hydraulic model of Prattville Intake when the intake is fitted with a curtain; and,
2. the curtain's ability to reduce the temperature of outflow water released through Prattville Intake.

Since tests with the hydraulic model showed that a skimming curtain would most effectively reduce the temperature of outflow from Prattville Intake, the testboxes were adapted for tests to confirm curtain performance. Two forms of curtain were tested. They are illustrated and described in Chapter 8, though a brief description ensues here.

Preliminary tests were done using a curtain consisting of a flat plate placed across the vertical sidewalls of the Bay testboxes. Subsequent tests, conducted at the end of the overall modeling work, and using the Open testboxes, were done using a more exact representation of the recommended curtain form and dimensions determined from tests with the hydraulic model. The curtain placed around the distorted testbox had the same form and dimensions as used in the hydraulic model. However, for the undistorted testbox, space and water-volume limitations, dictated by the dimensions of the hydraulic model basin in which the testboxes were placed, required that the curtain placed around the undistorted testbox be positioned proportionately closer to the simulated intake than was the case for the curtain in the hydraulic model and distorted testbox. The curtain around the undistorted testbox was at half the scaled distance from the intake, because there was insufficient cold water in the model basin to fill to an equilibrium thermal condition the large volume contained behind the curtain. The opening area beneath the curtain, though, was scaled in proportion to the equivalent area beneath the curtain in the hydraulic model. Flow-field observations during the initial tests with this curtain

configuration showed it to be an effective, undistorted-model equivalent of the curtain placed in the hydraulic model and around the distorted testbox.

In overall terms, it was important that the flow field at testboxes simulated the principal flow features occurring at Prattville Intake, as the flow field drew water of varied temperature to the intake. This requirement was met generally. It was not feasible to replicate an incised channel leading to the testboxes. Therefore, the curtain-performance tests with the testboxes do not take into account the curtain influence on water movement along the incised channel, and consequently on outflow temperature.

Additional sensitivity tests were done using shorter curtains around the testboxes and around Prattville Intake in the hydraulic model. Also, the incised channel in the hydraulic model was blocked so that its influence could be assessed. Those tests showed that the curtain arrangements used with the testboxes indeed adequately replicated curtain performance in the hydraulic model.

#### **4.6 Numerical Model of Testboxes**

The U<sup>2</sup>RANS numerical model was used to simulate the distorted and the undistorted Bay testboxes with the intent of validating the calibration factor,  $\alpha$ , determined from the testbox experiments. The stratification used in the simulation entailed the exact replication of the temperature profile measured for the series of testbox tests used for comparison.

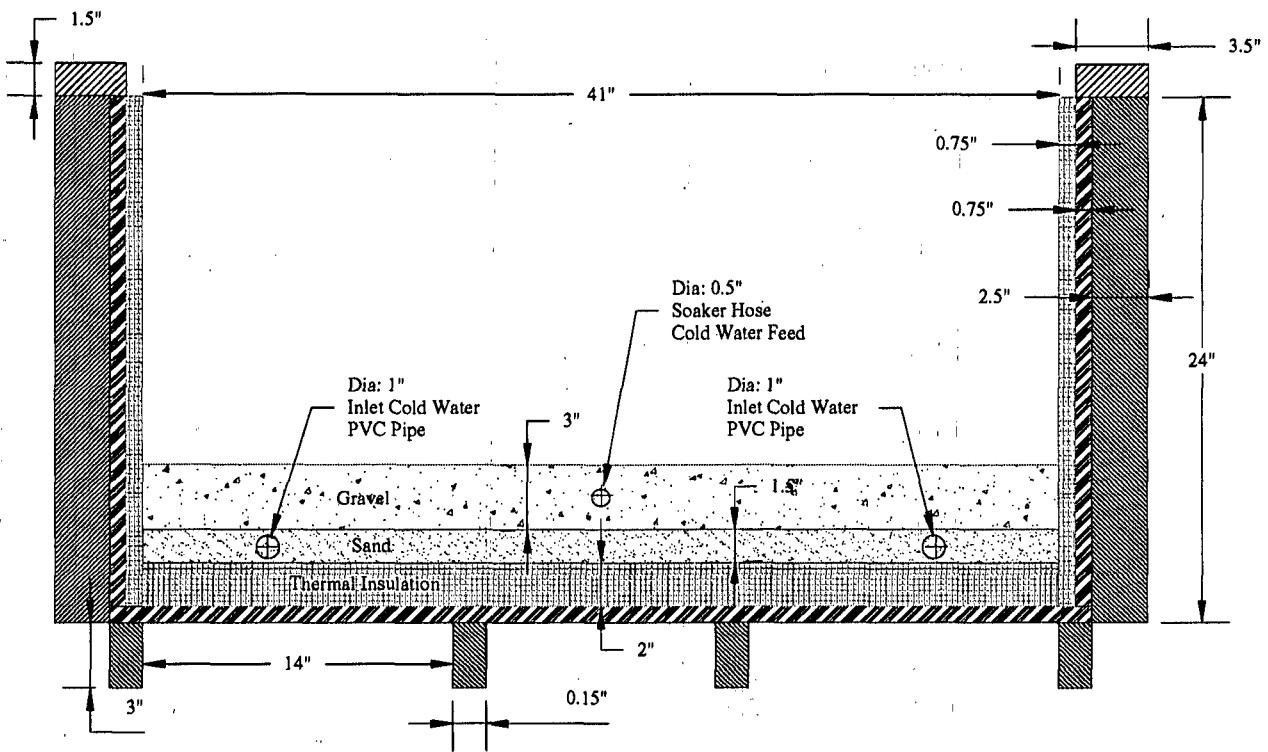
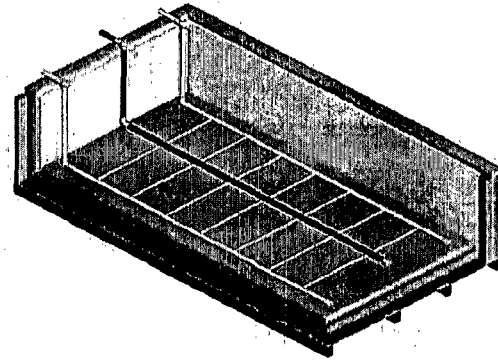
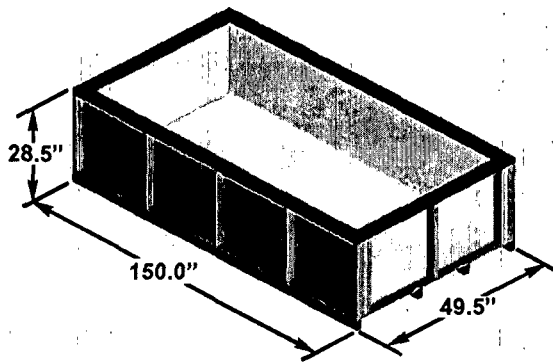


Figure 4-1. Views of the test tank: (a) perspective; (b) layout of water lines; (c) cross-section dimensions.

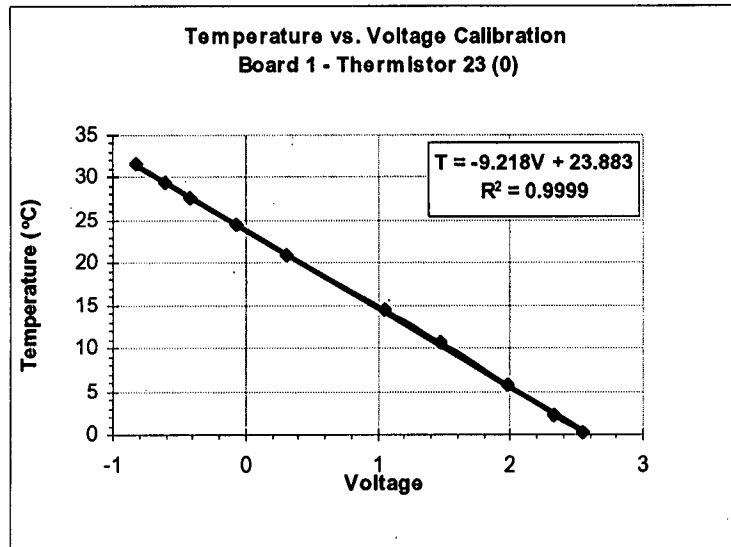


Figure 4-2. Example of thermistor calibration curve.

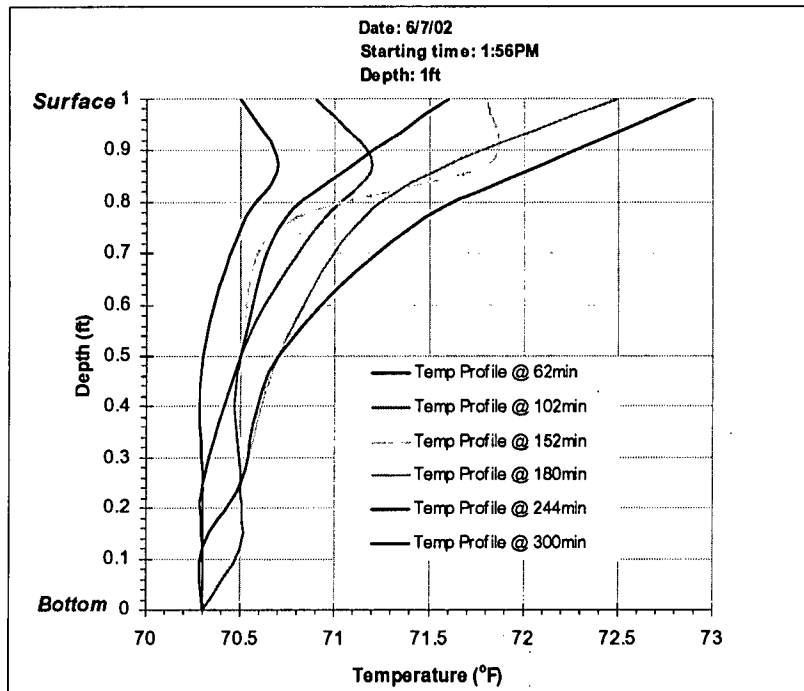
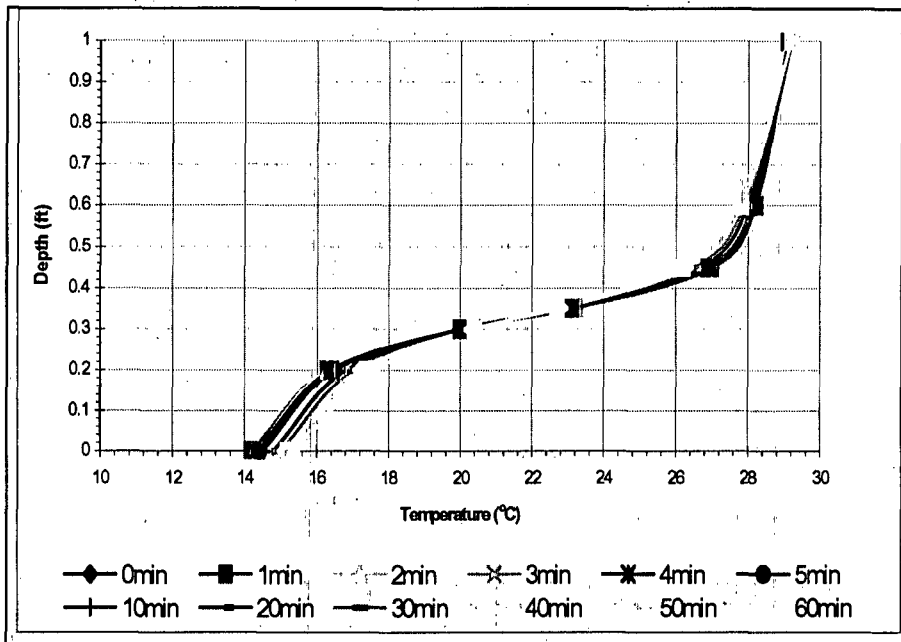
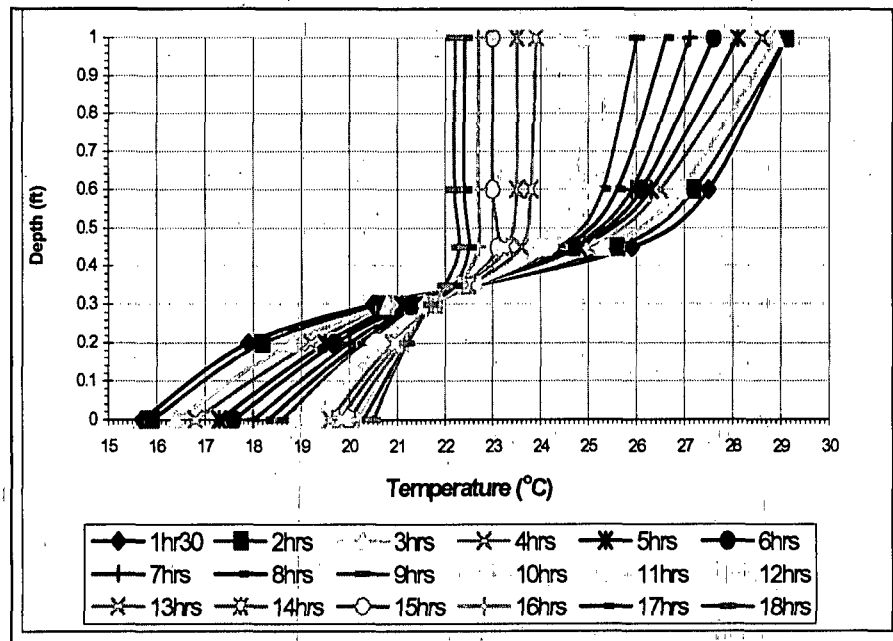


Figure 4-3. Temperature variation over time for a uniform body of water placed in the test tank.



(a)



(b)

Figure 4-4. Temperature variation over time for two layers of water fed in the test tank:  
 (a) during the first hour; (b) over 18 hours.

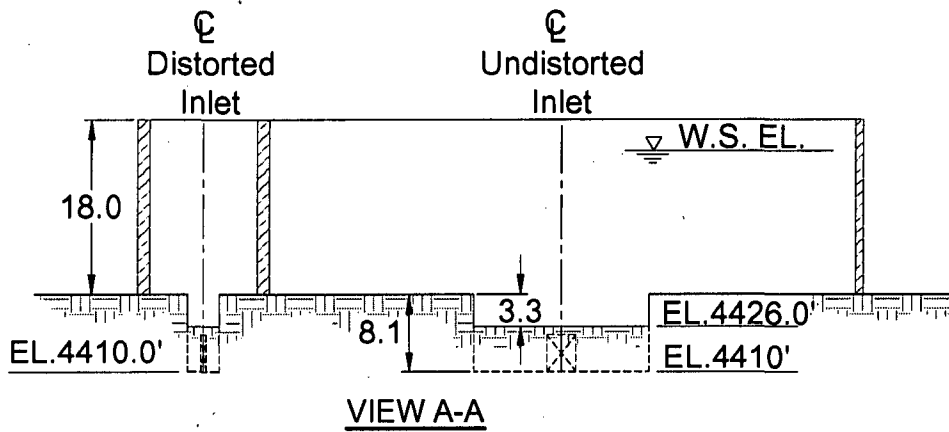
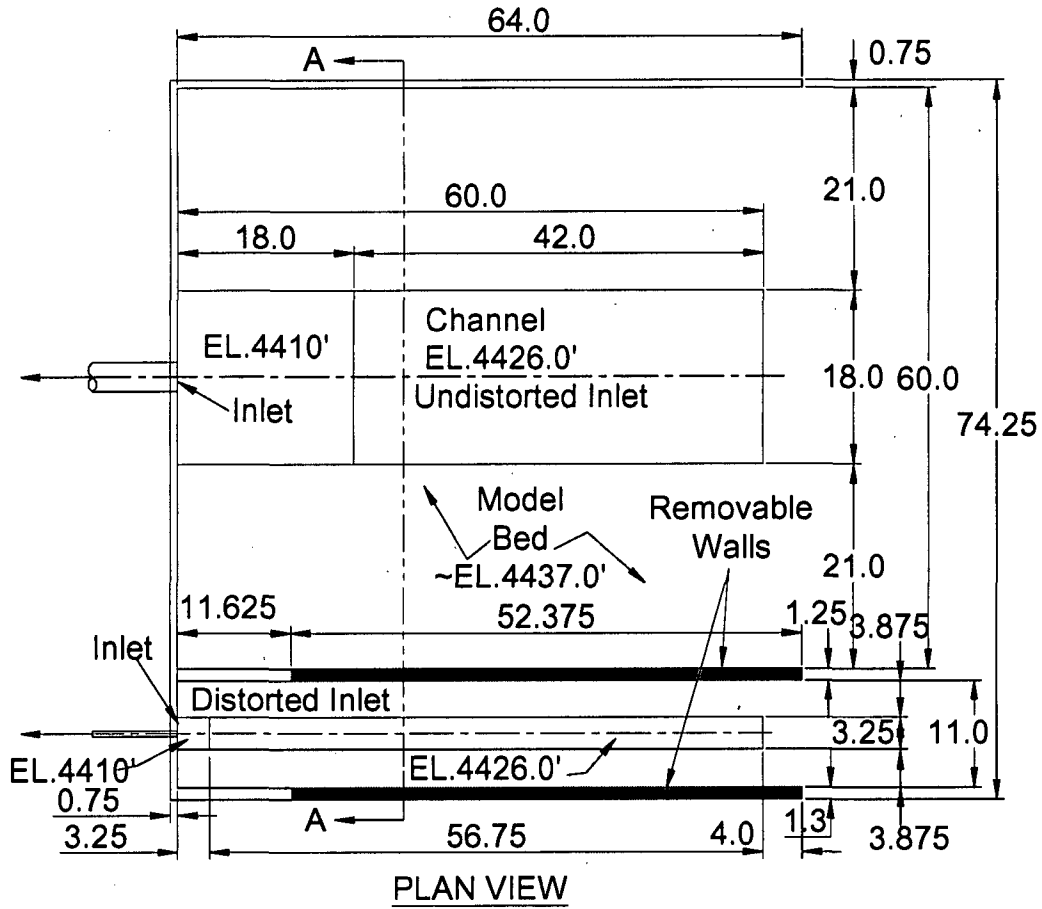


Figure 4-5. Layout and dimensions of the undistorted and distorted Bay testboxes.

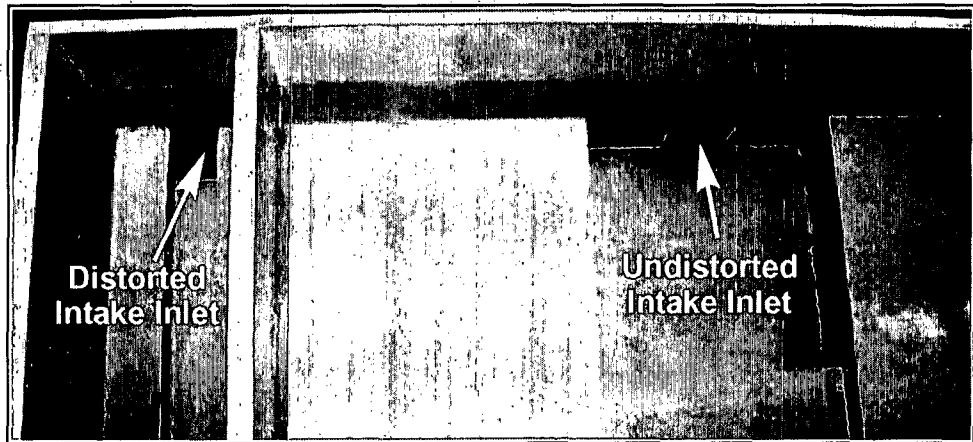
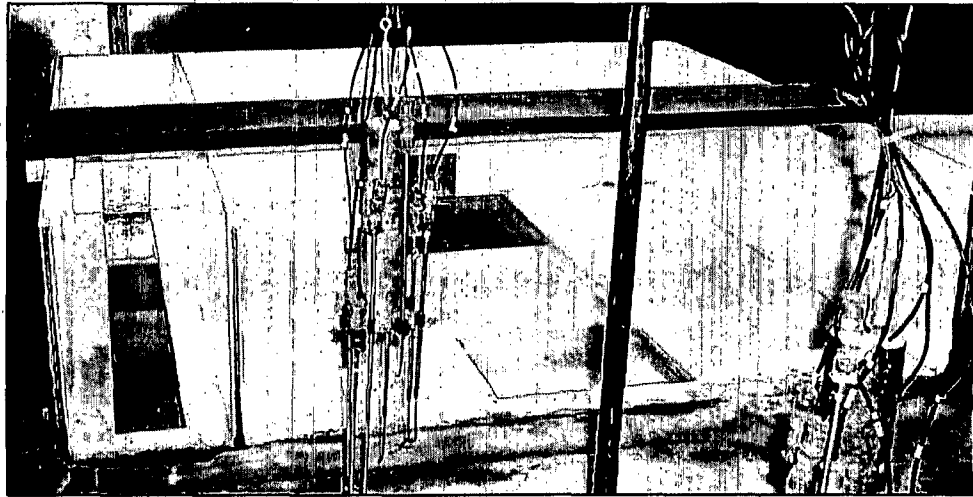
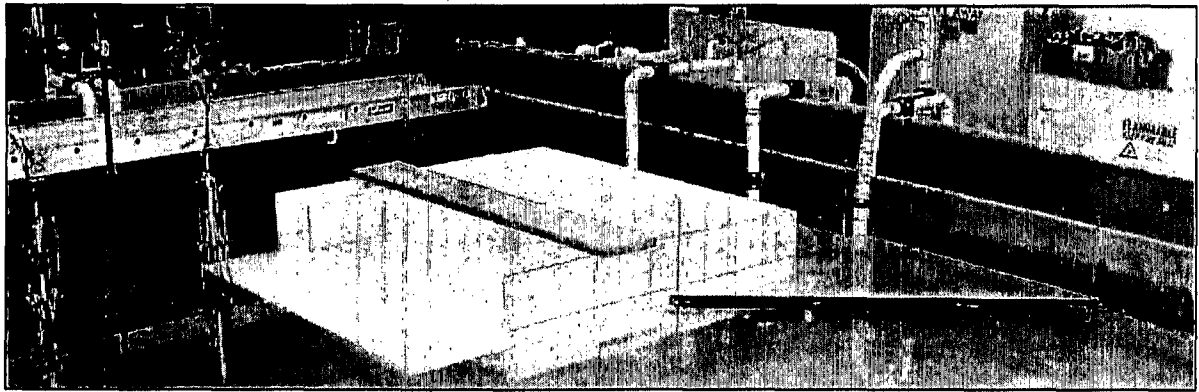


Figure 4-6. Photographs of the distorted and undistorted Bay testboxes. For each testbox the simplified intake was located in a recess below the replicated lakebed. The intake's invert was located at the actual elevation for Prattville Intake. The testboxes included a compound channel that approximately replicated the man-made channel excavated along the bed of Lake Almanor.

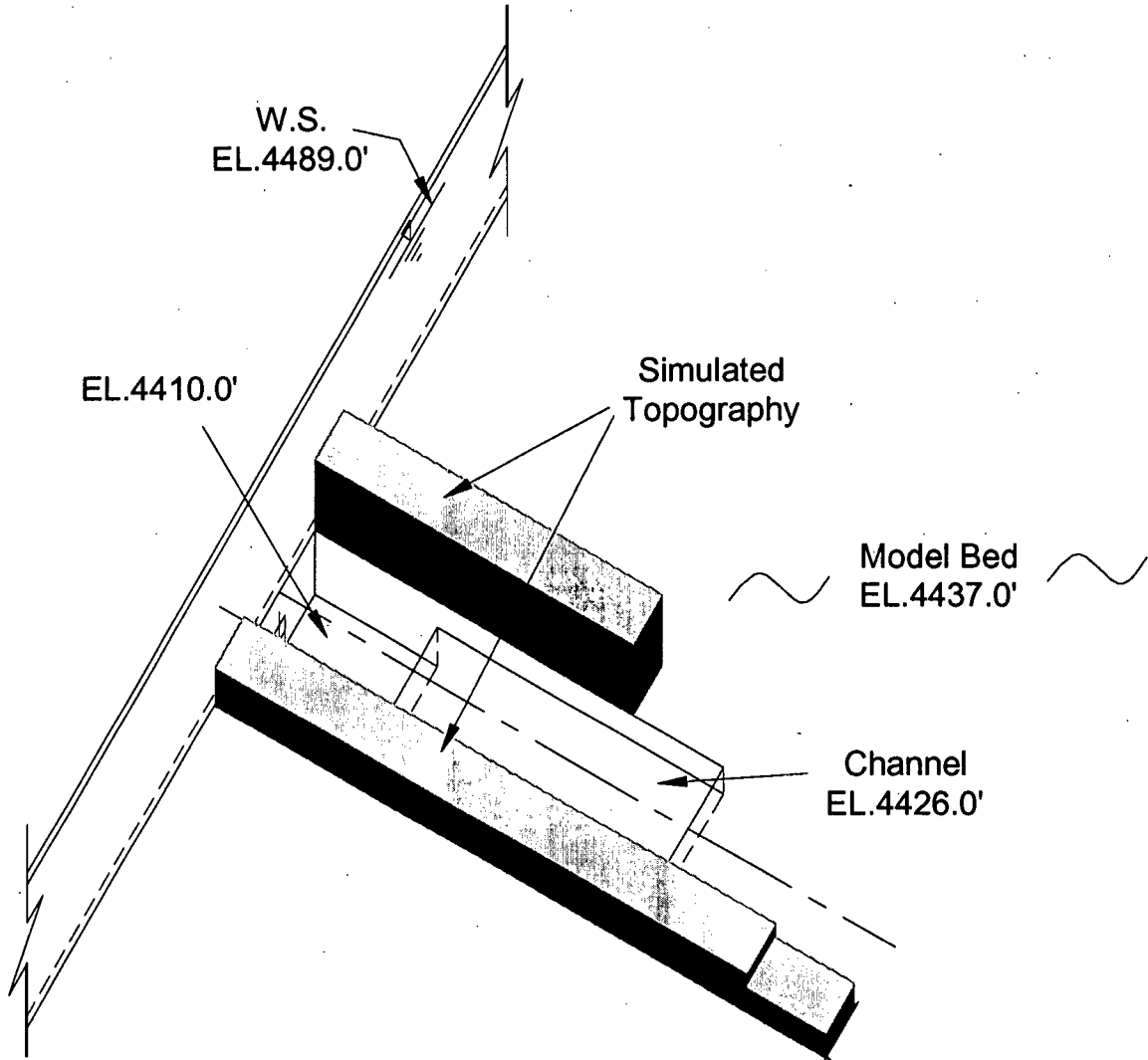


Figure 4-7. A perspective sketch of the undistorted Open testbox.



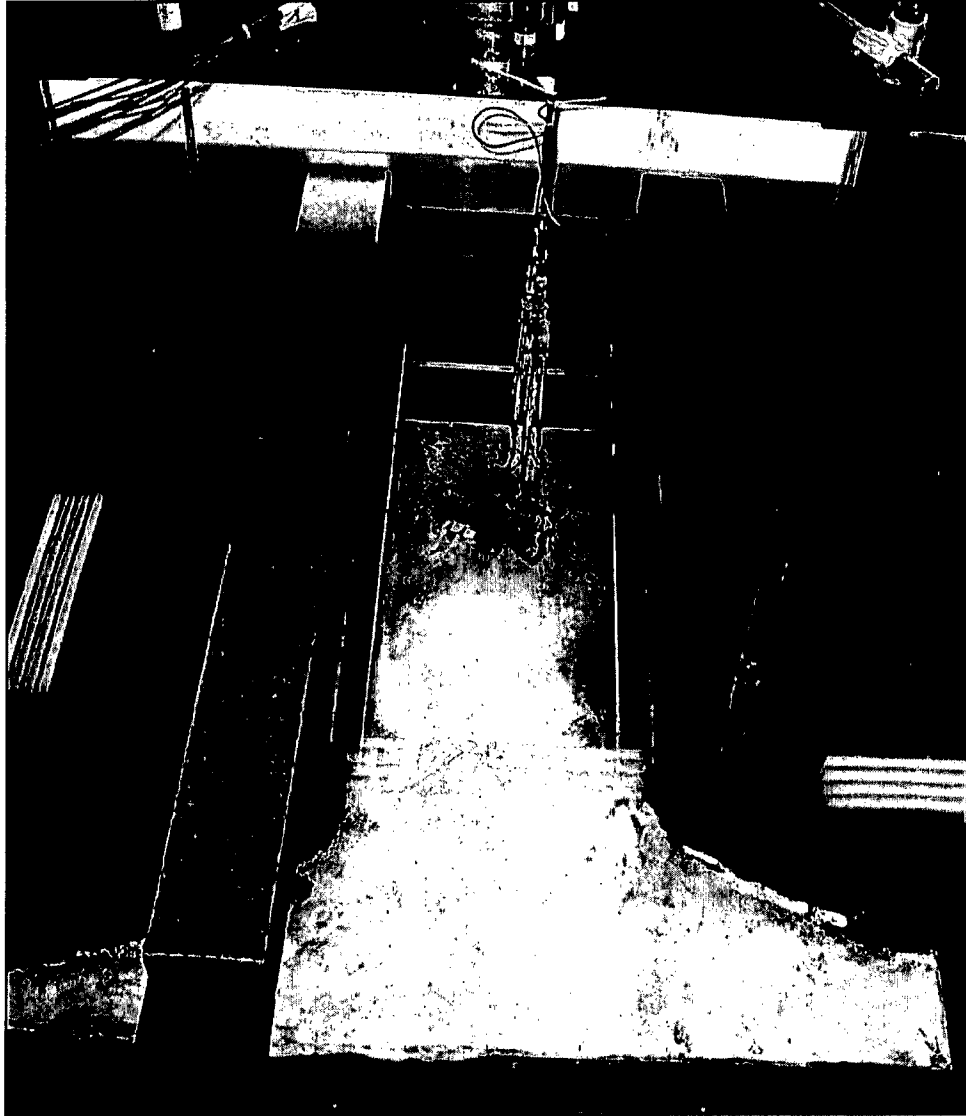


Figure 4-9. Photograph of the undistorted Open testbox.

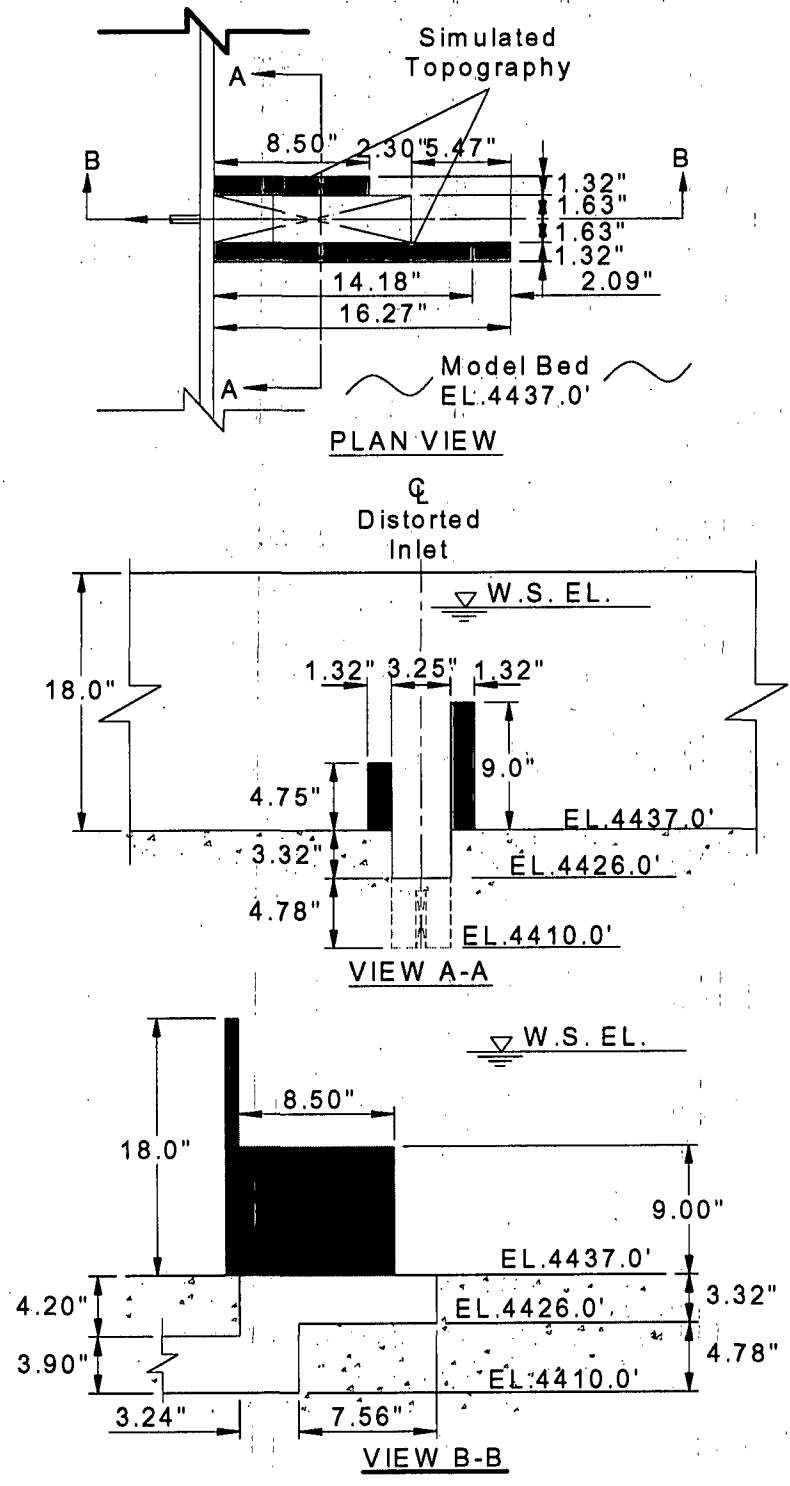


Figure 4-10. Layout and dimensions of the distorted Open testbox.

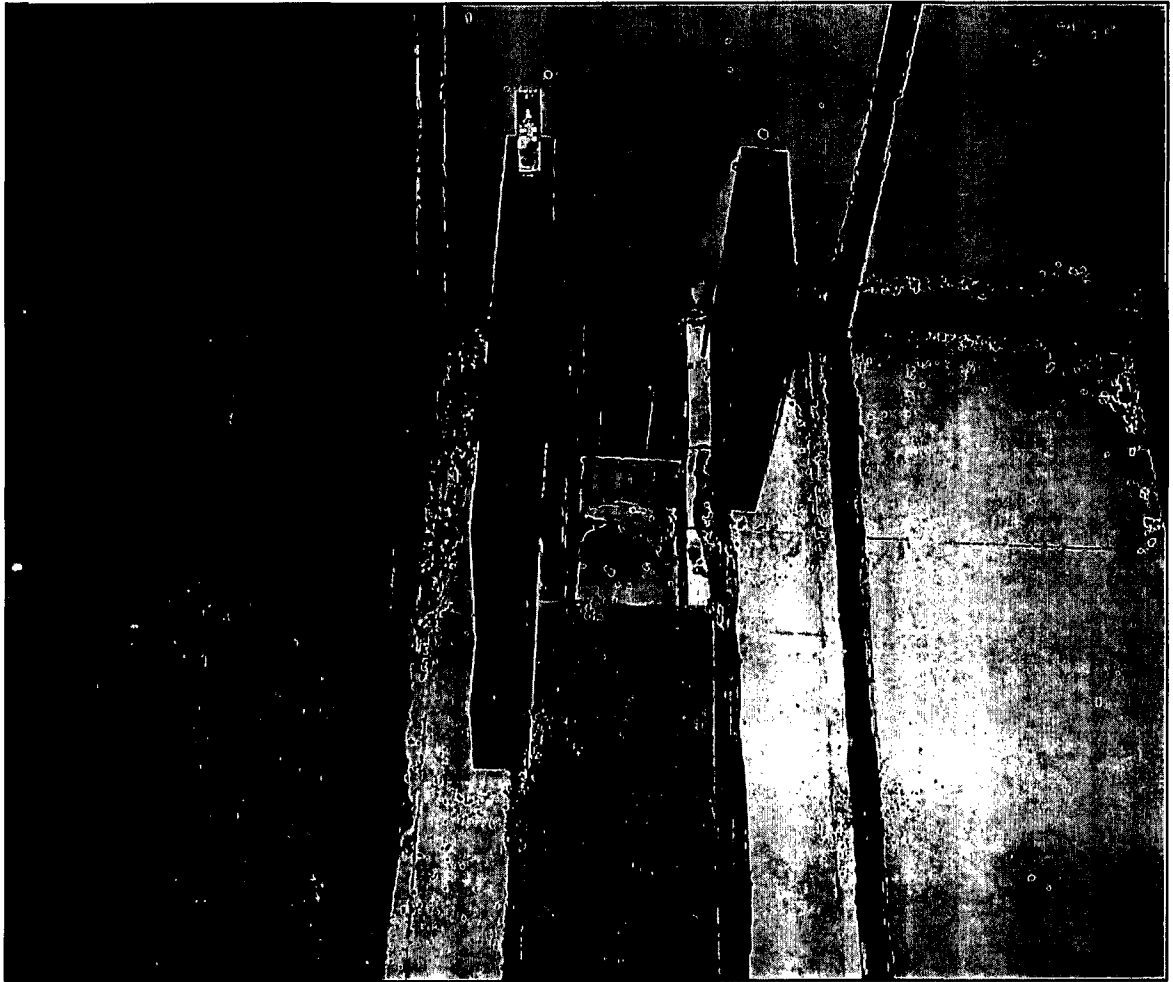


Figure 4-11. Photograph of the distorted Open testbox.

## 5. PROGRAM OF TESTS

### 5.1 Introduction

In accordance with the project's tasks listed in Table 1-1, the program of tests with the hydraulic model comprised the following arrangement of test series:

1. Calibration, validation, verification tests;
2. Baseline performance tests;
3. Modification screening tests; and,
4. Performance documentation and validation tests.

These test series were preceded by an extensive series of preliminary tests whose purpose was to enable the modelers to become familiar with the general operation of the model, and to assess the model's performance possibilities and limitations. Initial operational uncertainties, such as the stability of the hydraulic model, the number of test runs per body of water, and the difficulty of making structural changes (e.g., placement of a curtain), all had to be determined so that a test schedule could be planned in adequate detail. Such preliminary tests are important for a hydraulic model as complex as the present model. The results of those tests, nevertheless, are not presented in this report.

Tables 5-1a,b introduce and list the full number of baseline, screening, and documentation tests conducted with the hydraulic model. It also lists the calibration and validation tests conducted with the testboxes (Chapter 4). The tests are identified using a code string indicating test condition (e.g., existing configuration of Intake) and lake condition (e.g., August).

The ensuing sections of this chapter introduce the modifications tested, and describe the nature of each test series. Chapter 7 of the present report presents the results from the baseline tests, plus a selection giving the principal results from the modification screening tests. The results from the performance documentation tests are given in Chapter 8.

## **5.2 Modifications Tested**

Several design modifications were tested at the request of PG&E:

1. Skimming curtain (Figure 5-1);
2. Pipe with hooded inlet (short pipe, Figure 5-2; long pipe, Figure 5-3);
3. Levees of incised channel removed by excavation, (Figure 5-4);
4. Dredging of incised channel and approach channel (Figure 5-5); and,
5. Bottom sill (Figure 5-6).

The channel dredging and several extents of levee removal were tested in combination with the curtains and hooded-pipe inlets. In most of the cases, the lower-lip elevation of the curtains was set at EL. 4445ft. At this elevation the cold layer strata for any of the critical months (June, July, and August) could be withdrawn over an extended area in front of the Intake (see Figure 3-13c). For determining the sensitivity to operation, lip elevations at EL. 4447ft, EL. 4450ft and EL. 4443ft were also tested.

## **5.3 Calibration, Validation, Verification Tests**

These tests were done with the testboxes, as described in Chapter 4. It was common to conduct the calibration, validation, and verification tests in conjunction with tests carried out with the hydraulic model. By using the same body of water, it was possible to relate closely the results from the testboxes and the results from the hydraulic model. For example, occasionally one testbox could be operated at the same time the hydraulic model was operated. Tests in which the testboxes were used are designated as either calibration tests or validation tests. As described in Chapter 4, the calibration tests were conducted to determine the discharge coefficient  $\alpha$ . The validation tests were conducted to obtain data corroborating the value determined for  $\alpha$ .

## **5.4 Baseline Performance Tests**

The baseline tests documented the relationship between outflow temperature and outflow rate for Prattville Intake in its existing (as-built) state. These tests produced a set of

baseline performance curves corresponding to the June, July, and August conditions. The performance curves were supported by dye-visualization of the flow field developed by the Intake. Flow-field observations provided the insight needed to explain the performance of the Intake. The baseline tests involved repeated tests, conducted on different days, with the aim of ensuring that the baseline performance of the Intake was suitably documented, and to gauge the uncertainty associated with the Intake's performance.

### **5.5 Modification Screening Tests**

The modifications were assessed via a series of screening tests in which the capability of each modification to reduce the outflow temperature was evaluated. The screening tests were conducted for the August thermal condition and water-surface elevation of Lake Almanor. During August, the lake water is typically at its overall warmest condition and the lake's water level usually is low. Therefore the August condition is the critical test condition for assessing modification performance. The modification that produced the greatest reduction in temperature of outflow for the August condition was then tested thoroughly to document its performance.

The screening tests focused on retaining cold water during late Spring through to early Summer were conducted using the simulated June thermal condition, as that condition was closest to the thermal conditions prevailing in Lake Almanor during early Summer. These tests were done with the sill located around Prattville Intake.

### **5.6 Performance Documentation Tests**

The performance documentation tests were conducted to document the performance of the most promising modification, or set of modifications, that would enable Prattville Intake to release colder water during June, July, and August. Because an effective modification indeed was identified, and the course of the documentation tests concentrated on thorough investigation of the modification's performance, it is appropriate to mention at this point that the set of modifications found to best facilitate the release of colder water comprised a skimming curtain and minor bathymetry changes.

The performance documentation tests included tests on the sensitivity of outflow temperature to elevation of the curtain bottom.

Performance documentation tests were conducted also for the modification enabling the Intake to be operated so as to retain cold-water in Lake Almanor during earlier months; that modification is a bottom sill. The performance tests also involved repeated tests, conducted on different days, in order to ensure that the performance of the modification had been correctly assessed, and to gauge the uncertainty associated with the performance of the modification.

Table 5-1. List of the tests conducted with the Hydraulic Model and the Testboxes

The table lists the series of tests conducted after the model calibration/validation (the production run -PR- series). A series of 123 tests conducted prior the production runs for calibration-validation of the model (the E-series) are not listed in the table.

<p>Note on test coding:          Tests are labeled as a code string separated by dash; e.g., E-08-WL-P1. The significance of the group in the string is described below:</p> <ol style="list-style-type: none"> <li>1. The first string group designates the test objective and configuration.</li> <li>2. The second string group designates the time of the year for specification of the temperature profile</li> <li>3. The third string group indicates if the incised channel levees on the lakebed in front of Prattville Intake are removed (see Figure 5-4)</li> <li>4. The fourth string group designates the internal code for the test</li> </ol>			
---	--	--	--

Table 5-1. (a) Significance of strings in test labeling

Position in code string				Significance
<b>First group*</b>				
E				Prattville Intake, existing configuration
C				Prattville Intake & curtains. If a number is associated with the symbol C in the first string group (i.e., 45, 47, 50, etc) it designates curtain's bottom-lip elevation (i.e., EL. 4445ft, EL. 4447ft, EL. 4450ft, respectively)
LHPI				Prattville Intake & long pipe with hooded inlet (BOR design)
SHPI				Prattville Intake & short pipe with hooded inlet
SSHPI				Prattville Intake & shortest pipe with hooded inlet
F				Bottom sill (fence)
D				Prattville Intake & dredged channel
U				Undistorted Intake testbox
D				Distorted Intake testbox
UC				Undistorted Intake testbox & curtain
DC				Distorted Intake testbox & curtain
UH				Undistorted Intake testbox with simplified bathymetry around Prattville Intake
DH				Distorted Intake testbox with simplified bathymetry around Prattville Intake
<b>Second group</b>				
	06			June
	07			July
	08			August
<b>Third group</b>				
		WL		Levees in place
		WOL		Levees removed
<b>Fourth group</b>				
			P#	Production runs #

\* C added to the first group designates curtain added to the testbox tests

\*\*B added to the first group designates filled channel in front of the Prattville Intake

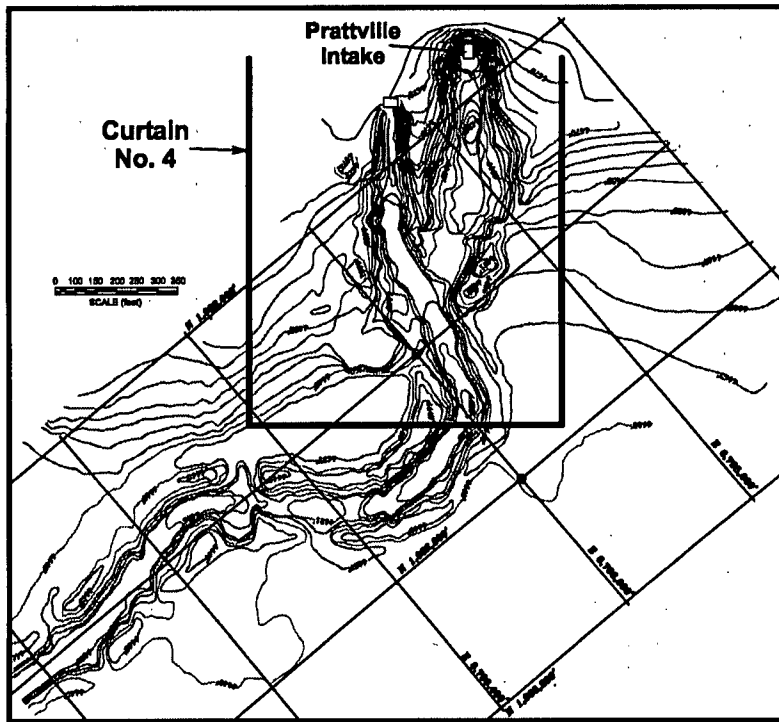
Table 5-1.(b). List of tests conducted in the Production Runs series

Test #	Run	Test configuration	Test type
1	PR1	C45-08-WOL-P1	screening
2	PR1	C45-08-WL-P1	screening
3	PR1	E-08-WL-P1	calibration/baseline
4	PR2	E-08-WL-P2	calibration/baseline
5	PR2	C45-08-WOL-P2	screening
6	PR2	C45-08-WL-P2	screening
7	PR3	C43-08-WL-P3	screening
8	PR3	C47-08-WL-P3	screening
9	PR3	C43-08-WOL-P3	screening
10	PR3	C45-08-WL-P3	screening
11	PR4	C45-08-WL-P4	screening
12	PR4	LHPI-08-WL-P4	screening
13	PR4	LHPI-08-WOL-P4	screening
14	PR5	LHPI-08-WL-P5	screening
15	PR5	C45-08-WL-P5	screening
16	PR5	LHPI-08-WOL-P5	screening
17	PR5	CC-08-WOL-P5	screening
18	PR6	C47-08-WL-P6	screening
19	PR6	C43-08-WL-P6	screening
20	PR6	C45-08-WL-P6	screening
21	PR6	C43-08-WOL-P6	screening
22	PR6	U-08-P6	screening
23	PR6	D-08-P6	calibration
24	PR7	CD-08-WL-P7	screening
25	PR7	CD-08-WOL-P7	screening
26	PR7	CDS-08-WOL-P7	screening
27	PR7	CDE-08-WOL-P7	screening
28	PR8	ED-08-PWL-P8	screening
29	PR8	LHPID-08-WL-P8	screening
30	PR8	C6DF-08-WOL-P8	screening
31	PR8	C45-08-WL-P8	screening
32	PR8	SSHPID-08-WOL-P8	screening
33	PR8	LHPID-08-PWL-P8	screening
34	PR8	C4DF-08-WOL-P8	screening
35	PR8	C4DF-08-WL-P8	screening
36	PR9	E-08-WL-P9	screening
37	PR9	E-08-WOL-P9	screening
38	PR9	EDF-08-WOL-P9	screening
39	PR9	C45-08-PWL-Q170-P9	screening
40	PR9	C45-08-PWL-Q100-P9	screening
41	PR9	C45-08-WOL-Q-P9	screening
42	PR10	C47-08-WL-P10	screening
43	PR10	U-08-P10	calibration

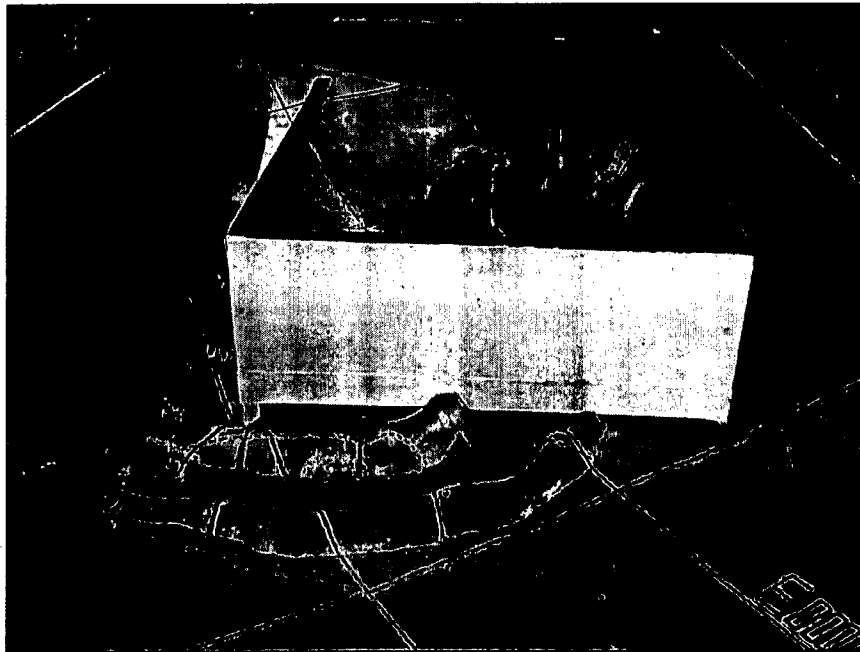
44	PR10	UC-08-P10	calibration
45	PR10	D-08-P10	calibration
46	PR10	DC-08-P10	calibration
47	PR11	E-07-WL-P11	calibration/screening
48	PR11	C45-07-WL-P11	validation
49	PR11	C45-07-WOL-P11	validation
50	PR12	C55-07-WOL-P12	performance
51	PR12	C55-07-WL-P12	performance
52	PR12	C50-07-WOL-P12	performance
53	PR12	C50-07-WL-P12	performance
54	PR12	C45-07-WOL-P12	validation
55	PR13	E-06-WL-P13	calibration/screening
56	PR13	F50-06-WL-P13	performance
57	PR13	F60-06-WL-P13	performance
58	PR14	E-06-WL-P14	calibration/screening
59	PR14	F50-06-WOL-P14	performance
60	PR14	F60-06-WOL-P14	performance
61	PR14	C4(45)-06-WL-P14	performance
62	PR15	C4(45)-08-WL-P15	performance
63	PR15	C4(45)-08-WOL-P15	performance
64	PR16	U-06-P16	calibration
65	PR16	UC-06-P16	calibration
66	PR17	UC-06-P17	calibration
67	PR17	U-06-P17	calibration
68	PR17	D-06-P17	calibration
69	PR17	DC-06-P17	calibration
70	PR17	E-06-WL-P17	Calibration/baseline
71	PR17	C4(45)-06-WOL-P17	validation
72	PR17	C4(45)-06-WL-P17	validation
73	PR18	U-06-P18	calibration
74	PR18	D-06-P18	calibration
75	PR19	August Flow Visual.	performance
76	PR20	August Flow Visual.	performance
77	PR21	August Flow Visual.	performance
78	PR22	US-08-P22	calibration
79	PR22	UC-08-P22	calibration
80	PR22	U-08-P22	calibration
81	PR22	UC-08-P22 (Curtain at the entrance)	calibration
82	PR23	U-08-P23	calibration
83	PR23	UC-08-P23	calibration
84	PR23	DS-08-P23	calibration
85	PR23	DSC-08-P23	calibration
86	PR23	D-08-P23	calibration
87	PR23	DC-08-P23	calibration
88	PR24	UHC-08-P24	calibration

89	PR24	UH-08-P24	calibration
90	PR24	DHC-08-P24	calibration
91	PR24	DH-08-P24	calibration
92	PR24	UHCE-08-P24	calibration
93	PR25	E-08-WOL-P25	verification
94	PR25	UH-08-P25	verification
95	PR25	UH-08-P25 (Different combinations)	verification
96	PR26	UH-08-P26	validation
97	PR26	EB-08-WOL-P26	verification
98	PR26	UHC-08-P26	validation
99	PR26	UHC-08-P26	validation
100	PR26	C-08-WOL-P26	validation
101	PR27	DH-08-P27	validation
102	PR27	UH-08-P27	validation
103	PR27	UHC-08-P27	validation
104	PR27	DHC-08-P27	validation
105	PR27	C45B-08-WOL-P27 (Half opening area)	verification
106	PR27	C47-08-WOL-P27	verification
107	PR27	EB-08-WOL-P27	verification
108	PR28	UH-08-P28	validation
109	PR28	D-08-P28	validation
110	PR28	DC-08-P28	validation
111	PR28	C45-08-WOL-P28	verification
112	PR28	C47-08-WOL-P28	verification
113	PR29	UH-08-P29	validation
114	PR29	D-08-P29	validation
115	PR29	DC-08-P29	validation
116	PR29	C4(45)-08-WOL-P29	verification
117	PR29	C4(47)-08-WOL-P29	verification
118	PR30	NA	validation
119	PR31	UC-07-P31	validation
120	PR31	DC-07-P31	validation
121	PR31	U-07-P31	validation
122	PR31	D-07-P31	validation
123	PR31	E-07-WL-P31	verification
124	PR31	CWF-07-WL-P31	verification
125	PR31	C50-07-WL-P31	verification
126	PR31	C50-07-WOL-P31	verification
127	PR31	C45-07-WL-P31	verification
128	PR31	C45-07-WOL-P31	verification
129	PR32	UC-07-P32	validation
130	PR32	U-07-P32	validation
131	PR32	DC-07-P32	validation
132	PR32	D-07-P32	validation
133	PR33	UC-07-P33	validation

134	PR33	U-07-P33	validation
135	PR33	DC-07-P33	validation
136	PR33	D-07-P33	validation
137	PR34	UC-07-P34	validation
138	PR34	U-07-P34	validation
139	PR34	DC-07-P34	validation
140	PR34	D-07-P34	validation
141	PR35	UC-07-P35	validation
142	PR35	U-07-P35	validation
143	PR35	DC-07-P35	validation
144	PR35	D-07-P35	validation
145	PR36	UC-07-P36	validation
146	PR36	U-07-P36	validation
147	PR36	DC-07-P36	validation
148	PR36	D-07-P36	validation



(a)



(b)

Figure 5-1. Simulated skimming Curtain No. 4: (a) Layout of Curtain No. 4 with respect to Prattville Intake; (b) View of the model Curtain No. 4.

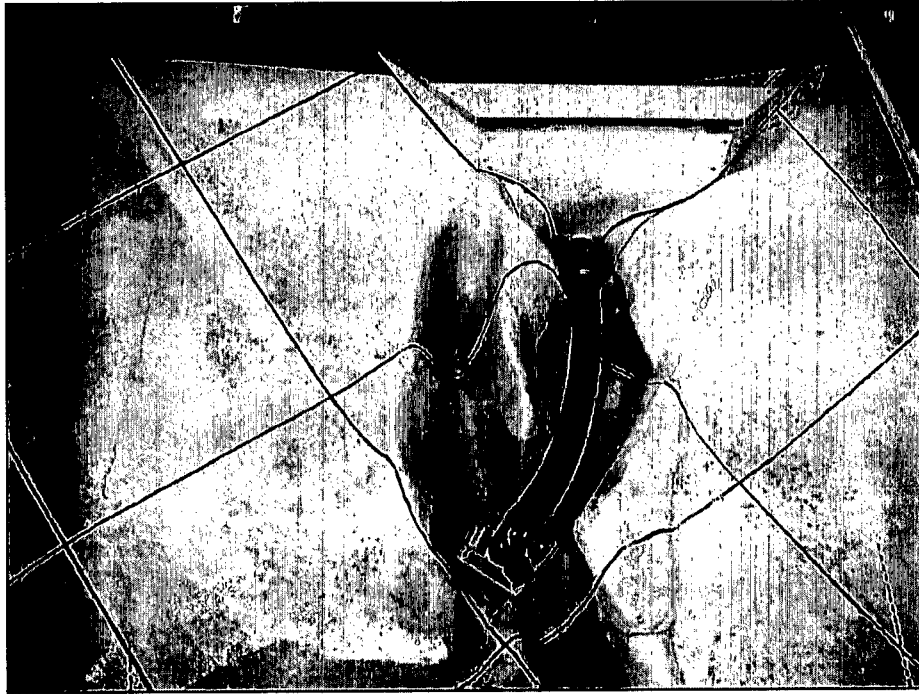


Figure 5-2. Short pipe with hooded inlet.

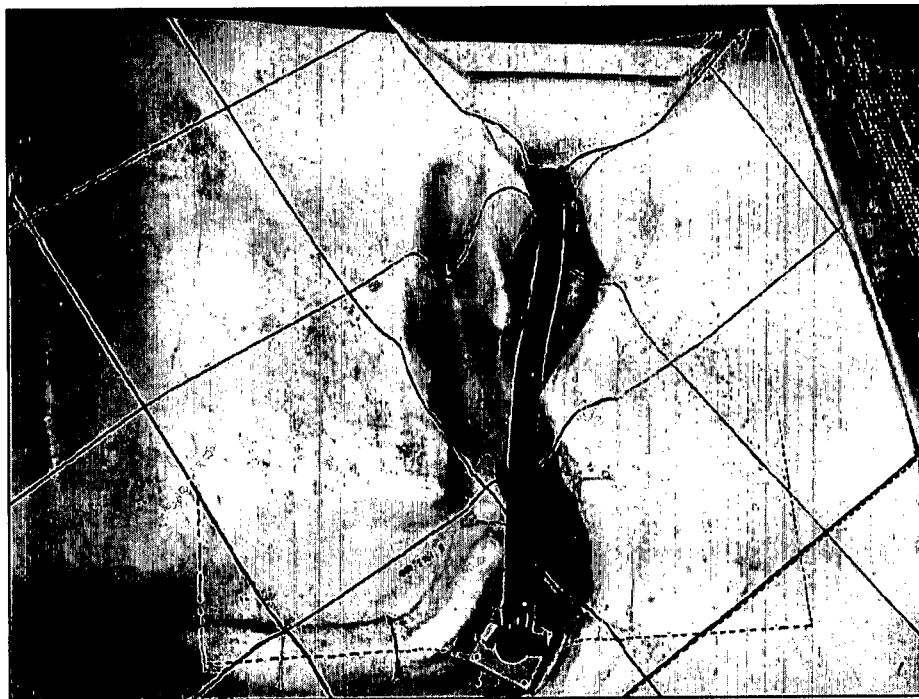


Figure 5-3. Long pipe with hooded inlet.

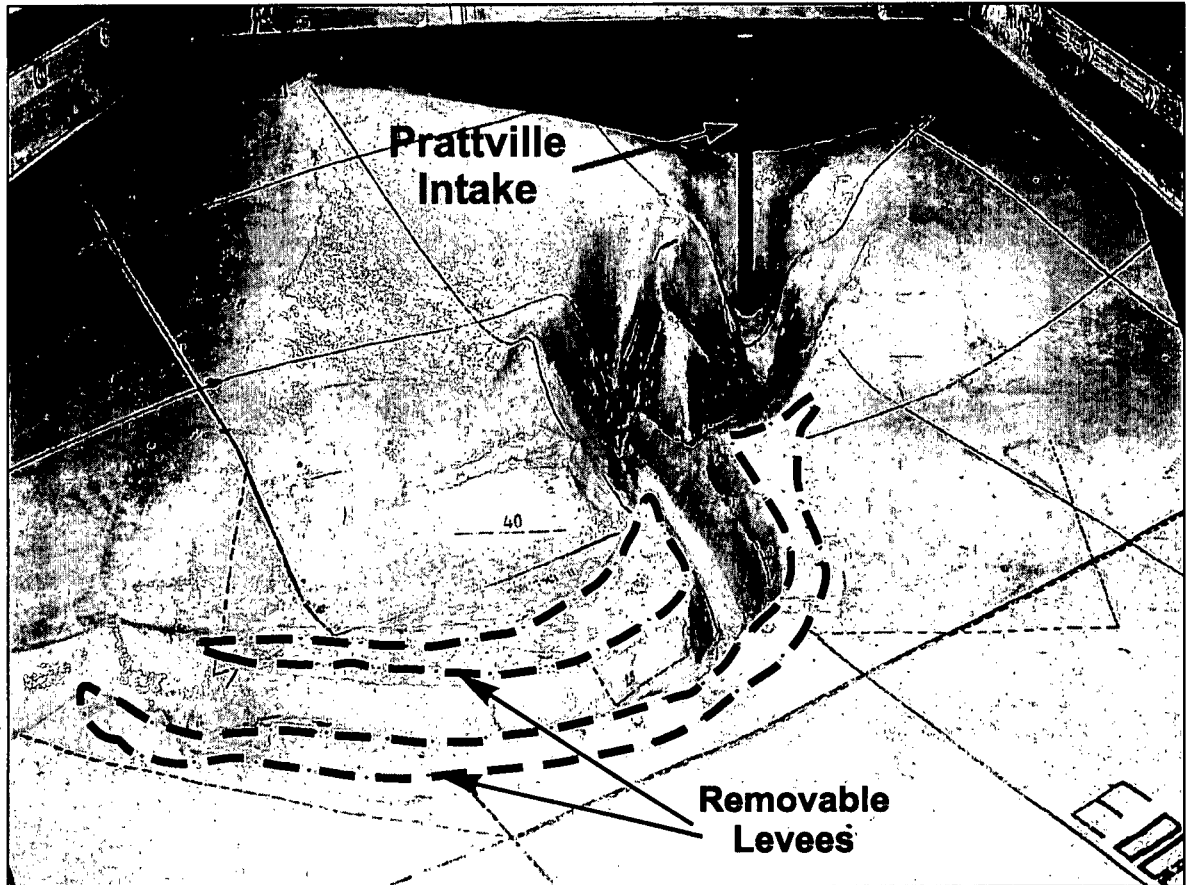
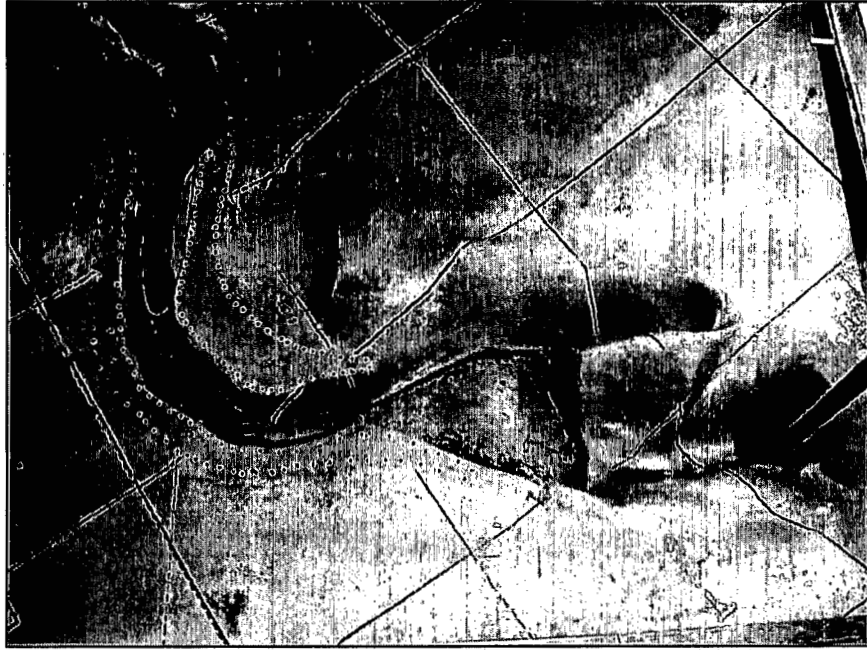


Figure 5-4. Levees removed from the incised channel near the Intake. Levee location is indicated by dashed lines.



(a)



(b)

Figure 5-5. Channel excavated in the confluence area near Prattville Intake: (a) general view with levees removed; (b) close-up view of the excavated area.

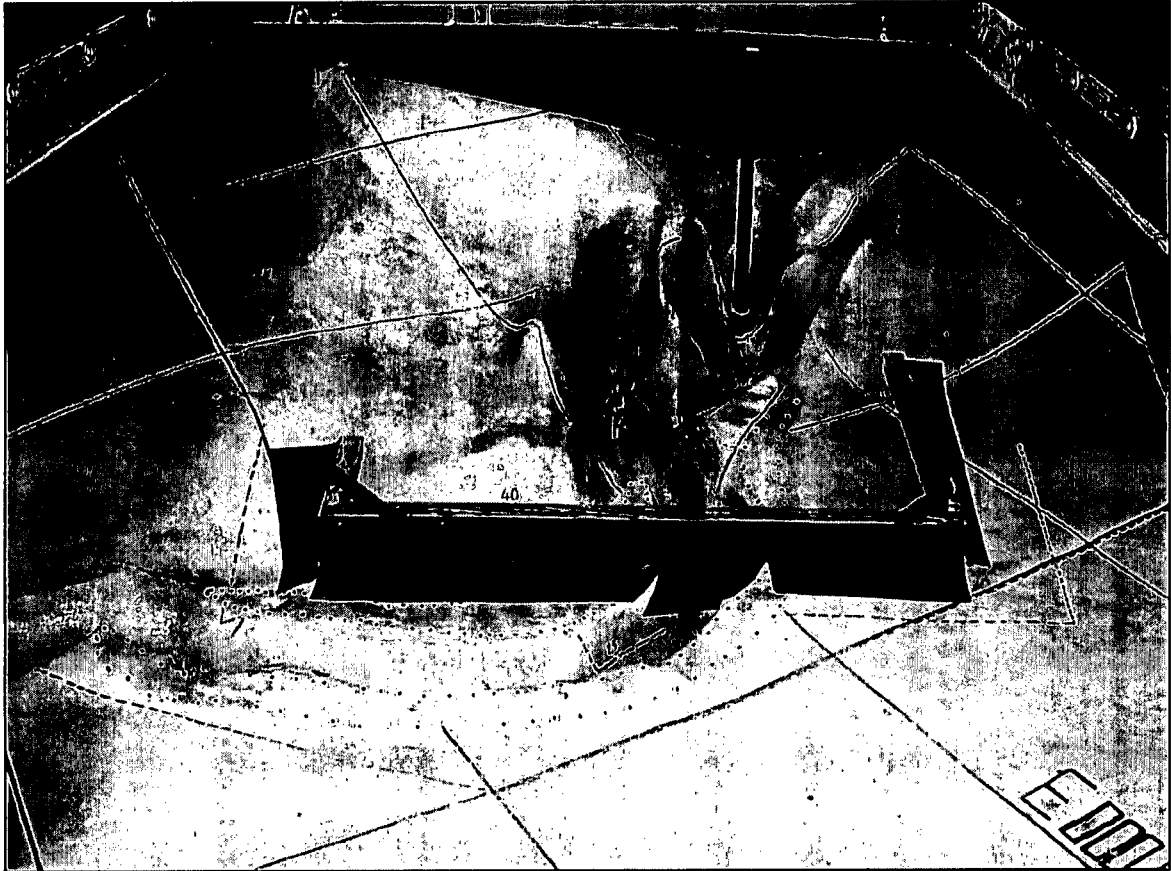


Figure 5-6. A view of the model bottom sill. The levees are removed.

## 6. TESTBOX RESULTS: EXISTING INTAKE CONFIGURATION

### 6.1 Introduction

The use of different length scales for vertical and horizontal dimensions (vertical distortion) in the hydraulic model requires that a calibration factor  $\alpha$  be applied in setting and interpreting the model-scale outflow discharges calculated using Eq. 4-1, and then applying those results in predicting the performance of Prattville Intake. This chapter presents and discusses the results from the following calibration procedure carried out using the laboratory testboxes and a numerical model applied to the existing configuration of Prattville Intake:

1. Calibration results for  $\alpha$  obtained from the testboxes subject to the July water-temperature and water-level conditions at Lake Almanor;
2. Validation results for  $\alpha$  obtained from the testboxes subject to the June and August water-temperature and water-level conditions at Lake Almanor;
3. Validation results for  $\alpha$  obtained from the numerical model simulating the water-temperature and water-level conditions typical of Lake Almanor during July; and,
4. Verification of  $\alpha$  obtained from comparison of results from the open testboxes and field measurements obtained from Prattville Intake during August, July and June 2000, and August 1994. The results presented in this chapter are based on the water-temperature profiles and water-surface elevations measured for those months (Figure 2-6).

Several questions had to be addressed in the course of the tests. One question was whether a single value of  $\alpha$  would be found for both pairs of testboxes. The second question was whether that value of  $\alpha$  would apply to the range of outflow discharges tested. A third question concerned how well the relationship between outflow

temperature,  $T_{out}$ , and discharge ratio,  $Q/Q_0$ , obtained from the testboxes would concur with that relationship as indicated by field data from Prattville Intake. Full agreement in this respect was not expected, because the testbox geometries did not fully replicate the geometry of Prattville Intake. Nonetheless, it was anticipated that the data from the undistorted Open testbox should reasonably agree with the field data.

A further verification check is given in Chapter 7, where data from the hydraulic model of Prattville Intake are compared to the field data mentioned in item 4 above. Moreover, additional verification is provided by in Chapter 8, which describes the outcome of the testbox work to check the temperature-reducing performance of the skimming curtain placed around Prattville Intake in the hydraulic model. Chapter 8 concludes with theoretical support ventured for the value of  $\alpha$  obtained from the testboxes and numerical model.

The present chapter begins by outlining and discussing the general trends that the testbox results delineate. The trends relate outflow temperature to outflow discharge for the distorted and undistorted testboxes, and provide a framework for discussing the data.

## 6.2 Outflow Adjustment Factor

The series of tests with the testboxes were aimed at determining the value, or value range, of the outflow adjustment factor  $\alpha$  in the expression (Eq. 4-3)

$$(Q_{0m})_{cal} = \alpha(Q_{0m}) = \alpha(Q_{0p} / Q_r) \quad (6-1)$$

in which the subscript 0 denotes the normal operating discharge of Prattville Intake; i.e., the prototype Intake releasing a discharge of 1,600cfs.

A theoretical value for the calibration factor  $\alpha$  would seem not to be readily determined by way of analysis, because the flow field in the testboxes, especially near their inlets, is markedly three-dimensional and includes significant differences in the size and strengths of flow swirl, eddies and turbulence. Moreover, the flow field changes as the rate of

outflow released through the inlet increases, especially in a situation involving the selective withdrawal of water from a thermally stratified water body. The factor  $\alpha$  must be determined from laboratory model tests by means of a set-up such as the present pair of testboxes, or perhaps from numerical simulation. Yet, in hindsight (as explained in Chapter 8), a simple theory evidently can be formulated to give a value for  $\alpha$ , at least for the present testboxes and hydraulic model, that agrees with the experimental results.

Though a value for  $\alpha$  can be assessed empirically from laboratory or numerical experiments comparing distorted and undistorted models simulating the same single regime and rate of outflow from a given geometric configuration of intake and surrounding bathymetry, it would seem that  $\alpha$  might vary somewhat in value as outflow rate and flow regime change. Indeed as the present investigation primarily was concerned with developing a design modification for Prattville Intake, which operates predominantly at its design outflow discharge,  $Q_0 = 1,600\text{cfs}$ , the calibration effort required determining a value of  $\alpha$  commensurate with that discharge. The calibration tests would show if  $\alpha$  varied for other flow conditions. The tests also would need to determine whether the value of  $\alpha$  at  $Q_0$  still applied when the intake design was modified and flow regime altered.

Figure 6-1 illustrates conceptually the relationship between the outflow temperature  $T_{out}$  and discharge ratio  $Q/Q_0$ , and indicates a shift in the relationships developed by the distorted and undistorted testboxes (implying the same shift for distorted and undistorted hydraulic models of Prattville Intake). The positions of the two curves indicate that  $\alpha \geq 1$ . A value of  $\alpha$  at  $Q/Q_0 \approx 1$  can be estimated from the offset between the two curves in Figure 6-1. That discharge condition value corresponds to the normal operating condition of Prattville Intake.

For very small outflow discharges, both the distorted and the undistorted testboxes would withdraw water predominantly from the hypolimnion. Therefore the values of  $T_{out}$  for the distorted and undistorted testboxes should be the same. Commensurately, for high values of outflow discharge, the inlets of both testboxes would withdraw water fully mixed over

the full depth of water. Therefore the values of  $T_{out}$  would be the same for both testboxes, and would equal the temperature resulting when the water is fully mixed. At the two extremes of the pair of curves,  $\alpha$  would be 1.

Between these two limits there would be a difference in the relationship between  $T_{out}$  and discharge ratio  $Q/Q_0$ , because of differences in the flow field developed in each testbox. By virtue of the greater lateral distance in the undistorted testbox, and commensurately in an undistorted version of the hydraulic model of Prattville Intake, greater mixing of water is expected to occur in the undistorted testbox. Therefore the undistorted-testbox curve in Figure 6-1 should lie above that for the distorted testbox. The unit discharge ( $Q/W$ , where  $W$  is testbox width) is equal in the distorted and the undistorted testboxes; the width of the distorted testbox is  $1/5.5^{\text{th}}$  of the width of the undistorted testbox, and the distorted testbox conveyed  $1/5.5^{\text{th}}$  of the flow conveyed by the undistorted testbox. However, the outer portions of the undistorted testbox conveyed flow of equal unit discharge that increasingly had to cross laterally to the intake at the end of the testbox. Thereby, opportunity for increased flow rotation, and more mixing, occurred in the undistorted testbox than in the distorted testbox.

Further, the greater width of the undistorted testbox is expected to admit more non-uniformity in approach-flow distribution, which in turn would cause locally increased water velocities and, thereby, increased entrainment of warmer water from higher elevations of the water column. All this leads to the likelihood of the undistorted testbox releasing water at a higher outflow temperature,  $T_{out}$ , when  $Q/Q_0 \approx 1.0$ .

The data from the testboxes enable estimation of factor  $\alpha$ . As estimation of  $\alpha$  is not a precise calculation, it is appropriate to include an estimation margin. The following format was adopted for estimating  $\alpha$ :

$$\alpha = \bar{\alpha} \pm M\% \quad (6-2)$$

where  $\bar{\alpha}$  is the average value estimated for  $\alpha$ , and is the value used when interpreting and assessing results from the hydraulic model;  $M$  is an uncertainty margin used herein to reflect the uncertainty in simulation and measurement. Such uncertainty is inevitable with laboratory experiments. The present experiments did not make possible a thorough, scientific evaluation of  $M$ , as so doing requires conducting many more tests than was feasible in the context of the overall study. Nevertheless, the tests were sufficient in number to determine a value of  $M$  in terms of an approximate round-number percentage; e.g., 10, 30, 50%. Section 6.3 further explains how the values of  $\alpha$ ,  $\bar{\alpha}$ , and  $M$  were estimated.

### 6.3 Normalization of Data

Several formats were considered for presenting the textbox data, as well as data from the hydraulic model. Two alternative formats in particular were considered:

1. Outflow temperature,  $T_{out}$ , plotted versus discharge ratio,  $Q/Q_0$ ; and,
2. Outflow temperature normalized as  $\frac{T_{out} - T_{hypo}}{T_{epi} - T_{hypo}}$  plotted versus discharge ratio,  $Q/Q_0$ .

Here  $T_{hypo}$  = the temperature in the hypolimnion at the textbox-invert level;  $T_{epi}$  = the temperature in the epilimnion at mid-height of the epilimnion;  $Q_0$  is the design outflow scaled in accordance with Eq. (3-1); and,  $Q$  is variable outflow discharge. Figure 6-1 could also be presented as  $\frac{T_{out} - T_{hypo}}{T_{epi} - T_{hypo}}$  plotted versus  $Q/Q_0$ . Other normalized, or non-dimensional, combinations of outflow temperature were considered; but were discarded in favor of the aforementioned combination.

The erstwhile advantage of the temperature normalization  $\frac{T_{out} - T_{hypo}}{T_{epi} - T_{hypo}}$  is that it may take into account differences in water-temperature profiles in the modeled lake. Yet that, or

similar normalizations of  $T_{out}$ , are themselves approximations. Though useful for comparing and generalizing findings obtained from quite different water bodies, they do not entirely account for variations in temperature distribution or water depth, nor do they add much information for tests done with practically the same water-temperature profile in the lake. For the present study, small variations in temperature and depth did occur (despite the considerable care taken in monitoring and replenishing water in the basin of the hydraulic model), but they were not large enough to obscure the test results.

Though there are advantages in using the fully normalized format (alternative format 2, above) for presenting the temperature results, it was decided that it is more practical to work mainly with plots of  $T_{out}$ , plotted versus discharge ratio,  $Q/Q_0$ . Such plots more clearly show to a broad audience how outflow discharge and design modifications influence outflow temperature. Use of these plots was made possible by the excellent repeatability of the water-temperature profiles developed in the modeled lake. For illustrative purposes, examples of the data plotted in format 2 are presented in Section 6.4.

#### 6.4 Calibration Tests: Testboxes

The data obtained for the testboxes, configured in the Bay and the Open forms (layouts given in Figures 4-8 and 4-10), and subject to the thermal conditions prescribed for Lake Almanor during July are shown respectively in Figures 6-2 and 6-3, which plot  $T_{out}$  versus  $Q/Q_0$ . The same data, plotted in normalized format as  $\frac{T_{out} - T_{hypo}}{T_{epi} - T_{hypo}}$  versus  $Q/Q_0$ , are shown in Figures 6-4 and 6-5.

The two pairs of figures show the same trends. As anticipated, the curves in Figures 6-2 and 6-3 show the same trend as indicated by the pair of conceptual curves in Figure 6-1. Additionally, the same trend is shown by the curves of normalized data in Figures 6-4 and 6-5.

The curves obtained from the Open testboxes, however, lie above those obtained from the Bay testboxes. The latter testboxes produced colder outflow. Flow-visualization observations using two colors of dye showed that for the lower flows, the intakes in each testbox withdrew colder water from the lower levels of the water column. As outflow discharge increased, a mix of water was withdrawn from over the full depth of water. For  $Q/Q_0 \approx 1.0$  in either of the Bay or Open testboxes, the intake replicated in the distorted testbox continued to withdraw overall colder water than did the intake replicated in the undistorted testbox. Consequently, the performance curve for the undistorted box lies above that for the distorted box, such that  $\alpha > 1$ .

It is evident by comparing the two sets of data that, as  $Q/Q_0$  increases, the temperatures of outflow from the Open testboxes are higher (Figure 6-3), by about 1.5 to 2°C, than are the outflow temperatures from the Bay testboxes (Figure 6-2). The higher temperatures of outflow from the open testboxes are attributable to a larger flow of warmer water from the upper layer (epilimnion) of water being drawn into the intake simulated as the Open testboxes. In particular, the submerged walls of the Open testboxes function to skim warmer water from regions to the sides of the intake in each testbox; this flow feature was observed also to occur for Prattville Intake in the hydraulic model. The upper asymptote (the practically constant value of about  $T_{out} \rightarrow 19.5^\circ\text{C}$  obtained when  $Q/Q_0$  exceeds approximately 2.5) approached by the Open-testbox data has the same value as the asymptote obtained with the hydraulic model of Prattville Intake.

For the calibration tests analyzed herein, the value of  $\alpha$  was determined as shown in Figures 6-3 and 6-5:

1. At the value of  $T_{out}$  read where  $Q/Q_0 = 1$  intersects the average curve for the data from the undistorted testbox, a line is extended across to intersect the average curve for data from the distorted testbox;
2.  $\bar{\alpha}$  is read as the value of  $(Q/Q_0)$  at the intersection of the average curve fitted through data from distorted testbox; and,

3.  $M\%$  is estimated in approximate terms from the spread of  $Q/Q_0$  about the average curve fitted through data from the distorted testbox, in the manner shown in Figures 6-3 and 6-5. The spread is determined from the spread in values of  $T_{out}$  about the mean curve found from the undistorted testbox. Accordingly, an uncertainty margin is indicated about the average curve obtained for the distorted testbox data.

This procedure was applied to all the results presented below. For the Bay testboxes (Figure 6-2), the method results in

$$\alpha = 1.7 \pm (\text{max deviation } 0.3)$$

or

$$\alpha = \bar{\alpha} \pm M\% = 1.7 \pm 18\%$$

For the Open testboxes (Figure 6-3), the method results in

$$\alpha = 1.7 \pm (\text{max deviation } 0.4)$$

or

$$\alpha = 1.7 \pm 24\%$$

The spread of data about the average curve for the Open testboxes is encompassed by the margin  $M = \pm 24\%$ . This margin means that values of  $\alpha$  are within the range  $1.3 \leq \alpha \leq 2.1$ .

The calibration tests show that, to produce the same water temperature of outflow from the distorted testbox as occurs for the undistorted model set at the design operating flow condition  $Q/Q_0 = 1$ , the discharge ratio for the distorted testbox must be set at  $Q = 1.7Q_0$ . In other words, this calibration result implies that the rates of outflow from the distorted hydraulic model of Prattville Intake,  $Q_{0m}$ , should be increased by an adjustment factor  $\bar{\alpha}$

= 1.7 to make the temperature of the outflow from the distorted hydraulic model equal to the temperature of the prototype outflow released by Prattville Intake.

It is intriguing, and appears somewhat of a mystery, to find that the same value of  $\bar{\alpha}$  was obtained for both the Bay and the Open forms of the testboxes, especially since the two geometries are significantly different, and that the Open testboxes released overall warmer water than did the Bay testboxes. The value of  $\alpha$  depends on the extent of mixing and disruption of water stratification in each testbox. In turn, mixing and layer disruption depend on flow turbulence, eddies, and shear stresses developed by flow drawn to the model intake; these flow features are affected by testbox geometry. Turbulence and shear stresses are manifestly unsteady phenomena quick to admit variations in  $T_{out}$  and therefore in  $\alpha$  estimates, as indicated for the margins  $M$ . The more complicated geometry of the open testboxes produced a slightly larger value of  $M$ .

It is relevant to note that work with the testboxes also showed that changes in outflow may cause thermocline oscillations, as evident in the oscillations in outflow temperature,  $T_{out}$ . The oscillations were of about 2 to 5 minutes in duration in the model, and were of about 0.5 to 1°C in magnitude. A value of  $T_{out}$  was recorded once the oscillations had dissipated. The oscillations were most pronounced for tests run with  $Q/Q_0 = 0.5$  to 1.0 for the August and July conditions of the lake. For larger values of this discharge ratio, outflow temperature seemed steadier subsequent to a change in flow rate. The oscillations also contribute to the uncertainty margin  $M$  values for the July and August conditions simulated.

### **6.5 Validation Results: Testboxes**

The data obtained from the Bay testboxes and the Open testboxes are shown in Figures 6-6 and 6-7 for the conditions prevailing for Lake Almanor during August, 2000. The figures relate  $T_{out}$  to  $Q/Q_0$ . The sets of curves in these figures indicate the same trends as in Figures 6-2 and 6-3, and give the calibration assessment  $\alpha = 1.7$ , when relating  $T_{out}$  values from the testboxes for the design operating condition  $Q/Q_0 = 1$  in the undistorted testbox.

The values for  $\alpha$  obtained for August concur with, and thereby lend validation to the value of  $\alpha$  obtained with the calibration tests done for the July, 2000 condition of Lake Almanor (Figures 6-2 and 6-3).

As evident in Figure 6-8, experiments with the Bay testboxes subject to the June, 2000 condition of Lake Almanor also resulted in  $\alpha = 1.7$ , when comparing  $T_{out}$  values for the undistorted and distorted testboxes operating at  $Q/Q_0 = 1$ . The June testbox data therefore further validate the calibration results obtained for the July condition.

The comparison of the curves shown in Figure 6-9 for the undistorted Bay testbox, for June, July, and August, illustrates an overall tendency of outflow warming as summer progresses (June through August) and Lake Almanor warms. This trend is to be expected, as it is in accordance with the overall warming of the lake's water.

The consistent value for  $\alpha$  (or  $\bar{\alpha}$ ) obtained for the Bay and the Open testbox forms, subject to the temperature profiles and water-surface elevations prescribed for June, July and August, indicates that increasing outflow discharge from the distorted testbox by the average calibration factor  $\bar{\alpha} = 1.7$  will produce essentially the same extent of mixing of water as occurs with an outflow of  $Q/Q_0 = 1$  through the undistorted testbox. The constancy of  $\bar{\alpha}$  for the two pairs of testboxes is intriguing. As mentioned in Section 4.4.1, an initial question was whether  $\bar{\alpha}$  would vary for the two pairs of testboxes, because their geometry differed substantially; a change in geometry would cause a flow field change that could respond differently to vertical distortion.

A further initial question concerned the applicability of  $\bar{\alpha}$  for the range of outflows tested. Figure 6-10 shows that the entire two curves in Figure 6-7 merge when the  $Q/Q_0$  values of the curve obtained from the undistorted testbox are multiplied by the factor  $\bar{\alpha} = 1.7$ . The merging suggests that  $\bar{\alpha}$  also applies generally for setting the range of outflows from the vertically distorted hydraulic model. Therefore, it follows that the factor  $\bar{\alpha}$  may be used to relate the curves of  $T_{out}$  versus  $Q/Q_0$ , as obtained from the distorted and the undistorted testboxes.

## 6.6 Validation Results: Numerical Model

The results from the U2RANS 3-D, numerical-model simulation of the distorted and the undistorted, Bay testboxes further validated the value of the calibration factor,  $\alpha$ , determined from the testbox experiments. The numerical model used the same temperature profile associated with the thermal stratification as for the test box experiment used in the comparison. The target temperature profile for the comparison was that for July. However, it was decided to use the actual profile prevailing in the hydraulic model during the period of testing. That profile differed slightly from the target July profile in the following manner: the bottom temperature was 12°C and the surface temperature 21°C; and the thermocline varied nearly linearly from 12°C at EL. 4440ft to 20.5°C at EL. 4470ft.

The results of the simulation are shown in Figure 6.11. This figure also shows the outflow temperatures measured in the companion testbox experiment. The value of  $\alpha$  is seen to be around 1.6, similar to that estimated from the testbox experiments themselves.

## 6.7 Comparison with Field Data

The essential purpose of the series of calibration, validation and verification tests conducted with the testboxes is to ensure that the hydraulic model accurately represents the outflow performance of Prattville Intake in its existing configuration and when modified. Meeting this purpose requires comparing hydraulic-model data with the field data available from Prattville Intake. That comparison is done in Chapter 7, where the value of  $\bar{\alpha}$  determined from the testboxes is used to relate the data from the vertically distorted hydraulic model to the available field data. Since the testboxes were used to calibrate the hydraulic model, it is useful to compare how well the outflow data from the testboxes, especially the undistorted Open testbox, compare with the available field data.

The undistorted Open testbox approximates an undistorted representation of the vertically distorted hydraulic model of Prattville intake and the lake bathymetry adjoining it. In particular, it is of interest to check whether the value of  $T_{out}$  obtained when  $Q/Q_0 \approx 1$  from that testbox is the same as produced by Prattville Intake operating at about its normal rate

of outflow. Figure 6-12 shows that the values of  $T_{out}$  at  $Q/Q_0 \approx 1$  produced by the undistorted Open testbox are in close proximity to the field data for the August 1994, August, and July 2000 conditions of Lake Almanor. However, the testbox data and the field data do not coincide exactly.

The field data were not expected to coincide exactly with the data from the undistorted Open testbox, because of differences in the geometry and location of the actual Intake in the field compared with the inlet geometry used for the testboxes. In particular, the testboxes only roughly simulate the lake bathymetry adjacent to the Prattville Intake, and the testboxes do not simulate the Intake as a free-standing tower structure. The Open-testbox data and field data, though, are in sufficiently close agreement as to confirm the appropriateness of the testboxes for calibrating the vertically hydraulic model.

The Bay testboxes are less geometrically similar to Prattville Intake and its surrounding lake bathymetry than are the Open testboxes. Consequently the data from the undistorted Bay testbox, though having the same overall trend as the field data (at least for August), do not lie close to the field data. The outflows from the undistorted Bay testbox (Figure 6-6) are generally cooler outflow temperatures than do the field data (Figure 6-12).

## 6.8 Comments

To address the uncertainty inherent in using a single value of discharge-calibration coefficient,  $\bar{\alpha}$ , it was decided that tests conducted with the hydraulic model should be conducted for the range of model discharges  $0.25 \leq Q/Q_0 \leq 2.75$ . This procedure ensures that testing encompasses the requisite model flow rate, and that it produces data trends sufficiently robust upon which to base decisions regarding the merits of a design modification to Prattville Intake. Furthermore, that range of  $Q/Q_0$  encompasses the operating range for outflows released from Prattville Intake.

From Eqs (4-1) and (4-2) in Chapter 4, the calibration coefficient  $\alpha$  should be within the range  $1 < \alpha < 5.5 (= X/Y)$ . The finding that  $\alpha$  is quite close to the lower limit would seem to reflect the largely two-dimensional (width-averaged) nature of the flow drawn

into the testboxes and to the simulated intake at the end of each testbox. The overall influences of turbulence and eddy-strengthening consequence of vertical distortion of flows around changes in boundary geometry do not seem to adversely affect model capability to simulate flow withdrawal and thermocline drawdown; in principle, strengthened eddies (and large-scale turbulence) would enhance mixing, notably at the entrance to the distorted testbox; if anything, therefore, greater mixing would have been anticipated. Yet, it is intriguing that the factor  $\bar{\alpha} = 1.7$  seems to apply on the average to all the testbox cases investigated.

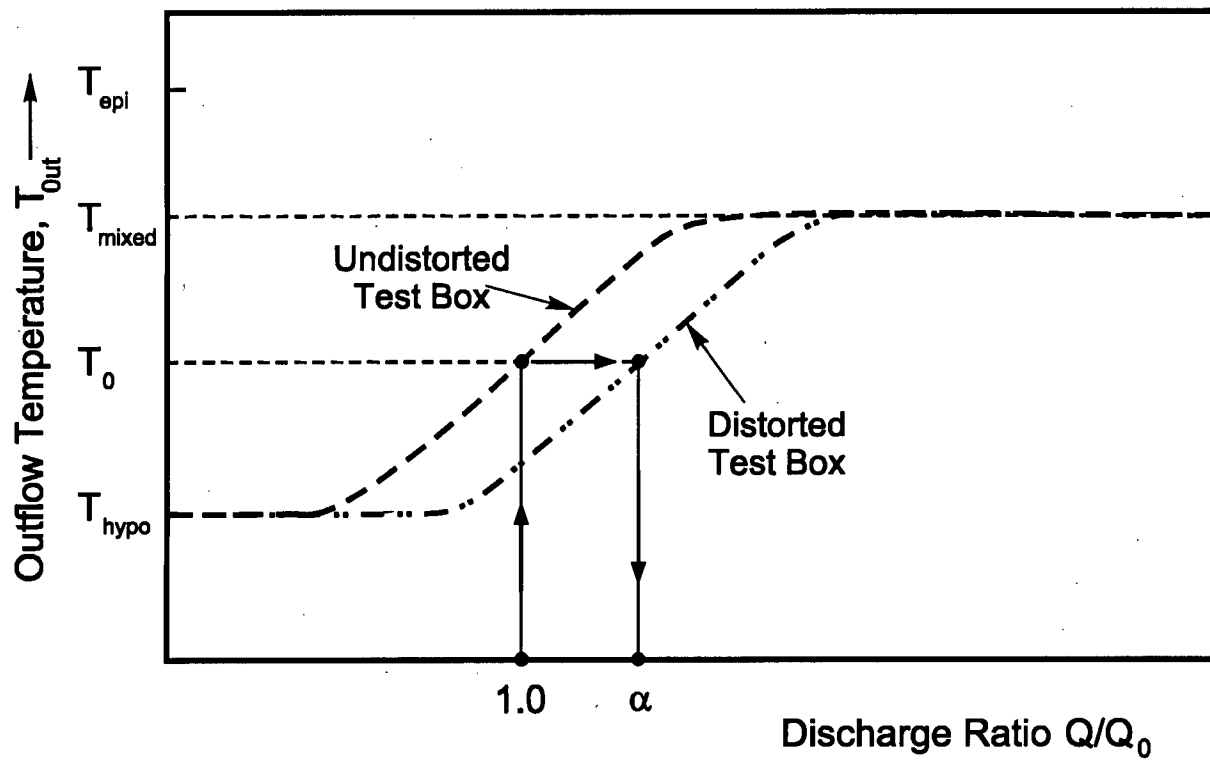


Figure 6-1. General relationship between the outflow temperature  $T_{out}$  and discharge ratio  $Q/Q_0$  for the distorted and undistorted testboxes.

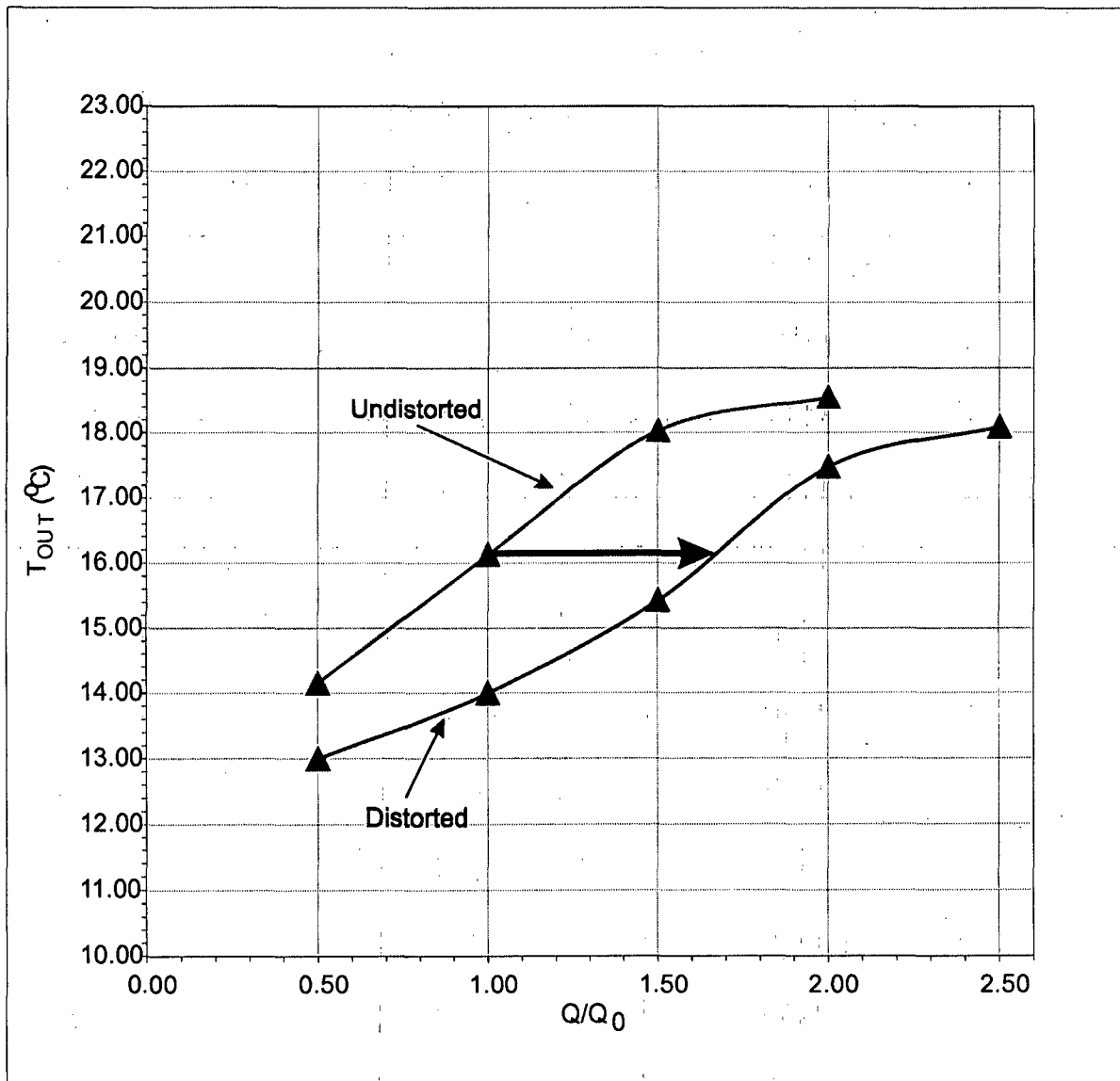


Figure 6-2. Results from Bay testboxes: July condition.

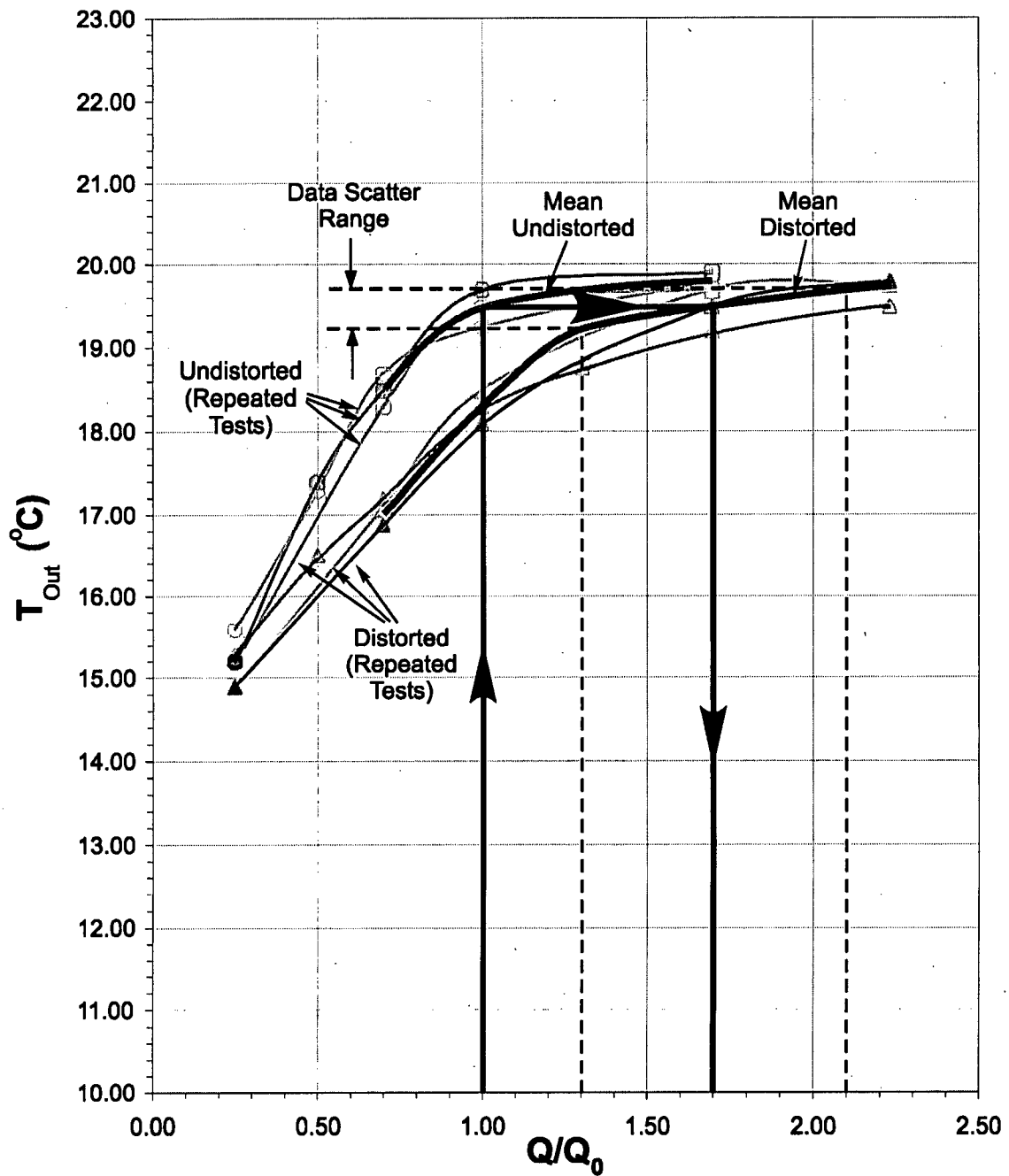


Figure 6-3. Results from Open testboxes; July condition.

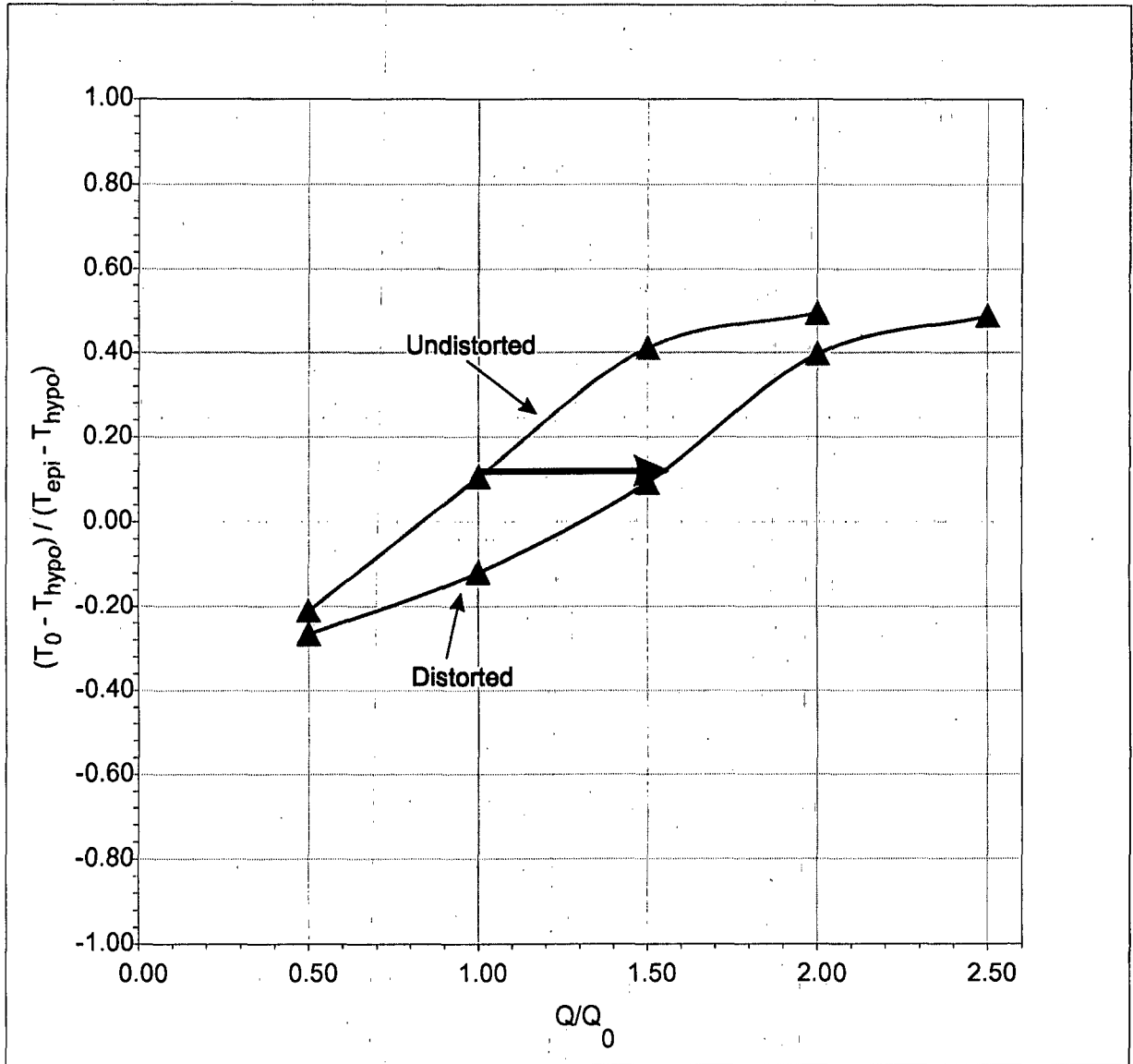


Figure 6-4. Normalized results from Bay testboxes; July condition.

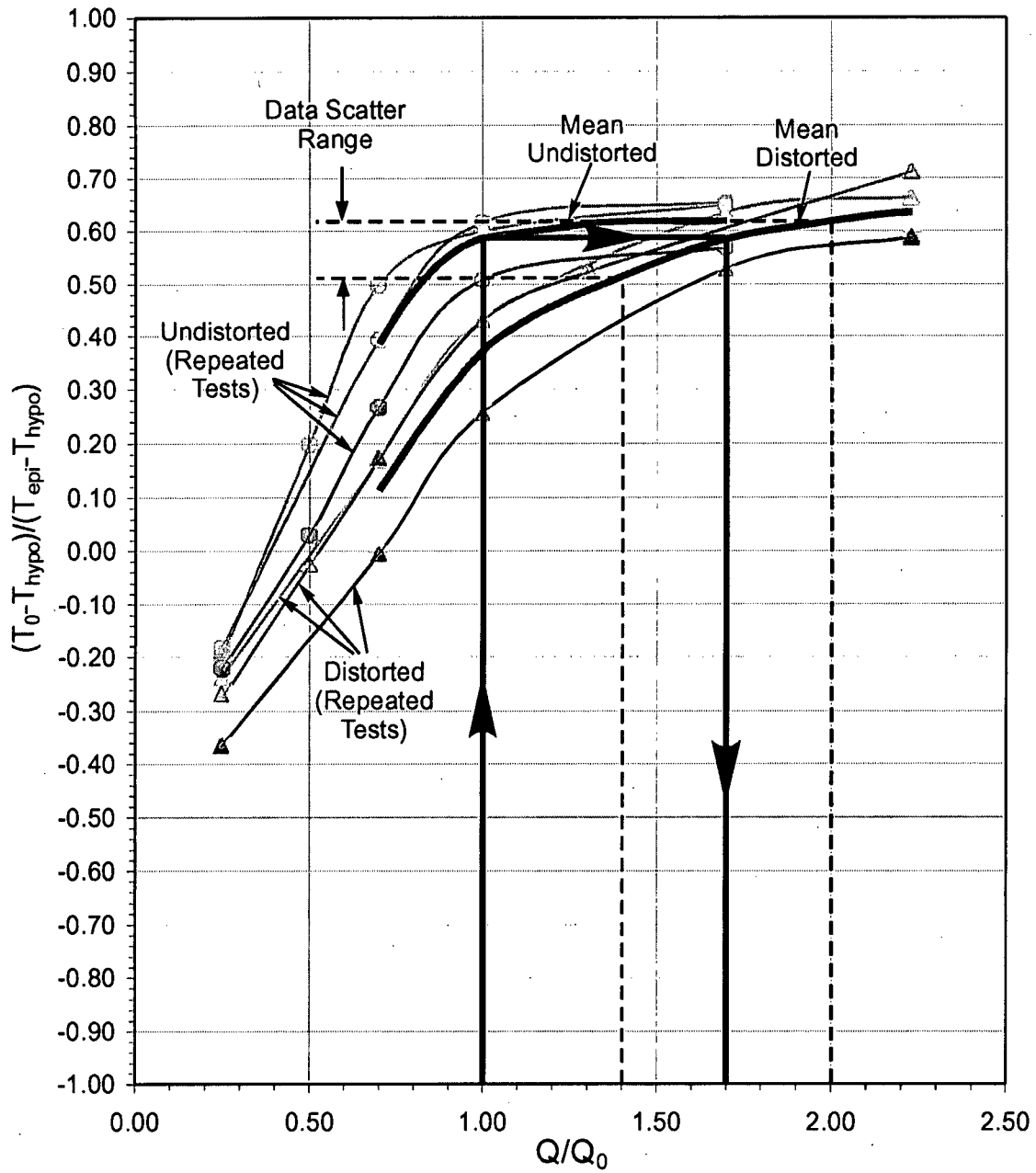


Figure 6-5. Normalized results from the Open testboxes; July condition.

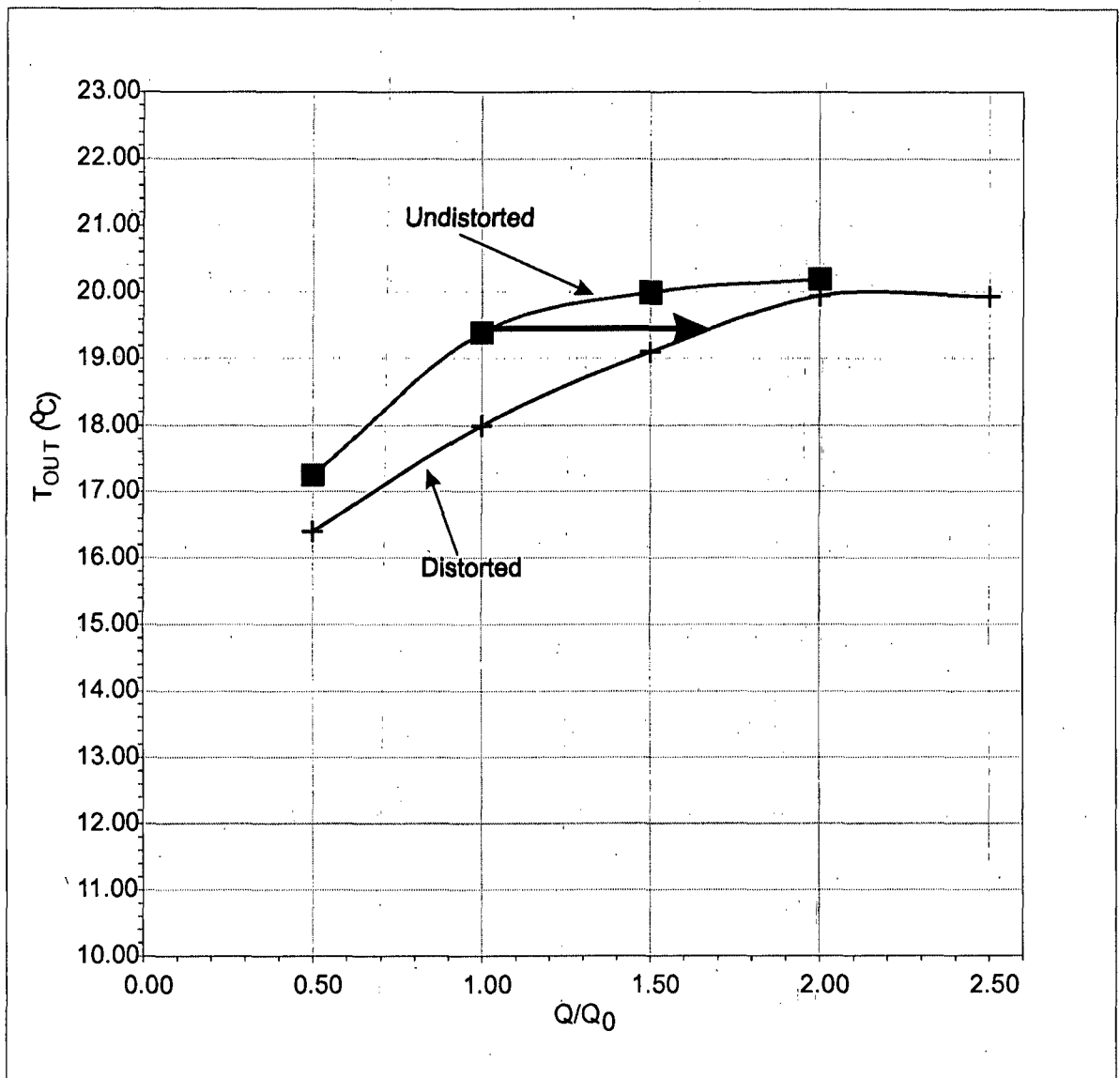


Figure 6-6. Results from Bay testboxes; August condition (no curtain).

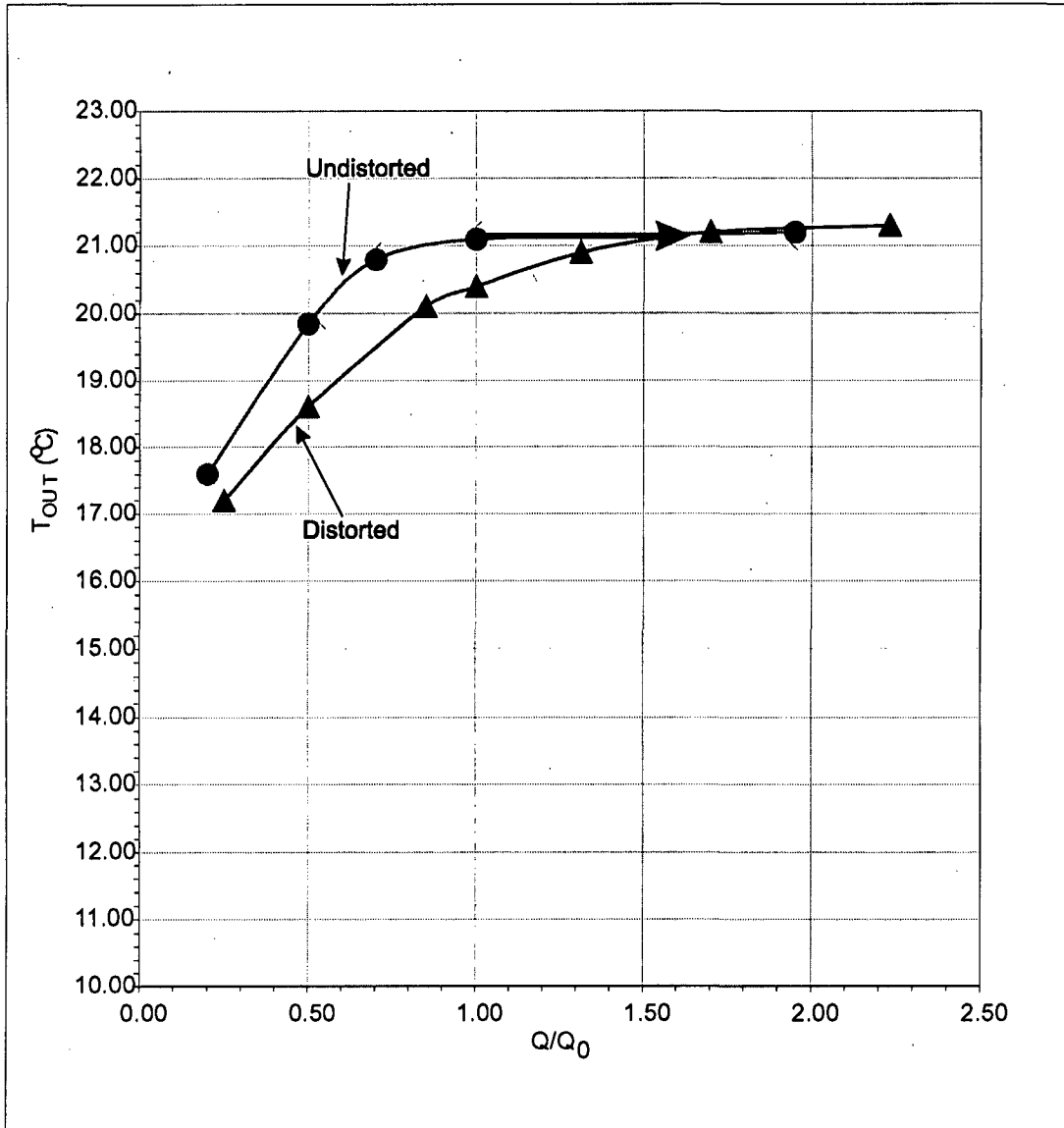


Figure 6-7. Results from Open testboxes; August condition (no curtain).

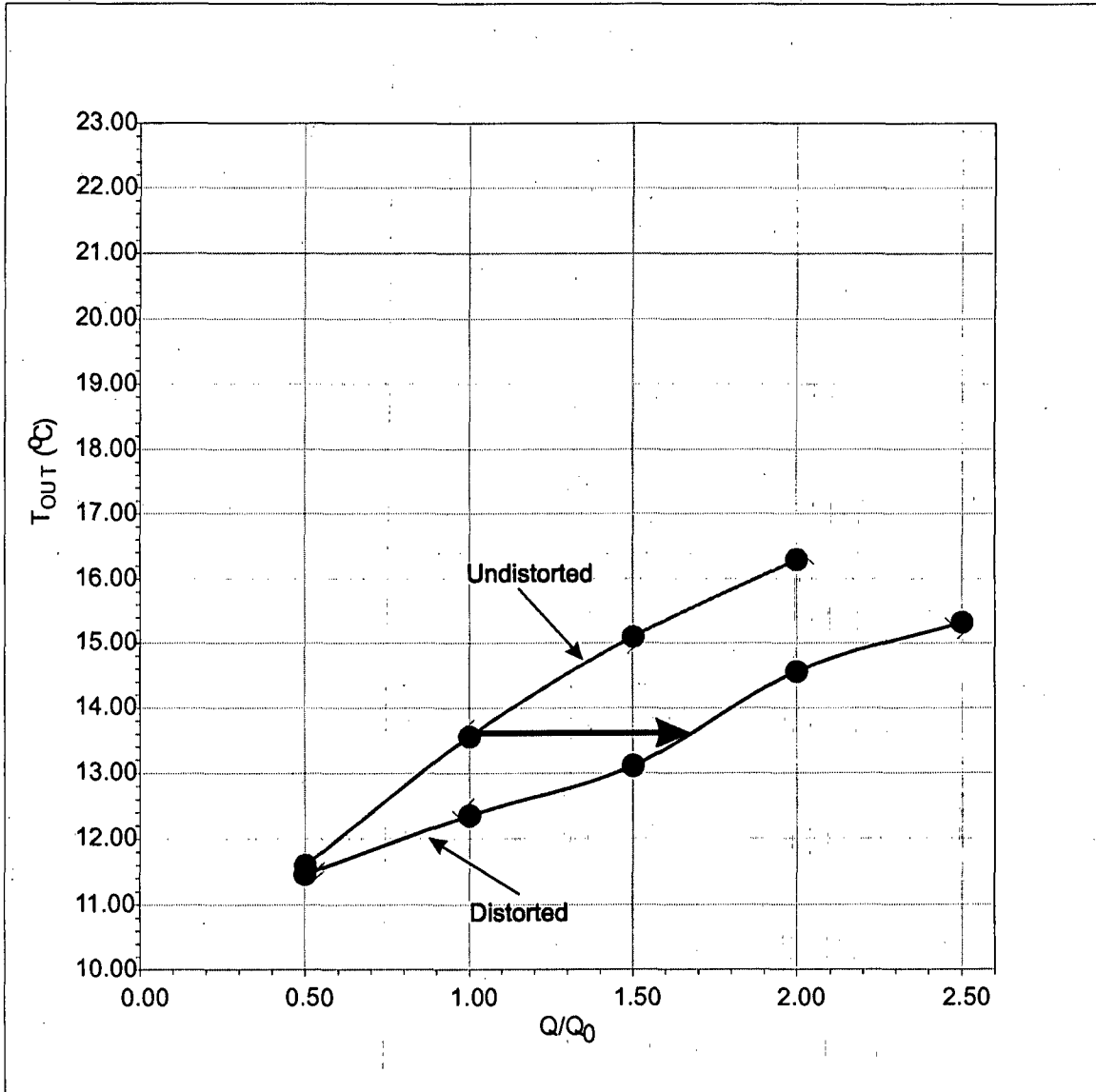


Figure 6-8. Results from Bay testboxes; June condition (no curtain).

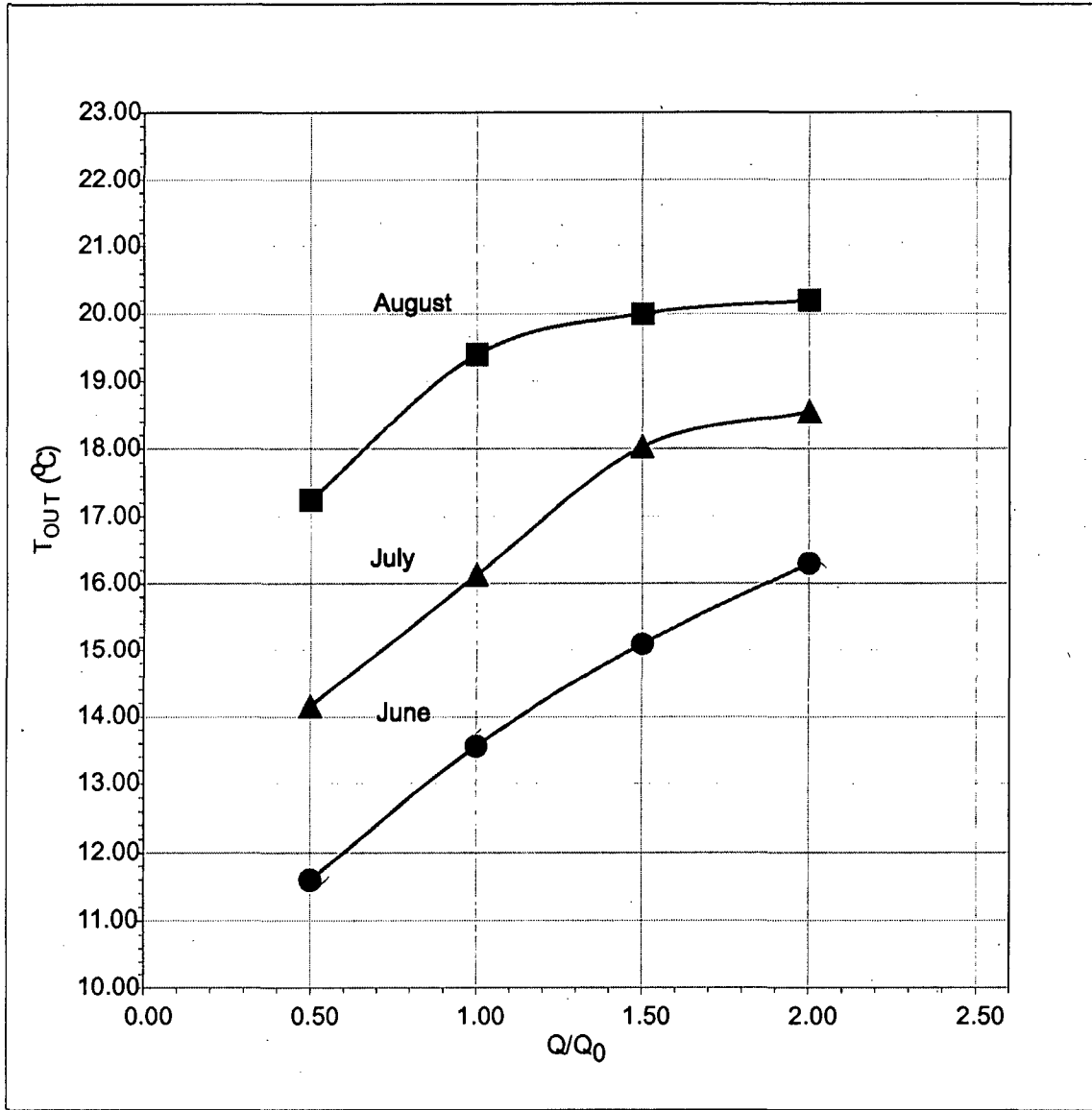


Figure 6-9. Variation of outflow temperature,  $T_{out}$ , with  $Q/Q_0$  for the Bay testboxes subject to June, July, and August conditions.

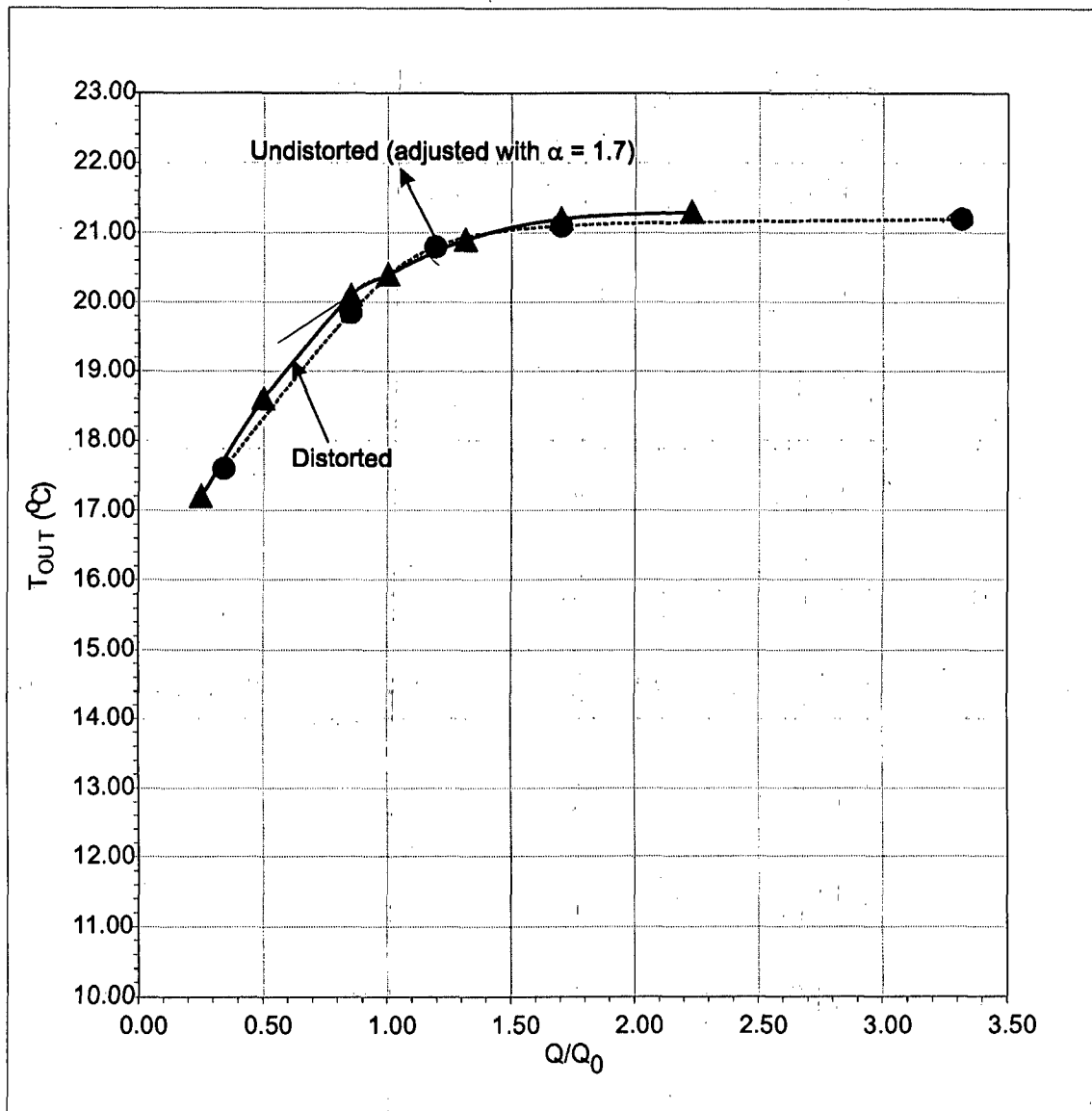


Figure 6-10. Comparison of results from the distorted Open testbox and from the undistorted Open testbox (adjusted with the calibration factor  $\alpha = 1.7$ ); August condition.

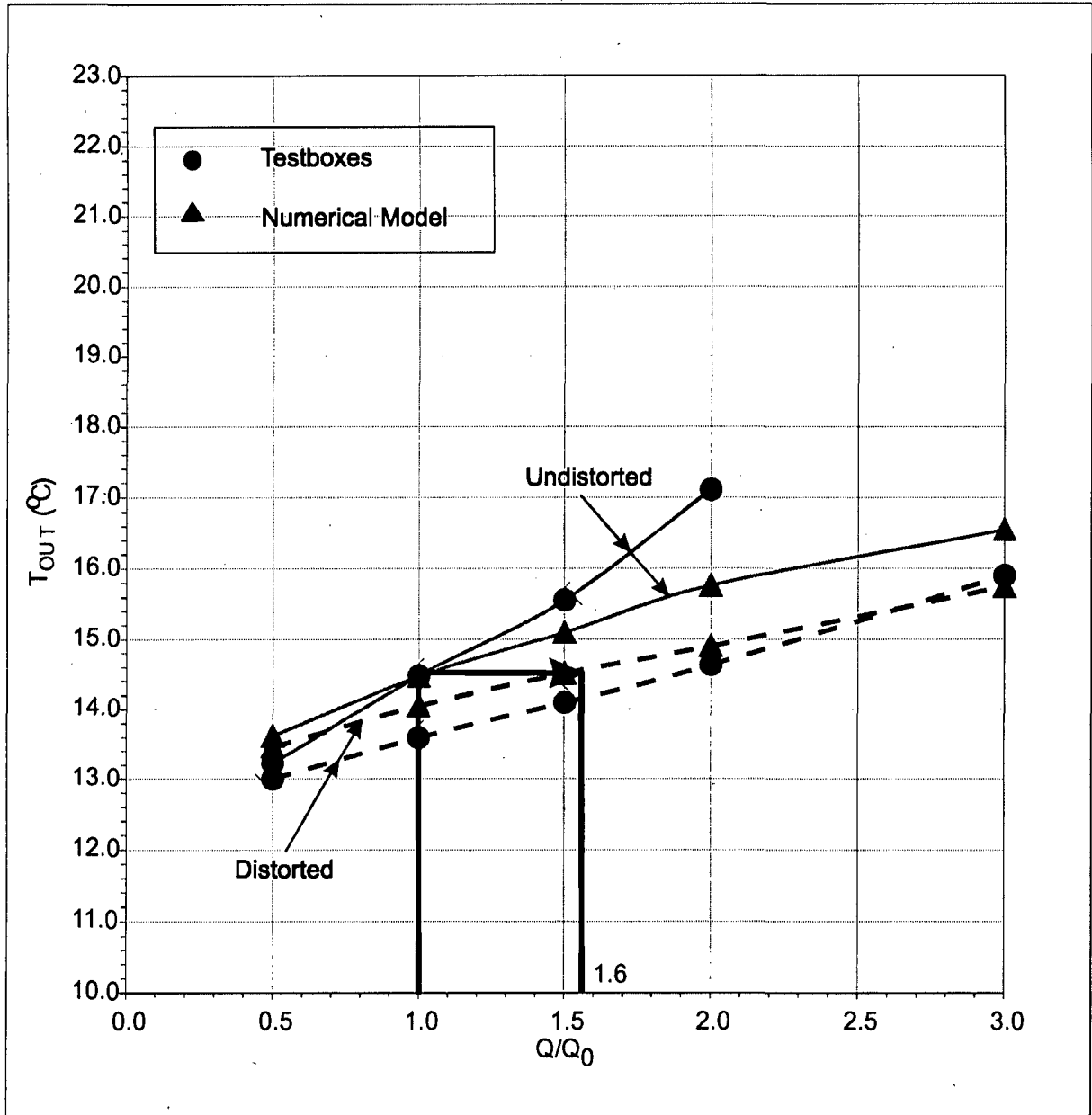


Figure 6-11. Comparison of results obtained from the testboxes and from the simulations of the testboxes; June condition (no curtain).

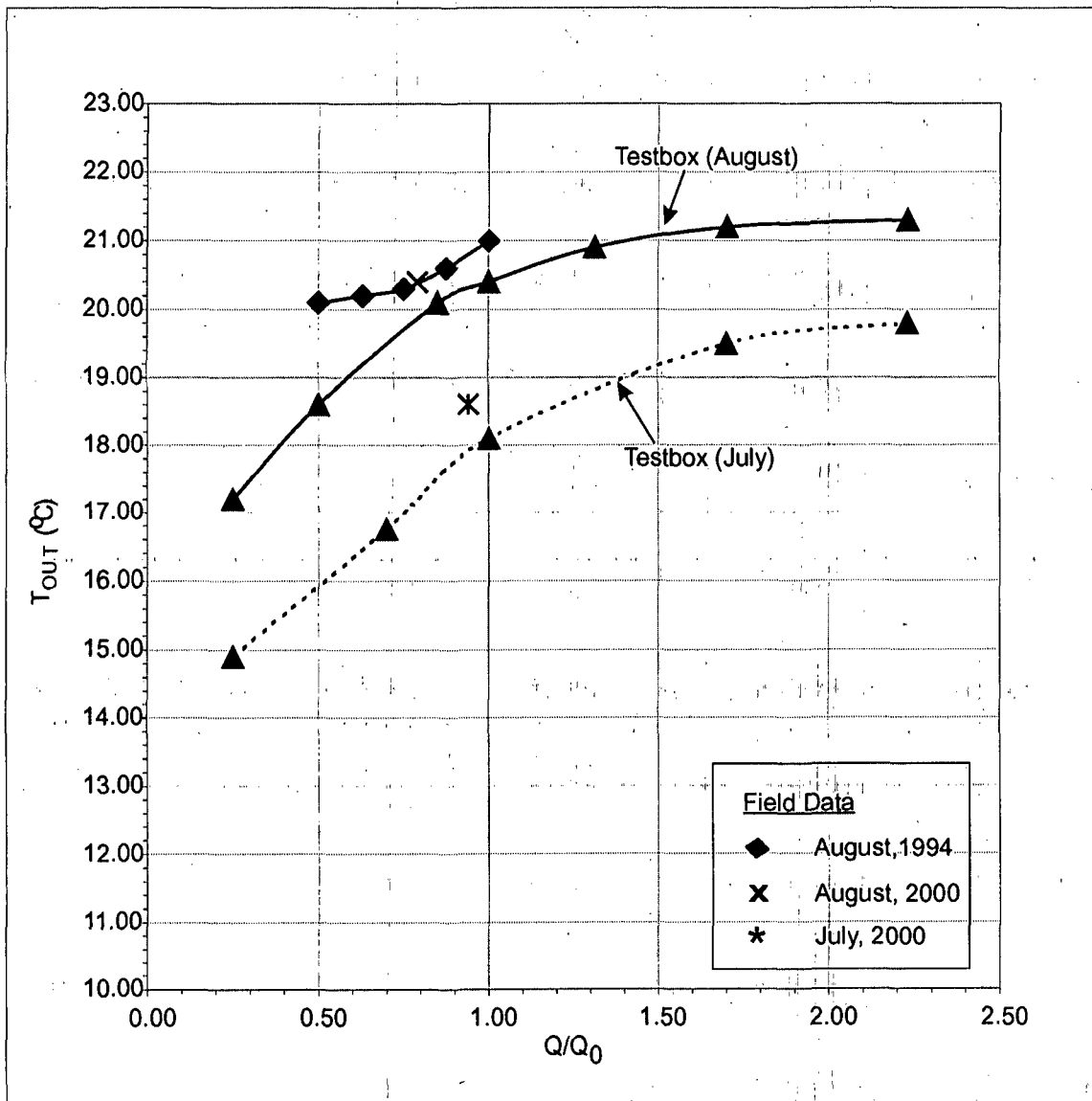


Figure 6-12. Comparison of results from the undistorted Open testbox with field data from Prattville Intake. The field data were measured during July 2000 and August 1994 and 2000 (no curtain).

## 7. RESULTS FROM HYDRAULIC MODEL

### 7.1 Introduction

The results obtained from tests with the hydraulic model of Prattville Intake provide detailed insights into the flow and water-mixing processes associated with operation of Prattville Intake in its present form. Additionally, the results lead to recommended design modifications for Prattville Intake.

The most promising set of modifications include a skimming curtain placed around Prattville Intake, and minor bathymetric adjustments made in the vicinity of the Intake. These modifications would enable Prattville Intake to release substantially colder water from Lake Almanor during summer months than the Intake in its present configuration can release. The present chapter gives the results from the baseline-performance and the screening-performance tests conducted with the hydraulic model. Results from the performance-documentation tests, aimed at confirming the capability of the most promising set of modifications to reduce outflow temperature, are given subsequently in Chapter 8.

Also given in this chapter are the results of tests conducted with the moveable sill located along more-or-less the same perimeter as the skimming curtain, but when the curtain is raised and not in use. The sill and the curtain could be supported by the same overall structure. In concept, the sill is intended to enable the Intake to be operated so as to conserve cold water in Lake Almanor during spring months.

The test results primarily comprise performance curves relating the bulk temperature,  $T_{out}$ , of outflow water drawn through the Intake versus Intake outflow rate normalized as  $Q/Q_0$ , in which outflow rate  $Q$  is normalized with the model-scaled value of the Intake's design outflow rate,  $Q_0$ . A model-scale value of  $Q_0 = 2.87 \times 10^{-2}$  cfs (1,600 cfs released from Prattville Intake) is used herein. Based on the calibration results from the testboxes, the discharge setting  $Q/Q_0 = 1.7$  in the hydraulic model is taken to be equivalent to  $Q/Q_0 = 1$  for the actual operation of Prattville Intake.

The performance curves are accompanied by illustrated descriptions of the flow and water-mixing processes associated with Prattville Intake. They are provided for the Intake in its existing configuration, and for the Intake fitted with the principal design modifications tested. In the course of the screening tests, some modification concepts that immediately proved entirely ineffectual were quickly abandoned, and therefore are not subject to detailed documentation tests. A sample set of plots is introduced in Section 7.2.

The test results obtained for Prattville Intake in its existing configuration, together with those for the Intake fitted with modifications, are presented in the following sequence:

1. Brief characterization of the water-temperature field in the model;
2. Performance curves giving  $T_{out}$  versus  $Q/Q_0$ ; and,
3. Illustrated description of the flow fields associated with the performance curves.

One figure giving the data in the fully normalized format ( $\frac{T_{out} - T_{hypo}}{T_{epi} - T_{hypo}}$  versus  $Q/Q_0$ ) is presented in Section 7.2 for Prattville Intake, to show how the performance trends in that format. As explained in Section 6.3, the water-temperature profiles obtained in setting up the hydraulic model were sufficiently repeatable that it was found more convenient to present the data directly as  $T_{out}$  versus  $Q/Q_0$ . Accordingly, this chapter does not use the fully normalized format for presenting the results.

## **7.2 Baseline Performance Tests: Prattville Intake**

Documentation of the baseline performance ( $T_{out}$  versus  $Q/Q_0$ ) of Prattville Intake, in its existing configuration, entailed measurement of the temperature field in the model, observation of the flow field established during Intake operation, and measurement of water temperature of the outflow discharge withdrawn by the Intake. The tests simulated

representative conditions of water-surface elevation and water-temperature stratification taken to prevail during June, July, and August.

### 7.2.1 Temperature Field

The temperature field, or distribution of water temperature, in the model was monitored using the three sets of temperature-measurement thermistors whose locations are indicated in Figure 3-15. The closest thermistor set was located 10ft (2,200ft in the lake) from the face of the Intake. The thermistor sets recorded the profile of water temperature over the full depth of water at each location.

Throughout each series of tests with a body of water, all the profiles were monitored to check how closely they conformed to the temperature profiles prescribed for water in Lake Almanor during June, July, and August. Figure 2-6 shows the prescribed water-temperature profiles used for all the tests simulating the June, July, and August conditions of the lake; the profiles also are given in Table 2-1. The temperature profiles, provided by PG&E, were measured on June 22, July 20, and August 17 during 2000. The elevations of the first data points in the temperature profiles indicate the water-surface elevation. As was shown in Figure 3-14, the temperature profiles in the model conform closely to those prescribed for Lake Almanor. Also, as the test series progressed, the water-temperature profiles in the model usually continued to conform closely to the prescribed profile for the duration (one to two hours) of the test series. As the water surface eventually lowered measurably, when the colder water was withdrawn from the lower elevations of water, the temperature profile and water level in the model were restored by discharging cold-water through the pop-up risers placed in the model's bed.

### 7.2.2 Variation of Outflow Temperature with Outflow Discharge

By virtue of the substantial mixing of flow entering the Intake, the swirl of flow within the Intake and the outflow pipe, and the location of the temperature-measurement point well downstream of the Intake's entrance opening, the outflow water can be treated as being fully mixed. Therefore, a single-point measurement of  $T_{out}$  is sufficient for characterizing the temperature of outflow water.

With increasing outflow discharge through the model Intake, the water temperature of the outflow increased, though asymptotically approaching an eventually constant outflow temperature equivalent to the fully mixed condition, as indicated in Figure 6-1 for the testbox simplification of the model of Prattville Intake. This result occurred for the temperature profiles prescribed for each month. Figure 7-1 shows, for the three summer months considered, the variation of outflow water temperature,  $T_{out}$  (in degrees centigrade), with discharge ratio  $Q/Q_0$ . The data and curves in Figure 7-1 are from actual tests whose results most closely aligned with the average trends obtained from several series of tests with the hydraulic model. Section 8.2 subsequently gives the spread of data about the average trend for each curve. This simplification in presentation allows crisper explanation of the influences of the modifications tested.

Also given in Figure 7-1 are field data for  $T_{out}$  versus  $Q/Q_0$  obtained from measurements conducted at Prattville Intake during August 1994 and 2000, and for June and July, 2000. The field data lie above the curves obtained from the hydraulic model. In Figure 7-2, the field data have been shifted in accordance with the calibration relationship developed from the testboxes,

$$(Q/Q_0)_{m-cal} = \alpha(Q/Q_0)_p \quad (7-1)$$

and using the average value of the discharge-calibration factor,  $\alpha = \bar{\alpha} = 1.7$ , applied to the field values of  $Q/Q_0$ . Figure 7-2 shows that the data from the hydraulic model align closely with the field data. This result adds validation support to the value of the calibration factor,  $\alpha = 1.7$ , as determined using the testboxes.

The hydraulic-model data giving the curves in Figure 7-1 are re-plotted in Figure 7-3 as

$$\frac{T_{out} - T_{hypo}}{T_{epi} - T_{hypo}} \text{ versus } Q/Q_0.$$

The fully normalized plots in Figure 7-3 show the same trends as the data in Figure 7-1. Because it easier to explain the results using  $T_{out}$  rather than a

normalized parameter, Figure 7-3 is the only fully normalized set of data presented in this chapter.

A feature of the data curves obtained from the hydraulic model (Figures 7-1, 7-2, and 7-3) is a small inflexion over the range  $Q/Q_0 \approx 0.75$  to 1.25. The inflexion occurs in the curves obtained for each of the three months. Though a detailed mapping of the flow field as it changed with  $Q/Q_0$  was not done, observations using dye indicated that the inflexion in each curve coincides with the visible strengthening of a vortex extending from the Intake's inlet to the water surface. As the vortex strengthened and became visible at the water surface, increased warm water was drawn into the Intake from the upper levels of the water column.

The uncertainties associated in estimation of  $\alpha$  are mostly generated by the slight differences between the stratifications obtained from one experiment to another and the changes in stratification due to heat transfer in the body of water. Besides these effects, it was noticed with the model that a sudden change in outflow discharge could produce waves in the thermocline. As a wave occurred, the measured value of  $T_{out}$  would slowly oscillate, as illustrated in Figure 7-4. Waves formed by a relatively rapid reduction in outflow discharge would travel across the model, and be reflected from solid walls bounding the model. The amplitude and period of such internal waves varied in accordance with magnitude of the reduction in outflow discharge, and the period over which the discharge changed. Though no systematic measurements were made of the wave periods, it was noticed that the periods could be as much as 10 minutes for short (about 15 second) reductions of about  $0.5Q/Q_0$  in magnitude. To diminish the occurrence of internal waves, adjustments in outflow were made in a gradual manner.

The range of outflow temperatures, and thereby the temperature asymptotes varied for the three months, June, July and August. As the overall profile of water temperature progressively shifted towards getting warmer, and the thermocline lowered (Figure 2-6) for June through August, the curve of outflow temperature inevitably shifted for each month. The shift for the upper asymptote of fully mixed flow is about 2 to 2.5°C between

July and June, as well as between August and July. The constant temperature at the asymptote of the curve for each month was not entirely attained during the tests. For each month the asymptote extends a little beyond the flow range used in the tests; i.e., beyond  $Q/Q_0 = 2.85$ . However, the following values for the asymptotes can be extrapolated from the curves: June, 18°C; July 20°C; and, August 22°C. These temperatures are about 1°C to 3°C lower than the water temperatures in the epilimnion formed in the lake during those months (Figure 2-6). For the model flow condition  $Q/Q_0 = 1.7$ ,  $T_{out} = 16.5^\circ\text{C}$ ,  $19.0^\circ\text{C}$ , and  $21.2^\circ\text{C}$ . These values of  $T_{out}$ , used subsequently for evaluating a modification's effect on outflow temperature, become closer to the asymptotic values as summer progresses and the lake warms.

The agreement between the field data and the model data is discussed further in Chapter 8, which focuses on confirming the results from the hydraulic model. Also discussed further in Chapter 8 are the uncertainties evaluated from data obtained from several series of hydraulic-model tests (conducted on different days) concerning the baseline performance of Prattville Intake.

### 7.2.3 Flow Field

The typical features of the flow field developed during the operation of the model Intake in its as-built condition are shown schematically in Figure 7-5a,b. The flow features were observed with the aid of dye visualization. Figures 7-5a,b are photographs depicting perspectives of the flow field. The flow features directly observable at the water surface were corroborated by anecdotal observations (from PG&E and Bechtel personnel) of water-surface movement at the actual Intake. One flow feature in particular, the counter-clockwise circulation of water around the Intake, was observable in both the model and at the site. As mentioned in Section 7.2.3, that circulation became more evident as  $Q/Q_0$  increased, and coincided with the inflexion in the data curves shown in Figures 7-1 through 7-3.

The Intake withdrew water from a region extending outward in a more-or-less radial arc out from the Intake's entrance opening. For the smaller rates of outflow tested, it

withdrew water from the lower levels of the water, directly in front of the entrance to the Intake. With increasing outflow discharge through the Intake, more water was withdrawn from over the full water depth in the vicinity of the Intake. In particular, the strengthening of the aforementioned circulation drew further warmer water to the Intake.

A related feature of the flow field became increasingly important when  $Q/Q_0$  exceeded about 0.7 in the model (750cfs for Prattville Intake). It was the long-shore flow of water at higher elevations. That flow occurred as the Intake increasingly drew water laterally from over the submerged ridges flanking the Intake. By virtue of the relative extents and elevations of the submerged ridges, the long-shore flow to the Intake was notably pronounced from along the shoreline to the northeast of the Intake. The dye paths in Figure 7-5b show this feature of the flow field. It is evident that the submerged ridges act as sills causing the Intake to skim warmer water from the upper elevations of the water column. The water moving long-shore to the Intake is warmer water from the lake's epilimnion.

For flows approximately exceeding  $Q/Q_0 \approx 0.7$ , the Intake drew water from over the submerged ridges that flanked the Intake. The position of the Intake between the ridges caused water in the vicinity of the Intake to circulate in a gradual, counter-clockwise rotation over much of the water depth around the Intake. The rotation is sketched in Figure 7-5b. As the Intake's outflow discharge increased, the circulation intensified such that a distinctly observable vortex developed. The vortex's vertical axis reached from the water surface and down into the Intake's entrance opening. The vortex, which dimpled the water surface, became observable when  $Q/Q_0$  for the model approximately equaled and exceeded a value of about 1.7. The presence of the vortex clearly showed that the Intake ingested and mixed water from over the full depth of water around the Intake.

There was no evidence that the Intake caused a significant amount of water to flow across the simulated, fairly flat bed of the lake's Chester branch, or along the incised channel. Dye placed on the simulated bed and in the incised channel did not disperse when the as-built Intake was operated over the range of model discharges ( $0.25 \leq Q/Q_0 \leq 2.85$ ).

Some sluggish movement of water was observed, by means of dye visualization, on the lake bed immediately adjoining the incised channel in front of the Intake. In comparison to water movement generally around the Intake, that movement appeared to contribute a minor amount of water to the outflow from the Intake.

### **7.3 Screening Tests: Modifications to Reduce Outflow Temperature**

The ensuing sections of this chapter give the performance curves ( $T_{out}$  versus  $Q/Q_0$ ) obtained when the Intake was fitted with the alternative modifications whose purpose is to enable the Intake to withdraw colder water from Lake Almanor during June, July, and August.

The principal modifications tested are as follow:

1. A large, skimming curtain placed around the Intake;
2. A long pipe fitted with a hooded inlet; and,
3. A short pipe fitted with a hooded inlet.

The modifications are illustrated in Figures 5-1 through 5-5. They are further described in the ensuing sections of the report.

Each modification involved tests conducted with the incised-channel as it presently exists, and subsequently with portions of the elevated levees flanking the incised channel removed. Additionally, for some tests, the incised channel was deepened by means of dredging. The results of tests with each modification are compared with the performance of the Intake in its existing condition.

Of focal interest is the extent to which each modification would lower the temperature of outflow water released from Prattville Intake for a range of outflow discharges ( $0 \leq Q/Q_0 \leq 3$ ) encompassing the actual operating range for Prattville Intake. The relative merit of

each modification or set of modifications was assessed in terms of the overall temperature reduction  $\Delta T_{out}$  it produced with the model values of  $Q/Q_0$  ranging from 1.0 to about 2.0 (the corresponding prototype outflows are about 950cfs to 1,900cfs).

## **7.4 Screening Tests: Skimming Curtain**

Described here is the performance of the Intake fitted with a skimming curtain placed over the existing bathymetry in the vicinity of the curtain. The influences on curtain performance of three separate bathymetric changes (levee removal, major excavation behind the curtain, and blockage of incised channel) are described subsequently.

### 7.4.1. Curtain Geometry

Several preliminary tests were carried out to determine the optimal deployment position of a skimming curtain. The preliminary tests examined the following geometric aspects of the curtain:

1. Plan layout of curtain; and,
2. Elevation of curtain bottom.

A series of screening tests examined the performances of six curtain layouts placed at different locations around the modeled Prattville Intake, and subjected to the August-condition water-temperature profile and water-surface elevation. The curtain layouts are indicated in Figure 7-6. For these tests,  $Q/Q_0 = 1.7$ . Table 7-1 summarizes the results of the screening tests.

Table 7-1. Summary of data from screening tests with skimming curtains; for the August condition of Lake Almanor and  $Q/Q_0 = 1.7$  in the model (the equivalent outflow from Prattville Intake is 1,600cfs).

Curtain Layouts (see Figure 7-6)	Outflow Temperature $T_{out}$ (°C)	Temperature Reduction $\Delta T_{out}$ (°C)
No curtain	21.2	-
Curtain No. 1	20.2	1.0
Curtain No. 2	18.7	2.5
Curtain No. 3	18.1	3.1
Curtain No. 4	17.7	3.5
Curtain No. 5	16.7	4.5
Curtain No. 6	18.2	3.0

Though Curtain No. 5 produced the largest reduction in temperature of the outflow, it would be a very large structure. It was thought that practically the same effect obtained with Curtain No. 5 could be obtained also with Curtain No. 4 if some relatively minor bathymetric adjustments were made, notably the removal of levees in front of the curtain. That thought, together with the results of the curtain screening tests, led to selection of the curtain (Curtain No. 4) whose layout and plan dimensions are provided in Figure 7-7. Elevation views of Curtain No. 4 are given in Figure 7-8, with the details on opening area given in Figure 7-9. Curtain No. 4 had a model-scale opening area of  $0.60\text{ft}^2$  ( $5,280\text{ft}^2$  in the prototype). A view of the model curtain is shown in Figure 7-10, as well as earlier in Figure 5-1.

Presented and assessed in more detail here below are the results from screening-performance tests with that curtain design. The curves relating outflow temperature and outflow discharge are given first. Discussed then is the flow field developed around and behind the curtain.

#### 7.4.2. Effect of Curtain No. 4 on Outflow Temperatures

The model curtain reduced the temperature of the outflow discharge released through the model Intake for each of the three months simulated. Figures 7-11a-c show the effects of Curtain No. 4 on the variation of  $T_{out}$  with discharge ratio  $Q/Q_O$  for the months of June, July, and August. Also presented in these figures are the curves for Prattville Intake operated in its existing condition (Figure 7-1). The curves show that the curtain decreases  $T_{out}$  by a differential of as much as about 4.3°C when  $Q/Q_O$  is in the range about 1 to 2.5.

Table 7-2. Summary of data from tests with Curtain No. 4 with  $Q/Q_{Om} = 1.7$  in the model (the equivalent outflow from Prattville Intake is 1,600cfs).

Month	Outflow Temperature, $T_{out}$ (°C) For $Q/Q_{Om} = 1.7$	Reduction in Outflow Temperature, $\Delta T_{out}$ (°C)
June	12.2	4.3
July	14.7	4.3
August	17.7	3.5

The effect of Curtain No. 4 is compared for the three months in Figure 7-12, which shows, as expected, that the outflow is still warmer as summer progresses from June through August. Table 7-2 summarizes the results obtained by placing the curtain around Prattville Intake, for the normal operating discharge in the model ( $Q/Q_{Om} \approx 1.7$ ).

The performance curves obtained with the curtain are drawn as a general framework in Figure 7-13. Based on the curves in Figures 7-11a-c, Figure 7-13 illustrates the following general trends:

1. For small outflows ( $Q/Q_O$  less than say 0.25), the curtain reduces outflow temperature,  $T_{out}$ , by about 1°C for the June and August conditions, and about 2°C for the July condition. This comparatively small change in outflow temperature is

to be expected, because for such small flows, the Intake is withdrawing water locally from the lower depths of the water column near the Intake;

2. As  $Q/Q_0$  increases over the range of flow rates tested, the curtain suppresses  $T_{out}$  with a temperature difference  $\Delta T_{out}$  that increases as  $Q/Q_0$  increases up to about 2. For values of  $Q/Q_0$  nominally ranging from about 1.5 to 2.5,  $\Delta T_{out}$  remains approximately constant. The maximum value of  $\Delta T_{out}$  in that outflow range is about 4.3°C for the June and July conditions, reducing to about 3.5°C during the August condition; and,
3. For comparatively large outflows, the two curves are expected to merge. At such very high outflows the thermocline is drawn down at the curtain entrance, thereby causing the outflow water to be mixed to essentially the same extent as occurs for the Intake operating without the curtain present. The two curves merge for outflow discharges well beyond the maximum rate of outflow release from the Intake, and for values of  $Q/Q_0$  that substantially exceed the range of flows tested. Extrapolation of the curves suggests that the two curves would merge when  $Q/Q_0$  exceeds a magnitude in excess of 10. Beyond that limit, the flow fully mixes as it approaches and passes beneath the curtain. Consequently, the outflow temperature then would be the same as obtained were the present configuration of Prattville Intake operated at such a large value of  $Q/Q_0$ .

#### 7.4.3 Flow Field at Curtain No. 4

Skimming Curtain No. 4 substantially altered the flow field in the vicinity of the Intake. The curtain caused the Intake to draw water substantially from the lower and cooler elevations of lake water immediately outside the curtain. As the outflow discharge from the Intake increased, water from increasingly higher elevations of the water column outside the curtain was drawn below the curtain.

Flow visualization by means of dye revealed the major features of flow toward, under, and behind the curtain, as illustrated in Figures 7-14a,b, which show the overall features

of the flow field. The flow features were revealed with the aid of dye paths formed from dye released along lines near the lakebed and near the water surface outside the curtain. The photograph in Figure 7-14a depicts the main features of the flow approach toward and under the curtain. Figure 7-14b illustrates the flow paths under the curtain and then toward the Intake. Together, the photographs in Figures 7-14a,b show the following flow features:

1. Water near the lakebed converged to the curtain and is drawn through the curtain opening;
2. The curtain blocked the warmer water at higher elevations near the lake shore from entering the Intake;
3. The curtain caused a substantial flow of colder water to be drawn along the incised channel. Dye released in the incised channel revealed that the curtain causes water to be drawn along the incised channel for a distance extending into the Hamilton Branch of Lake Almanor. This was an especially intriguing feature of flow generated by the Intake fitted with the curtain. A veritable submerged stream of dye-colored water flowed from the Hamilton Branch to the curtain.

A calculation based on the average drift velocity (nominally depth-average in the order of  $5 \times 10^{-2}$  ft/s at model scale) midway along the channel, together with an average cross-sectional area of the incised channel (about  $0.13 \text{ ft}^2$ ), gives a flow discharge of  $0.65 \times 10^{-2}$  cfs, which corresponds to approximately 13.3% of the  $1.7Q_0$  discharge released through the Intake (for the model Intake,  $1.7Q_0 = 1.7 \times [2.87 \times 10^{-2} \text{ cfs}] = 4.88 \times 10^{-2} \text{ cfs}$ ) of flow to the Intake is drawn along the incised channel

Water in the incised channel, however, was measured to be on average about  $2^\circ\text{C}$  to  $3^\circ\text{C}$  cooler than water at the bed level of the Chester Branch in a region immediately out from the Intake;

4. Flow on the lakebed region in front of the curtain is drawn to the curtain, but must rise to pass over the outer levee in front of the curtain. The flow rises and passes smoothly over the levees, though it mixes slightly with warmer water above the levee;
5. Whereas water near the curtain opening essentially flows directly towards and under the curtain, the flow field in front of the curtain itself is subtly complex, involving several circulating currents. Other than briefly describing the main flow features observed, the full complexity of the flow is not detailed here. The flow field was marked by slow-moving currents generated by lower-elevation water drawn to the curtain opening. Those currents were influenced by local bathymetry in the vicinity of the curtain, and by the curtain face. The local bathymetry determined the lateral distribution of the open area beneath the curtain, and thereby influenced the lateral distribution of flow along the curtain opening; and,
6. Prominent amidst the currents is a slow, long-shore current, or drift, around the curtain. The current was generated by the asymmetry of opening beneath the curtain. The opening area was larger along the curtain's northeast half, than its southwest half (Figure 7-9). The long-shore current generated two large patterns of slow circulation near the water surface along the front of the curtain.

Flow passing beneath the curtain mixed with the water volume behind the curtain. The extent of mixing increased with outflow discharge. Flow passing beneath the bottom of the curtain generated a system of large flow-separation eddies and vortices that were effective in mixing water behind the curtain. As shown in Figure 7-14b, eddies and vortices commonly extended over the entire water depth behind the curtain. The strength of eddies and vortices increased as the outflow discharge increased; and commensurately, the period needed for the outflow water to attain a constant temperature decreased with increasing outflow discharge. Figure 7-15 presents a series of temperature profiles taken

at one vertical location in the water enclosed by the curtain (white curve at Station 1), and a vertical outside the curtain (green curve at Station 3). As the outflow ratio  $Q/Q_O$  increased the profiles became flatter as the temperature difference diminishes, indicating increased mixing. For the range of  $Q/Q_O$  values considered, the water volume behind the curtain did not become completely mixed. An upper layer of warmer water persisted, though it thinned as  $Q/Q_O$  increased.

Figure 7-16 gives a sense of the period of time needed for water behind the curtain to attain an equilibrium state of mixing, and thereby for the outflow temperature to attain a constant value. The top chart in the figure shows that  $T_{out}$  initially rose when  $Q/Q_O$  was set at 2.25, then shows how  $T_{out}$  decreased. Eventually (beyond the period shown),  $T_{out}$  leveled to a constant value. During the tests, the period ranged from about 5 to about 10 minutes for the range of  $Q/Q_{Om}$  tested; the variability in period relates to the initial condition of the water enclosed by the curtain, and magnitude of change in outflow rate, such that only an approximate estimation of period to equilibrium is meaningful. The equivalent prototype periods can be assessed by way of a calculation based on the time required to fill the volume behind the curtain; i.e.,

$$t_p = t_M \left( \frac{\text{volume scale}}{\text{discharge scale}} \right) = t_M \left( \frac{V_r}{\bar{\alpha} Q_r} \right) \approx t_M \left( \frac{X_r^2 Y_r}{\bar{\alpha} X_r Y_r^{3/2}} \right) \approx t_M \left( \frac{X_r}{\bar{\alpha} Y_r^{1/2}} \right) \approx 21 t_M \quad (7-1)$$

in which  $t_p$  and  $t_m$  are prototype and model periods, respectively. In accordance with Eq. (7-1), the period to reach equilibrium temperature of outflow would vary from about  $21 \times 5$  minutes = 105 minutes to about  $21 \times 10$  minutes = 210 minutes. So, it would be anticipated that about 2 to 4 hours would be required for the temperature of outflow released by Prattville Intake to become steady.

## 7.5 Screening Test: Curtain, Levees Removed

Removal of the levees in the vicinity of the Intake enhanced the skimming performance of Curtain No. 4 for the July and August conditions of Lake Almanor, though levee removal did not significantly alter curtain performance for the June condition. Figure 7-

17 indicates the locations of the removed levees relative to curtain position, while Figure 7-18 provides a view of this configuration in the hydraulic model. The curtain geometry and dimensions are the same as presented in Section 7.3.

### 7.5.1 Influence on Outflow Temperature

Figures 7-19a-c show that removal of the levees further reduced the outflow temperature,  $T_{out}$ , for each of the test months. The further reduction was greatest for the August condition, about 1.5°C to 2.0°C. For the July condition, the reduction was approximately 1°C to 1.5°C. Only small reduction, less than 1°C, was obtained for the June condition. Consequently, for the flow range tested ( $0.25 < Q/Q_o < 3.0$ ), the overall maximum reductions in outflow temperature are  $(\Delta T_{out})_{max} = 5.2^\circ\text{C}$ ,  $5.8^\circ\text{C}$ , and  $4.5^\circ\text{C}$  for August, July and June conditions, respectively. Accordingly, for the normal operating discharge (adjusted using the discharge correction factor),  $Q/Q_{om} \approx 1.7$ , the modifications of placing the curtain and removing the levees result in outflow temperatures listed in Table 7-3. The general conceptual trends shown in Figure 7-13 illustrating the curtain effect on outflow temperature also pertain when the levees are removed, though the numerical locations of the two curves may be altered somewhat.

Table 7-3. Summary of data from tests with Curtain No. 4 with levees removed, for model discharge set at  $Q/Q_o = 1.7$  (the equivalent outflow from Prattville Intake is 1,600cfs).

Month	Outflow Temperature, $T_{out}$ (°C)	Reduction in Temperature $\Delta T_{out}$ (°C)
June	12.0	4.5
July	13.2	5.8
August	16.0	5.2

Table 7-3 in conjunction with Table 7-2 indicates that the temperature-reducing effect of the levee removal mildly increases as summer progresses. The reductions in  $\Delta T_{out}$  increase from June through August, even though the outflow temperature increases from June through August, as shown in Figure 7-20. This effect of levee removal is

attributable to the role levees play in partially obstructing cold-water movement to the curtain. As the thermocline lowers and the hypolimnion thins during summer (see the temperature profiles in Figure 2-6), that role becomes greater. Accordingly, the temperature-reducing influence of having the levees removed mildly increases during summer.

#### 7.5.2 Flow Field When Levees Removed

Removal of the levees substantially modified the flow field immediately outside the curtain. The main flow features are illustrated with photographs of dye visualization and schematically in Figure 7-21a,b.

Levee removal caused water near the lakebed to flow directly toward and through the curtain opening. Consequently, the curtain caused the Intake to draw water more directly from lower elevations of the water column covering the region of the lakebed out in front of the curtain. Also, as revealed by dye observations, levee removal did not appear to substantially reduce the rate of water flow along the incised channel.

An intriguing flow feature observed in the model was the movement of water along the incised channel when the curtain was placed around the Intake. Intake operation drew water along the channel all the way from the channel's juncture with the Hamilton Branch of Lake Almanor. Viewed with the aid of dye, water movement along the incised channel appeared as a submerged stream. Except for regions near the curtain, comparatively negligible flow occurred above the incised channel, or on the lakebed near the incised channel. The sequence of photographs in Figure 7-22 show how a dye placed in the incised channel moved along the channel. The arrowed dye mass within the incised channel flowed at a speed of about 0.5ft/minute along the incised channel when  $Q/Q_0 = 1.7$ . The adjoining dye mass placed above the channel moved much more slowly.

Near the curtain, the incised channel received much lateral inflow from the lakebed offshore from Prattville Intake. The incised channel then served also as a collector and a local mixer of cold water, blending the much colder water conveyed along the channel

with cold water drawn over the lakebed. The flow rate in the channel increased markedly near the curtain, such that the channel became an important conduit of water under the curtain.

The curtain's improved facility to draw water directly from the lake bed in front of the curtain, without the mild blocking action of the levees, slightly diminished the size of the circulation patterns occurring over the upper levels of the water in front of the curtain. Comparison of Figures 7-14b and 7-21b shows that levee removal mildly simplified the flow field in front of the curtain. The overall flow field in front of the curtain, though, still remained markedly three-dimensional, and included the drift of surface water across the face of the curtain, the presence of a flow-separation eddy at the curtain's northeast corner, and the non-uniform distribution of unit discharge through the opening beneath the curtain.

To delineate the effect of lake stratification on the flow field at the curtain and on the temperature of outflow from Prattville Intake, a test with non-stratified, uniform temperature body of water was conducted. Figure 7-23 shows photographs of dye visualization. It can be seen from the paths of dye released at the top and bottom of the water column that water from over the entire water column in front of the curtain was drawn beneath the curtain. However, when temperature stratification was established in the model, the upper (and warmer) layers in front of the curtain were not drawn down and did not pass beneath the curtain. The curtain's selective withdrawal of colder water from the hypolimnion, and exclusion of the epilimnion water, is a pronounced difference in the flow fields generated by the curtain when it is placed in thermally stratified water as opposed to iso-thermal water. These differences would occur in the field as in the hydraulic model.

## **7.6 Screening Test: Curtain, Levees Removed, Further Excavation**

Testing showed that further modification of the lake's bathymetry in front of the curtain, or modification of curtain geometry, did not result in significant lowering of outflow-

water temperature released through the Intake. For example, deepening of the incised channel in front of the curtain did not result in lower temperature of outflow.

Another prospective modification tested was the excavation of a region behind the curtain and in the approach to the curtain. It was thought that further excavation, to the extent shown in Figures 7-24 and 5-5, might increase the amount of colder water drawn under the curtain, and thereby enhance curtain performance and further reduce outflow temperature. In part, this thought was prompted by an interest in evaluating additional excavation work, besides levee removal, that might enhance curtain performance.

Testing showed that the additional excavation work did not significantly alter the performance of Curtain No. 4. Moreover, further excavation adjustments of bathymetry behind the curtain proved to have negligible effect on outflow temperature, as illustrated in Figure 7-25. Included in the adjustments were exploratory tests to see how outflow temperature would be influenced if the original approach channel adjacent to the current approach channel to the Intake were blocked or in-filled, such as by the placing of soil excavated from the levees. Those exploratory tests revealed  $T_{out}$  to be insensitive to bathymetry changes behind the curtain. Once flow passed under the curtain, it rose and mixed over much of the water column behind the curtain before being drawn to the Intake.

### **7.7 Screening Tests: Short-pipe with Hooded Inlet**

Described here is the performance of the Intake modified so that water is withdrawn from Lake Almanor by way of a relatively short pipe that extends out to the approach channel about 250ft out from the Intake. The pipe's inlet was covered with a low cap or hood. The modification tested entailed the placing of a barrier wall immediately in front of the model Intake. The wall isolated the Intake from the lake. The pipe was connected to a hole in the barrier wall. The Intake withdrew water from the small reservoir created by the barrier wall. The concept of the short pipe with hooded inlet (SPHI), location, and a photograph of the pipe in the model are shown in Figures 7-26a,b, as well as earlier in Figure 5-2. For ease of modeling, the pipe inlet was coupled to the top of the top of the

hood (Figure 7-26b). If actually constructed, the pipe inlet could be positioned immediately under the hood. The bottom elevation of the hood relative to the local bathymetry is shown in Figure 7-27. Figure 7-28 is a view of the SPHI placed in the hydraulic model. Also shown is the barrier wall formed around the simulated Prattville Intake.

The elevation difference between the water surface of the lake and that of the small reservoir created a pressure head that pushed flow through the pipe to the Intake. As the discharge increased through the inlet, the difference in water-surface elevations increased. In the model, the head difference was about 0.2ft for the model operated at  $Q/Q_0 = 1.7$  (prototype condition of  $Q/Q_0 = 1$ ).

The short pipe with hooded inlet did not cause the Intake to release outflow at water temperatures as low as those obtained using the curtain or the long pipe with hooded inlet. Moreover, the depth of excavation needed to locate the inlet posed construction concerns that would make this modification impractical. The concerns included the geotechnical stability of the sideslopes of the lakebed ridges flanking the inlet (a sense of the sideslope steepness is evident from the view in Figure 7-28). Also, use of the Intake would be significantly interrupted during the excavation and the construction of the barrier wall around the Intake. Therefore, this modification was not pursued further, and the results obtained from it are covered only briefly here.

#### 7.7.1 Influence on Outflow Temperature

Use of a short pipe fitted with a hooded inlet reduced the outflow temperature,  $T_{out}$ , for each of the test months, but the reductions were much smaller than were obtained using the curtain. The performance curve obtained for the short pipe with hooded inlet in August is given in Figure 7-29. The reduction for the August condition was only about  $2.1^{\circ}\text{C}$  for the flow range tested ( $0.25 < Q/Q_0 < 3.0$ ). At the model condition  $Q/Q_0 = 1.7$ ,  $T_{out} = 19.1^{\circ}\text{C}$ .

### 7.7.2 Flow Field

The location of the hooded inlet for the short pipe was too far removed from the source of the colder water needed to substantially reduce the temperature of the outflow through the Intake. The pipe drew water from a wide arc around its inlet. Though the pipe drew water from directly out in the reservoir, it also drew significant quantities of water from along the shoreline south of the Intake. Figure 7-30 depicts flow paths revealed with the aid of dye visualization.

Dye visualization showed that the short pipe was not close enough to the incised channel and the flat lakebed beyond. The pipe's inlet did not produce the same magnitude of flow velocity along the incised channel that the curtain developed. Also, the inlet did not produce the same magnitudes of flow velocity on the lakebed immediately out from the incised channel. These differences are evident when the flow field illustrated in Figure 7-30 is compared with the flow field illustrated in Figures 7-14b for the Intake fitted with Curtain No. 4 and with the levees still in place.

Water drawn along the shoreline originated from the higher elevations of the lake's water column, as evident in Figure 7-30. That water was warmer than water drawn from the incised channel and from over the lakebed. The significant vortex formed over the hooded inlet acts further to mix water drawn into the inlet. Consequently, the outflow from the pipe is warmer than that obtained with the curtain. Given this modest performance, and the construction concerns mentioned above, the use of the short pipe with hooded inlet was not investigated further for the July and June conditions.

## **7.8 Screening Tests: Long-pipe with Hooded Inlet**

Described here is the performance of the Intake modified so that water is withdrawn from Lake Almanor by way of a long pipe that extends out to the incised channel at a location adjoining the lakebed. Figure 7-31 indicates the location of the long pipe with hooded inlet (LPHI) relative to Prattville Intake. The long pipe was connected to the same barrier wall used for the short pipe, and it extended such that its inlet was located within the incised channel slightly beyond the location suggested for Curtain No. 4. Figure 7-32

indicates the elevation of the hooded inlet relative to the bathymetry of the incised channel. The lower surface of the hood over the inlet was at elevation EL.4440ft. Figure 7-33, together with Figure 5-3 earlier, provides a view of the LPHI as simulated in the hydraulic model.

The performance of the LPHI was tested for the following local bathymetry conditions: levees as presently exist, levees removed, and incised channel blocked. The LPHI performed best with the levees removed, but its performance was not as effective in reducing the temperature of the outflow as was the curtain. For this reasons, and because of similar concerns regarding construction as mentioned in Section 7-7 for the short pipe, the long pipe was not tested for the June and July water-temperature conditions of Lake Almanor.

#### 7.8.1 Influence on Outflow Temperatures

Figures 7-34 shows the variation of outflow temperature,  $T_{out}$  with  $Q/Q_0$  obtained with the LPHI in a simulated August condition for Lake Almanor. Also shown is the variation of  $T_{out}$  with  $Q/Q_0$  for the model of the existing Intake operating during the August condition of the lake. The LPHI reduced outflow temperature by about 2.0°C for flows in the range  $0.7 < Q/Q_0 < 2.0$ . This reduction, however, was not as large as the reduction in  $T_{out}$  obtained using Curtain No. 4 with the levees; values of  $T_{out}$  were about 1.5°C higher for outflow drawn through the LPHI.

Removal of the levees, as indicated in Figure 7-35, resulted in a further reduction of outflow temperature such that the total overall reduction of about 3.8°C, which is a smaller reduction than the reduction obtained with a curtain and the levees removed (5.2°C).

#### 7.8.2 Flow Field Generated by Long-pipe with Hooded Inlet

Views of flow paths revealed by means of dye are shown in Figures 7-36a,b. The long pipe with hooded inlet drew water predominantly from the lower elevations of the water column in the lake. Views taken with the underwater camera (provided in the

visualization clip) show the vertical distribution of flow velocity toward the hooded inlet. The flow on passing over the levees mixes with water at higher elevations before entering the hooded inlet.

The long pipe with hooded inlet produced approximately the same average flow rate along the incised channel as did the curtain. However, with increasing  $Q/Q_0$  the hooded inlet more quickly drew down the thermocline than did the curtain. This result is attributable to the larger velocity of flow entering the perimeter opening of the hooded inlet. The opening area of the hooded inlet was about  $0.30\text{ft}^2$ ; about half of the opening area beneath the curtain, which in the model was about  $0.60\text{ft}^2$ .

Removal of the levees enabled the hooded inlet to draw colder water than when the levees were present (Figure 7-36b). The flow was drawn directly along the lakebed toward the inlet. The larger average velocity of flow entering the perimeter of the hooded inlet, compared to flow entering the curtain opening, caused the hooded inlet still to draw warmer water than did Curtain No. 4 with the with levees removed.

Though the data are not presented here, it was found that enlarging the incised channel for a short distance upstream of the hooded inlet did not result in colder outflow temperature. Though water was drawn along the incised channel, the channel primarily served as a collector of cold water drawn over the lakebed and towards the inlet.

Given that the long pipe with the hooded inlet did not perform as well in reducing outflow temperature as did the curtain with the levees removed, it was decided not to continue further testing with the long pipe. Some additional, tentative adjustments were made to the hooded inlet, such as removal of levees and altering the elevation of the hood. However, measurements of  $T_{out}$  and observations of the flow field indicated that the long pipe with hooded inlet could not be developed further to produce lower temperatures of outflow than did the curtain when the levees were removed.

## 7.9 Screening Test: Bottom Sill to Conserve Colder Water

The concept of a submerged fence or bottom sill was proposed as a prospective means for managing or conserving the amount of cold water released through the Intake during months when it will not be necessary to release cold water. While the Intake is used mainly during summer and autumn, conservation of cold water is not an important consideration for Intake operation. Nonetheless, the hydraulic model offered a convenient opportunity to determine in principle whether a bottom sill could be used to conserve cold water.

The sill potentially could be placed during spring and early summer to impede large rates of cold water from entering the Intake then removed when the Intake needed to withdraw cold water. The tests focused on determining an effective crest elevation for the sill.

The tests, conducted with June temperature profile simulated in the model, led to the layout and dimensions of the sill indicated in Figure 7-37. The photographs in Figures 7-38a,b, and earlier in Figure 5-6, show the sill configuration tested in the hydraulic model. The performance of a bottom sill was first tested for the case when the levees are in place.

### 7.9.1 Influence on Outflow Temperature

After a set of preliminary tests tentatively investigating the influence of crest elevation on outflow temperature, two sets of tests were conducted for two crest elevations of a bottom sill:

1. Crest at EL. 4450ft; and,
2. Crest at EL. 4460ft.

Figures 7-39 gives a set of performance curves relating outflow temperature,  $T_{out}$  and  $Q/Q_0$  for sills with the two crest elevations for the June condition of Lake Almanor. By way of comparison, the curves for the performance of the existing Intake are given too.

The average elevation of the top of the levees at the lakebed in front of the Intake is EL. 4440ft.

The curves show that a sill with crest at EL 4460ft, and with the levees in place, resulted in an increase of  $T_{out}$  by about 1.0 to 2.0°C for the flow range  $1 < Q/Q_0 < 2.25$ , compared to outflows from the existing Intake. At the nominal design discharge condition,  $Q/Q_0 = 1.7$ ,  $T_{out}$  was raised 1.8°C, to about 18.3°C. By way of comparison  $T_{out}$  for outflow from the existing Intake (no modifications) was about 16.5°C for the June conditions.

With the levees removed, the presence of the sill resulted in  $T_{out}$  of about 17.8°C for the model outflow set at  $Q/Q_0 = 1.7$ . With the sill also removed,  $T_{out}$  for outflow from the existing Intake (no modifications) was about 15.8°C. The sill therefore raised  $T_{out}$  by about 2.0°C for the Intake's normal rate of outflow release. Figure 7-40 gives the curves for the sill performance when the levees were removed.

The sill with crest elevation 10ft lower at EL 4450ft did not substantially alter the outflow temperature  $T_{out}$  compared to values produced by the existing Intake (Figures 7-39 and 7-40). When the levees were removed, the sill resulted in lower values of  $T_{out}$ . These results indicate that the sill should have a crest elevation at EL. 4460ft or more in order for the sill to substantially limit the release of colder water from the lower level of Lake Almanor.

### 7.9.2 Flow Field

Views of flow paths revealed by means of dye, when compared with the illustrations of the flow field around the existing configuration of the Intake (Figures 7-5b), showed that the sill, with a crest at EL. 4460ft, partially hampered the Intake's capacity to draw colder water from the lakebed and the incised channel, and caused the Intake to draw water from higher elevations of the lake's water column. For flows in the range  $Q/Q_0$  in excess of about 0.7, the Intake still drew much of its water from over the full depth of water immediately around the Intake. The removal of the levees did not markedly alter the flow field at the Intake, though the region of colder water at lower elevations on the

lakebed was observed to move a little more directly at lower elevation towards the Intake and produce a slightly colder outflow.

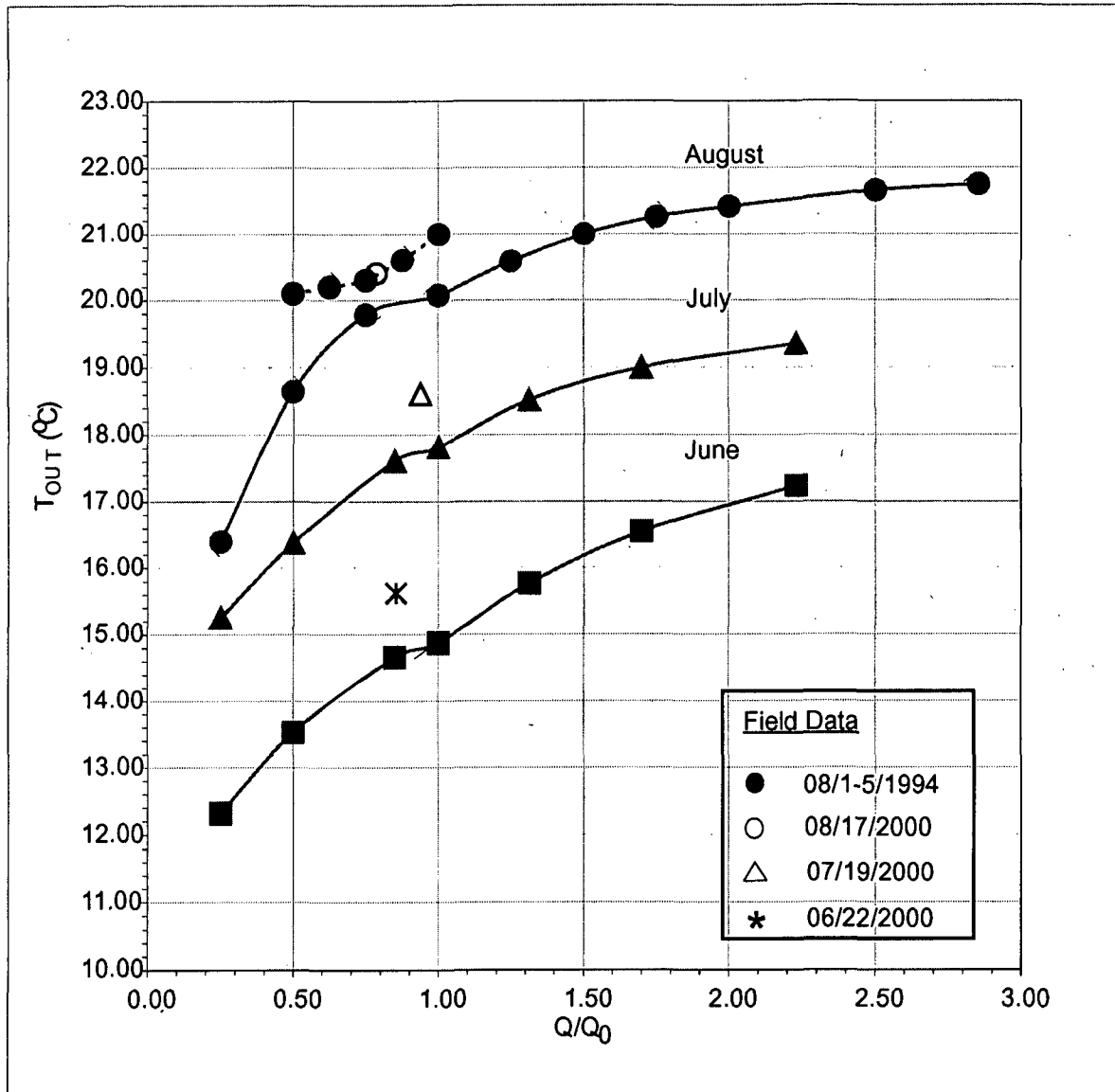
The sill with crest elevation at EL. 4450ft was insufficiently high above the levees to alter the flow field in the immediate vicinity of the Intake. As observed when the sill elevation was at EL. 4460ft, removal of the levees enabled water near the lakebed to drift a little more directly to the Intake, but the water velocities were very small.

### 7.10 Screening Tests: Summary of Results

Table 7-4 summarizes the principal results from the screening tests carried out to identify the modification that would produce the coldest outflows from Prattville Intake operating at the discharge condition  $Q/Q_0 = 1.7$  in the model, which is taken to be equivalent to Prattville Intake operating at  $Q/Q_0 = 1.0$  (releasing 1,600cfs). The table shows that the set of modifications comprising the skimming curtain whose bottom elevation is at EL. 4445ft, together with the removal of levees, would enable the Intake to release the coldest outflow.

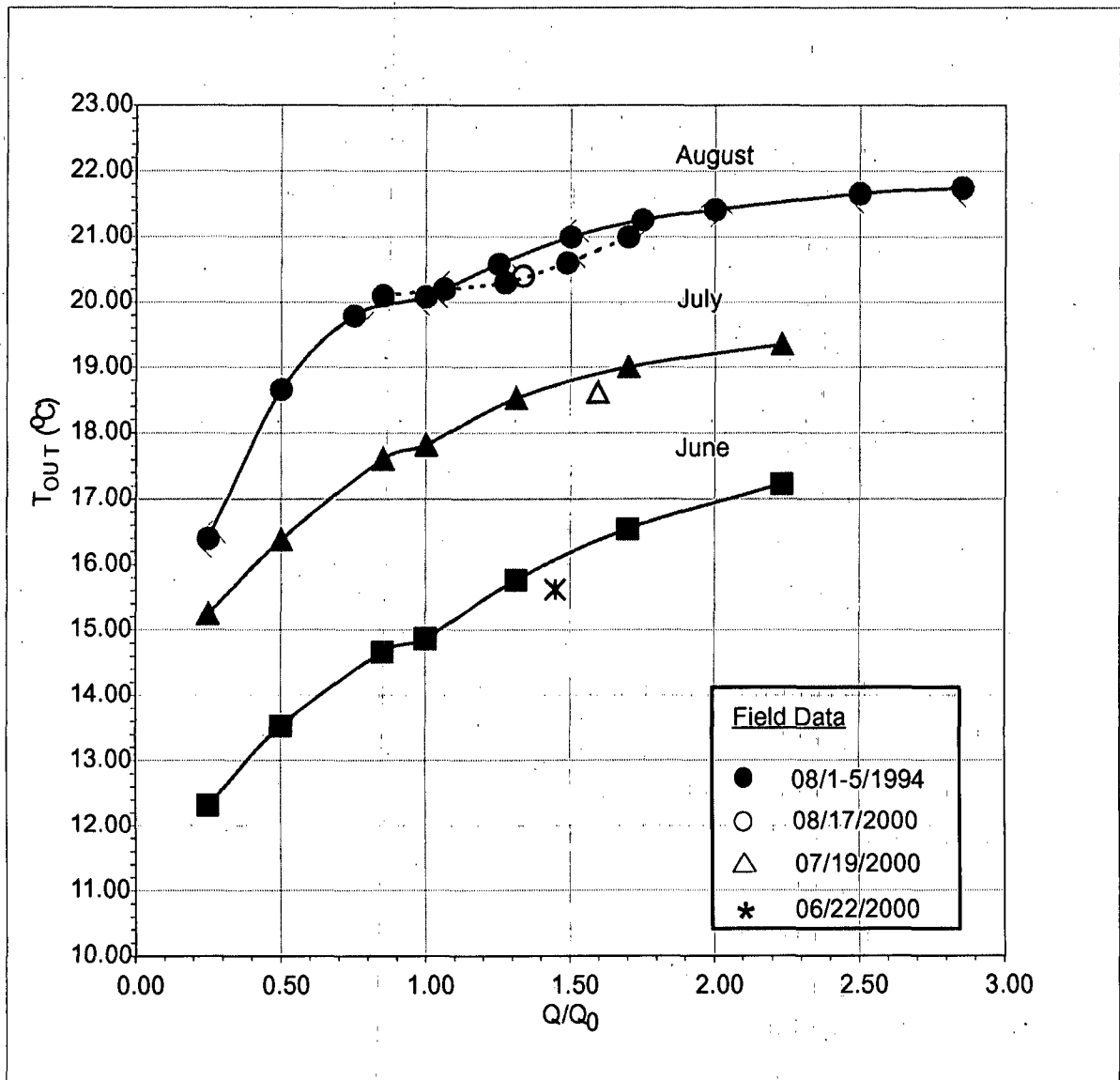
Table 7-4. Summary of screening-performance data (to reduce  $T_{out}$ ) for the August condition of Lake Almanor, and  $Q/Q_0 = 1.7$  in the model (the equivalent outflow from Prattville Intake is 1,600cfs)

Modification to Prattville Intake	Outflow Temperature $T_{out}$ (°C)	Temperature Reduction $\Delta T_{out}$ (°C)
Baseline test: existing design	21.2	-
Screening test: Curtain No. 4	17.6	3.6
Screening test: Curtain No. 4, with levees of incised channel removed	16.0	5.2
Screening test: long pipe with hooded inlet	19.2	2.0
Screening test: long pipe with hooded inlet, with levees removed	17.4	3.8
Screening test: short pipe with hooded inlet in dredged channel, with levees removed	19.1	2.1



(a)

Figure 7-1. Variation of outflow temperature from Prattville Intake for June, July and August. Also shown are field data from Prattville Intake.



(b)

Figure 7-2. The field data, adjusted with discharge calibration factor,  $\alpha = 1.7$ , align with results from the hydraulic model.

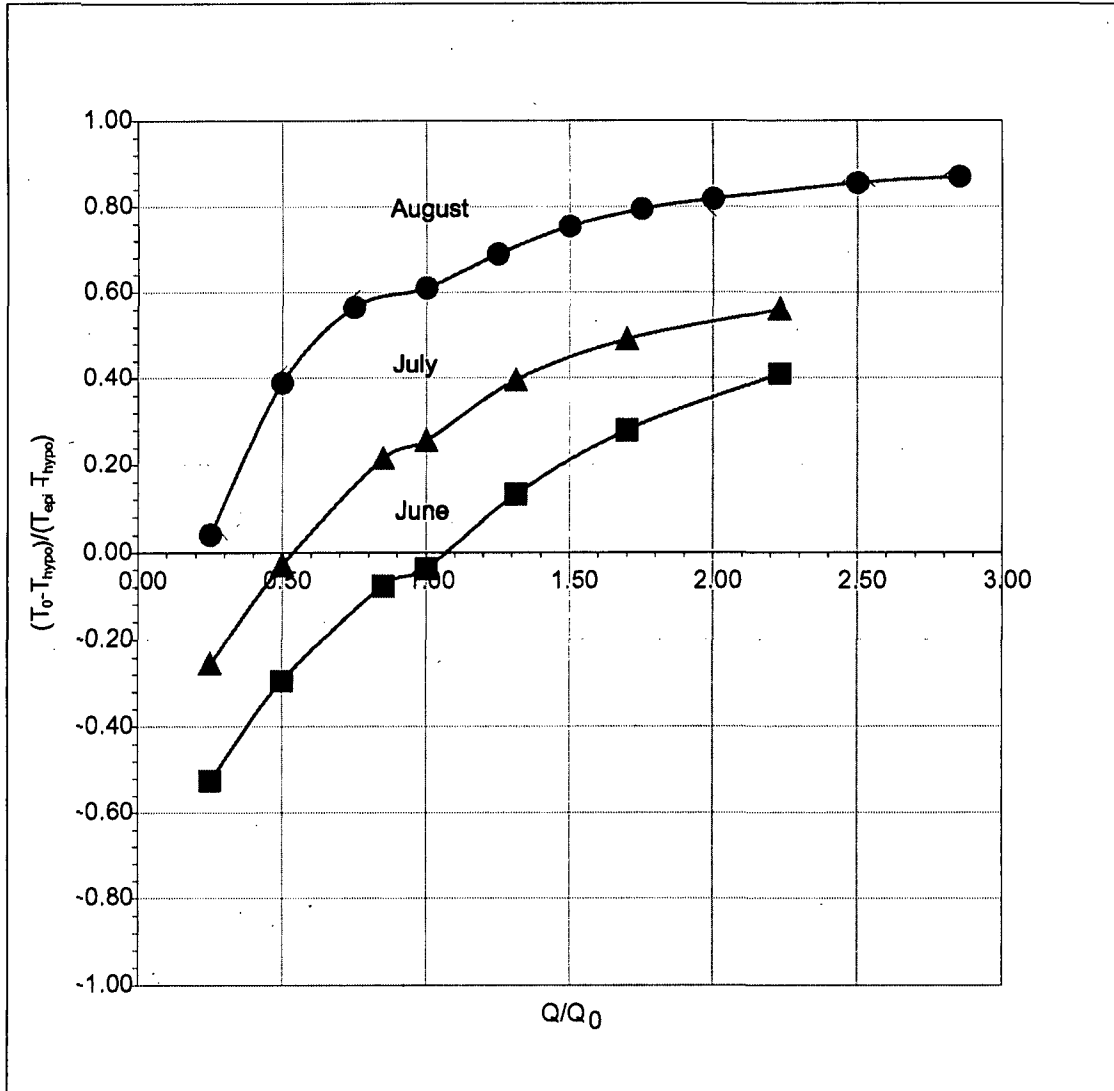


Figure 7-3. Normalized outflow temperature obtained with the hydraulic model for June, July and August.

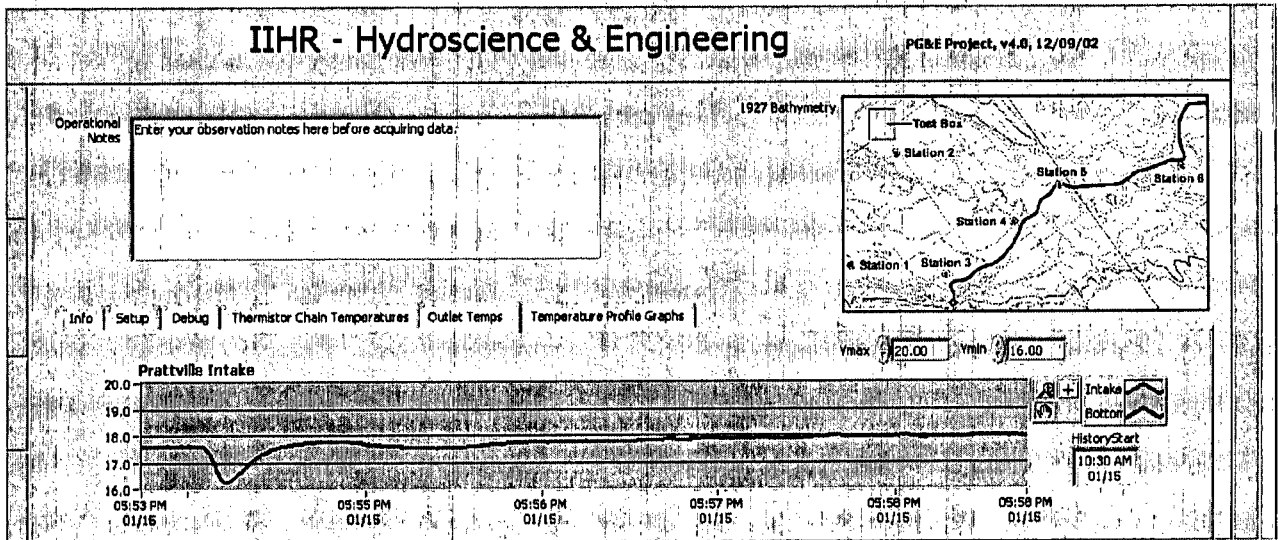
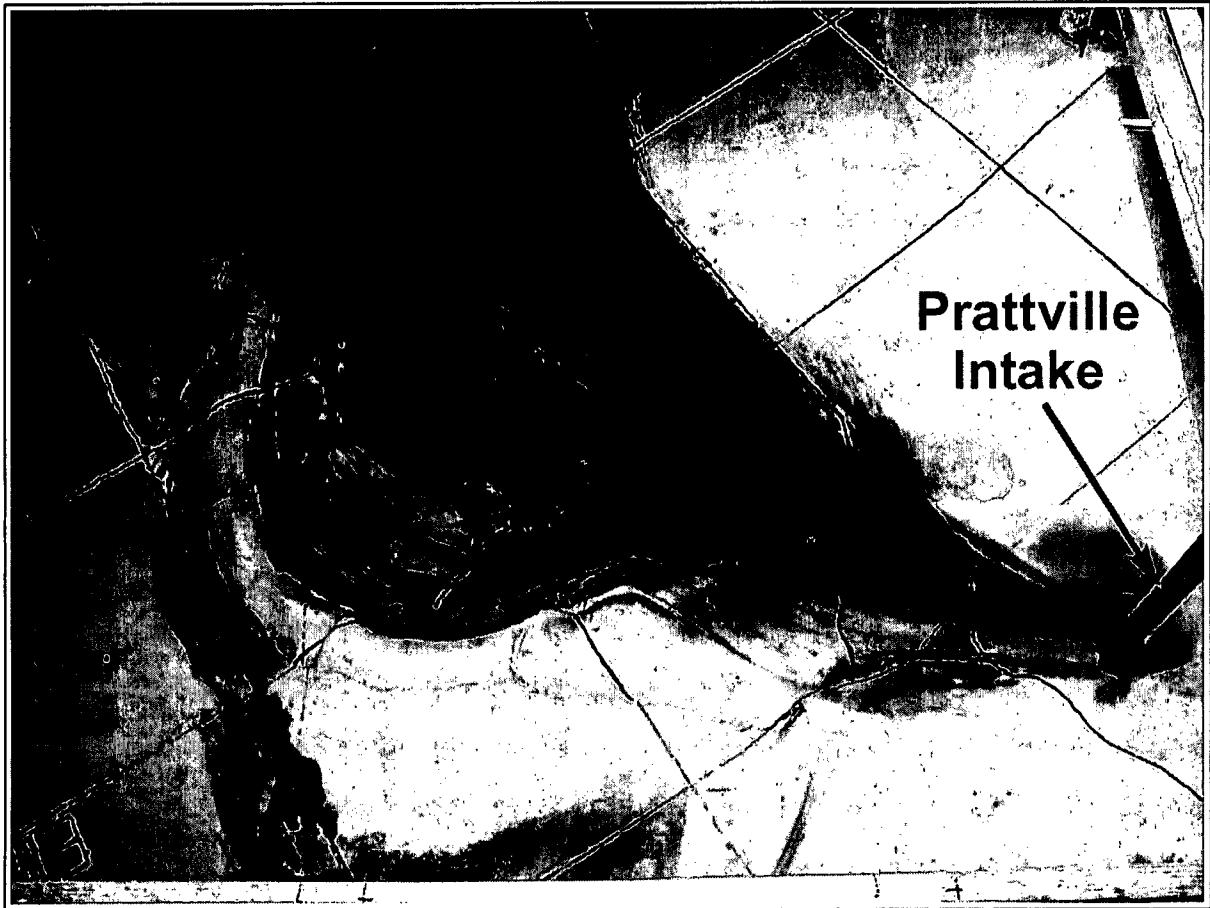


Figure 7-4. Oscillation of outflow temperature after a change in Intake outflow discharge.



(a)

Figure 7-5. Visualization of flow to Prattville Intake ( $Q/Q_0 = 1.7$ , August condition).  
(a) Visualization with dye. Dye is released into approach flow outside the incised channel, blue dye into colder bottom layer and red dye into the warmer surface layer. The intake withdraws predominantly warm surface water.



(b)

Figure 7-5 continued. (b) Photograph with arrows indicating flow paths of flow to Prattville Intake ( $Q/Q_0 = 1.7$ , August condition). Arrow size approximately indicates magnitude of the velocity vector.

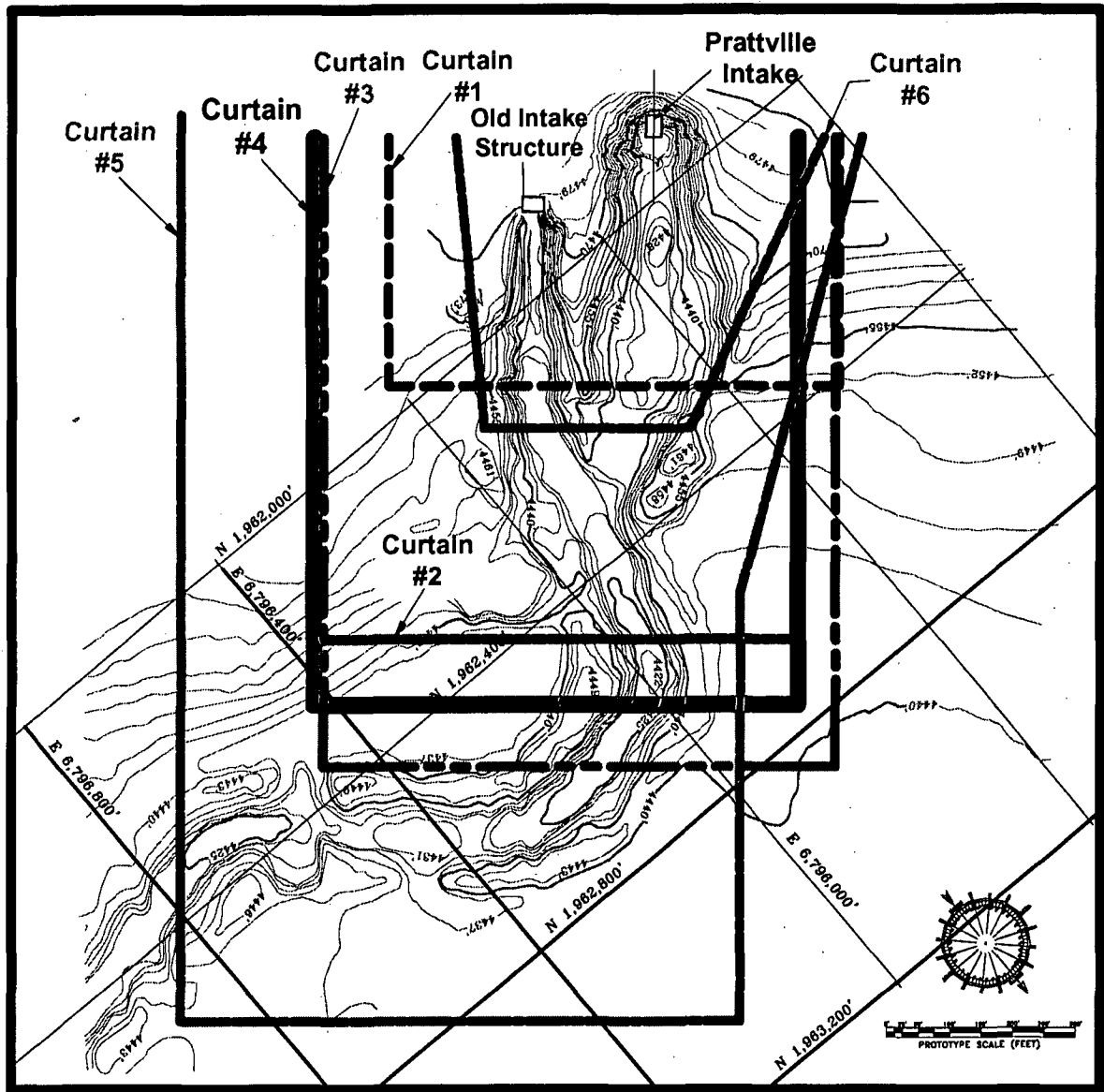


Figure 7-6. Layouts of the curtains tested. Curtain No. 4 was selected for further testing.

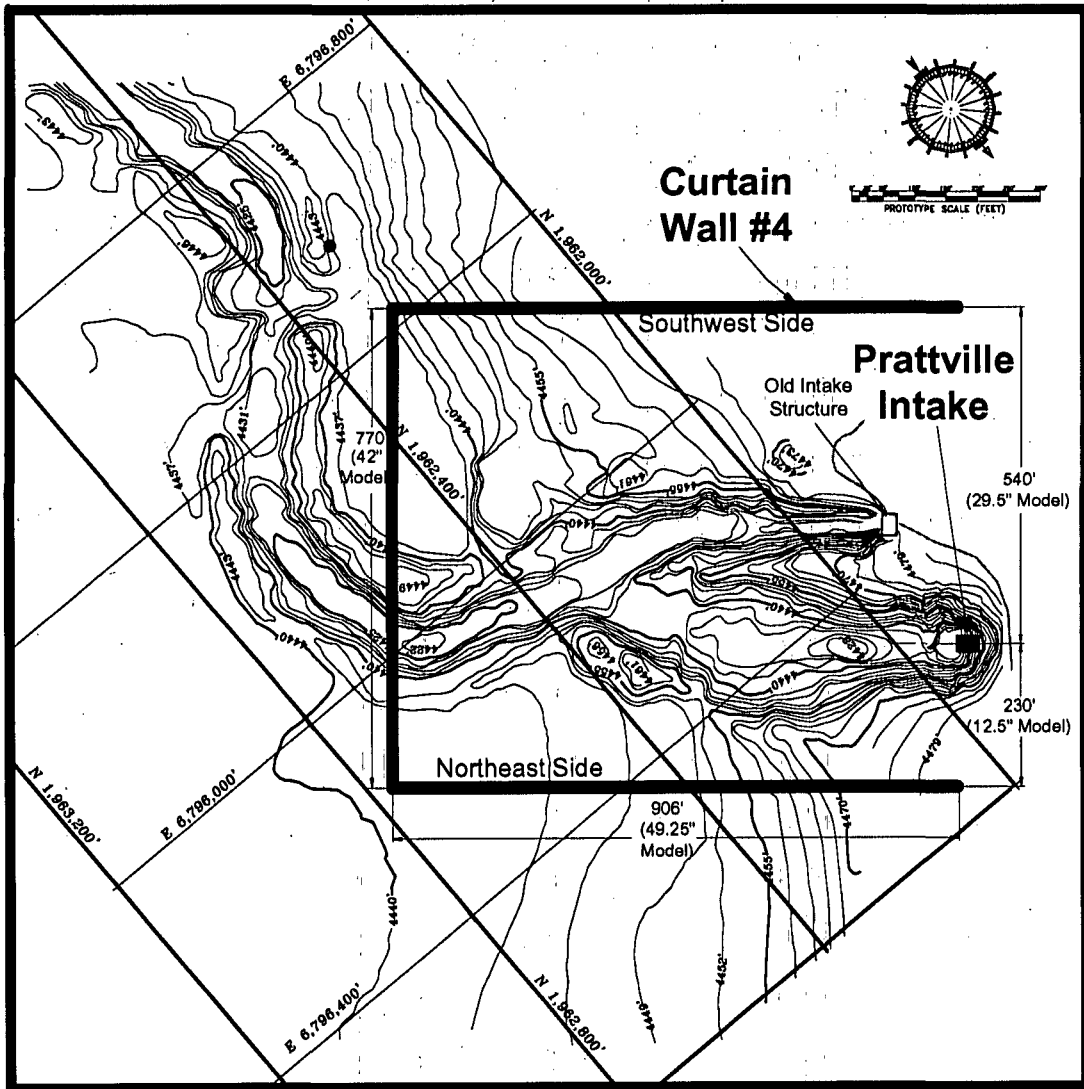


Figure 7-7. Layout and dimensions of Curtain No. 4

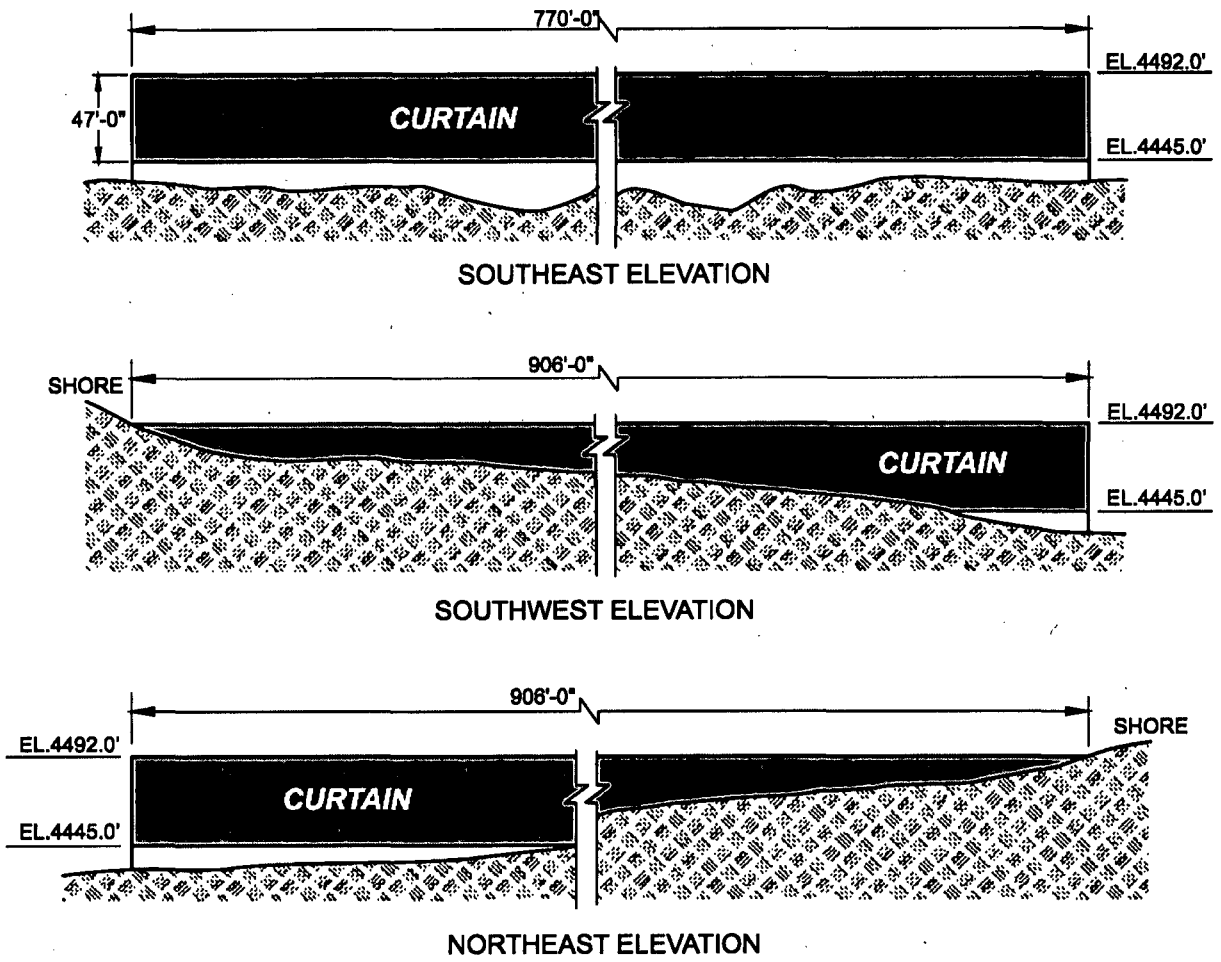
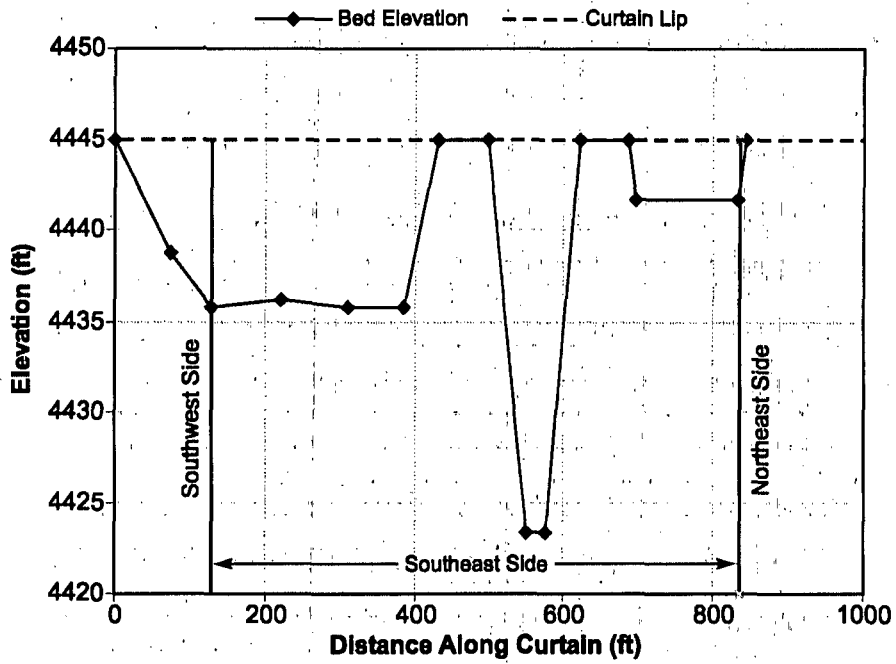
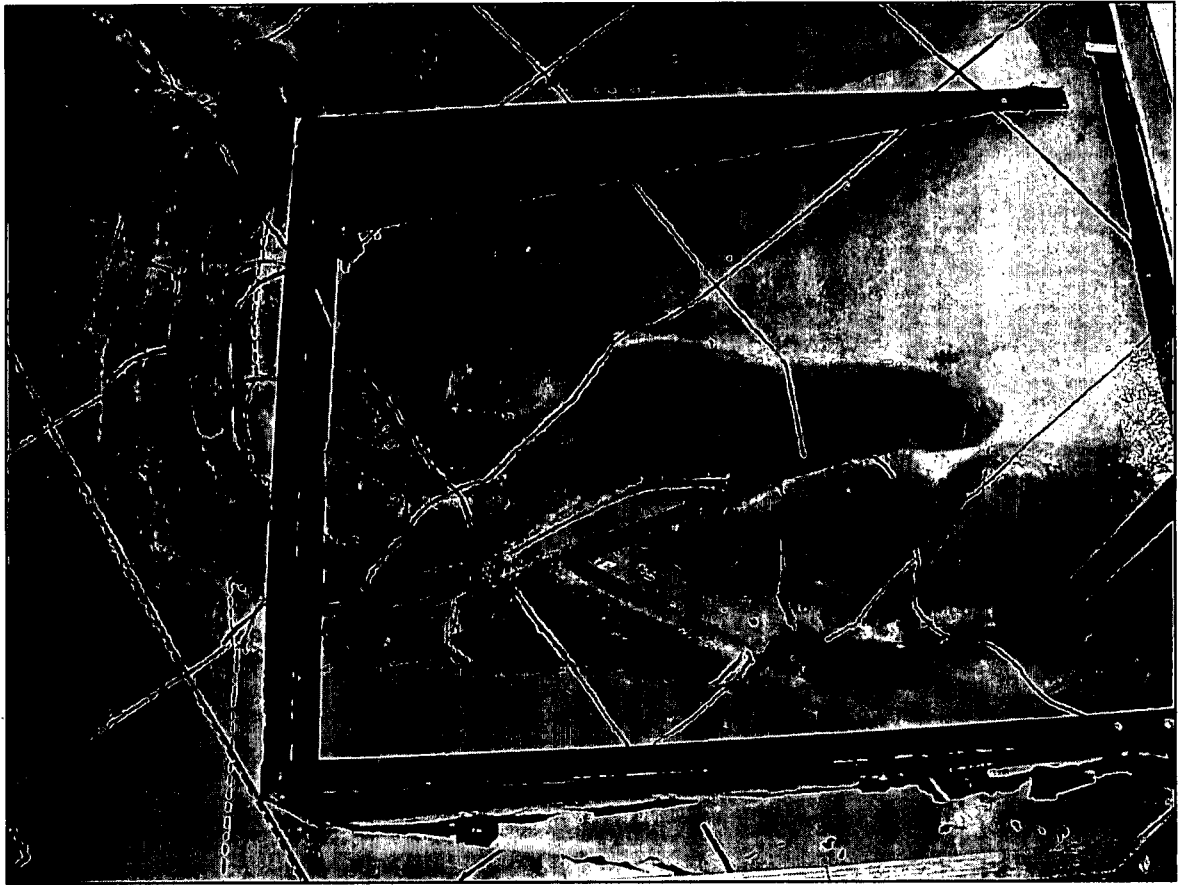


Figure 7-8. Elevation views of Curtain No. 4 (prototype dimensions).

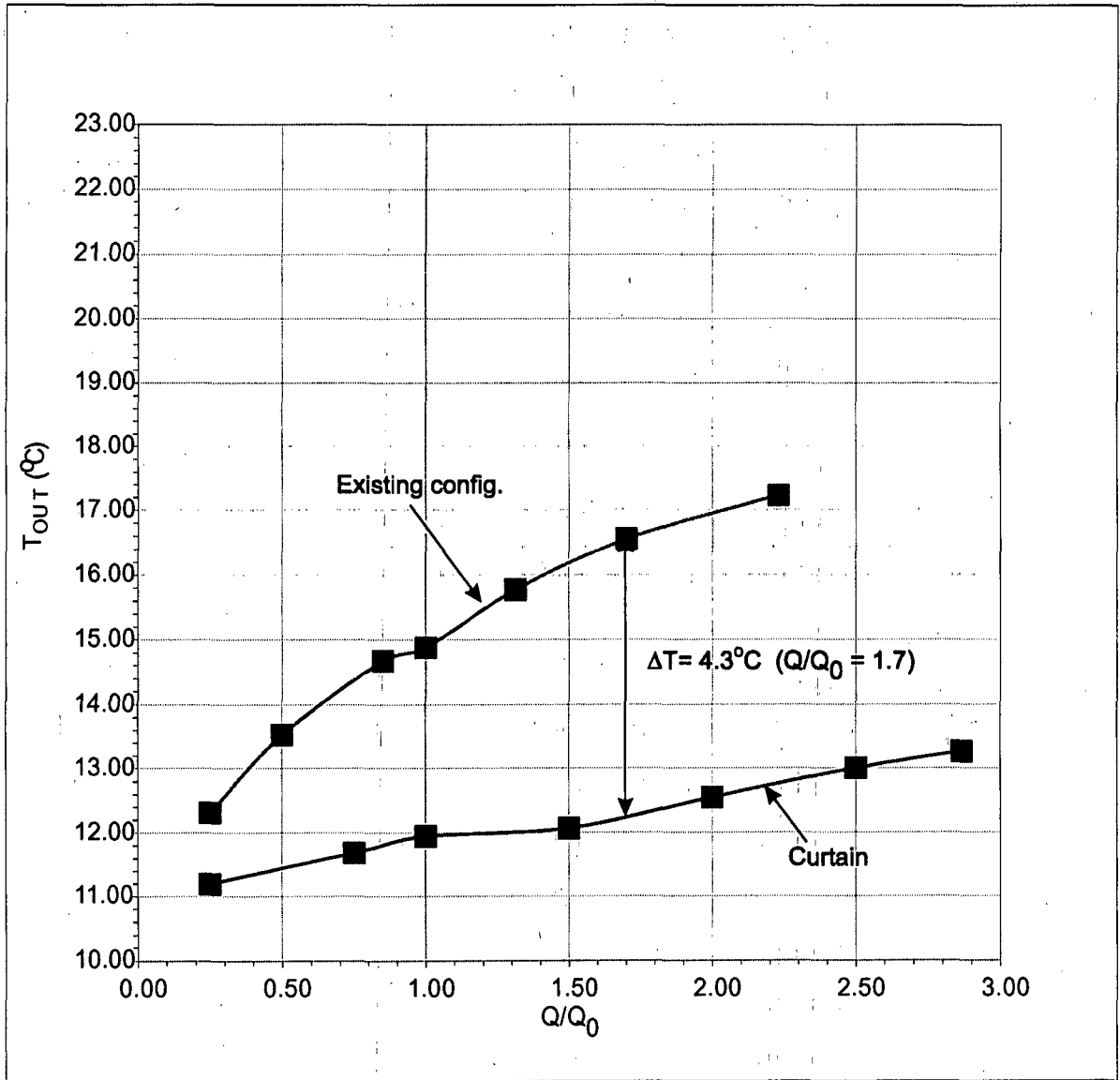


Curtain 4					
Distance model in	Depth model in	Area model in <sup>2</sup>	Distance proto ft	Elevation proto ft	Area proto ft <sup>2</sup>
0.00	0	0	0.0	4445.0	0
4.00	1.88	3.75	73.3	4438.8	229
7.00	2.75	6.94	128.3	4435.8	424
12.00	2.63	13.44	220.0	4436.3	821
17.00	2.75	13.44	311.7	4435.8	821
21.00	2.75	11.00	385.0	4435.8	672
23.50	0.00	3.44	430.8	4445.0	210
27.25	0.00	0.00	499.6	4445.0	0
30.00	6.50	8.94	550.0	4423.3	546
31.38	6.50	8.94	575.2	4423.3	546
34.00	0.00	8.53	623.3	4445.0	521
37.50	0.00	0.00	687.5	4445.0	0
38.00	1.00	0.25	696.7	4441.7	15
45.50	1.00	7.50	834.2	4441.7	458
46.00	0.00	0.25	843.3	4445.0	15
Area (model in <sup>2</sup> )		86.41	Area (prototype ft <sup>2</sup> )		5,280

Figure 7-9. Opening area between the curtain lip and lakebed for Curtain No. 4.

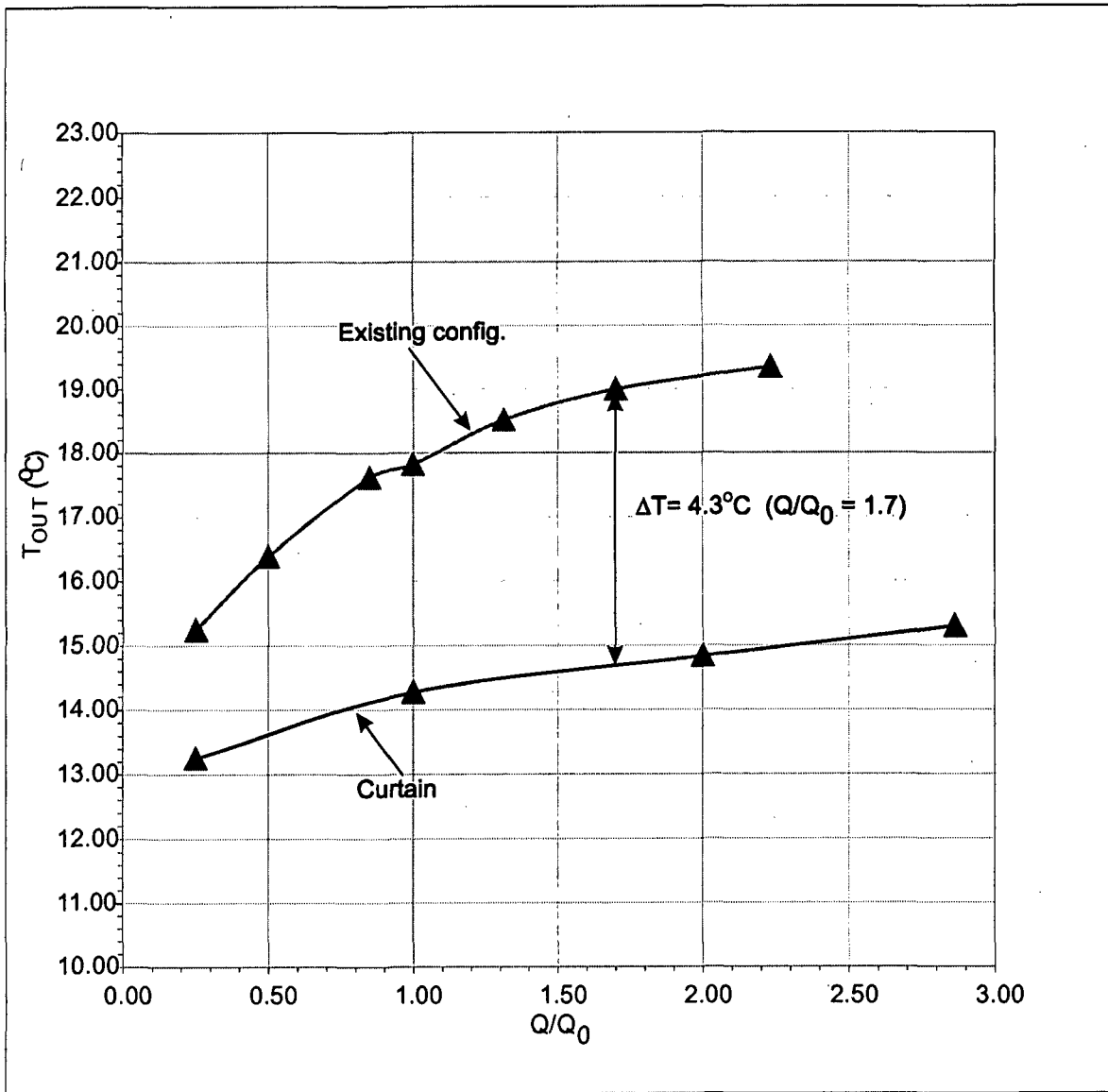


*Figure 7-10. View of Curtain No. 4.*



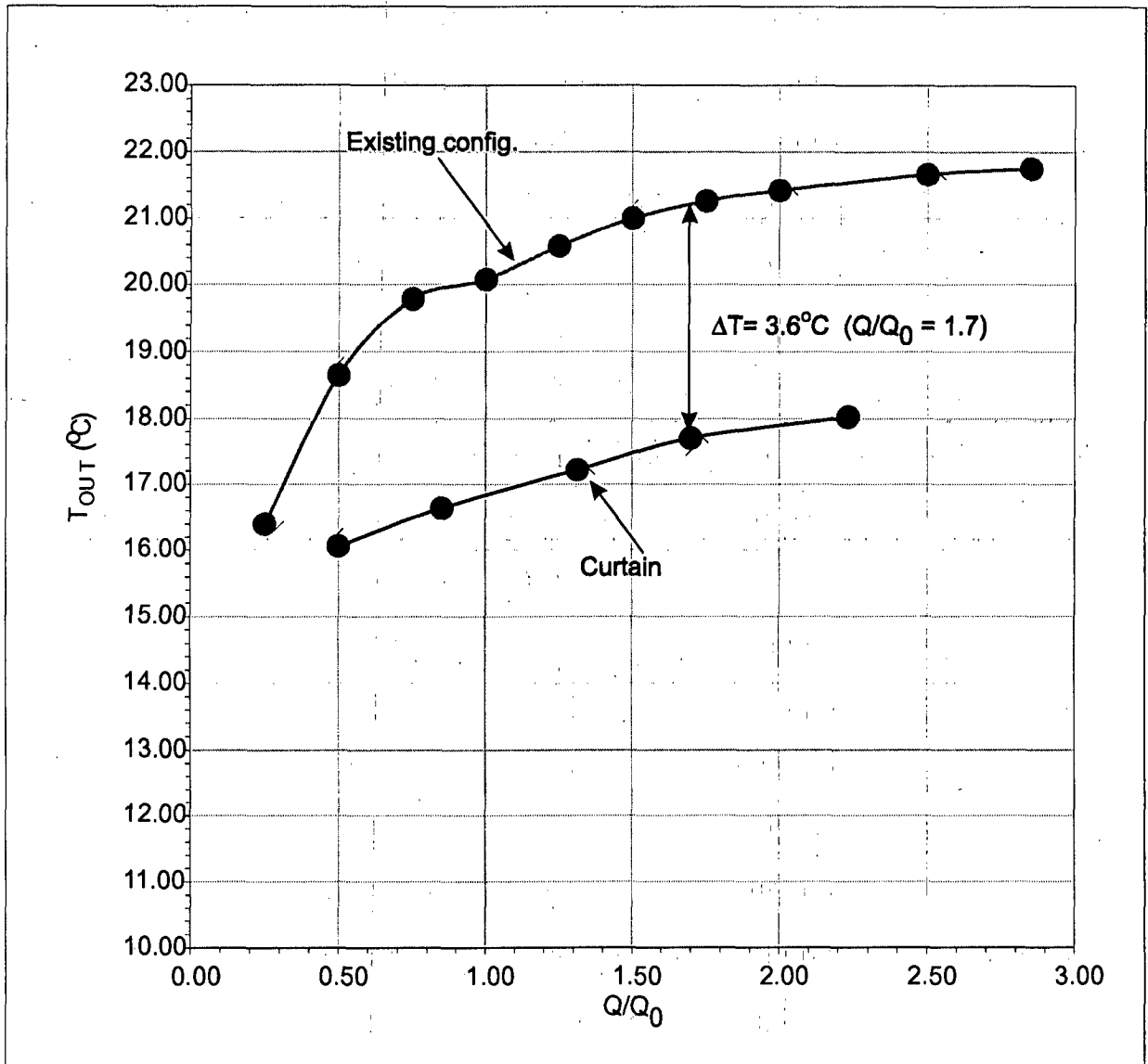
(a)

Figure 7-11. Effect of Curtain No. 4 on outflow temperature: (a) June condition.



(b)

Figure 7-11 continued. (b) July condition.



(c)

Figure 7-11 continued. (c) August condition.

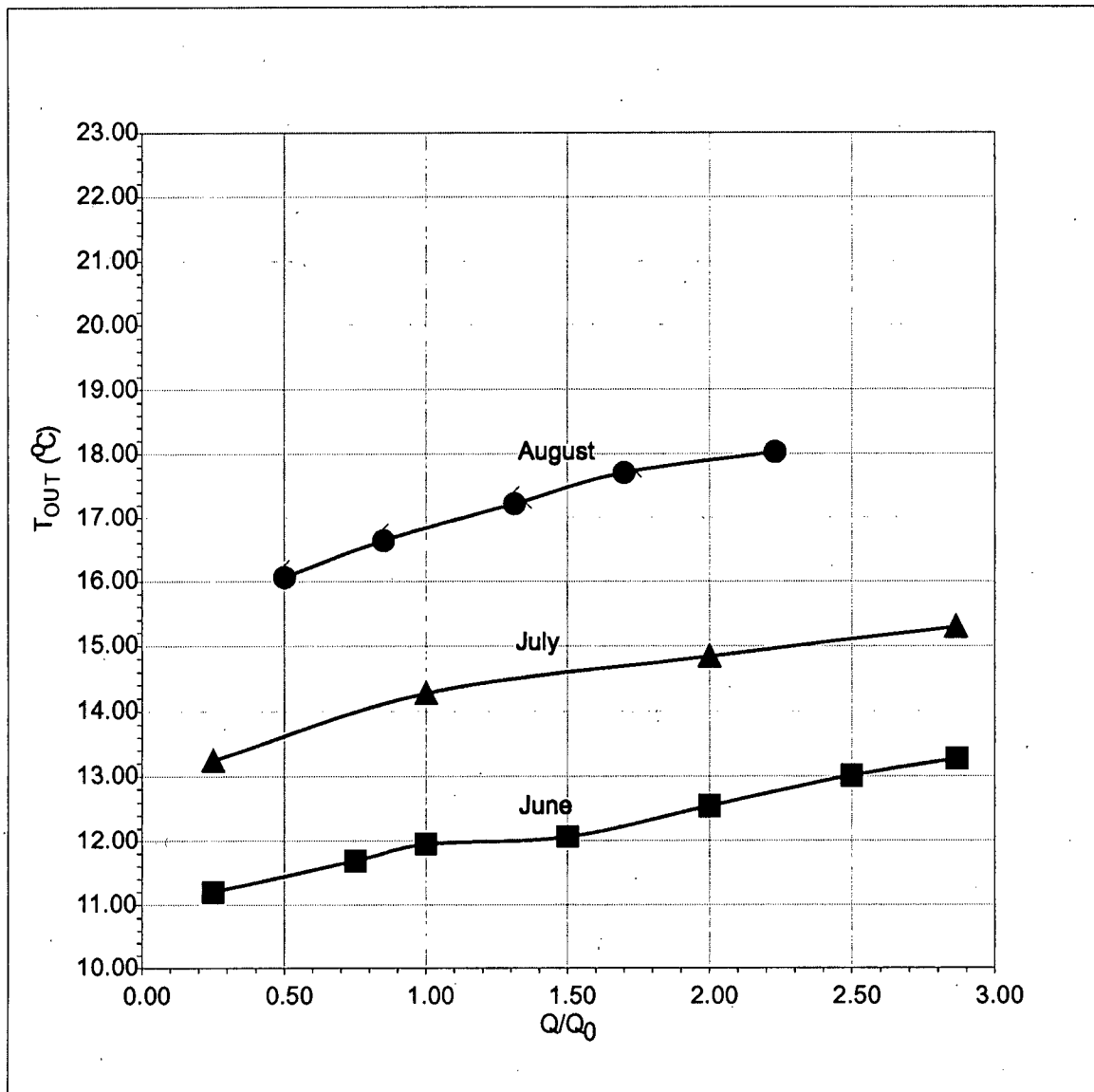


Figure 7-12. Comparison of Curtain No. 4 effects on outflow temperatures for June, July, and August conditions.

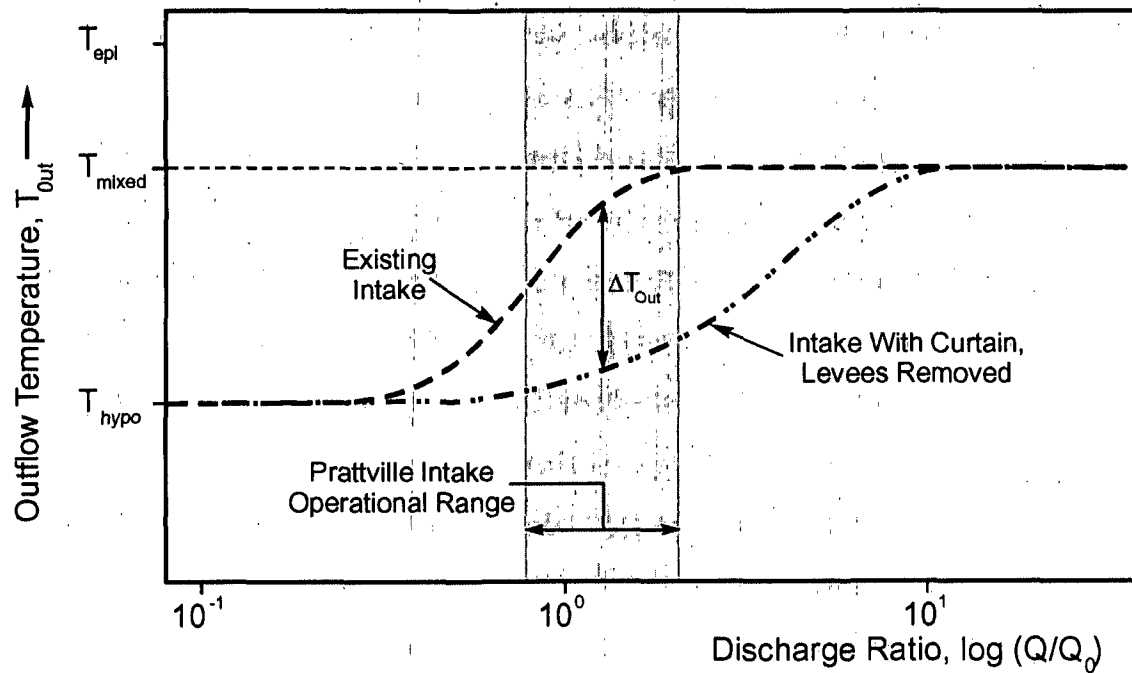
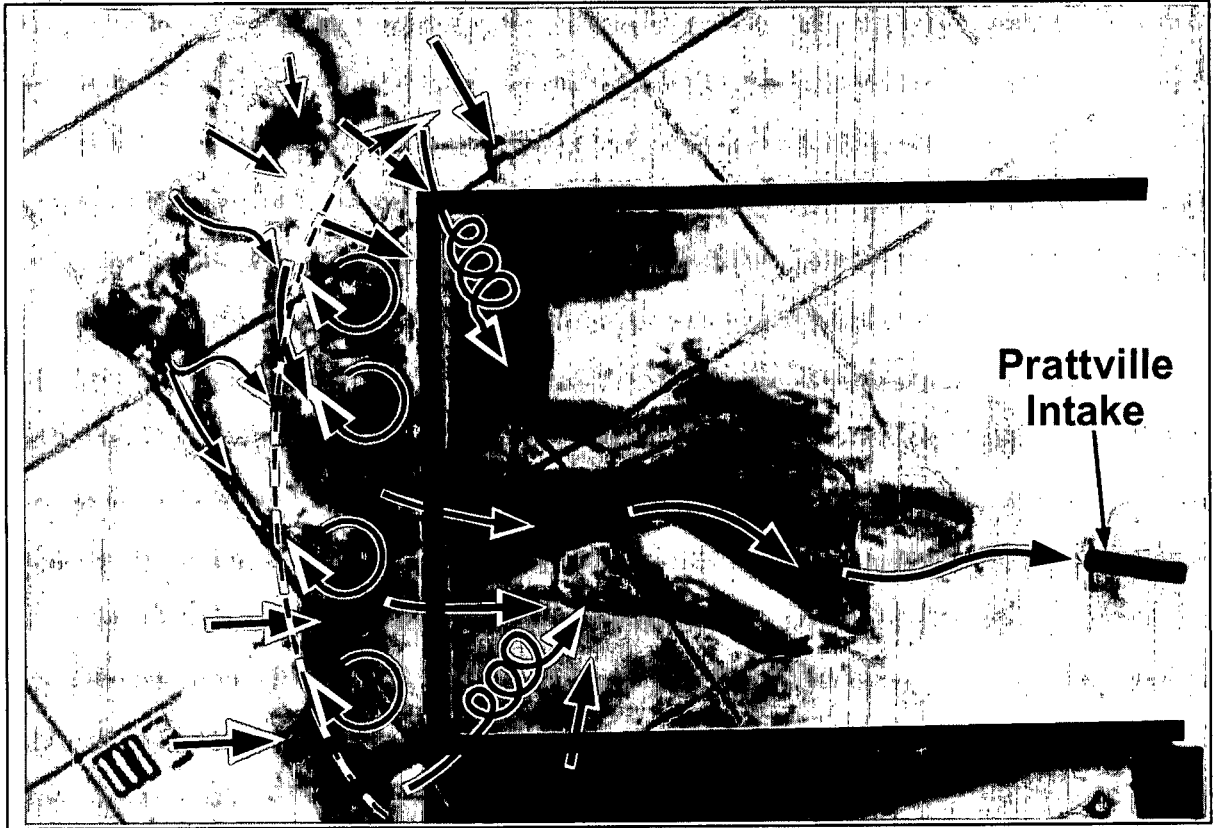


Figure 7-13. Conceptual trends showing the reduction in outflow temperature when the intake is fitted with a curtain. At very low rates of outflow, only cold water is withdrawn. At higher flow rates, the curtain's effectiveness decreases because fully mixed water passes beneath the curtain.



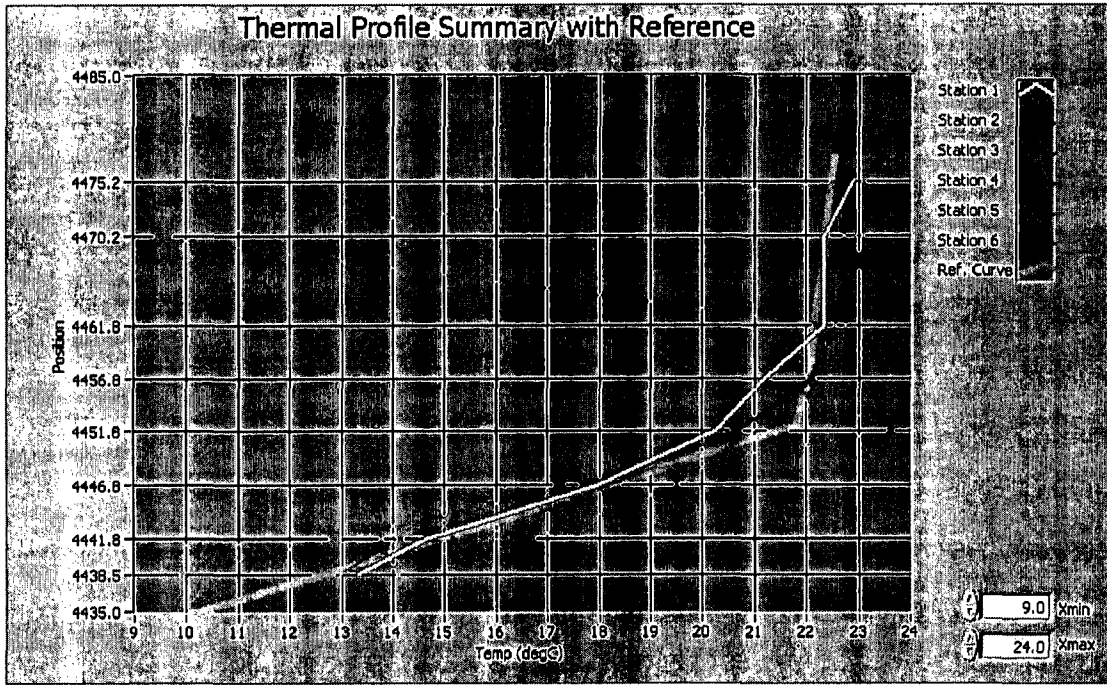
(a)

Figure 7-14. Visualization of flow to Prattville Intake fitted with Curtain No. 4 ( $Q/Q_0 = 1.7$ , August condition). (a) Visualization with dye. Dye is released into approach flow outside the incised channel; blue dye is in the colder bottom layer; and red dye is in the warmer surface layer.

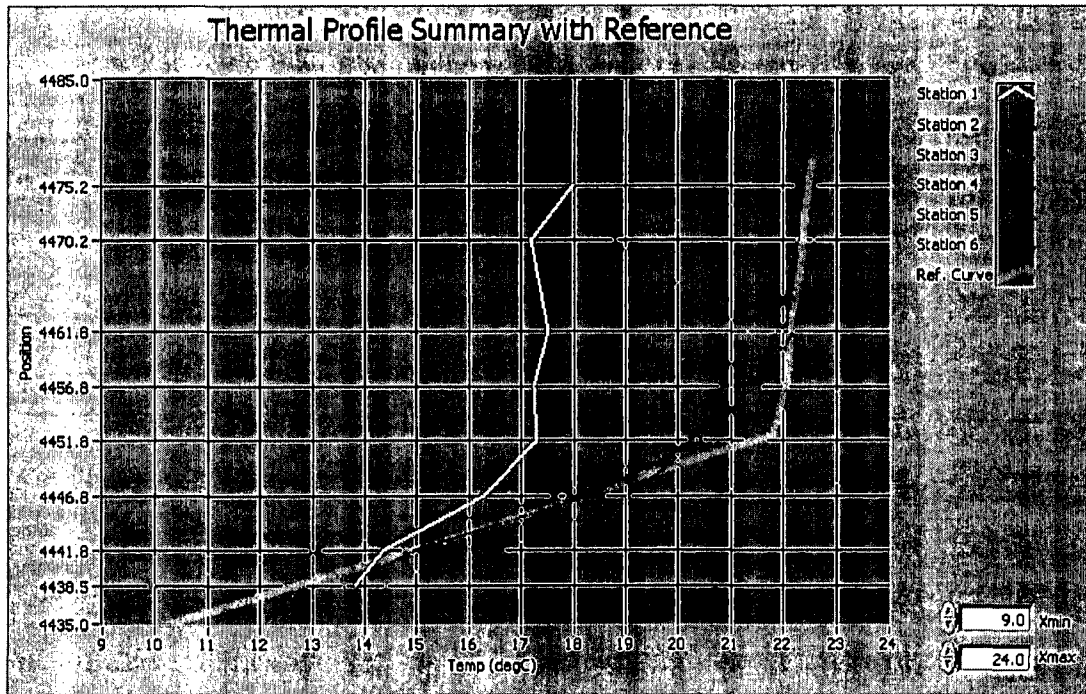


(b)

Figure 7-14 continued. (b) Photograph with arrows indicating flow paths toward Prattville Intake fitted with Curtain No. 4 ( $Q/Q_0 = 1.7$ , August condition).



(a)



(b)

Figure 7-15. Variation of water temperature profiles inside the curtain: (a) initial temperature profiles inside (white line) and outside the curtain (green line); (b) temperature profile inside the curtain when outflow temperature is steady at  $T_{out} = 17.4^{\circ}\text{C}$ .

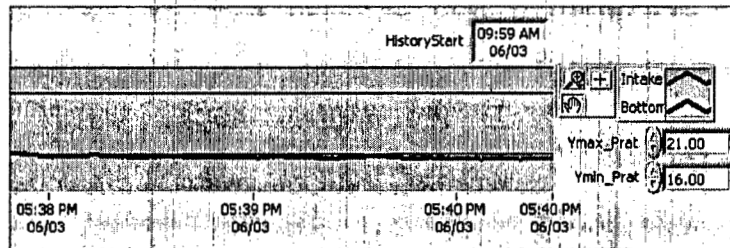
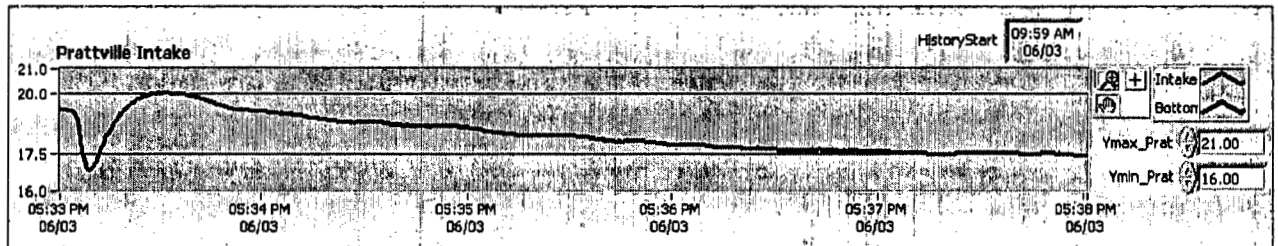


Figure 7-16. Variation of outflow temperature until steady temperature at  $T_{out} = 17.4^{\circ}\text{C}$  is obtained (the two successive screens are equivalent of 7 minutes of intake operation);

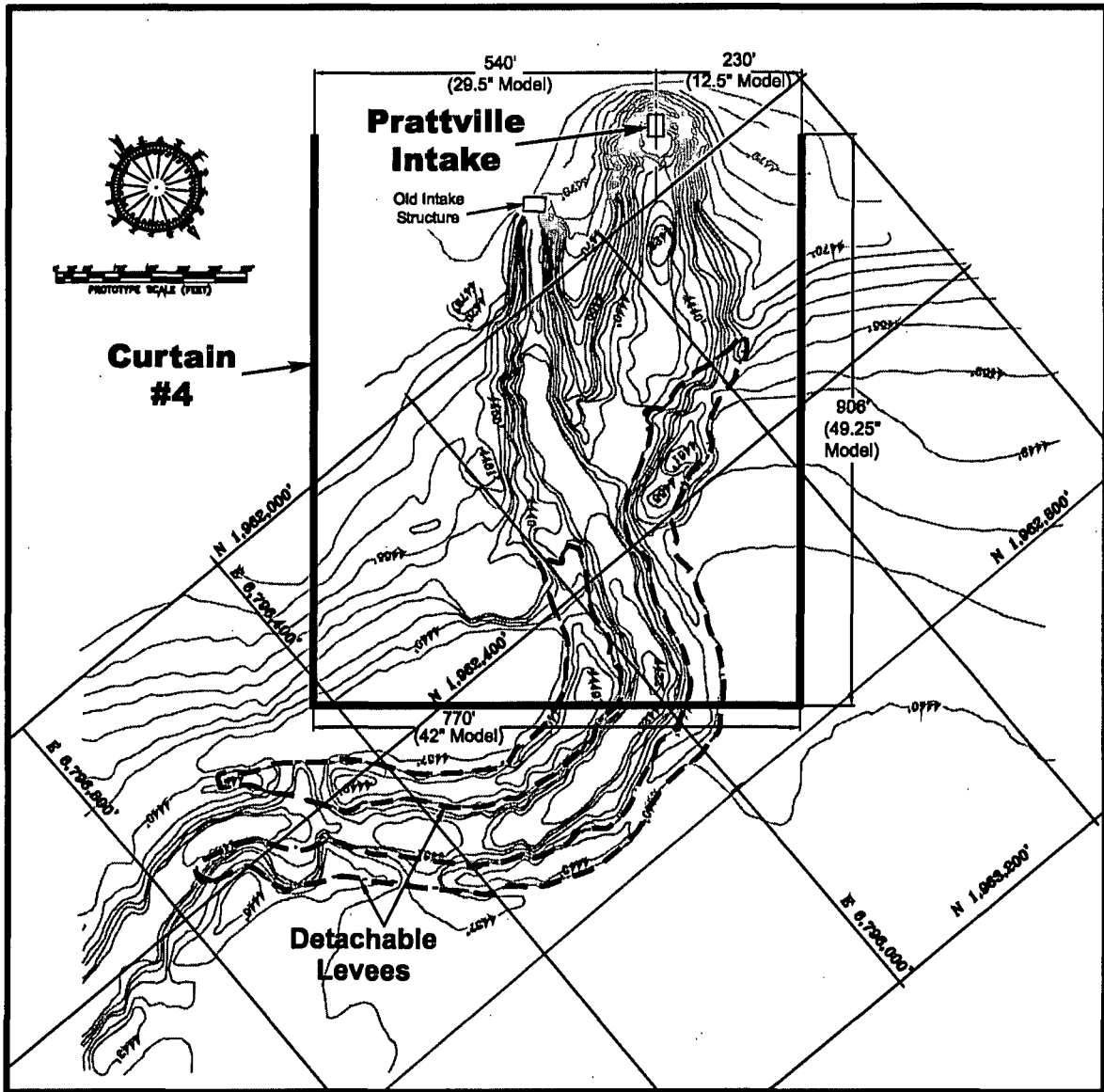


Figure 7-17. Curtain No. 4 with levees removed

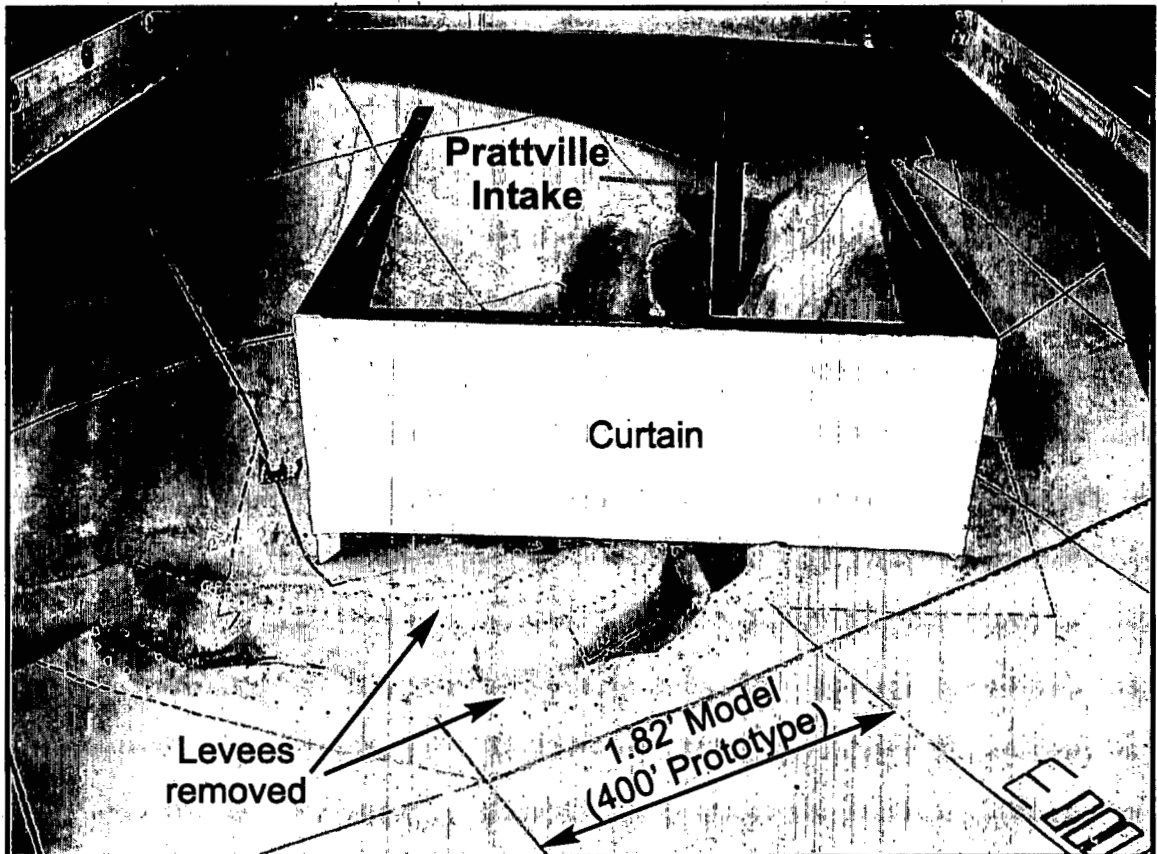
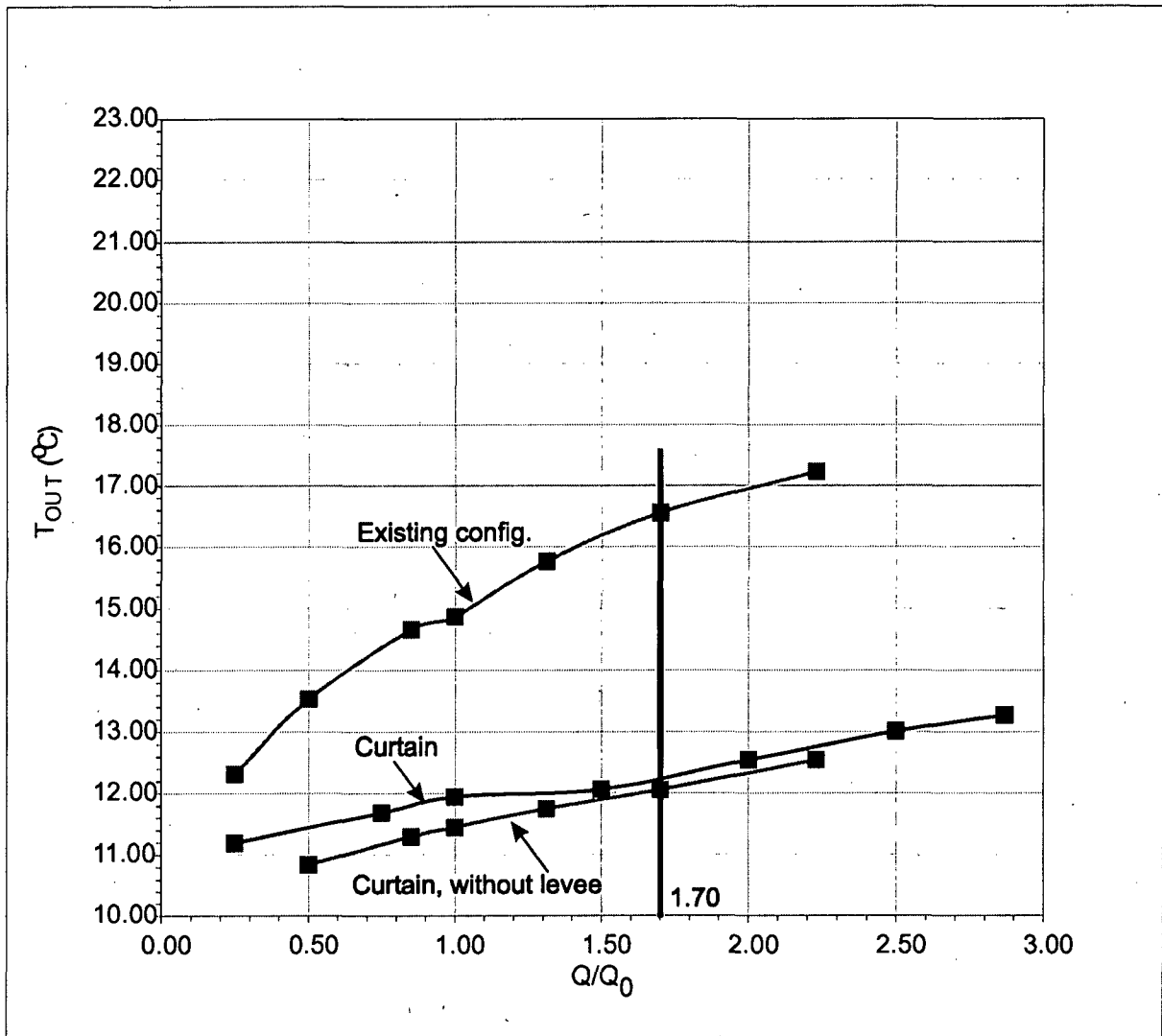
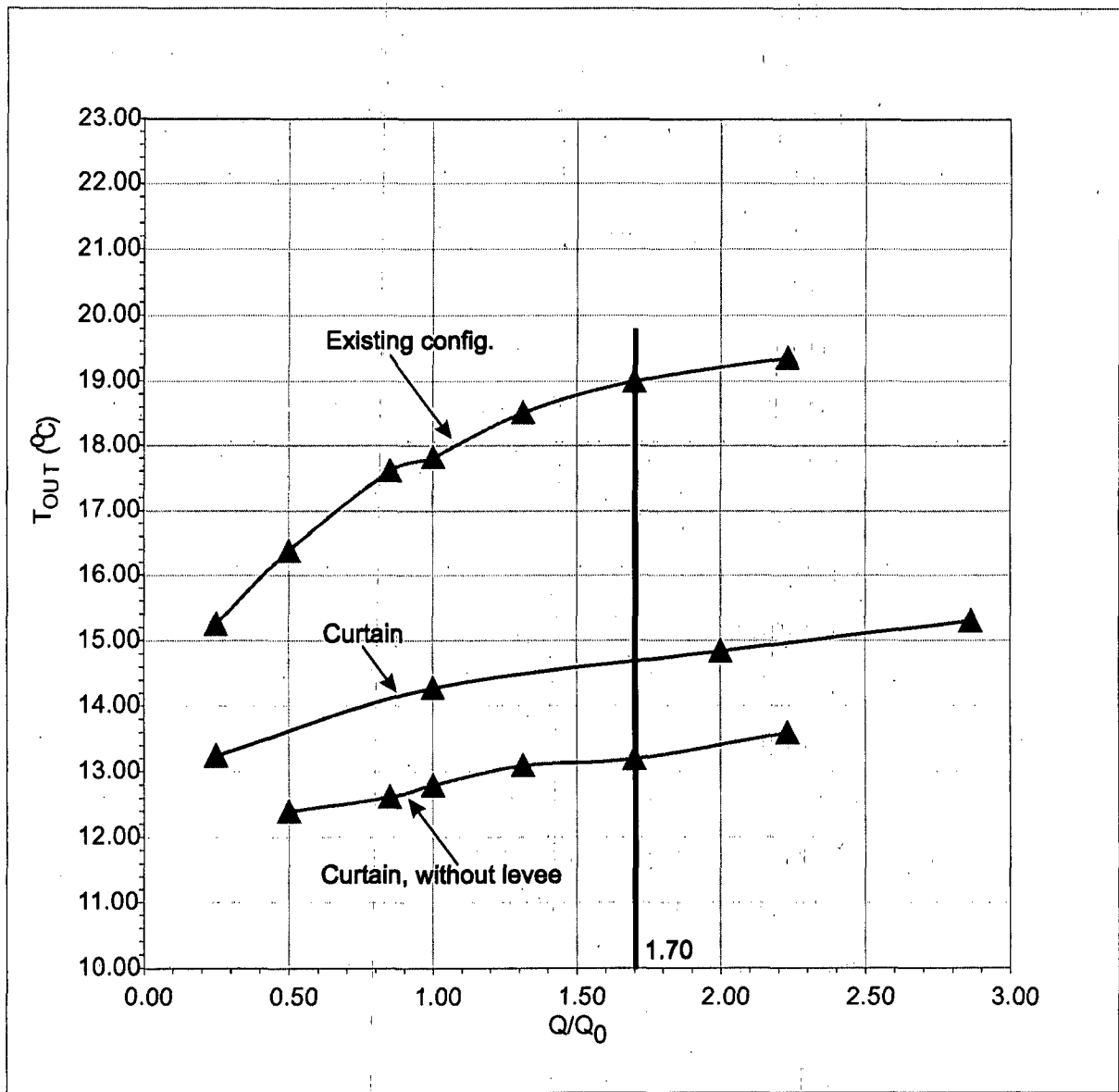


Figure 7-18. View of Curtain No. 4 with levees removed.



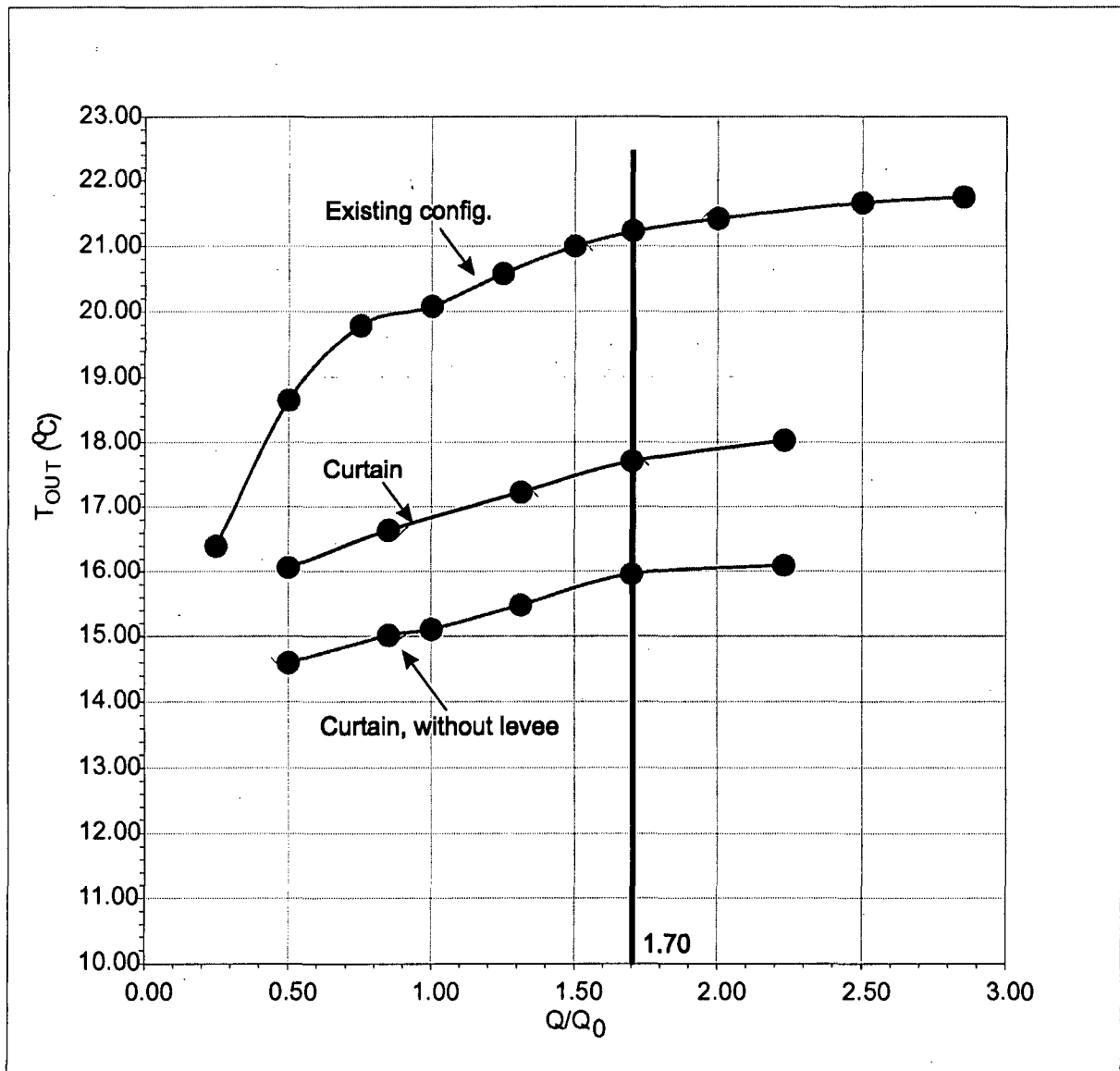
(a)

Figure 7-19. Reduction in outflow temperature produced by Curtain No. 4 with levees removed: (a) June condition.



(b)

Figure 7-19 continued. (b) July condition.



(c)

Figure 7-19 continued. (c). August condition

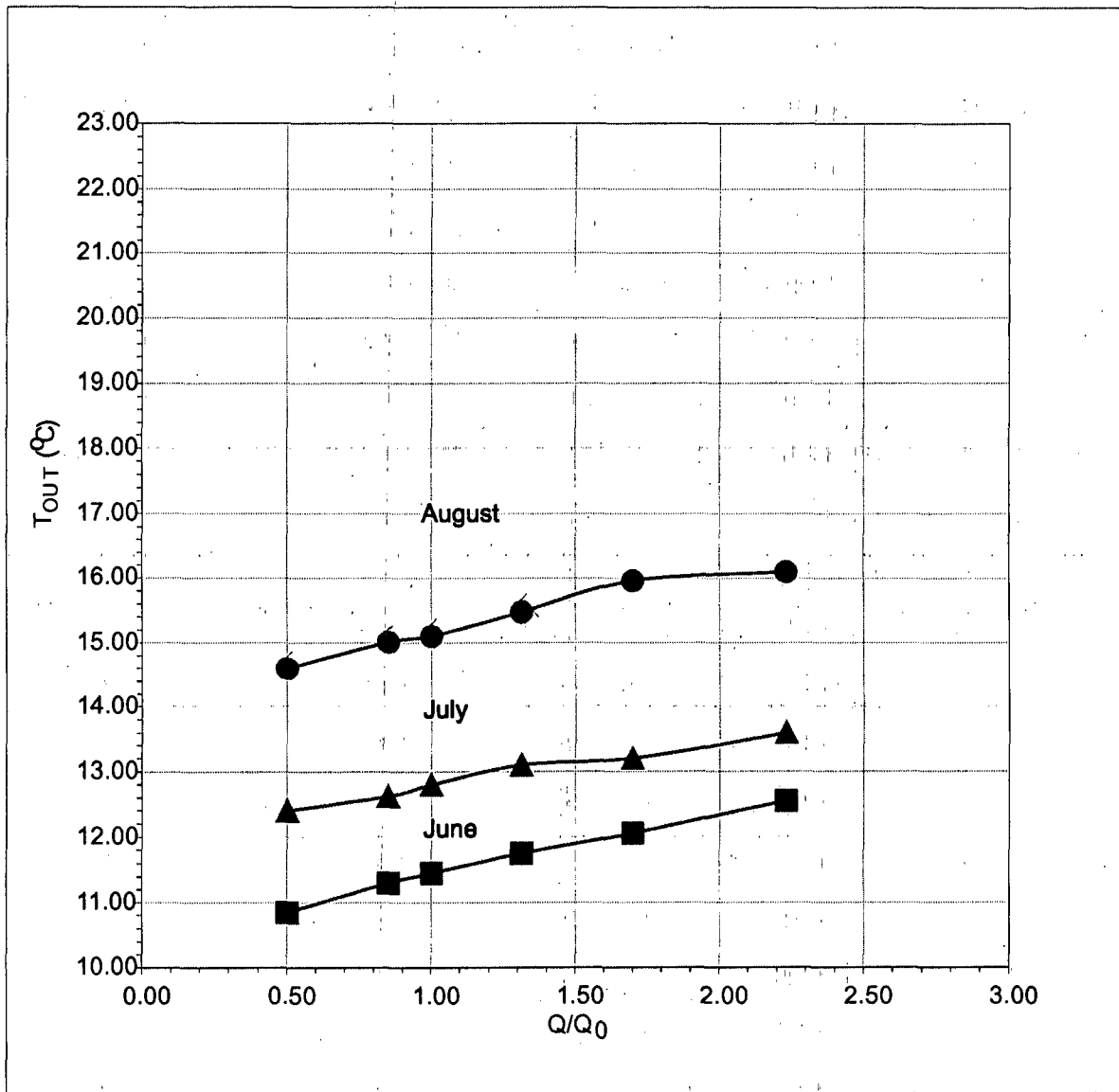
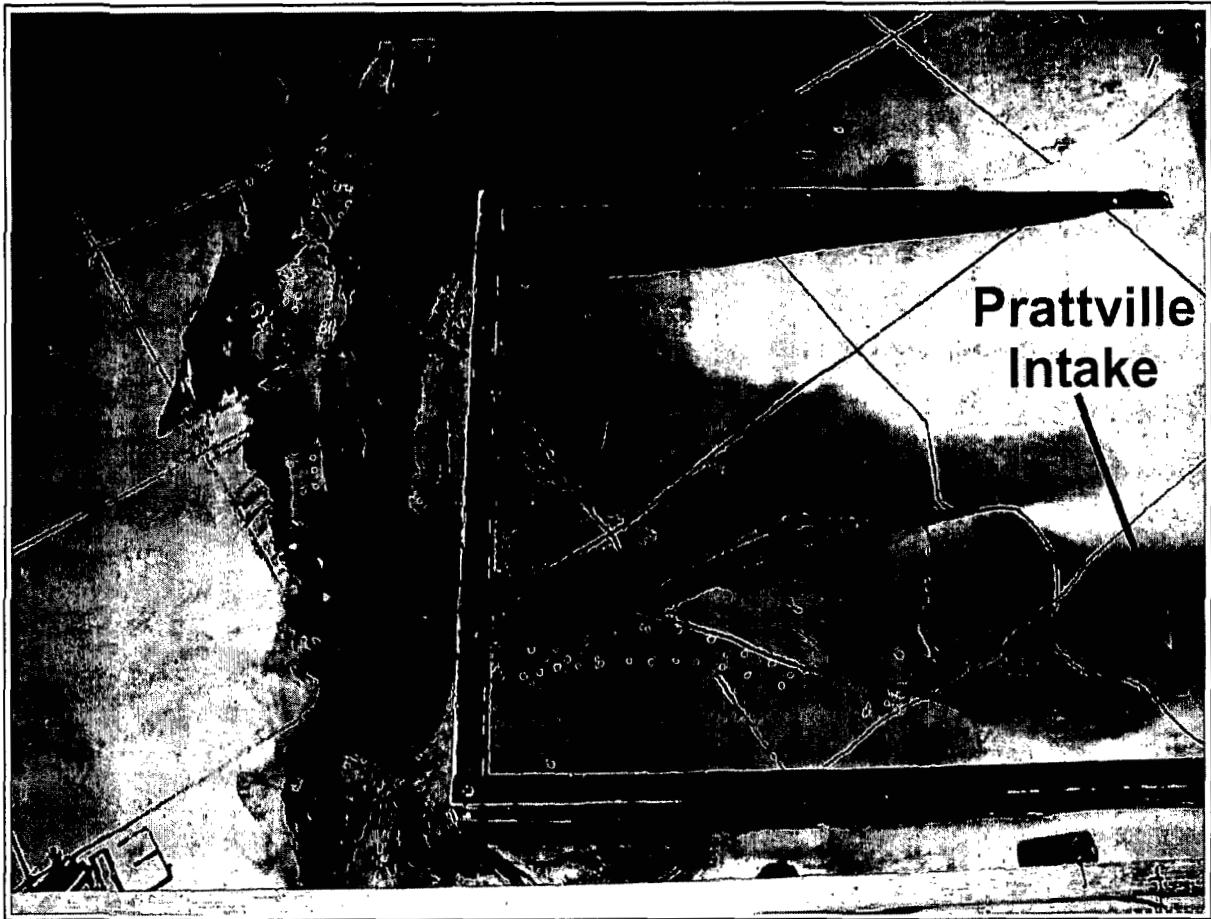
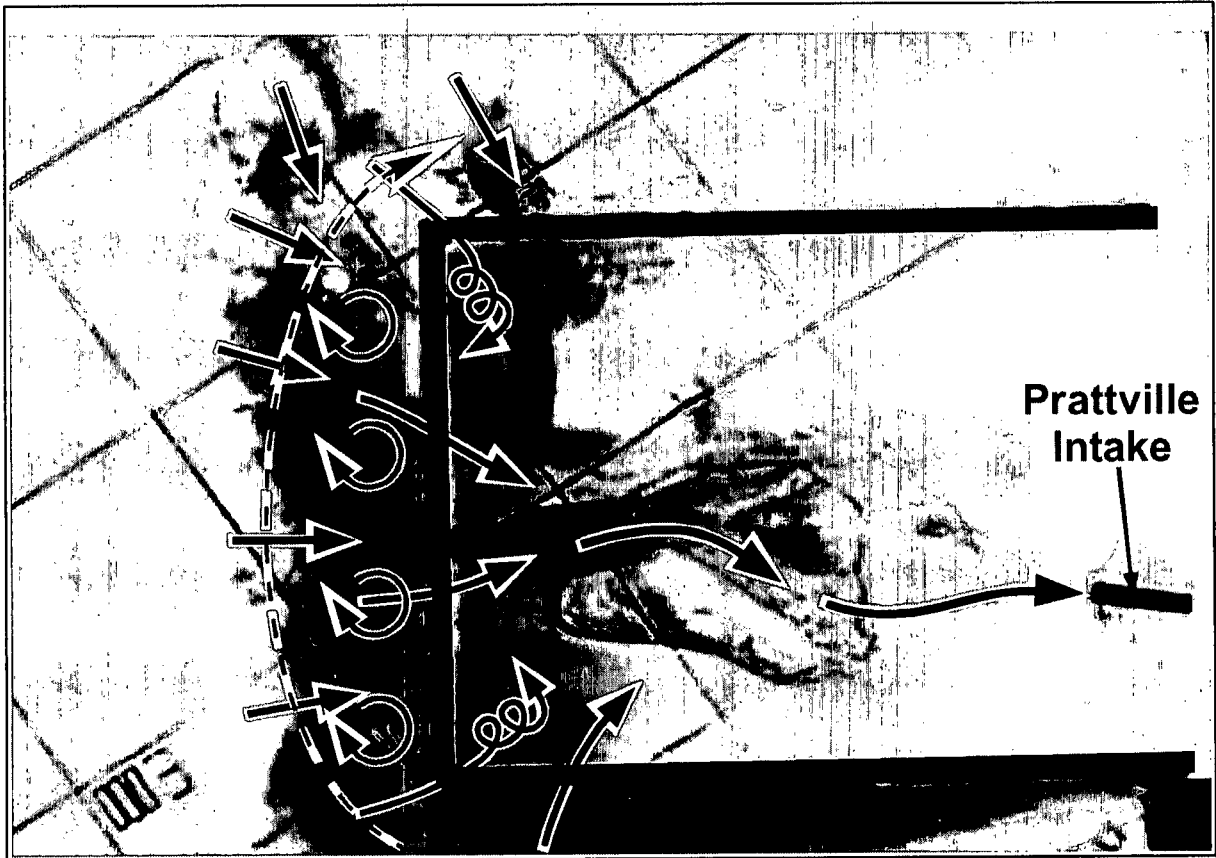


Figure 7-20. Outflow temperature obtained with Curtain No. 4 and levees removed, for the June, July, and August conditions.



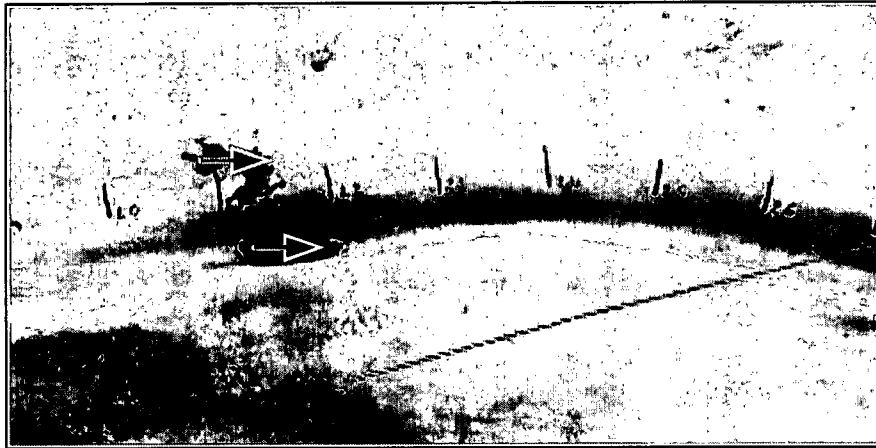
(a)

Figure 7-21. Visualization of the flow approaching and passing Curtain No. 4, when levees are removed ( $Q/Q_0 = 1.7$ , August condition). (a) Visualization with dye. Dye is released into approach flow outside the incised channel; blue dye is in the colder bottom layer; and red dye is in the warmer surface layer.

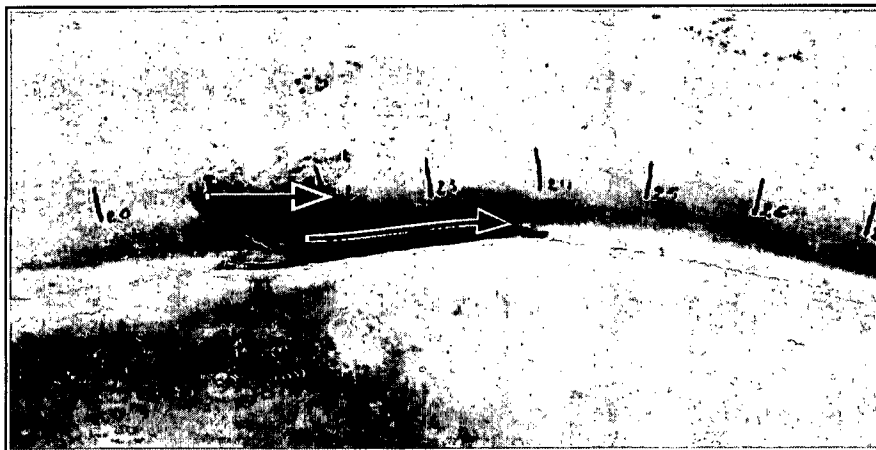


(b)

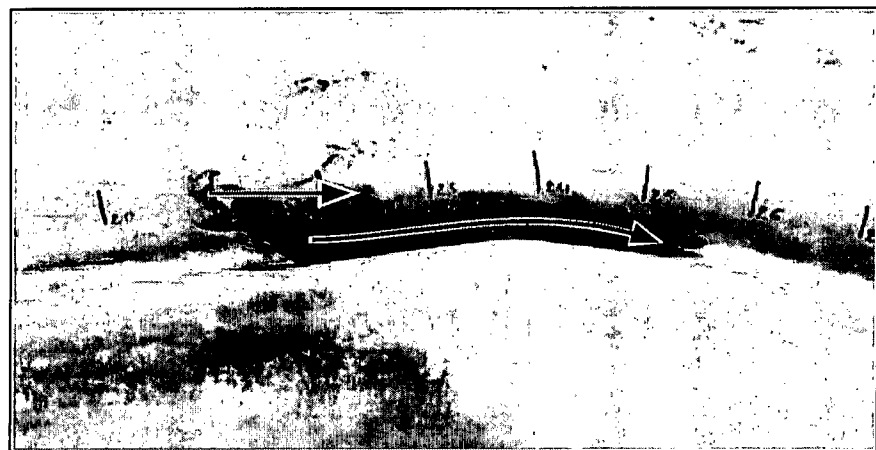
Figure 7-21 continued. (b) Photograph with arrows indicating flow paths.



(a)



(b)



(c)

Figure 7-22. Flow along the incised channel approx 15ft (3,300 ft prototype) upstream from the Intake. Sequential photographs (a to c) were used to determine the velocity in the incised channel.

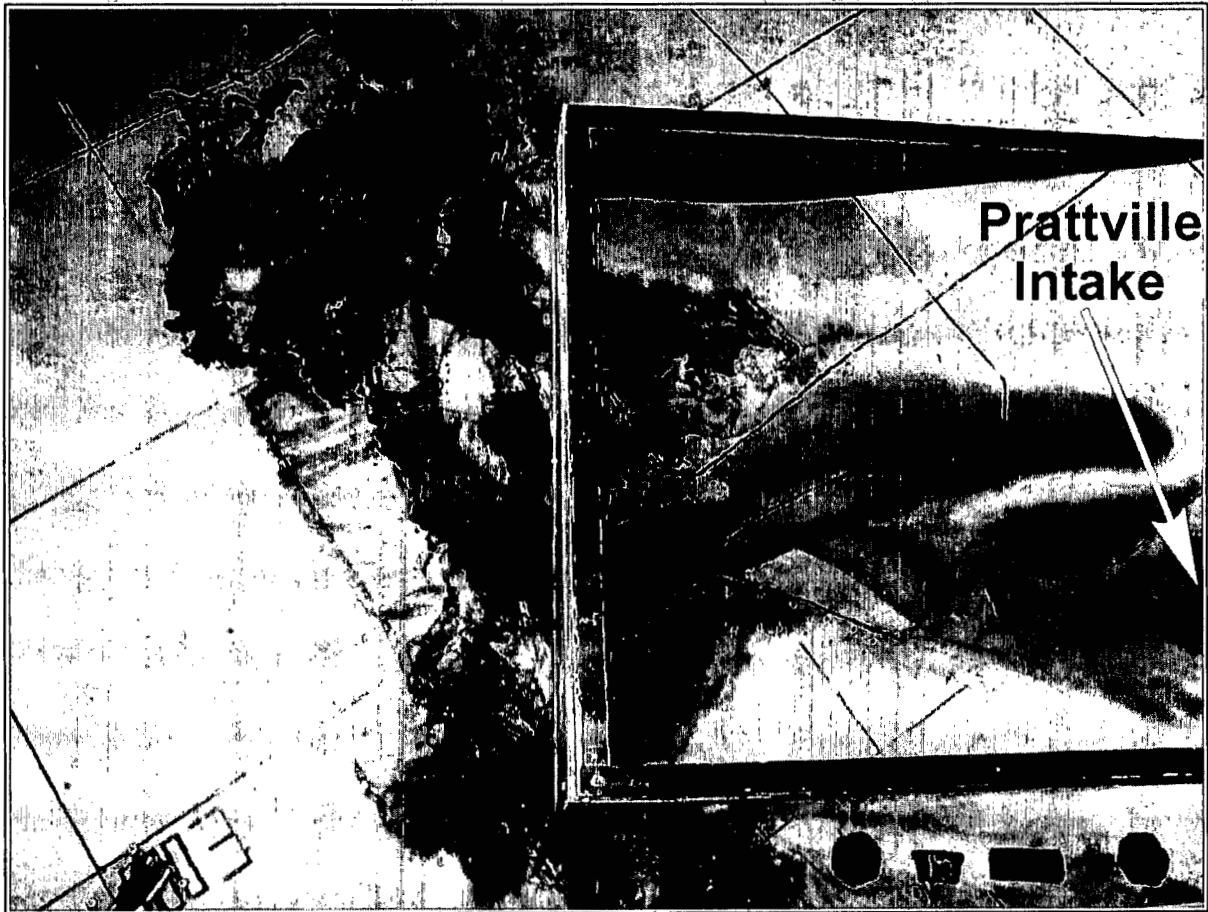
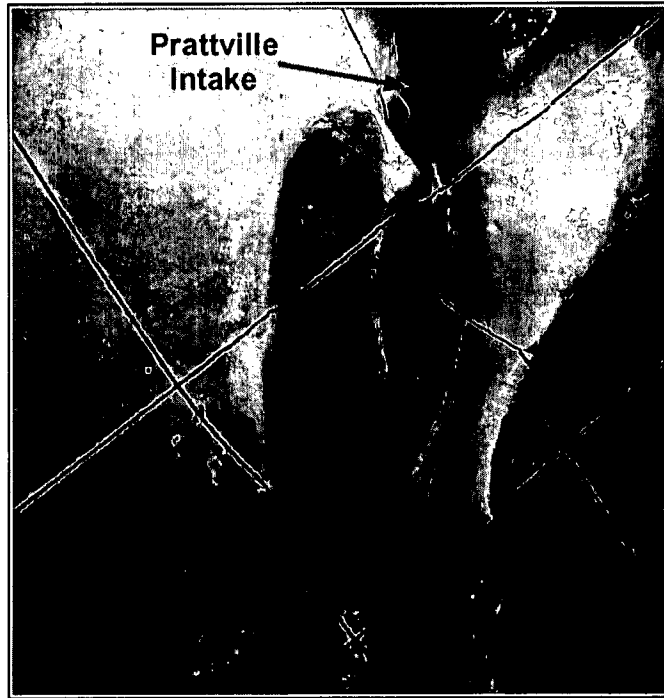
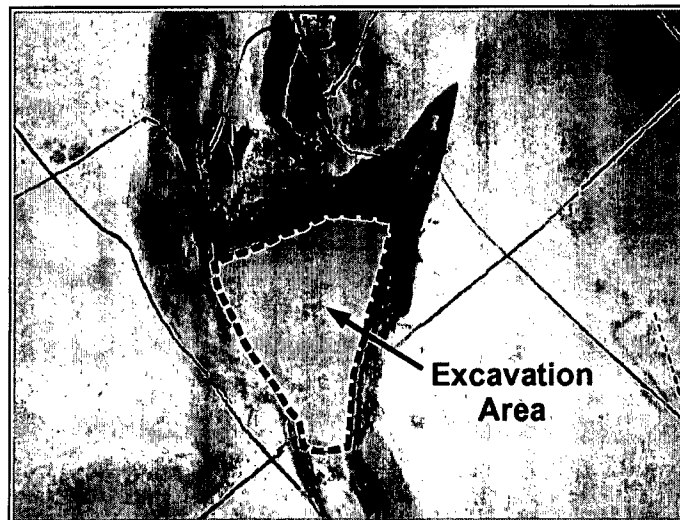


Figure 7-23. Visualization of the flow approaching and passing Curtain No. 4 without levees, operating without thermal stratification in the lake ( $Q/Q_0 = 1.7$ , water surface for August condition). Dye is released into approach flow outside the incised channel; blue dye is in colder bottom layer; red dye is in the warmer surface layer.



(a)



(b)

Figure 7-24. Excavation near the Intake: (a) original bathymetry; (b) bathymetry with excavation.

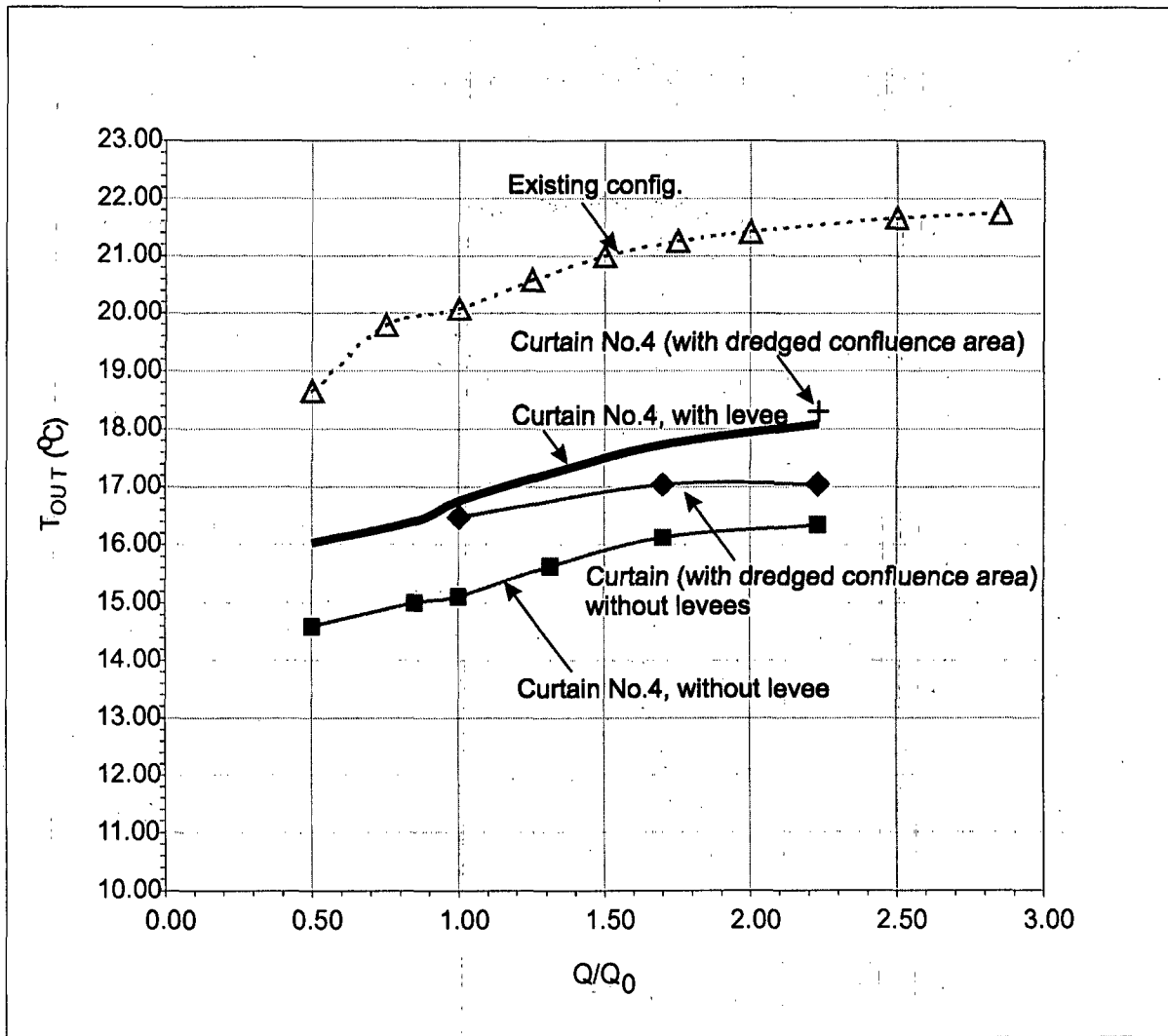
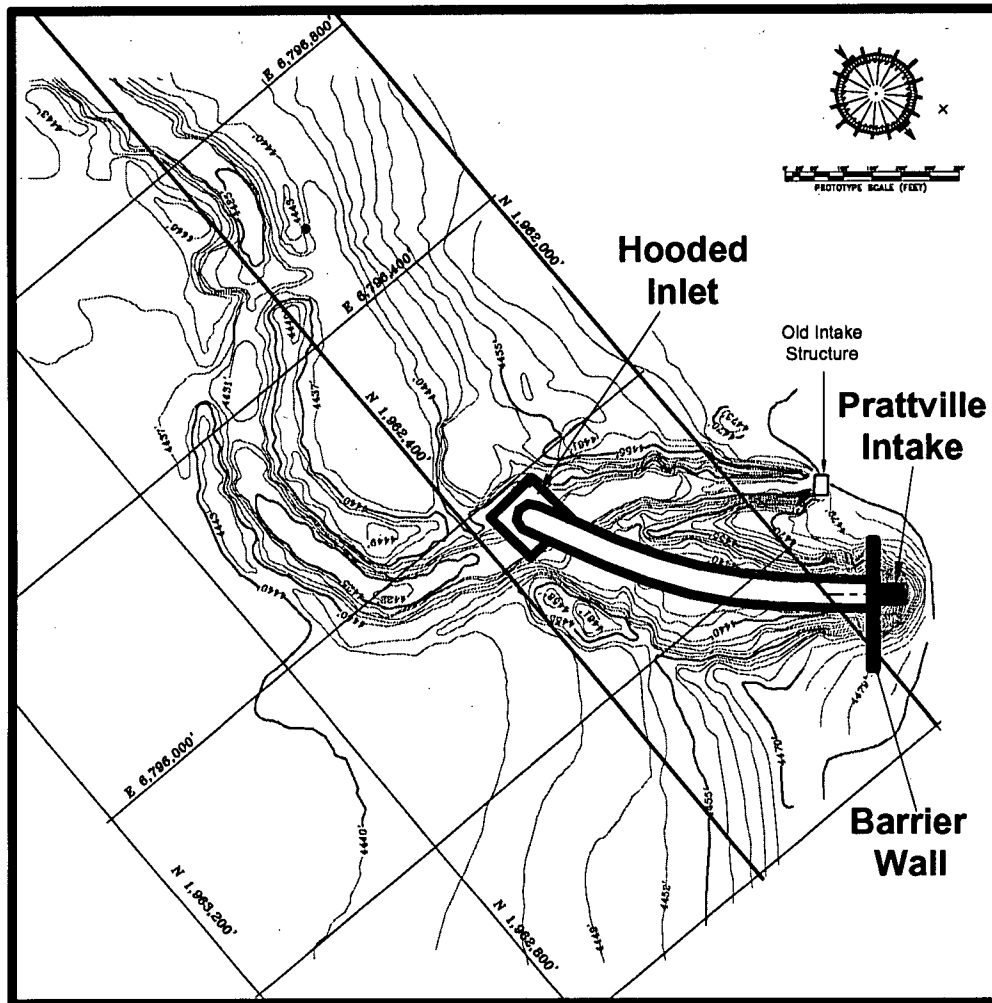
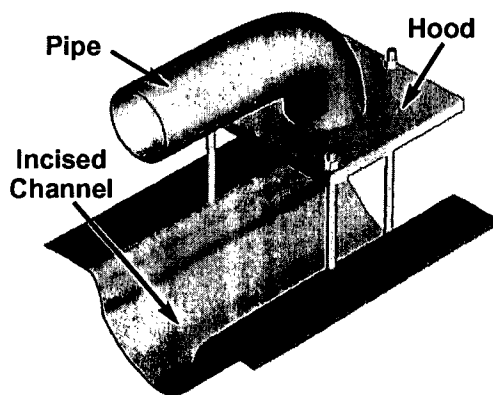


Figure 7-25. Comparison of the performances of Curtain No. 4 (with and without levees) with additional excavation in the confluence area; August condition.



(a)



(b)

Figure 7-26. Short pipe with hooded inlet (SPHI): (a) location of the SPHI; (b) conceptual sketch of the modeled SHPI.

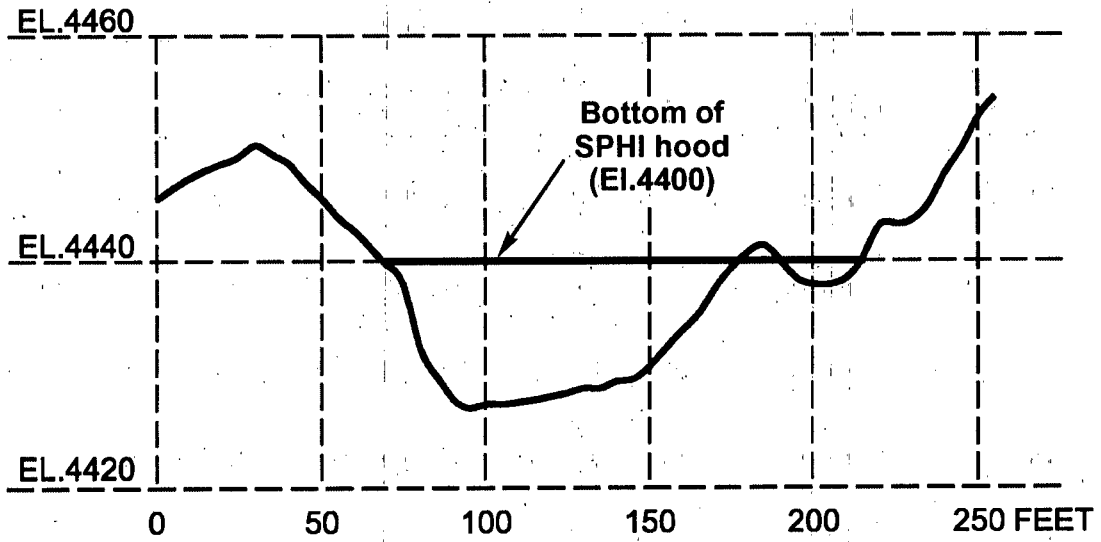


Figure 7-27. Elevation view of the cross-section through the hood and the incised channel (prototype dimensions) for the modeled SPHI.

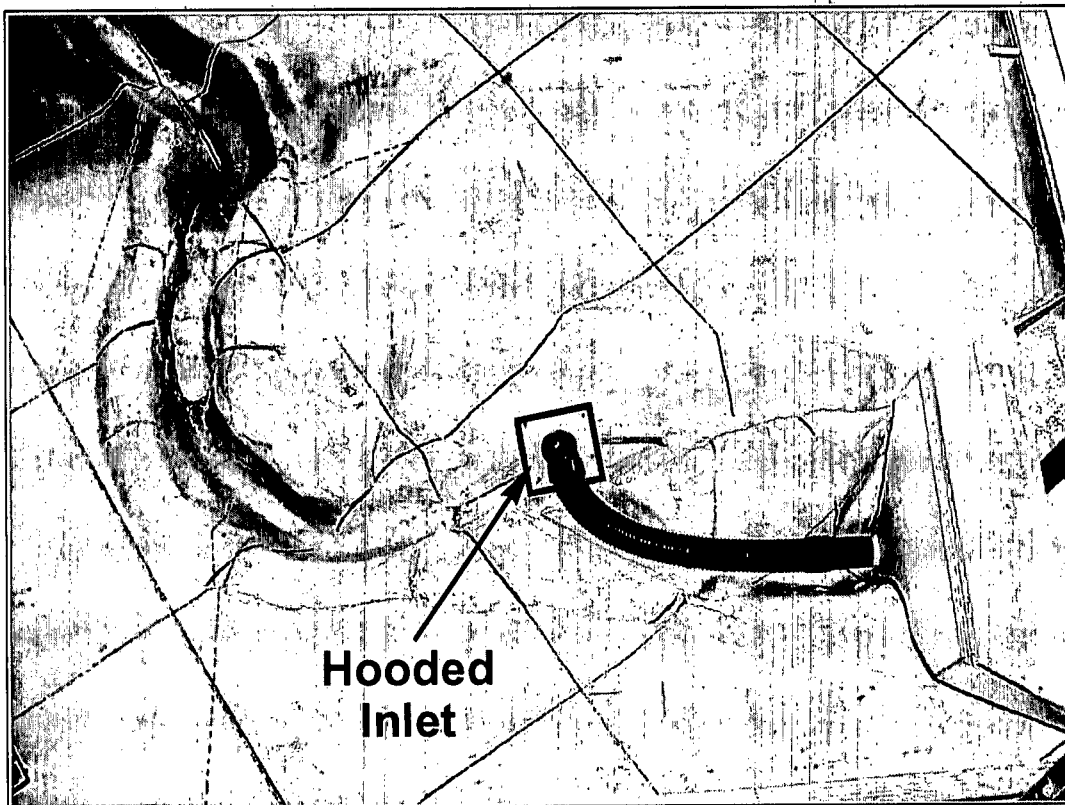


Figure 7-28. View of the SPHI in the model.

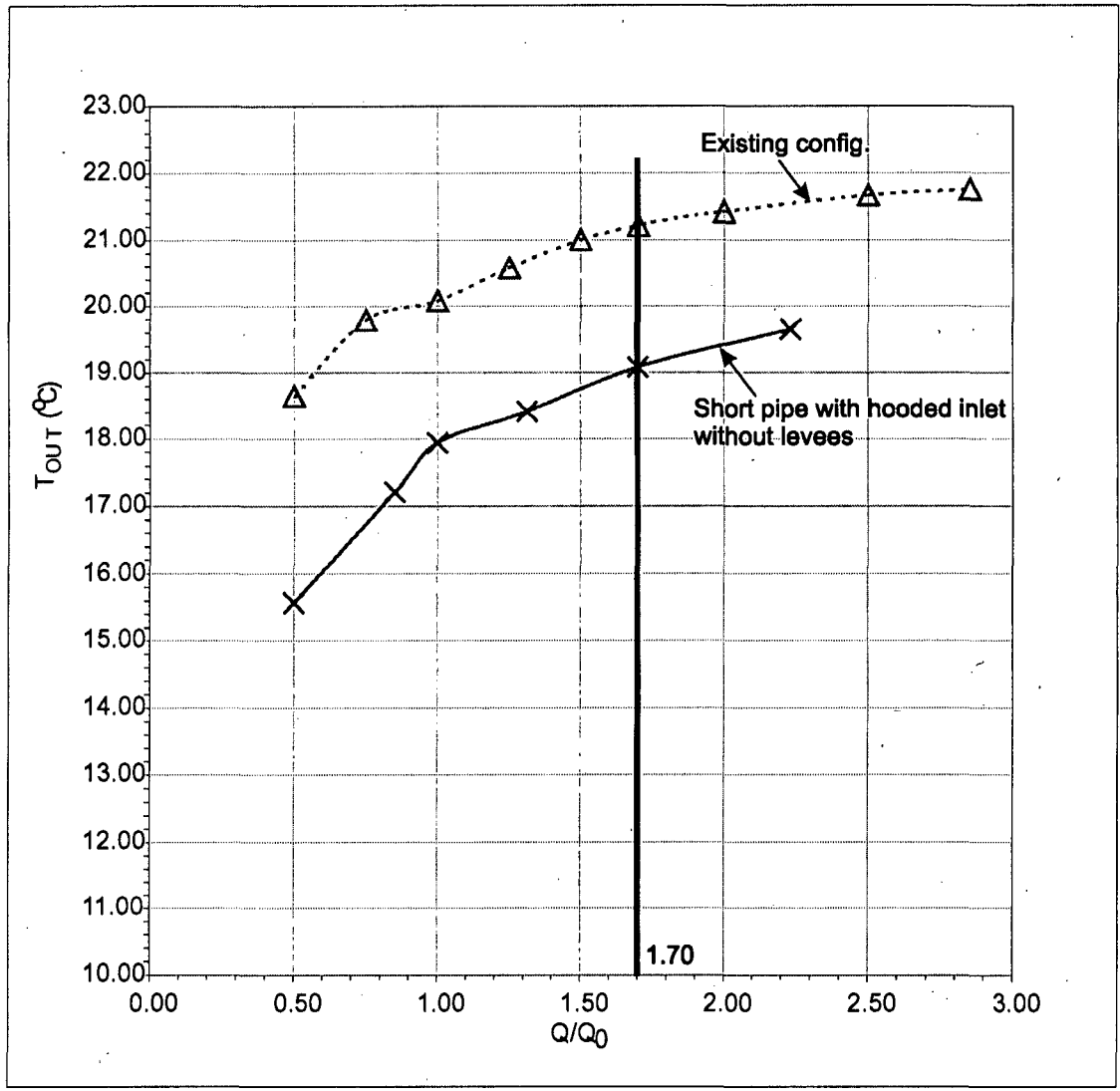


Figure 7-29. Effect of the short-pipe with hooded inlet without levees on outflow temperature; August condition.

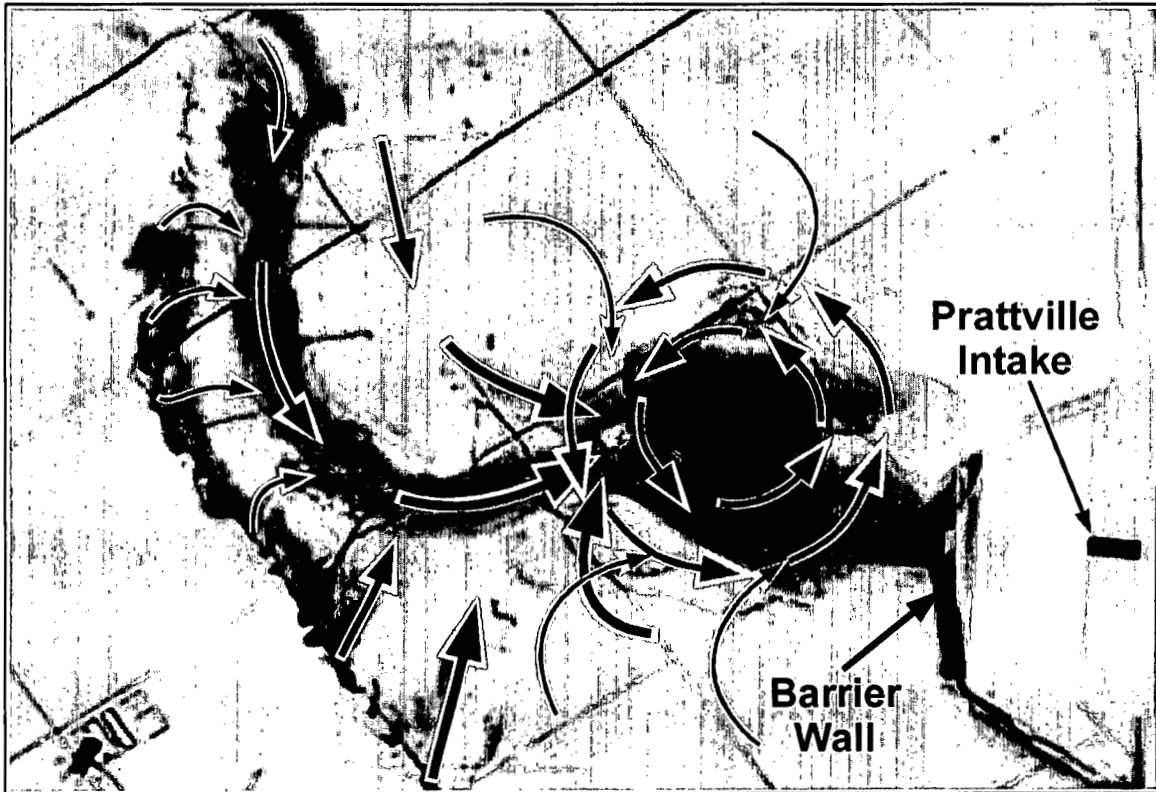


Figure 7-30. Visualization of the flow approaching the SPHI. The arrows indicate flow paths produced by the short pipe with hooded inlet.

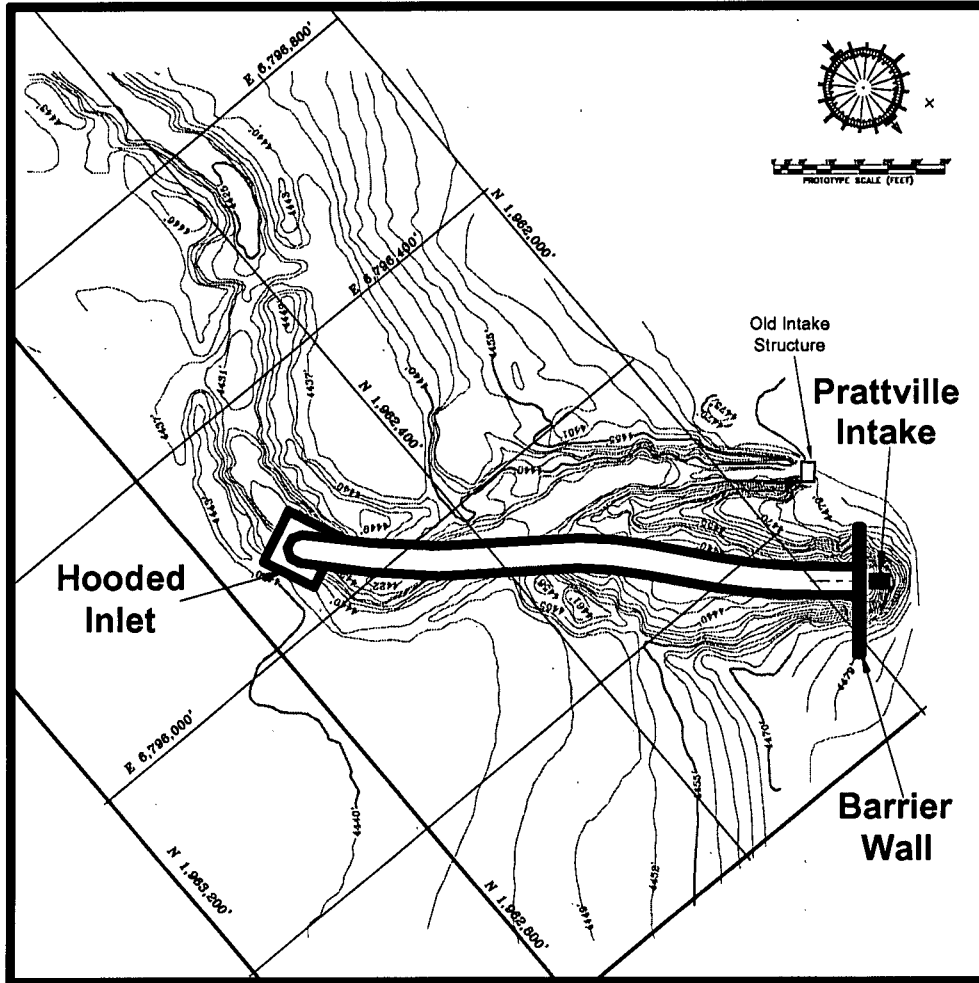


Figure 7-31. Location of the long pipe with hooded inlet (LPHI) relative to Prattville Intake.

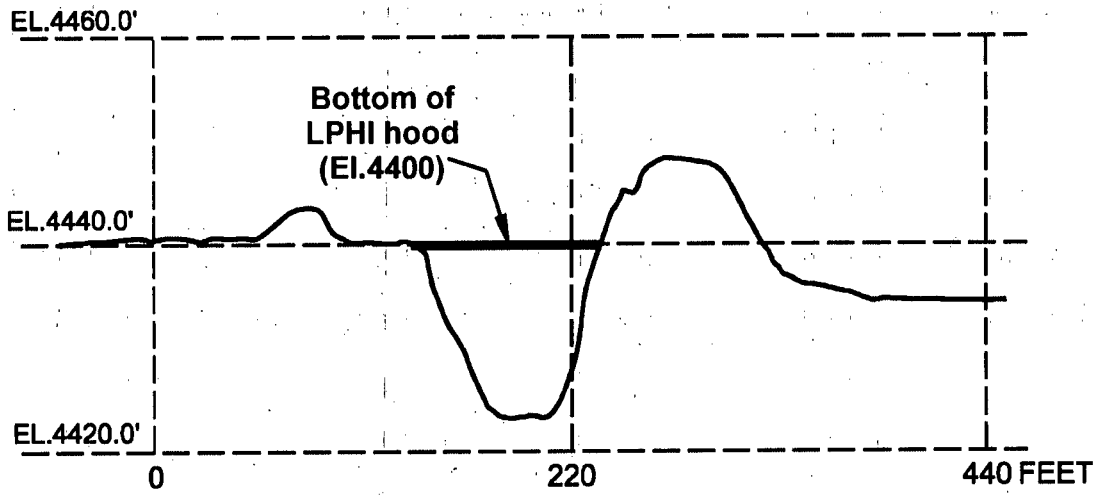


Figure 7-32. Elevation view of the cross-section through the hood and the incised channel (prototype dimensions) for the modeled LPHI.

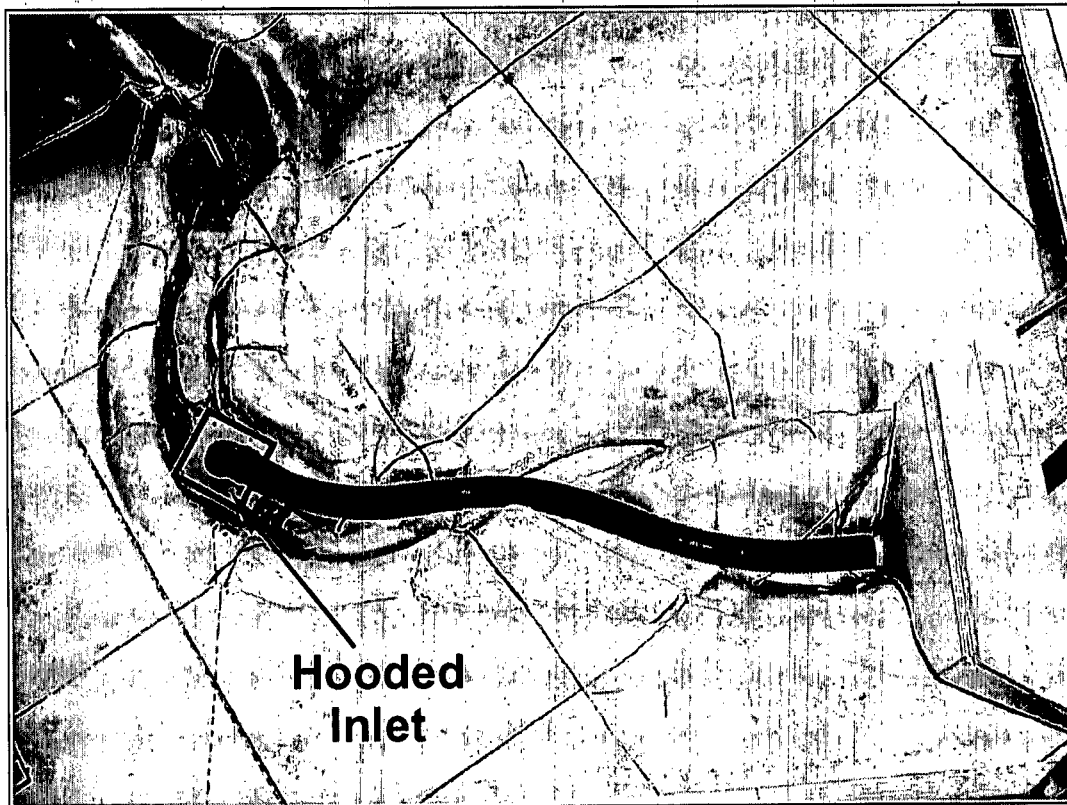


Figure 7-33. View of the LPHI in the model.

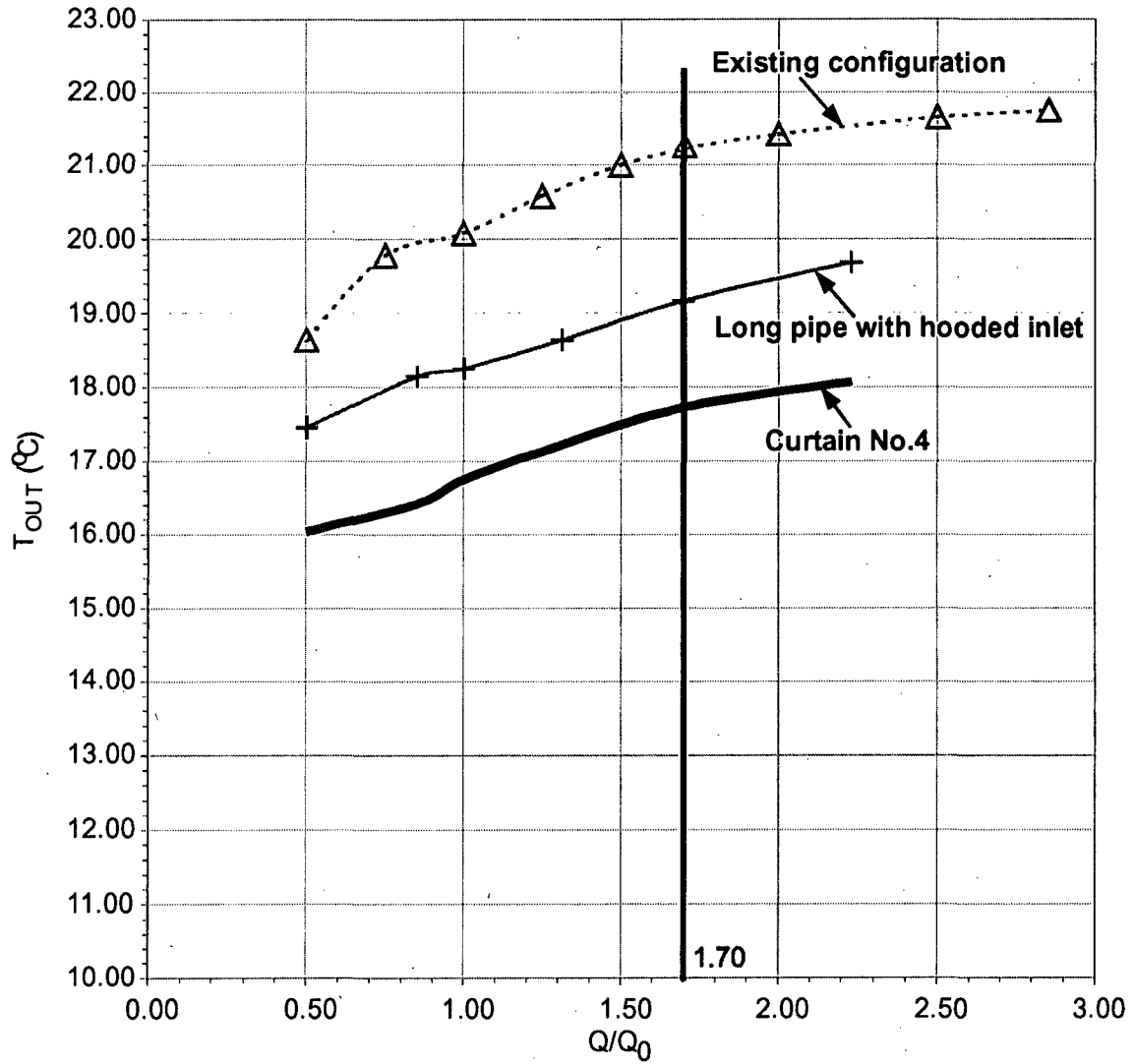


Figure 7-34. Comparison of the performances of the LPHI with levees not removed and Curtain No. 4 for August condition.

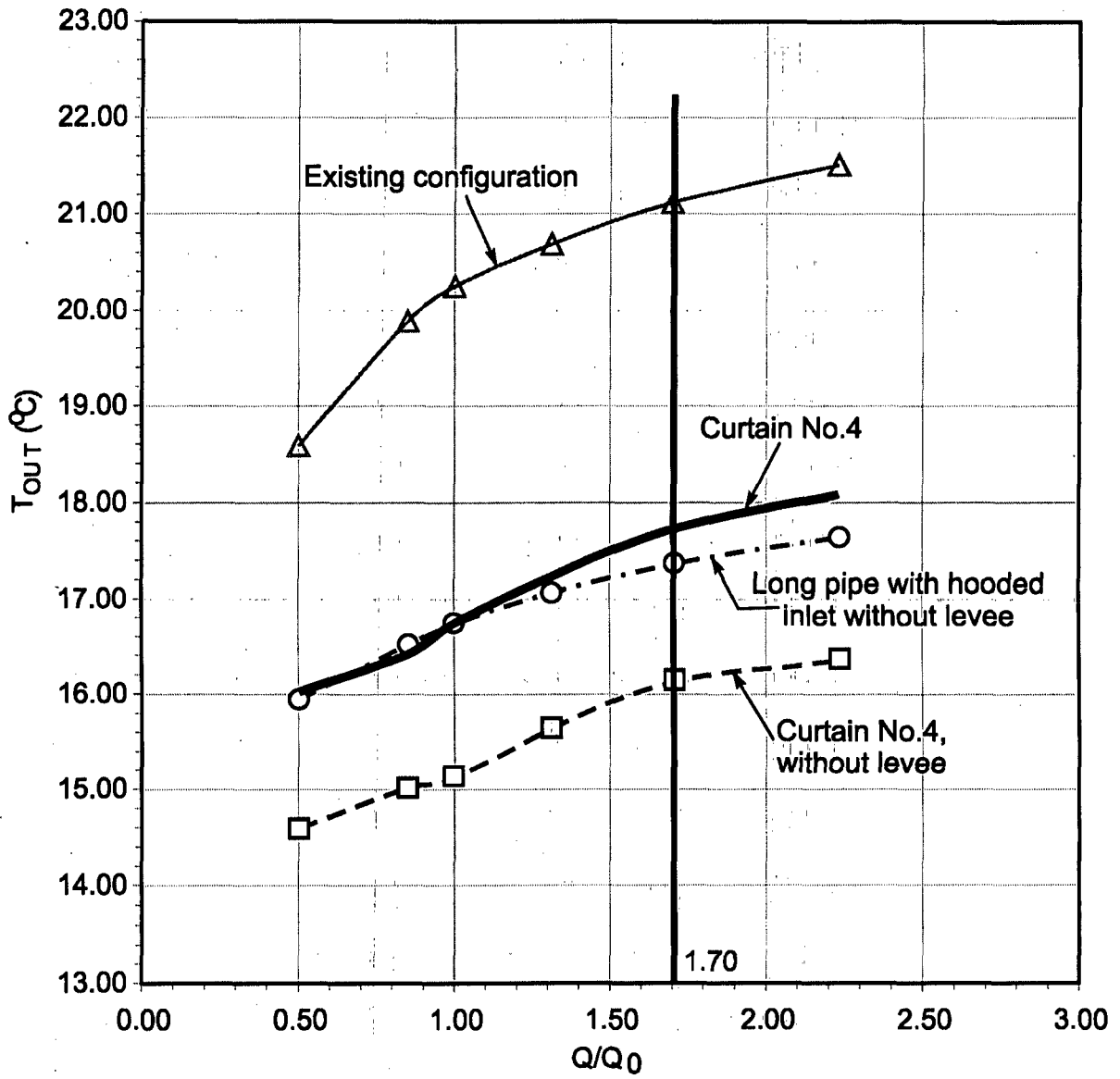
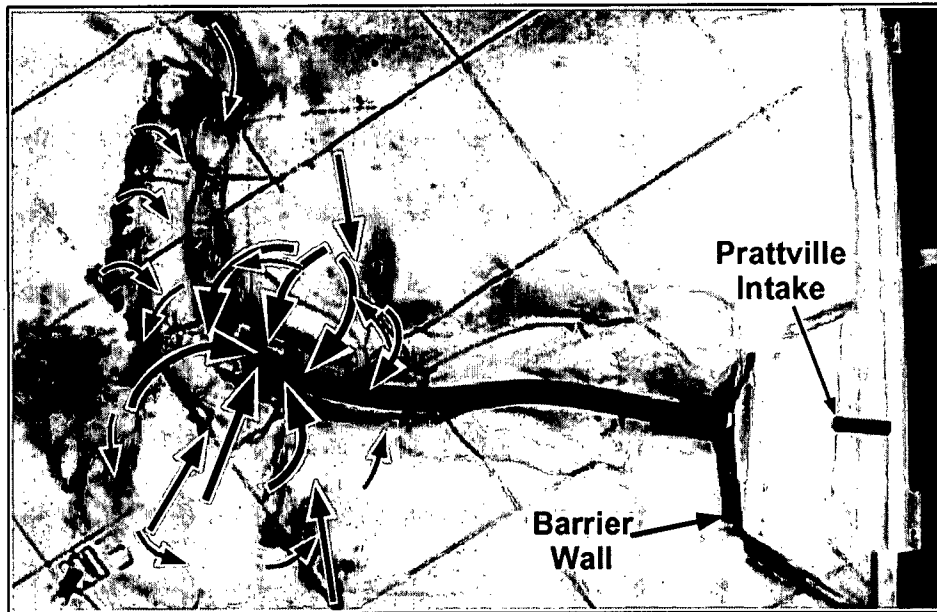
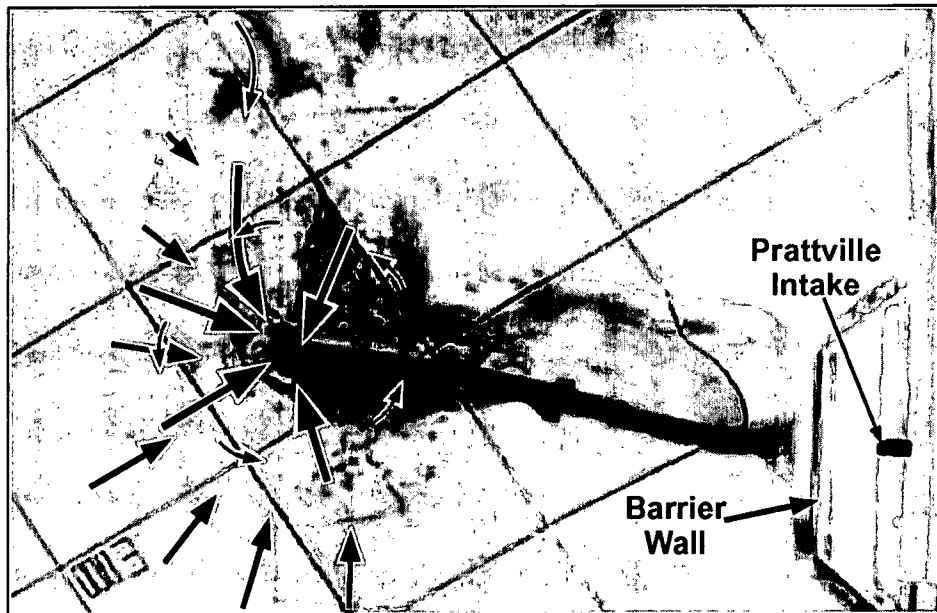


Figure 7-35. Comparison of the performances of LPHI with levees removed and Curtain No. 4 (with and without levees); August condition.



(a)



(b)

Figure 7-36. Visualization of the flow approaching the LPHI. Arrows indicating flow paths produced by the long pipe with hooded inlet (LPHI): (a) LPHI with levees; (b) LPHI without levees.

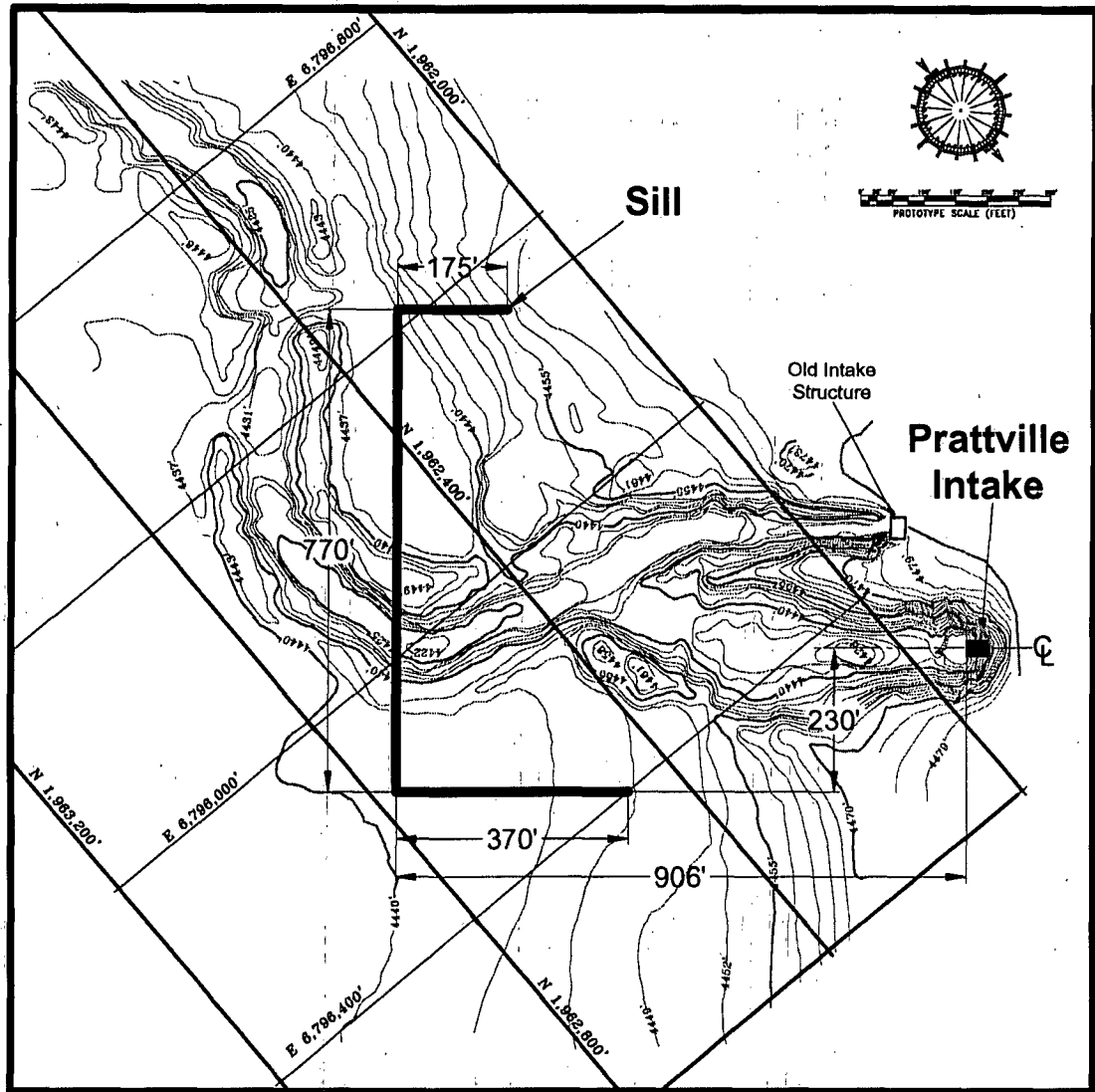
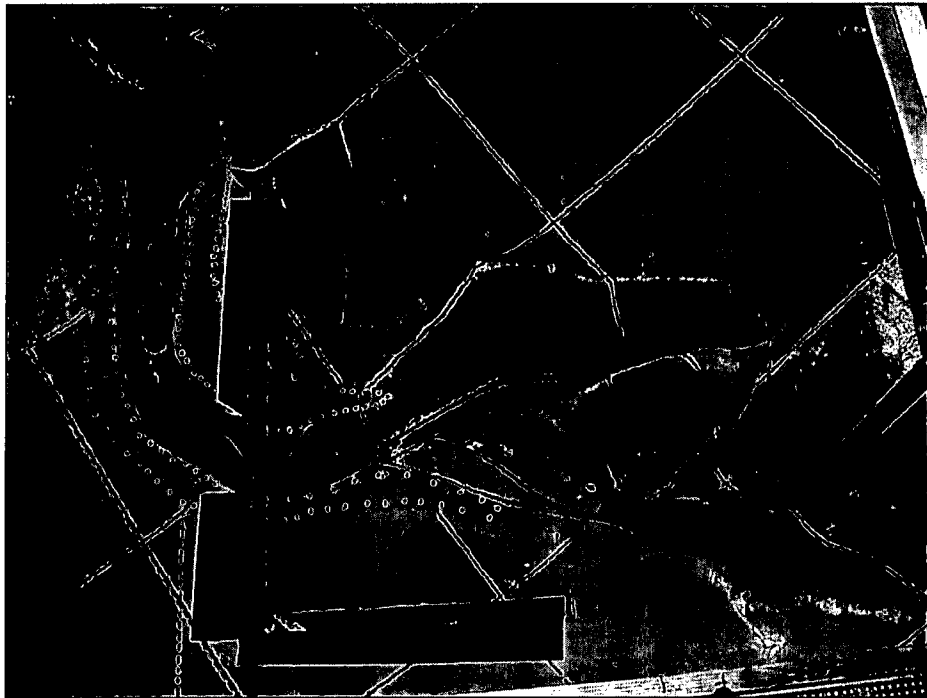


Figure 7-37. Layout of the bottom sill. The sill crest is at 4450 ft.



(a)



(b)

Figure 7-38. View of the sill with levees (a) and without levees (b).

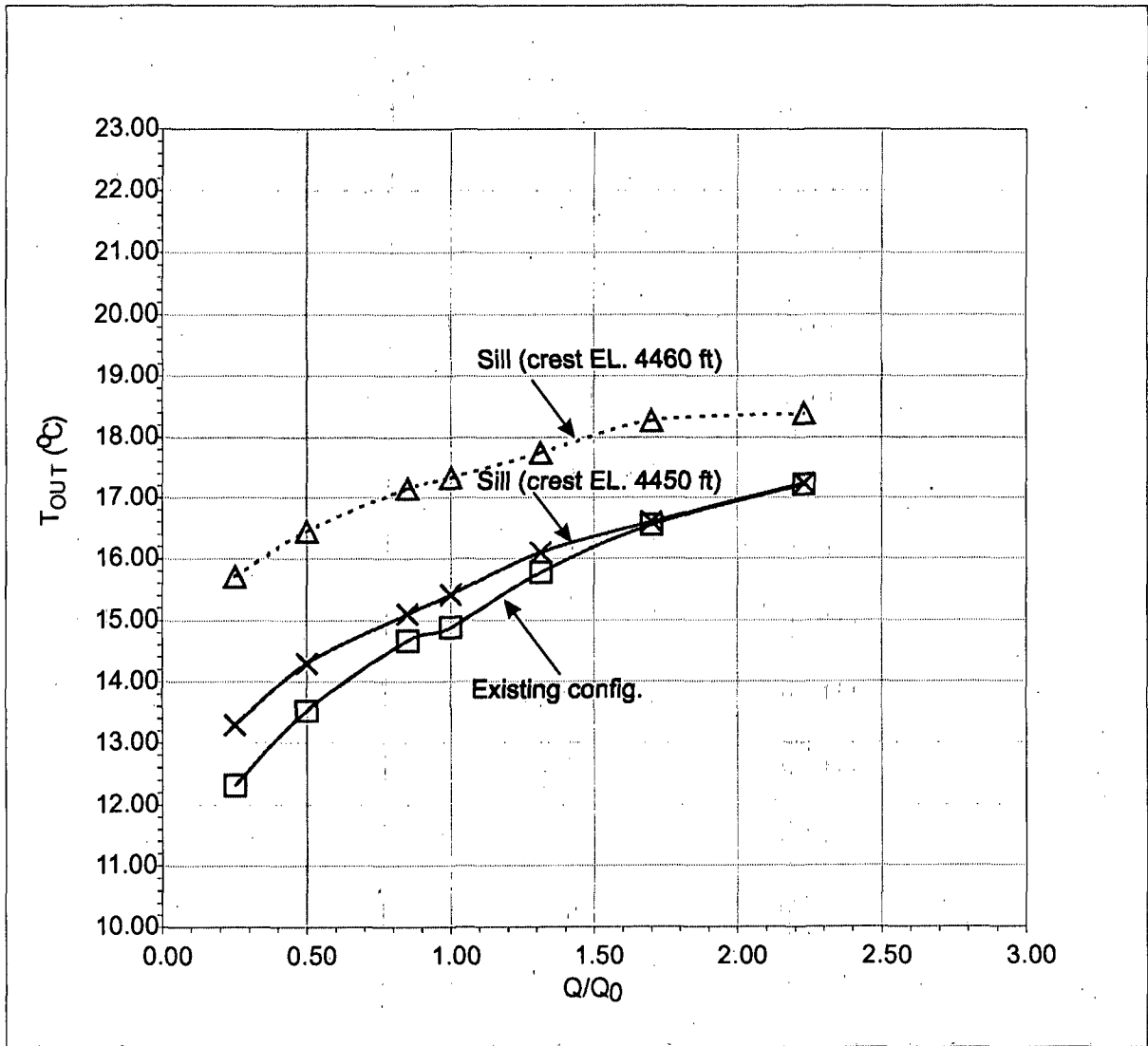


Figure 7-39. Comparison of the outflow performance produced by a sill at either of two crest elevations; levees in place, June condition.

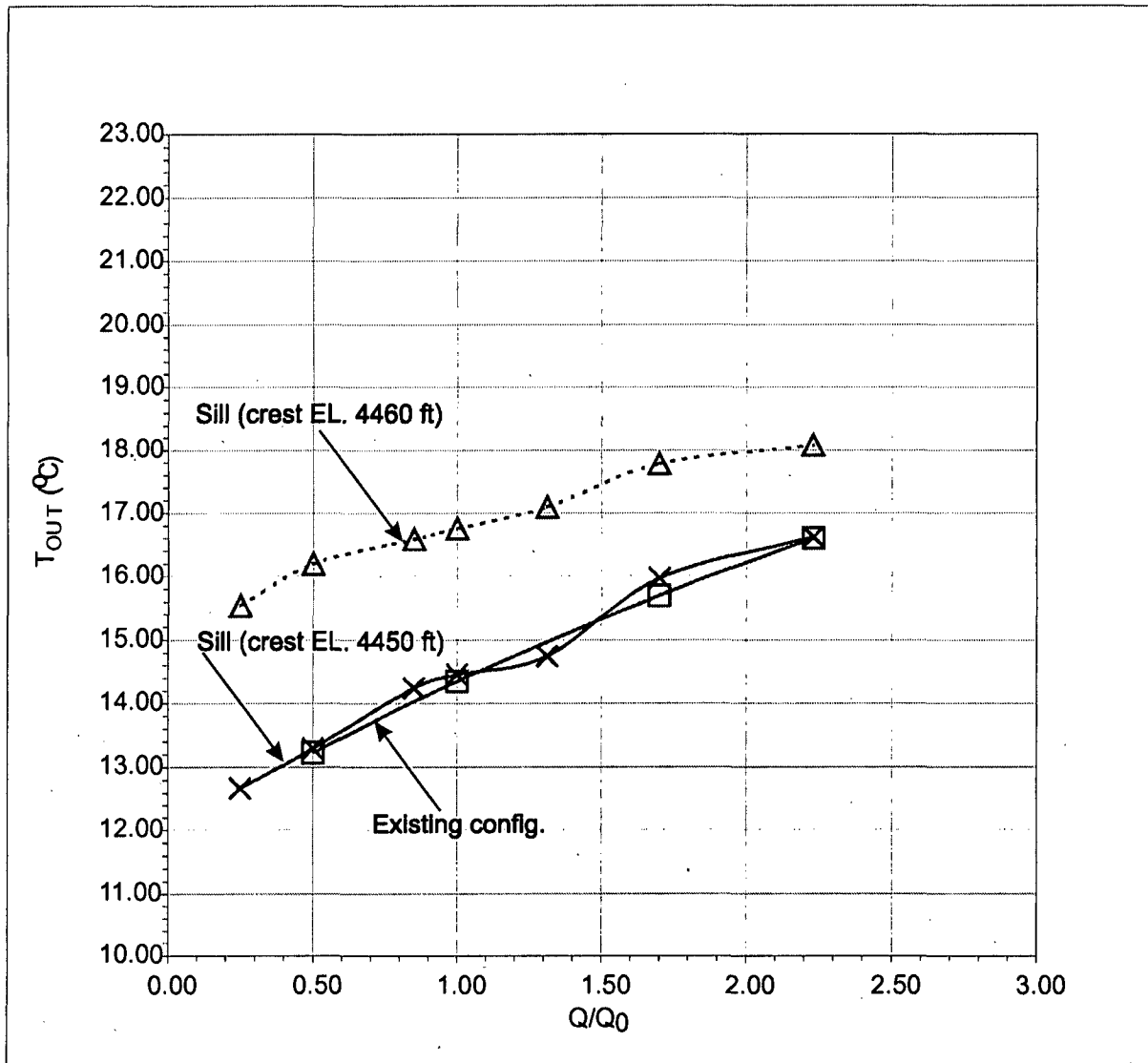


Figure 7-40. Comparison of the outflow performance produced by a sill at either of two crest elevations with levees removed; June condition.

## 8. PERFORMANCE DOCUMENTATION AND VALIDATION

### 8.1 Introduction

The results from the performance-screening tests reveal a set of practicable modifications that hold promise for enabling Prattville Intake to release colder water than it currently releases during summer months. The modifications comprise a skimming curtain configured as shown in Figures 7-7 through 7-10, and removal of the levees flanking a length of the incised channel in the immediate vicinity of the curtain as indicated in Figures 7-17 and 7-18. To confirm and document the performance of this set of modifications, three series of additional tests were conducted:

1. Performance-documentation tests with the modifications installed in the hydraulic model;
2. Validation tests with the testboxes; and,
3. Validation tests with the numerical model.

The validation tests with testboxes and the numerical-model provide an essential check as to whether the results from the vertically distorted hydraulic model also would have been obtained by means of an undistorted hydraulic model and a numerical model. The results from these tests are presented and compared in this chapter. At this opening point of the chapter it is necessary to mention that the numerical model, an auxiliary study in support of the hydraulic-model study, proved to be only partially helpful in validating the results from the hydraulic model. Complexities in configuration of computational mesh, the need for a shorter computational time step, together with the prolonged periods of time incurred with completing simulation runs, hampered full utilization of the numerical model.

The chapter concludes with a discussion regarding the discharge-calibration coefficient  $\alpha$  used for setting and interpreting the outflow performance of Prattville Intake as simulated in the hydraulic model with Curtain No. 4 placed around the Intake. The accumulated

observations and experience gained with the hydraulic model and testboxes lead to a comparatively simple approximate justification for the average value determined for  $\alpha$ .

## 8.2 Performance-Documentation Tests

As a preamble to discussing confirming the outflow performance ( $T_{out}$  versus  $Q/Q_0$ ) of a modified Prattville Intake, it is important to show that the average curves coincide very well with the field data obtained from the Intake once the discharge coefficient  $\alpha = 1.7$  is used to adjust values of  $Q/Q_0$ . The agreement shown in Figure 8-1 confirms that the hydraulic model indeed predicts the outflow performance of Prattville Intake.

A series of tests were carried out with the hydraulic model to document the model performance of Prattville Intake in its existing condition, and then when the Intake was fitted with a skimming curtain, and then again for the curtain with the levees removed from along the portion of incised channel immediately near the curtain. One series checked the sensitivity of outflow temperature to bottom elevation of curtain. The other series of tests were repeat tests with Curtain No. 4 (curtain bottom elevation at EL. 4445ft), done to gauge margins of uncertainty associated with use of the curtain.

The series of tests to check the influence of curtain bottom elevation examined three bottom elevations when the lake is in the August condition, the most pressing condition for assessing curtain performance: EL. 4443ft, EL. 4445ft, and EL. 4447ft. The results are shown in Figure 8-2, from which it can be concluded that, with the levees present, the performance is not particularly sensitive to curtain bottom elevation for the variation considered. However, when the levees were removed, a bottom elevation of EL. 4445ft produced the lowest outflow temperatures. The curtain with bottom elevation EL. 4443ft was close in its performance, but the higher velocities under that curtain were larger than for the curtain at EL. 4445ft, which arguably could ease more cold water under itself and toward the Intake. Further performance tests therefore concentrated on Curtain No. 4 with bottom elevation at EL. 4445ft.

Series of repeat tests were done with Curtain No.4 for the lake conditions prescribed for the June, July, and August conditions of Lake Almanor. The repeated tests sought to confirm an average curve for Intake performance and an approximate margin of

uncertainty for the average value of outflow temperature,  $T_{out}$ , obtained for each value of  $Q/Q_0$  tested. Figures 8-3a-c give the curves and uncertainty margins assessed from the series of repeated tests. The uncertainty margins bracket the extremes in  $T_{out}$  measured for each  $Q/Q_0$  setting. The numbers of repeat tests were insufficient for more formal estimation of the uncertainties.

The repeated tests confirm the capacity of a modified Prattville Intake to release colder water. The reductions in water temperature over the model outflow range  $Q/Q_0 = 1.0$  to  $1.7$  are  $4.5^\circ\text{C}$ ,  $5.8^\circ\text{C}$ ,  $5.2^\circ\text{C}$  for the lake water conditions corresponding to the June, July and August conditions, respectively (Figures 8-3a-c). For the actual Intake operating at  $Q/Q_0 = 1$  (i.e., 1,600cfs), the outflow temperature is estimated to be  $12.0^\circ\text{C}$ ,  $13.2^\circ\text{C}$ , and  $16.0^\circ\text{C}$  for the June, July, and August conditions, respectively. The margins of uncertainty associated with these temperatures are within  $\pm 0.5$  to  $0.7^\circ\text{C}$ . The data resulting from the use of Curtain No. 4, and with the levees removed, on the whole have lesser margins of uncertainty. Removal of the levees simplified the approach flow field toward the curtain, and thereby lessened variations in outflow temperature.

### 8.3 Validation Tests with Testboxes

The validation tests with the testboxes sought to check two aspects of the performance of Prattville Intake fitted with a curtain, and with the levees removed:

- 1 Whether the value of discharge-calibration factor  $\alpha = 1.7$  applies when Prattville Intake is fitted with a curtain; and,
- 2 Whether an undistorted model of the curtain and Intake would produce the same magnitudes of water temperature drop,  $\Delta T_{out}$ , in outflow water as was obtained during tests with the vertically distorted hydraulic model.

A series of initial tests were conducted with the Bay testboxes (Figure 4-5) in which a simple skimming wall was placed between the vertical sidewalls of the distorted and the undistorted bay testboxes. The curtains had a bottom elevation of EL. 4445ft, and were positioned at 9 inches and 4.2ft from the entrance of the distorted and undistorted testboxes, respectively. These tests resulted in  $\alpha = 1.7$  for the August condition of Lake

Almanor. The same value was obtained with tests done for the June and July conditions of the lake. Figure 8-4 gives the test results.

The main series of tests were conducted using the Open-form testboxes, as those testboxes more closely replicated the bathymetry around Prattville Intake. The tests were done in a sequential process whereby the curtain was placed around one testbox (e.g., the distorted testbox), while the bathymetry around the other testbox (e.g., the undistorted testbox) was leveled; once measurements were completed, a curtain was placed around the other testbox. The curtain had the same form and dimensions as used in the hydraulic model, though, as explained in Chapter 4, the curtain for the undistorted testbox was placed closer to the simulated intake than was the case for the curtain in the hydraulic model and distorted testbox; the curtain around the undistorted testbox was at half the scaled distance from the intake. A bottom elevation of EL. 4445ft was used for the curtains around each of the distorted and undistorted testboxes, the same elevation as for the curtain in the hydraulic model (Figure 7-8). The testbox tests did not include the incised channel, which is a significant bathymetric feature between Prattville Intake and the Hamilton Branch of Lake Almanor. Figure 8-5 is a perspective sketch illustrating the Open testbox surrounded by the equivalent of Curtain No. 4. The curtains layout and dimensions are given in Figure 8-6. A view of the curtain around the undistorted testbox is provided by the photograph in Figure 8-7. The layout and dimensions of the equivalent curtain placed around the distorted Open testbox is given in Figure 8-8, while Figure 8-9 is a view of the curtain around the distorted Open testbox.

The Open-testbox results are given in Figures 8-10a,b for the July and August water conditions of Lake Almanor. These figures show the curves  $T_{out}$  versus  $Q/Q_0$  obtained for the testboxes with and then without the curtains. The curves in these figures provide information confirming the results obtained from the vertically distorted hydraulic model:

- 1 The value of discharge calibration factor,  $\alpha$ , obtained for the open testboxes each fitted with a curtain, concurs with the value obtained with tests with only the open testboxes; i.e.,

$$\alpha = 1.7 \pm 0.3$$

- 2 A curtain placed around the undistorted testbox produced a temperature drop of  $\Delta T_{out} = 4.0$  to  $4.5^{\circ}\text{C}$  in the July condition and  $2\text{-}3^{\circ}\text{C}$  in the August condition over the range  $Q/Q_0 = 1.0$  to  $1.7$ . The same values of  $\Delta T_{out}$  were measured for the distorted testbox with a curtain.

These results confirm that a skimming curtain, of the layout and dimensions given in Figure 7-7 through 7-10, could enable Prattville Intake to release significantly colder water. Moreover, they demonstrate that use of the calibration factor  $\alpha$  enables the results from the hydraulic model to be scaled to the prototype conditions occurring at Prattville Intake.

#### **8.4 Validation Tests with Numerical Model**

The U2RANS code was used to develop a numerical model that replicates a major portion of the hydraulic model. In a separate report, Lai et al. (2004) describe the numerical model in detail. Figure 8-11 shows a comparison between the outflow temperatures computed using this model and outflow temperatures measured in the vertically distorted hydraulic model for the cases with the levees in place, both with the lake in the August condition. The agreement is excellent.

The code was also used to develop a numerical model replicating a virtual, undistorted version of the hydraulic model. This model turned out to be considerably more complex than originally anticipated. It required a more comprehensive computational mesh, shorter time steps, and consequently longer run time for each simulation. Although additional development effort is needed on this model, the preliminary results are encouraging. The preliminary results are shown in Figure 8-12. The results are also for the lake in the August condition. It is seen that the model predicts outflow temperatures that are comparable to those measured in the field. The model also supports the finding of the hydraulic model (and the numerical model of the hydraulic model) that Curtain No. 4 is effective in reducing outflow temperatures. The level of reduction predicted (about 2.8 degrees) is not quite that predicted by the hydraulic model (about 3.5 degrees), however, the discrepancy is attributed to the preliminary nature of the numerical model of the undistorted hydraulic model.

## 8.5 Discussion

Given the structural differences involved, it may seem a little surprising that the discharge-calibration coefficient  $\alpha$  has the same value for the testboxes with and without a curtain fitted (and in their Open as well as Bay forms). A curtain would seem to make the flow approach to the testbox more two-dimensional, and therefore would suggest that  $\alpha \approx 1$ , with the discharge ratio  $Q_r$  being in accordance with Eq. (4-1).

Yet, in viewing the distribution of approach flow to the testboxes, and in recalling that the same geometric distortion ( $X_r/Y_r$ ) exists between the distorted and undistorted testboxes and curtains, it can be argued readily that  $\alpha$  should retain the same value, at least its average value. On the other hand, the margin of uncertainty,  $M$ , may vary because some of the testbox configurations admit a few more opportunities for flow-field variability and measurement uncertainty; e.g., the extended length time needed to complete some tests with the undistorted, open testbox fitted with a curtain. The approach flow toward each testbox was largely two-dimensional for flows over most of the  $Q/Q_0$  range tested; indeed the flow approaching each testbox is essentially a radial, two-dimensional distribution, though somewhat skewed owing to the position of the testbox in the hydraulic-model basin. Therefore placing the curtain in the largely two-dimensional flow field around an open testbox should not cause  $\alpha$  to be less than the value obtained from the testbox without a curtain. Furthermore, dye visualization of flow showed that the curtain's influence on flow structure behind the curtain was qualitatively comparable to the influence of the sidewalls or submerged ridges of the testboxes. In other words, the influence of vertical distortion on turbulence generation and flow mixing was the same as vertically distorting any other part of the testbox, as would be expected since  $X_r/Y_r$  is constant.

The foregoing argument can be extended to include the screening tests investigating the efficacy of the hooded-inlet pipes to reduce outflow temperature. The approach flow to the hooded inlets is essentially radial and two-dimensional in the far field, but three-dimensional locally at the hooded inlets.

The argument in the preceding paragraphs assigns the differences in flow field between the distorted and the undistorted testboxes to strengths or intensities of eddies and turbulence. Such strengths or intensities usually are characterized in terms of a flow property called vorticity, a measure of the intensity, or strength of rotation, of an eddy or turbulent rotation of flow. In simple terms vorticity,  $\omega$ , expresses flow-path length,  $L$ , divided by flow velocity,  $V$ . The units of vorticity are length/velocity. The prior studies of flow in stratified water bodies do not take into account the influence of the three-dimensional and rotating features of flow on the stability of such flows. The similitude relationships proposed by Stolzenbach and Harleman (1967), for example, are intended for idealized two-dimensional flow, and do not fully describe water mixing in the near field region around a water intake.

By comparing the scaling ratios of vorticity for the flow fields formed by the undistorted testbox and the distorted testbox, it is possible to venture an explanation for the value determined for the coefficient  $\alpha$  during the calibration work with the testboxes. Essentially, the explanation is that flow vorticity in the distorted testbox is over-scaled relative to flow vorticity in the undistorted testbox. In other words, in the distorted testbox, most forms of vortices, eddies, and turbulence were reduced in strength compared to the flow in the undistorted testbox, such that local mixing of flow is not as pronounced in the distorted testbox. To increase flow mixing in the distorted testbox entails increasing flow vorticity in the near field of the intake at the end of the distorted testbox. The question then concerns by how much should the vorticity be increased.

Comparison of the scales for vorticity in the flow fields formed by the undistorted testbox and the distorted testbox (and hydraulic model), yields an explanation as to the value determined for the calibration factor  $\alpha$ . The explanation leads to a simple relationship with which to estimate  $\alpha$  for vertically distorted hydraulic models. For an undistorted model operated in accordance with Froude-number similitude; flow vorticity,  $\omega$ , scales as

$$\omega_r = V_r/L_r = L_r^{1/2}/L = L_r^{-1/2} \quad (8-1)$$

here,  $L_r$  and  $V_r$  are scales of length and velocity, respectively. Flow vorticity in the flow field formed in a vertically distorted hydraulic model will be less than that in an undistorted model built at length scale  $L_r = Y_r$ , though it is greater than in an undistorted model built at a scale  $L_r = X_r$ .

In each distorted testbox and the hydraulic model itself, large-scale turbulence and flow vorticity overall was reduced in strength compared to vorticity in each undistorted testbox or an undistorted hydraulic model. Because vorticity scales as  $\omega_r = L_r^{-1/2}$ , the smaller the scale reduction in flow length ( $L_r$ ) from prototype to model, the stronger is flow vorticity in the model; recall that  $\omega_r = (\text{vorticity in prototype})/(\text{vorticity in model})$ . Consequently, local mixing of flow was not as pronounced in each of the distorted testboxes (and the distorted hydraulic model) as in the undistorted testboxes, because the reduction in flow length was greater for the distorted testboxes. To increase flow mixing in the distorted testbox entails increasing flow vorticity in the distorted testbox. For a given geometry of flow, a vorticity increase can be achieved by increasing flow velocities in the distorted model. The question is: By how much should the vorticity be increased?

For the undistorted testbox, built at length scales  $L_r = Y_r = 40$ , flow vorticity scales as  $\omega_{r(L_r=Y_r)} = L_r^{-1/2} = 0.159$ . In comparison, flow vorticity in the flow field of a smaller undistorted testbox built at length scales  $L_r = X_r = 220$ , would scale as  $\omega_{r(L_r=X_r)} = L_r^{1/2} = 0.068$ . Then for the flow field in a vertically distorted hydraulic model built with  $Y_r = 40$  and  $X_r = 220$ , the scale of flow vorticity lies somewhere between 0.158 and 0.068, the scale ratios for vorticity in the two sizes of undistorted testbox. It is reasonable to assume that the overall or average vorticity scale for the distorted testbox ( $X_r = 220$ ,  $Y_r = 40$ ) is the average of 0.158 and 0.068; i.e., for the distorted testbox,  $\bar{\omega}_r = (0.158 + 0.068)/2 \approx 0.113$ .

In answer to the preceding question, the vorticity of flow in the distorted testbox and the hydraulic model has to be comparable to that in the undistorted testbox. This consideration requires increasing vorticity by a factor of  $0.113/0.068 = 1.66 \approx 1.7$ . For a given geometry or cross-section of flow, this increase can be achieved by increasing outflow rate from the distorted model by a factor of 1.7. This value agrees with the

average value of the outflow factor coefficient,  $\alpha$ , found from the testbox effort, and suggests that  $\alpha$  can be estimated as

$$\alpha = \bar{\omega}_r / \omega_{r(L_r=X_r)} = (X_r^{-0.5} + Y_r^{-0.5}) / 2X_r^{-0.5} = 0.5[1 + (Y_r/X_r)^{0.5}] \quad (8-2)$$

in which  $\bar{\omega}_r$  is the average of the vorticity scales for corresponding undistorted models built at horizontal- and vertical length scales  $X_r$  and  $Y_r$ , respectively; usually  $X_r > Y_r$ . Also,  $\omega_{r(L_r=X_r)}$  is the vorticity scale for a model built at undistorted scale  $L_r = X_r$ .

The inference of Eq. (8-2) is that, for vertically distorted models, the Froude-number similitude criterion expressed in Eq. (3-2) be adjusted as

$$F_{Dr} = 1/\alpha \quad (8-3)$$

Though Eq. (8-2) enables a calibration factor  $\alpha$  to be estimated, calibration tests still would be needed to verify the estimated value of that factor.

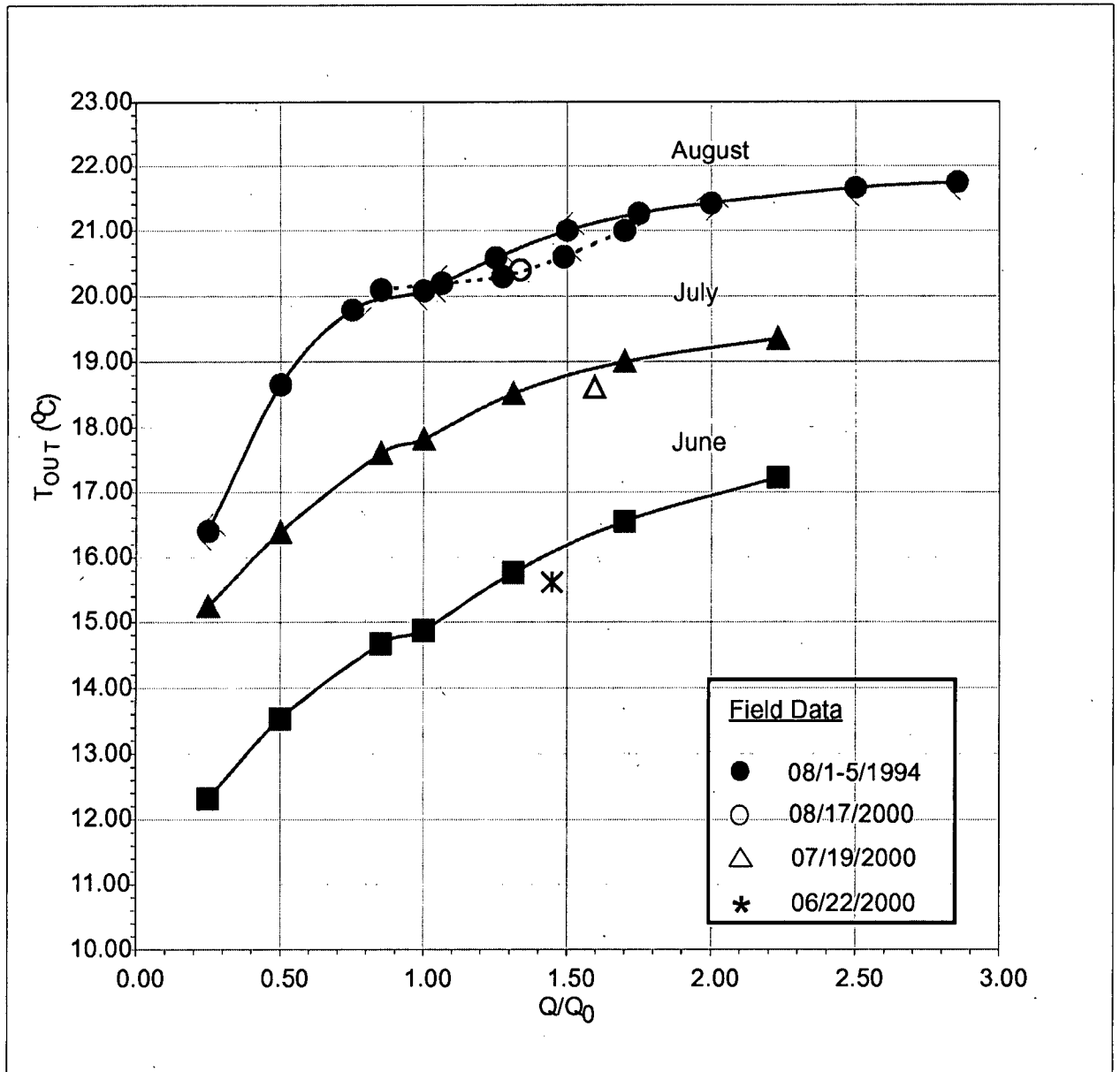


Figure 8-1. Validation of the hydraulic model results with field data. The field data are adjusted by factor  $\alpha = 1.7$  applied to  $Q/Q_0$ .

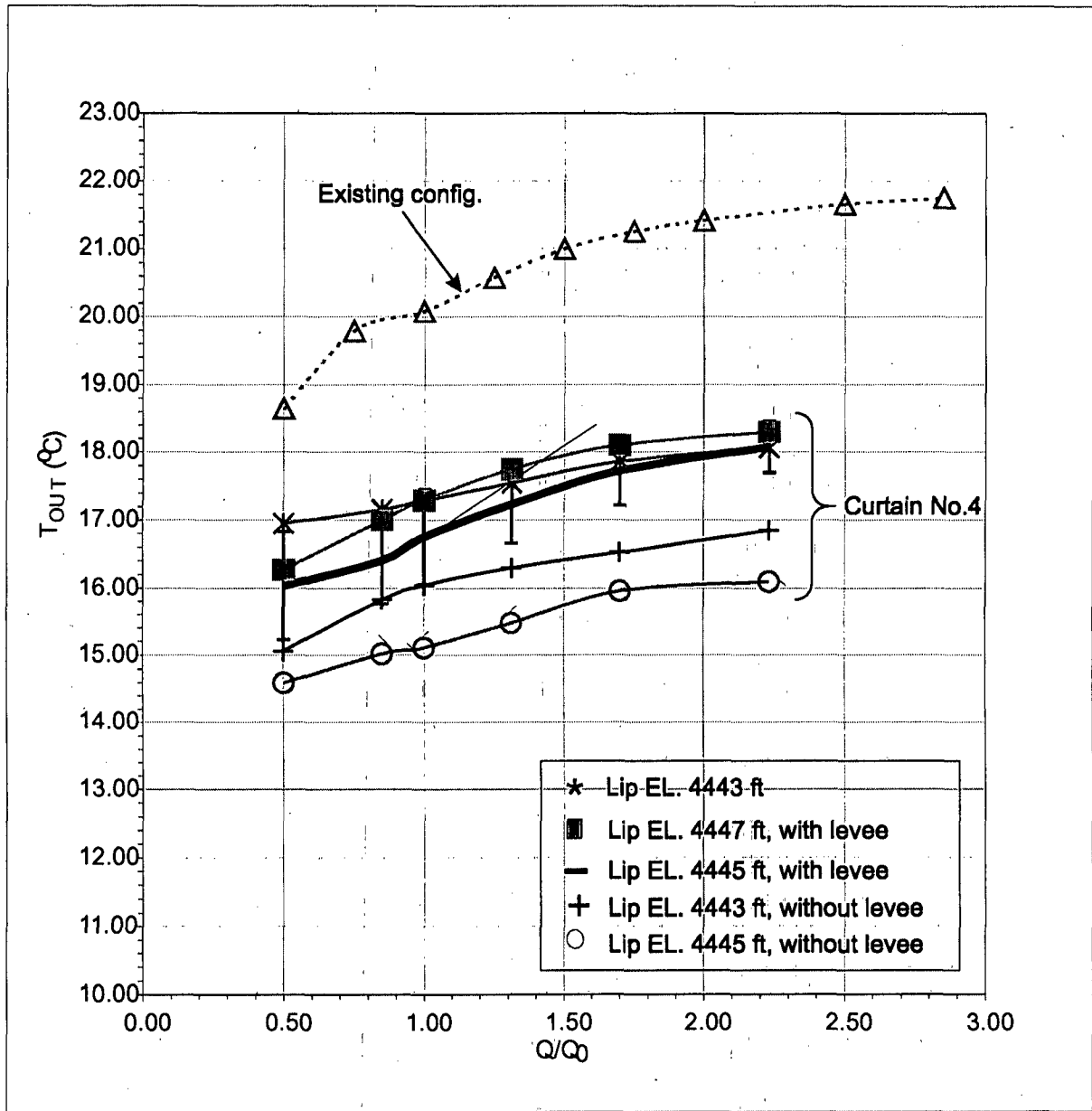
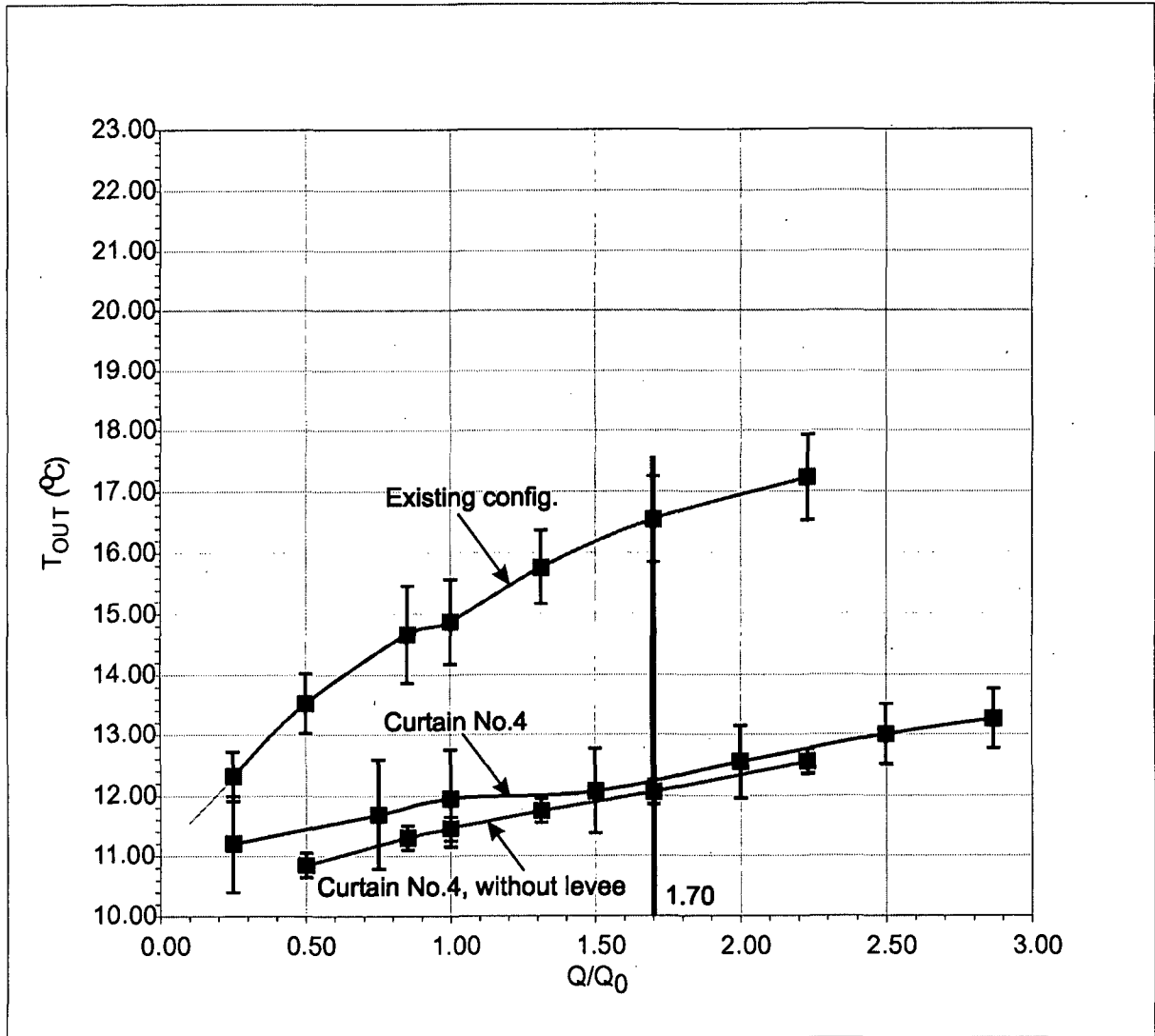
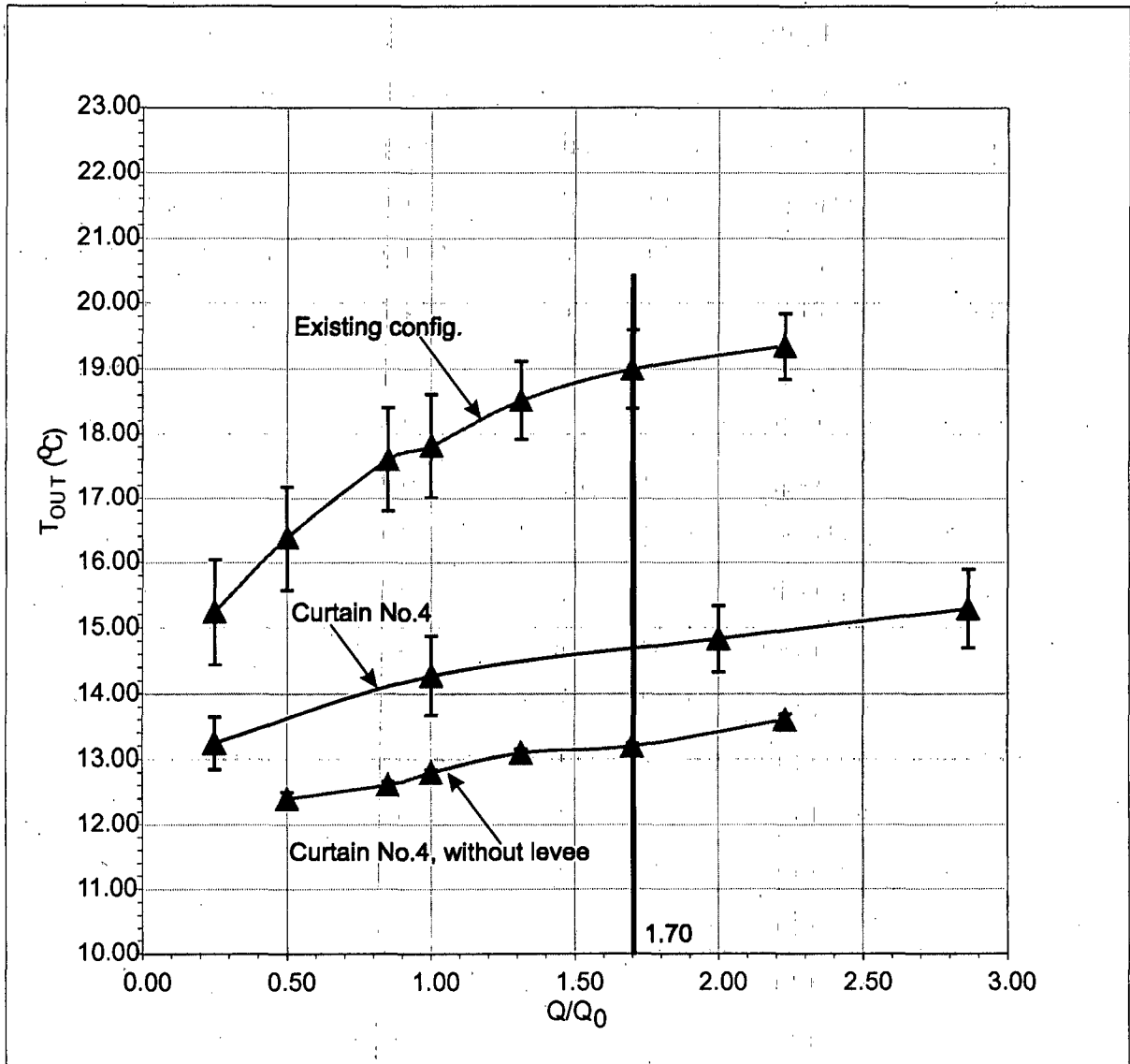


Figure 8-2. Sensitivity of Curtain No. 4 with variation of lip elevation (tests conducted for August condition).



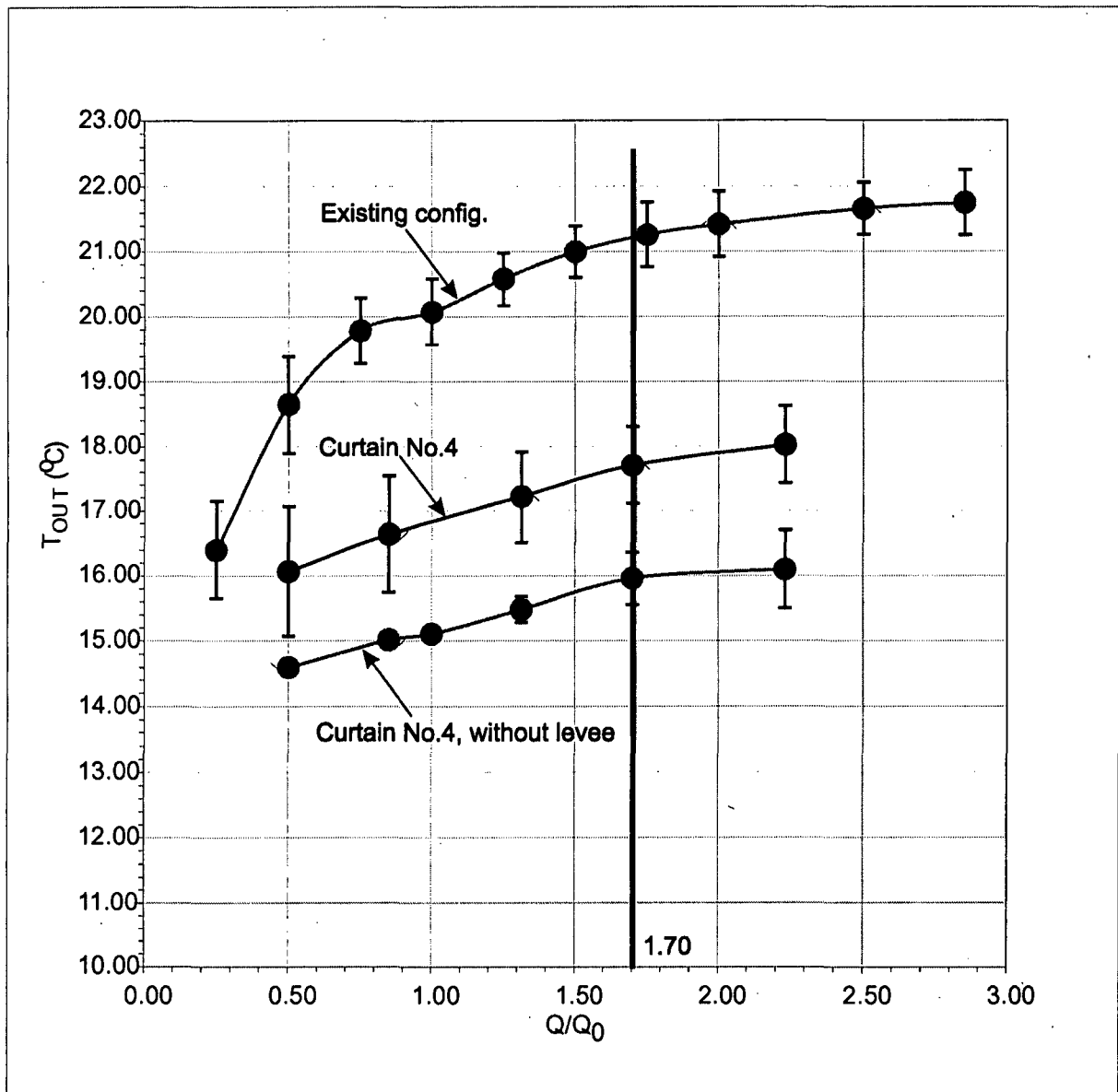
(a)

Figure 8-3. Performance curves with margins of uncertainty: (a) June condition.



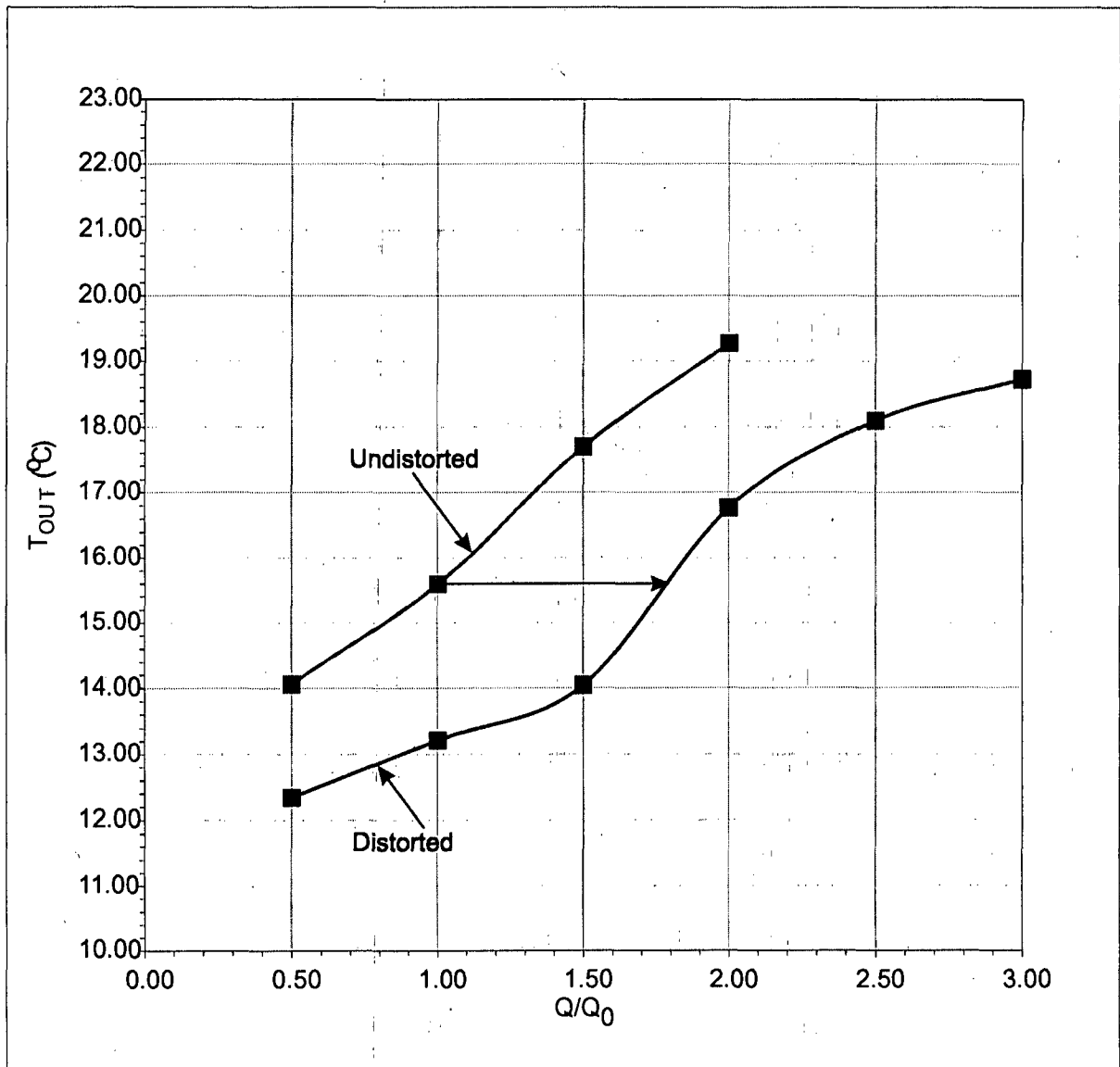
(b)

Figure 8-3. continued. (b) July condition.



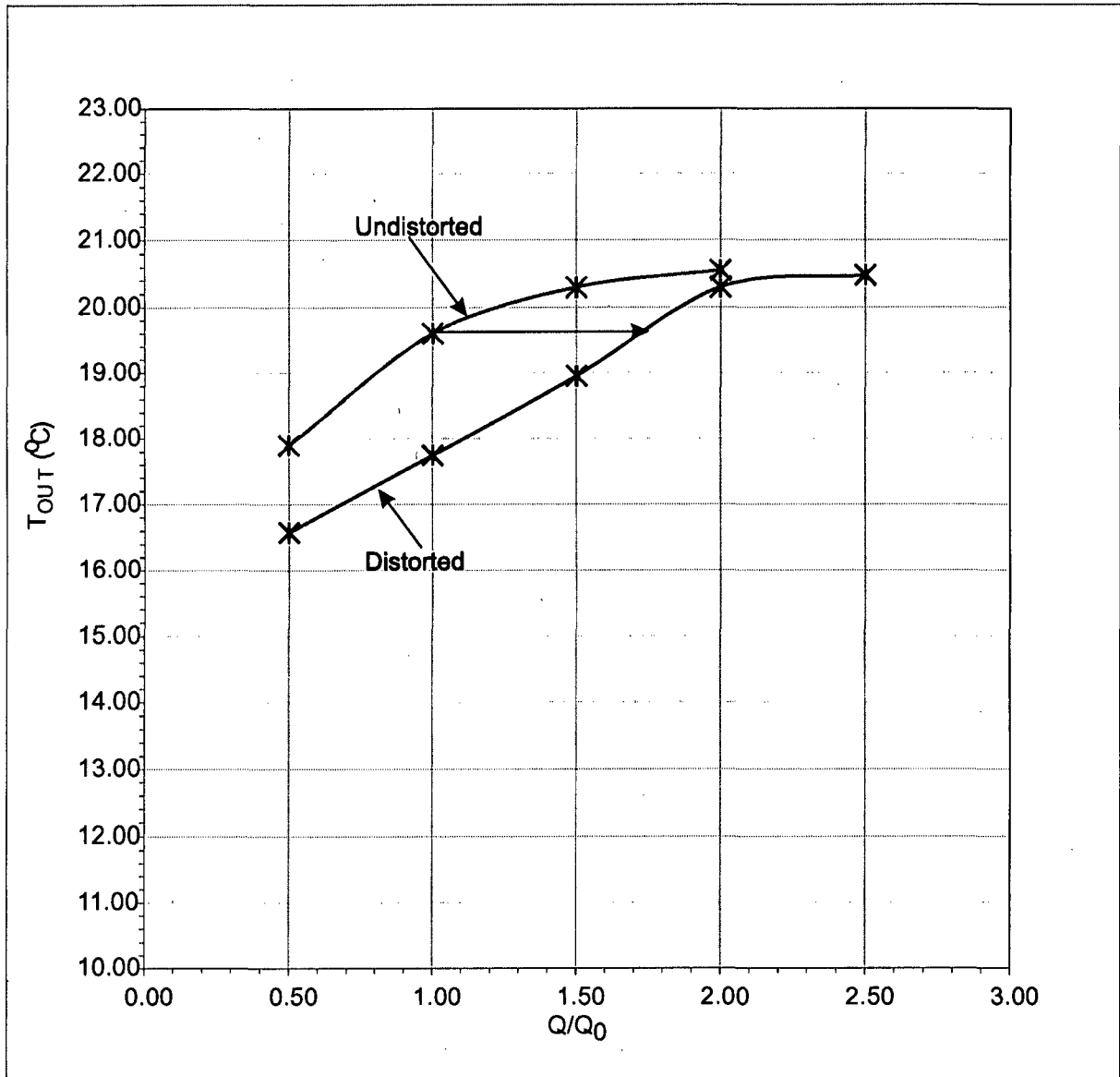
(c)

Figure 8-3. continued. (c) August condition.



(a)

Figure 8-4. Performance of the Bay testboxes fitted with skimming walls: (a) July condition.



(b)

Figure 8-4 continued. (b) August condition.

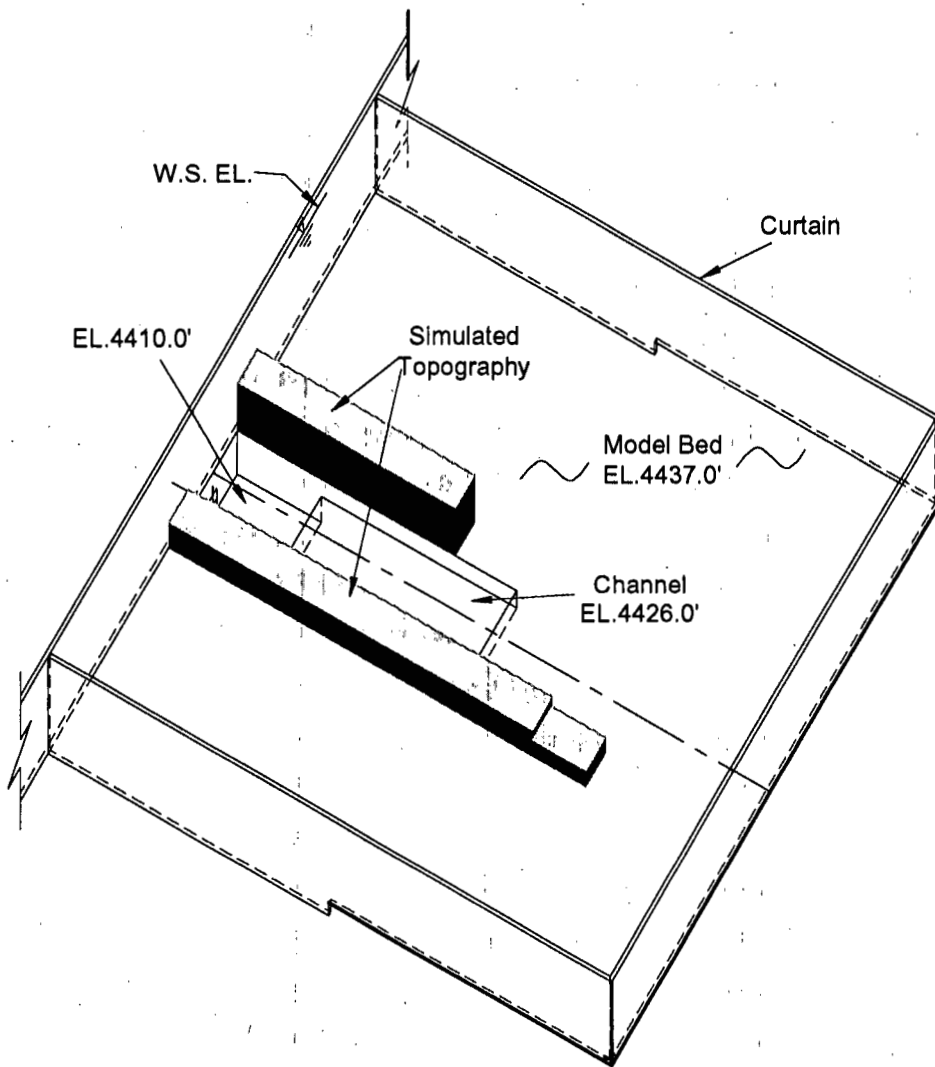


Figure 8-5. Perspective view of the undistorted Open testbox with curtain.



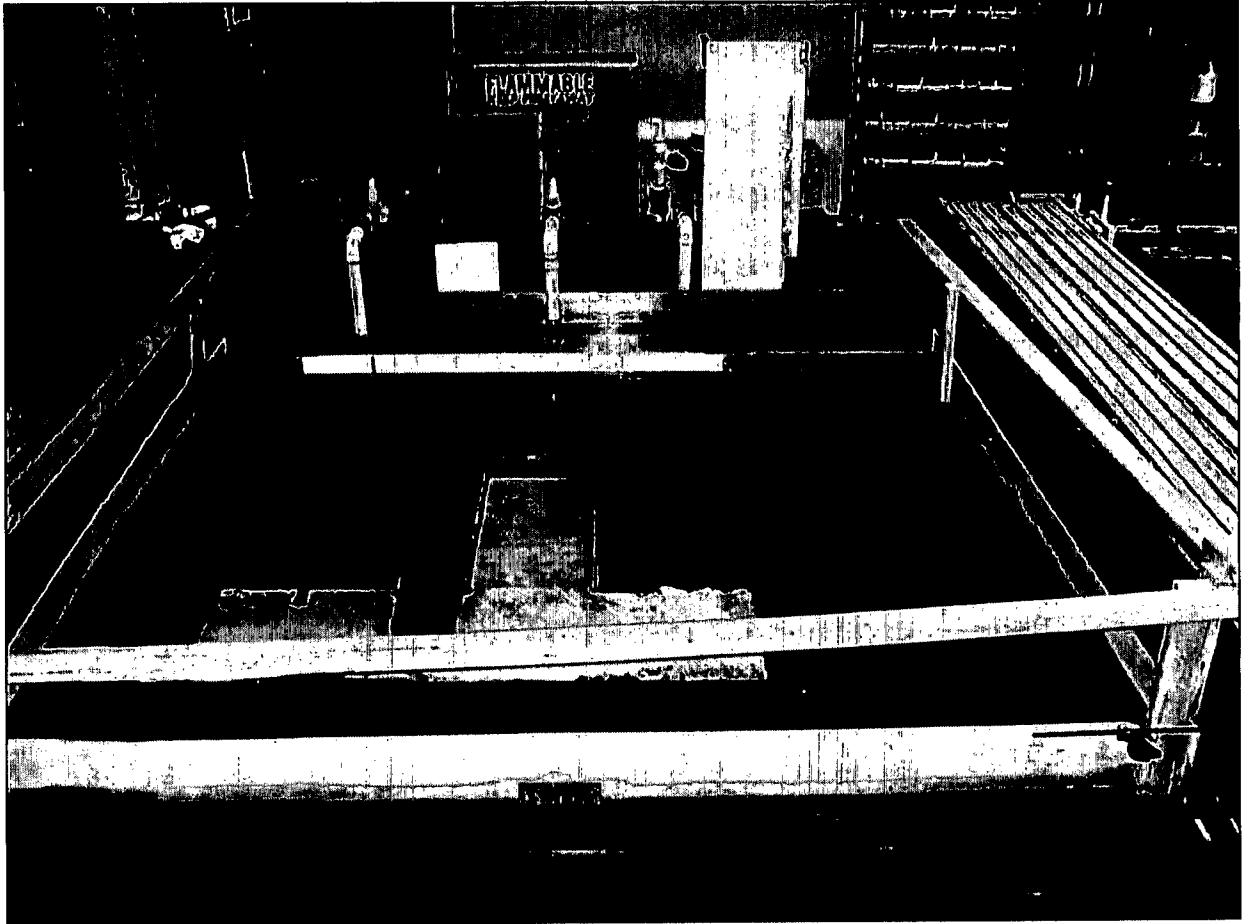


Fig. 8-7. View of the undistorted Open testbox with curtain.

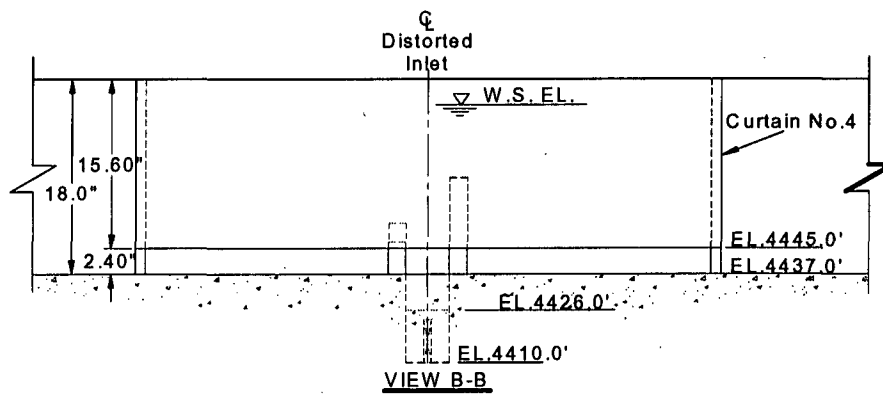
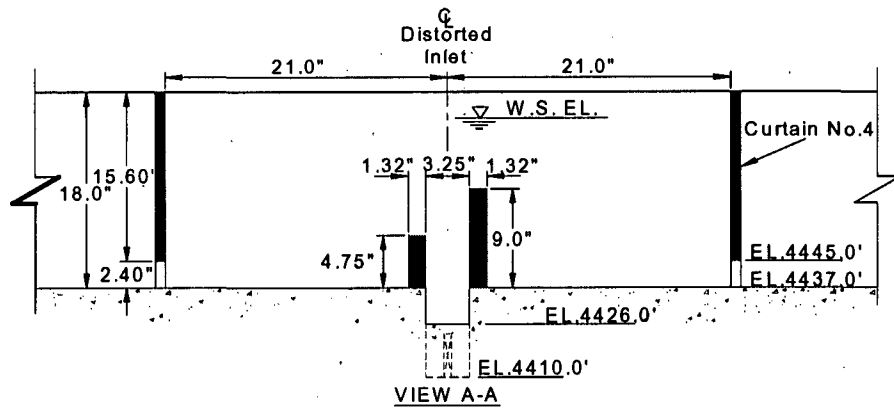
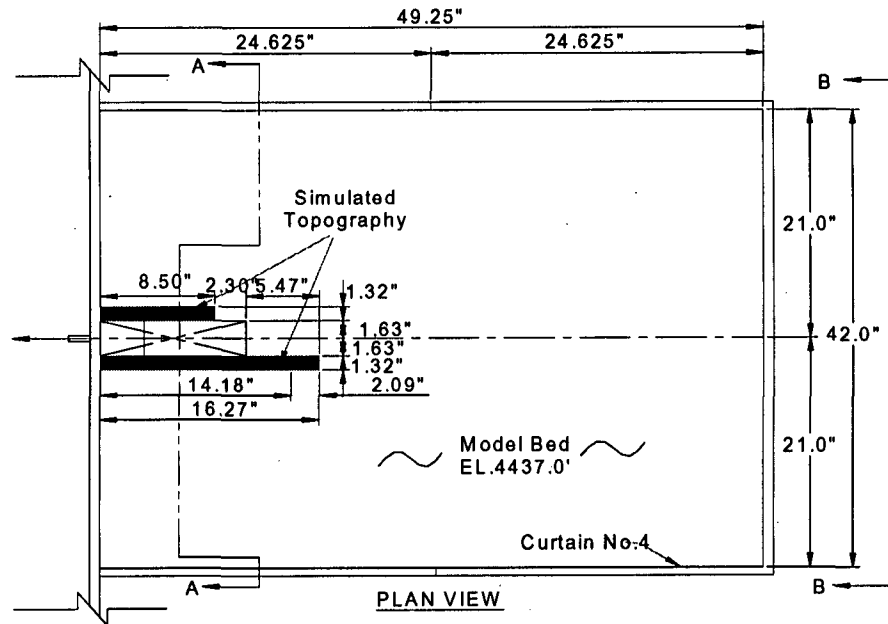


Figure 8-8. Layout and dimensions of Curtain No. 4 placed around the distorted Open testbox.

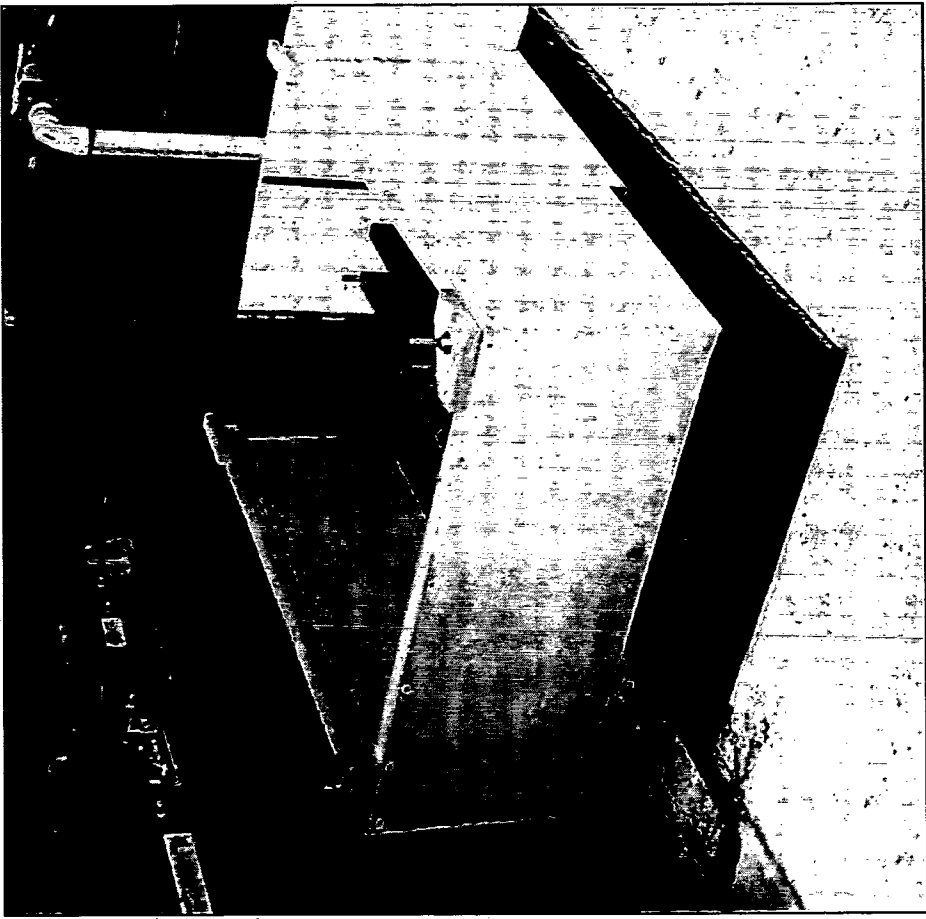
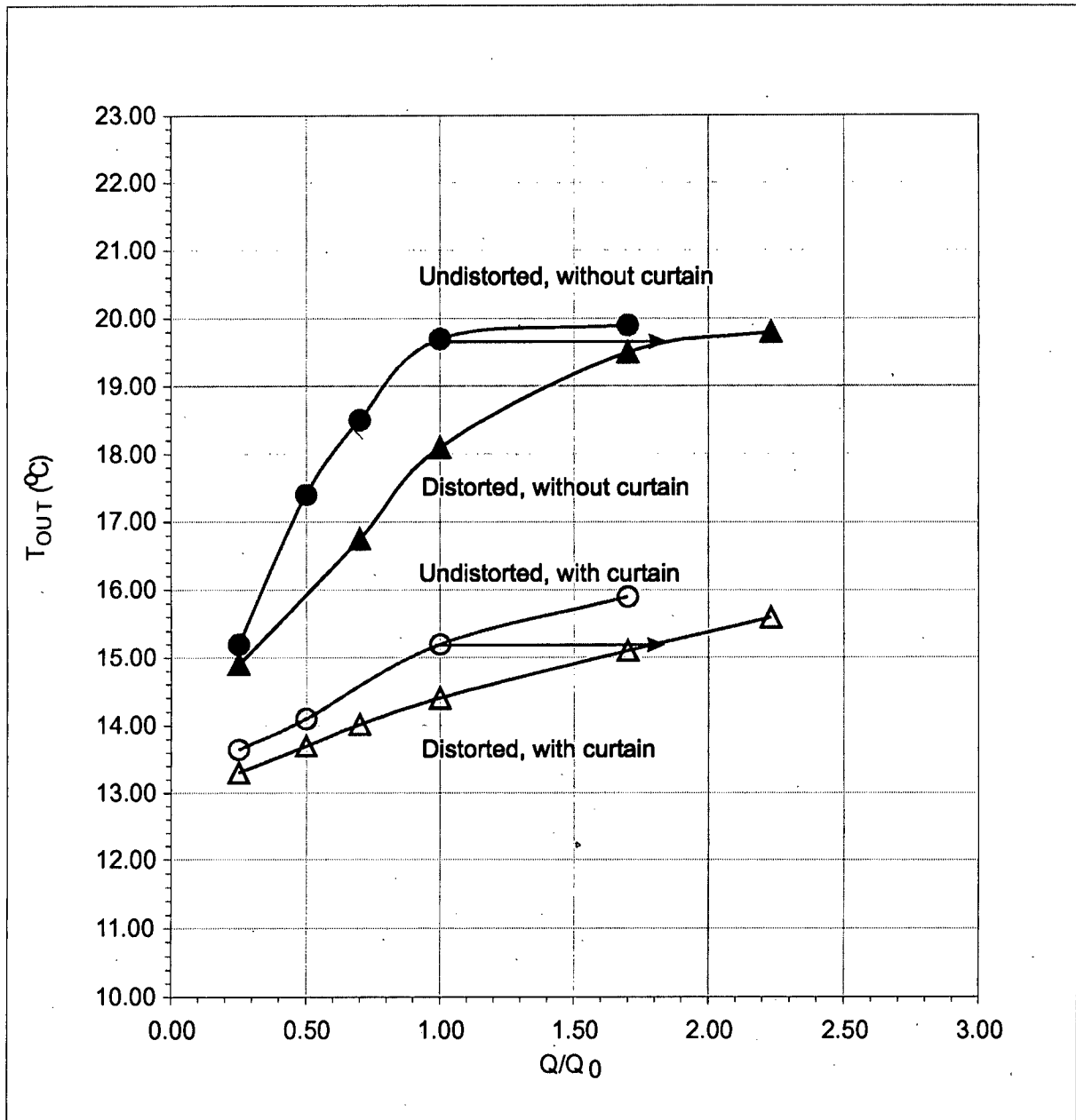
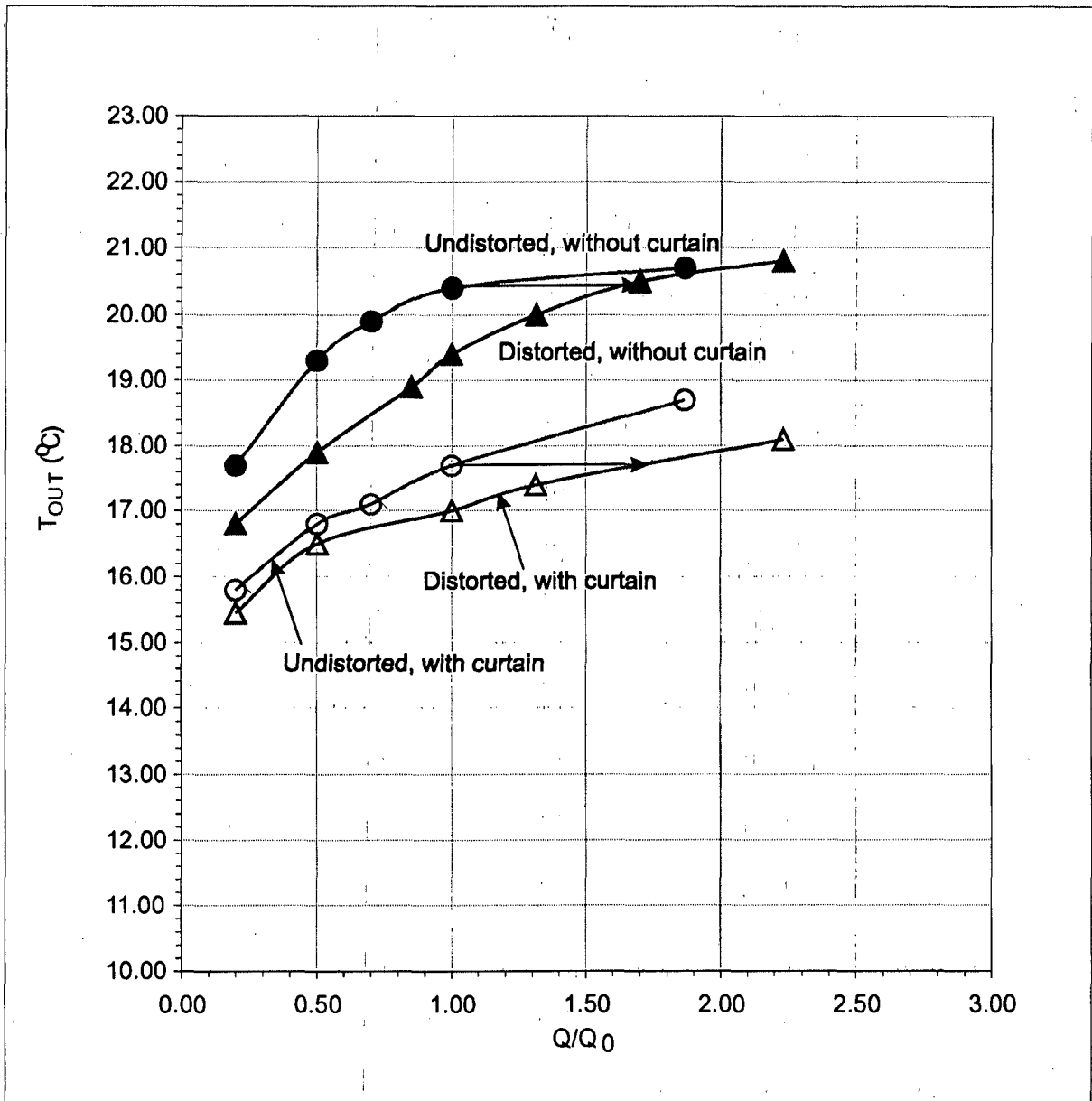


Figure 8-9. View of the distorted Open testbox with Curtain No. 4.



(a)

Figure 8-10. Performance of the Open testboxes fitted with curtains: (a) July condition.



(b)

Figure 8.10 continued. (b) August condition.

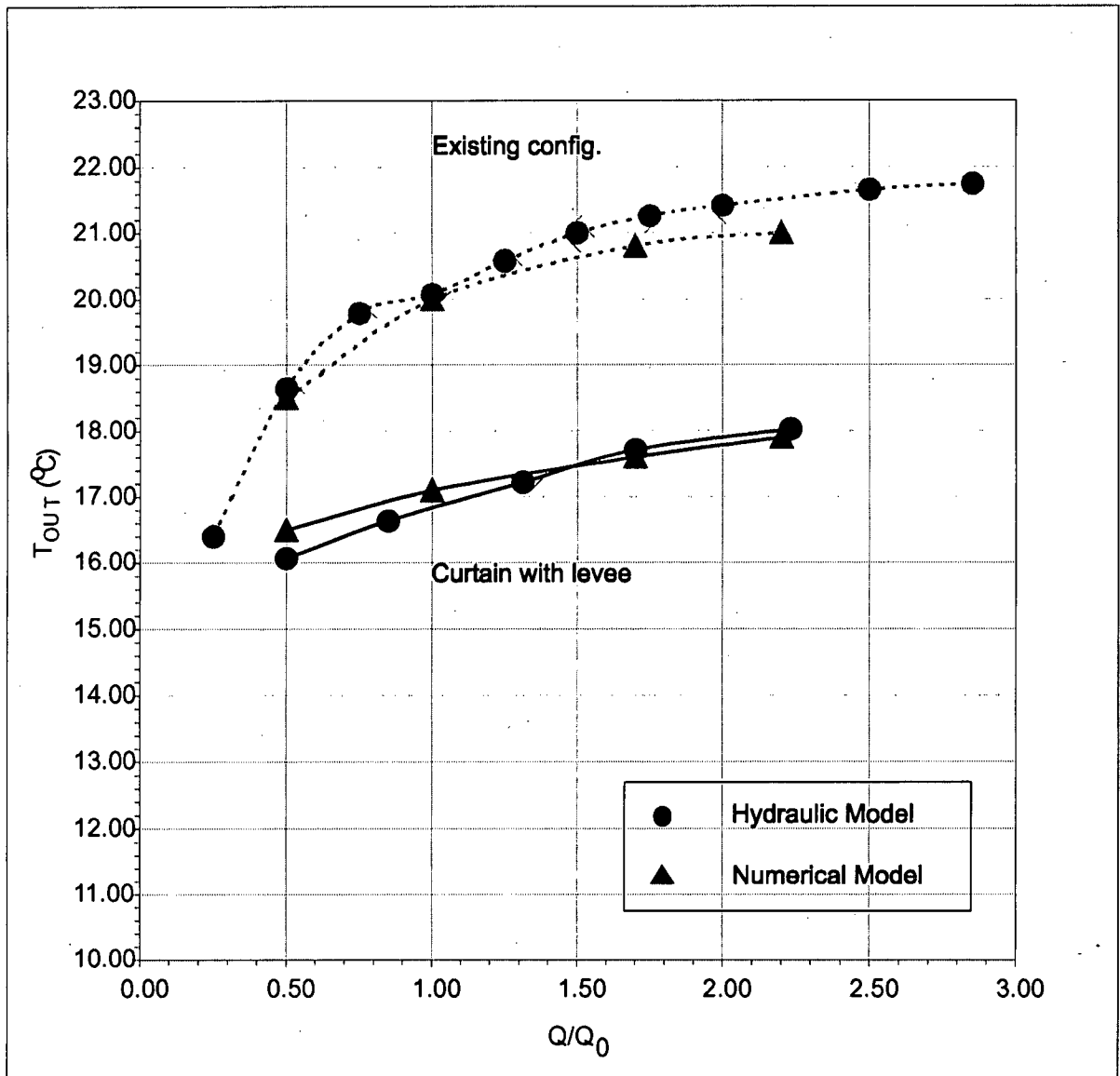


Figure 8-11. Comparison of numerical-model and hydraulic-model results for vertically distorted representation of Prattville Intake. The results are for the Intake with and without Curtain No. 4 for August condition. Note that the levees were not removed.

## 9. CONCLUSIONS AND RECOMMENDATIONS

This chapter summarizes the conclusions drawn from the results obtained from the hydraulic model of Prattville Intake, and leads to recommendations regarding design modifications to the Intake.

### 9.1 Summary

Prattville Intake releases water from Lake Almanor, a storage reservoir that becomes thermally stratified during summer (mid-June through to mid-September). The Intake in its existing configuration releases water whose temperature environmental interests consider too warm for trout in the North Fork of the Feather River downstream from Lake Almanor. For its normal operating outflow of 1,600cfs, the Intake presently draws water from over the full depth of water in the lake, especially from the warm upper layer that develops in the lake during summer. Several modifications were identified as potentially enabling the Intake to draw more cold water from deeper in the lake, and thereby significantly reduce the temperature of the outflow it releases:

1. A skimming curtain placed around the Intake;
2. A short pipe (with hooded inlet) extending out from the Intake; and,
3. A long pipe (with hooded inlet) extending from the Intake out to the lakebed.

The modifications were investigated successfully in an extensive program of laboratory tests carried out using a unique hydraulic model. The model had to encompass a large portion of Lake Almanor surrounding the Intake in order to link the Intake to the main source of cold water which lay in Lake Almanor's Hamilton Branch. Additionally, it was necessary to have sufficient volume of water so that the model could release water at a steady outflow temperature. Further, the model had to be sufficiently deep so as to simulate the flow of water in the stratified lake, as well as to facilitate adequate measurement of flow and temperature variables. To meet these requirements, the

hydraulic model had to be vertically distorted, whereby its vertical-length scale<sup>1</sup> was smaller than its horizontal-length scale. The model's horizontal-length and vertical-length scales were 220 and 40, respectively.

To address the influence of vertical distortion on the model's results, and to aid validation of hydraulic-model results, laboratory tests were conducted on a pair of testboxes that served as distorted and undistorted replications of Prattville Intake and its surrounding bathymetry; moreover, a comprehensive computer simulation was undertaken using a set of numerical models of Prattville Intake.

Work with the testboxes and the numerical models showed that a discharge-adjustment coefficient,  $\alpha$ , was needed for operating the hydraulic model and interpreting results from it. The coefficient, found to have an average value of 1.7, had to be applied to the model discharge determined from theoretical scale ratio considerations. The value of 1.7 also was found to be appropriate for adjusting flow from the hydraulic model so that the outflow temperature closely matched field measurements of outflow temperature. Accordingly, the flow-field conditions associated with an outflow setting of  $Q_0 = 1,600\text{cfs}$  at Prattville Intake had to be replicated in the hydraulic model using an outflow of 1.7 times the theoretical model-scale equivalent of  $Q_0$ .

The model results contain much data concerning the outflow performance of Prattville Intake under its existing condition and when the Intake was fitted with the alternative modifications intended to enable it to release colder water during the summer months of mid-June through to mid-September. Those modifications, the curtain and the hooded pipes mentioned above, were augmented with sundry excavation adjustments to the bathymetry near the Intake.

Additionally, the opportunity was taken to use the hydraulic model to determine the effectiveness of a submerged sill that could enable the Intake to conserve colder water

---

<sup>1</sup> Herein, scale = (prototype value)/(model value)

during late spring and early summer. Though this modification presently is not needed, information on its performance was considered useful for possible future reference.

## 9.2 Conclusions

Tests with the hydraulic model led to the following conclusions:

1. Prattville Intake operated at its normal discharge ( $Q_0 = 1,600\text{cfs}$ ) presently withdraws water from over the full depth of water around the Intake. In addition to withdrawing water from immediately out in Lake Almanor, the Intake withdraws water from along its adjoining shoreline, especially the shoreline running northeast of the Intake. Selective withdrawal at the Intake's normal operating discharge is not possible unless the Intake is modified.
2. The temperature of the outflow increases as outflow from Prattville Intake increases, until reaching asymptotic values of  $22^\circ\text{C}$ ,  $20^\circ\text{C}$ , and  $18^\circ\text{C}$  for the temperature-profiles representative of Lake Almanor during August, July, and June, respectively.
3. The vertically distorted hydraulic model simulated the main flow features observable at Prattville Intake. However, a sequence of calibration, validation, and verification activities involving the pair of testboxes that simulated the Intake, and comparison with limited field data from Prattville Intake, were required to establish the effects of vertical distortion on data obtained from the hydraulic model. Those activities show that outflow discharges in the hydraulic model should be increased by a factor about 1.7 in order for the model's performance (the curve – outflow temperature versus rate of outflow) to coincide with those of the actual Intake, and take into account effects attributable to the vertical distortion of the model. By virtue of the vertical distortion, the flow patterns in the model required slight adjustment so as to replicate the amount of water mixing that would occur in the field. As noted in Section 9.1, the factor led to close agreement between data from the distorted model and the available field data.

4. The results from the program of tests conducted with the hydraulic model indicate the feasibility of reducing the temperature of outflow water released through Prattville Intake when the reservoir is thermally stratified during summer and early autumn.
5. A skimming curtain, together with removal of segments of the levees bordering the submerged (incised) channel, comprise the modification best enabling Prattville Intake to release colder water during June, July, and August. The layout recommended for the skimming curtain is shown in Figures 7-7 and 7-8. The most effective elevation of the curtain bottom is EL. 4445ft. Figure 7-17 delineates the extent of levee removal recommended.

The performance curves relating outflow temperature ( $T_{out}$ ) to outflow rate (normalized as  $Q/Q_0$ ) for the modified Intake (curtain and the levees removed) are given in Figures 8-3a-c for the temperature profiles representative of Lake Almanor during June, July, and August.

6. As listed in Table 9-1, tests with the hydraulic model of Prattville Intake fitted with a curtain for the August, July, and June temperatures of Lake Almanor show that the curtain, with the levees removed, reduces outflow temperature by 5.2, 5.8, and 4.5°C for the August, July, and June conditions, respectively. These data pertain to the hydraulic model simulating Prattville Intake releasing its normal operating discharge of 1,600cfs; the equivalent flow condition in the hydraulic model being taken herein as  $Q/Q_0 = 1.7$ .
7. Removal of the levees accounts for approximately a 1.5°C to 1.7°C reduction in outflow temperatures for the August and July conditions, respectively if the curtain is installed.

8. The submerged (incised) channel contributes a relatively small amount of cold water to Prattville Intake when the curtain is in position; an estimate indicates only about 3% when  $Q/Q_0 = 1.7$  in the model (equivalent to a release of 1,600cfs from Prattville Intake). Nevertheless, the water from the incised channel is appreciably colder than elsewhere near the Intake. As measured in the hydraulic model, water temperatures varied from about 8.5°C to 9.5°C over the depth of the incised channel, whereas the water temperature at the surrounding lakebed was about 10.5°C to 11.0°C. Moreover, the model showed that Prattville Intake with a curtain could draw water along the incised channel over a distance extending to the "Narrows" region linking the Chester and Hamilton Branches of Lake Almanor.
9. A particularly intriguing flow phenomenon observed in the hydraulic model was the flow of water along the incised channel when Curtain No. 4 was placed around the Intake. The model showed that the Intake fitted with the curtain could draw water along the channel all the way to the channel's juncture with the Hamilton Branch of Lake Almanor. Viewed with the aid of dye, flow along the incised channel appeared as a submerged stream (Figure 7-22). Rather little flow occurred on the lakebed flanking the incised channel, except regions immediately surrounding the curtain. An approximate estimate indicates that the incised channel contributes about 13.3% of the outflow released through the model Intake operated at the  $Q/Q_0 = 1.7$ .
10. Tests show that the outflow temperature of water released by Prattville Intake is not significantly affected by dredging behind the curtain, or by other bathymetric changes behind the curtain such as infilling of regions not in the direct flow path to the Intake.
11. The performance data obtained from the hydraulic model (notably of Prattville Intake with curtain and levees removed) are supported by data obtained from an undistorted, though simplified, hydraulic model of the Intake and surrounding

bathymetry. That model, herein termed the undistorted testbox, produced the same outflow temperatures measured from Prattville Intake in the hydraulic model. The undistorted testbox surrounded by a skimming curtain produced a similar drop in temperature of outflow as occurred for the hydraulic model fitted with a comparable curtain.

12. The alternative modifications tested – (1) a long pipe with hooded inlet, (2) a short pipe with hooded inlet, and, (3) sundry excavation and reshaping of the lakebed in the vicinity of Prattville Intake) – enabled the modeled Prattville Intake to release colder water. However, none of these alternatives was found to be as effective as the modification comprising the curtain and levee removal. For example, the long pipe fitted with a hooded inlet (Figure 7-31), and with the levees removed, operated at the normal outflow rate for the August condition reduced outflow temperature by about 3.8°C, whereas the curtain with levees removed reduced outflow temperature by 5.2°C.
  
13. Conservation of cold water in Lake Almanor during the spring months preceding June (and including June) could be feasible with the aid of a removable bottom sill whose crest elevation is at EL. 4460ft (Figure 7-37). A sill, with the same plan location as the curtain, would be removable and form part of the overall structure incorporating the curtain. For the lake's June condition, and if the levees were removed, the sill would raise outflow temperature by about 2.0°C.
  
14. A further intriguing outcome of the modeling warrants mention at the close of the report. It is the value of the discharge-calibration factor  $\alpha$ , which laboratory testing and numerical simulation determined to be 1.7 on average. This value was found to pertain to tests with Prattville Intake in its existing configuration and when the Intake was modified. A simple explanation ventured on the basis of scaling flow vorticity leads to the same value for  $\alpha$ .

Table 9-1. Summary of hydraulic-model data on outflow temperatures,  $T_{out}$ , and temperature reductions,  $\Delta T_{out}$ , obtained when  $Q/Q_0 = 1.7$  in the model (an equivalent outflow of 1,600cfs from Prattville Intake). Also indicated is the water-surface elevation for each month.

Intake Configuration	June (EL. 4491.5ft)		July (EL. 4489.0ft)		August (EL. 4482.5ft)	
	$T_{out}$ (°C)	$\Delta T_{out}$ (°C)	$T_{out}$ (°C)	$\Delta T_{out}$ (°C)	$T_{out}$ (°C)	$\Delta T_{out}$ (°C)
Existing configuration	16.5	-	19.0	-	21.2	-
Intake modified to release colder water						
Curtain added	12.2	4.3	14.7	4.3	17.7	3.5
Curtain added and levees removed	12.0	4.5	13.2	5.8	16.0	5.2
Long pipe with hooded inlet, and levees removed	-	-	-	-	17.4	3.8
Short pipe with hooded inlet, and levees removed	-	-	-	-	19.1	2.1
Levees removed, no curtain	15.8	0.7	-	-	-	-
Intake modified to conserve colder water						
Existing configuration, sill added	18.3	-1.8 (16.5 - 18.3)	-	-	-	-
sill, when levees removed	17.8	-2.0 (15.8 - 17.8)	-	-	-	-

Note: the highlighted row is modification set giving greatest reduction in outflow temperature.

### 9.3 Recommendations

The conclusions lead to recommendations to be considered further by PG&E and the Ecological Resource Committee established under the operating license for Prattville Intake, FERC 1962:

1. The following set of modifications produced the largest drop in water temperature of outflow released from Prattville Intake, and is recommended for implementation:
  - (a). a 770-ft-wide skimming curtain placed 906ft offshore from the Intake, with bottom elevation at EL. 4445ft, and whose plan layout is shown in Figure 7-7, and bottom-lip elevation is given in Figure 7-8.
  - (b). removal of the levees flanking the incised channel immediately in front of Prattville Intake, as indicated in Figure 7-17.
2. A moveable sill whose crest elevation is EL. 4460ft, and whose dimensions and layout are as given Fig 7-37, is recommended as a feasible means for Prattville Intake to conserve cold water during spring months preceding and including June. The sill could be positioned at the same location as the skimming curtain, and be supported by the same structure.
3. Recommended for further development are the numerical models for simulating an undistorted version of the hydraulic model, and the modeled area at prototype dimensions. The requirements for further developing the model are defined in Section 8.4 of the present report. Those requirements entail an effort that is beyond the resources available for the work done in completing the present report.

## REFERENCES

- Chen, Z., Ettema, R., and Lai, Y., (2003). "Ice-Basin and Numerical Studies of Frazil Ice at a Submerged Water Intake." Report in Press, IIHR-Hydroscience and Engineering, The University of Iowa, Iowa City, IA.
- Fleenor, F. and Schladow, G.S., (2002). "Lake Almanor – A Field Study." Report UCD Agreement 01-01034V, Environmental Dynamics Laboratory, University of California, Davis, CA.
- Goldring B.T., (1989). "Capped Water Intakes in a Stratified Crossflow." Journal of Hydraulic Engineering, 115(2), pp228 – 243.
- Harleman, D.R.F. and Elder R.A., (1965). "Withdrawal from Two-Layer Stratified Flows." Journal of the Hydraulics Division, ASCE, 91(HY4), pp43-58.
- Harleman D.R.F. and Gooch, R., and Ippen, A.T., (1958). "Submerged Sluice Control of Stratified Flow." Journal of the Hydraulics Division, ASCE, 84(HY2), pp43-58.
- Harleman, D.R.F. and Stolzenbach, K.D., (1967). "A Model Study of Thermal Stratification Produced by Condensed Water Discharge," Hydrodynamics Laboratory, Massachusetts Institute of Technology, Report No. 107, Cambridge, MA.
- Jirka, G., (1979). "Super-critical Withdrawal from Two-layered Fluid Systems, Part 1. 2D Skimmer Wall." Journal of Hydraulic Research, IAHR, 17(1), pp43-51.
- Johnson, P.T. and Vermeyen, T., (1993). "A Flexible Curtain Structure For Control of Vertical Reservoir Mixing Generated by Plunging Inflows." Proceedings ASCE Conference Hydraulic Engineering '93, San Francisco, CA, pp2377-2382.
- Johnson, P.T., Vermeyen, T., and O'Haver, G., (1993). "Use of Flexible Curtains to Control reservoir Release Temperatures: Physical Model and Field Prototype Observations." Proceedings of US Committee on Large Dams (USCOLD), Annual Meeting, Chatanooga, TN.
- LabVIEW (1996). Data Acquisition Basics Manual. National Instruments Inc., San Diego, CA.
- Lai, Y., Odgaard, A.J., Ettema, R., and Muste, M., (2004). "Lake Almanor Cold-water Feasibility Study: Numerical Modeling." Report in Press, IIHR-Hydroscience and Engineering, The University of Iowa, Iowa City, IA.

- Muste, M., Xiong, Z., Bradley, A., and Kruger, A., (2000). "Large-Scale Particle Image Velocimetry – a Reliable Tool for Physical Modeling." Proceedings of ASCE 2000 Joint Conference on Water Resources Engineering and Water Resources Planning & Management, Minneapolis, MN (CD-ROM).
- Nystrom, J.B., Hecker, G.E., and Moy, H.C., (1981). "Heated Discharge in Estuary: Case Study." Journal of the Hydraulics Division, ASCE, 107(11), pp1371 – 1406.
- Pacific Gas & Electric Company, (2001). "Physical and Numerical Modeling of Cold Water Feasibility Study through Prattville Intake at Lake Almanor in North Fork Feather River." Request for Proposal No. 111501-TSJ, PG&E, Hydro Generation Department, San Francisco, CA.
- Ryan, P.J. and Harleman, D.R.F., (1973). "An Analytical and Experimental Study of transient Cooling Pond Behavior." Ralph M. Parsons Laboratory for Water Resources and Hydrodynamics, Massachusetts Institute of Technology, Report No. 161, Cambridge, MA.
- Vermeyen, T., (1995). "Prattville Intake, Lake Almanor, California, Hydraulic Model Study on Selective Withdrawal Modifications." US Department of the Interior, Bureau of Reclamation, Report R-95-07, Denver, CO.
- Vermeyen, T. and Johnson, P.T., (1993). "Hydraulic Performance of a Flexible Curtain Used for Selective Withdrawal: A Physical Model and Prototype Comparison." Proceedings ASCE Conference Hydraulic Engineering '93, San Francisco, CA, pp2371-2376.
- Wilkinson, D.L., (1991). "Model Scaling Laws For Tunneled Ocean-Sewage Outfalls." Journal of Hydraulic engineering, ASCE, 117(5), pp547-424.
- Woodward-Clyde Consultants, (1986). "Rock Creek-Cresta Project Cold Water Feasibility Study." Report submitted to Pacific Gas & Electric, San Ramon, CA.
- Zeng, P., Chen, H., Ao, B., Ki, P., Wang, X. and Ou, Z. (2002). "Transport of Waste Heat from a Nuclear Power Plant into Coastal Water." Proceedings of Coastal Engineering 44, pp301-319

**APPENDIX A**

**PHASES OF THE HYDRAULIC MODEL CONSTRUCTION**

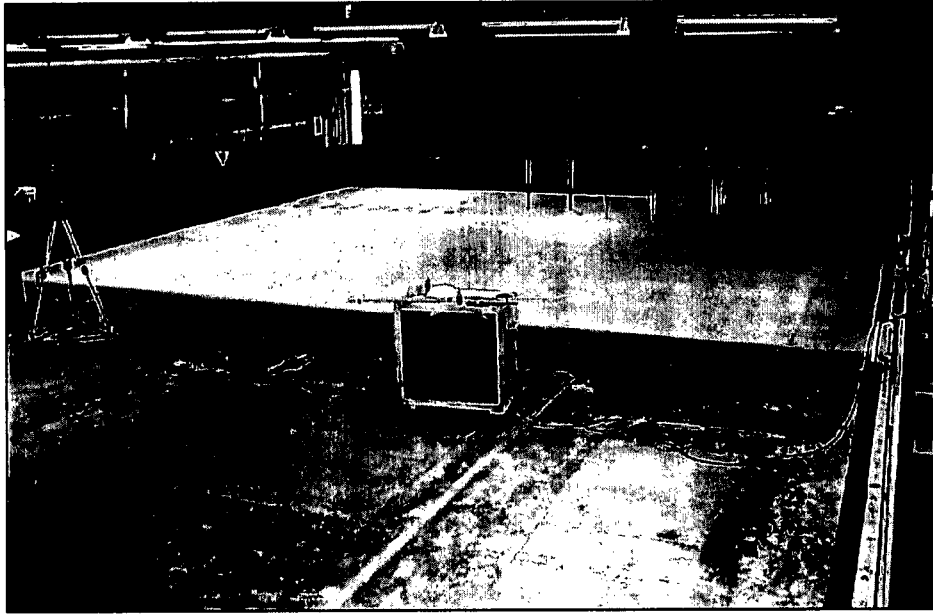


Figure A.1. Layout of the model boundaries (concrete-block walls) scaled and fitted thermal insulation

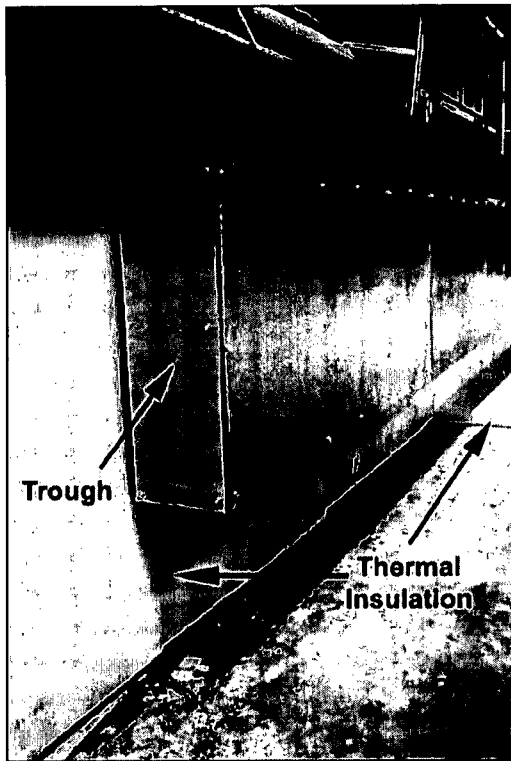


Figure A.2. Detail of insulation positioning (1 inch-thick insulation on wall; 1.5 inch-thick insulation on the model floor)

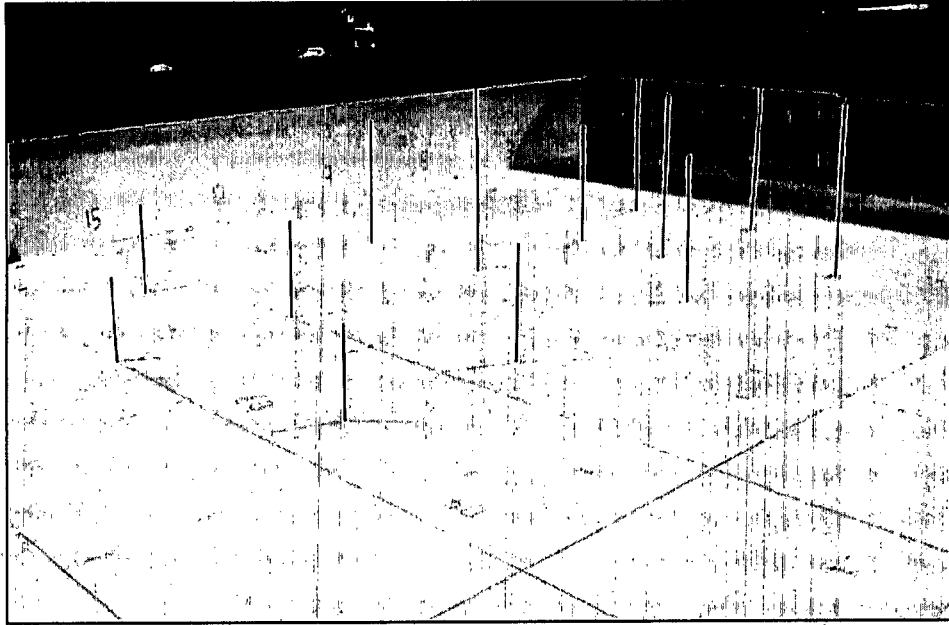


Figure A.3. Grade pins used for setting model bathymetry

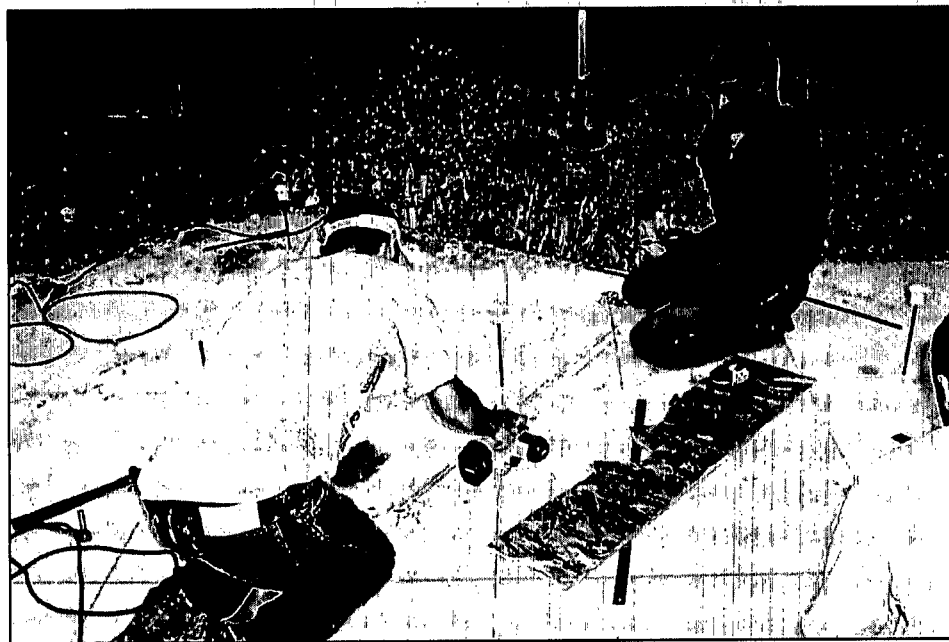
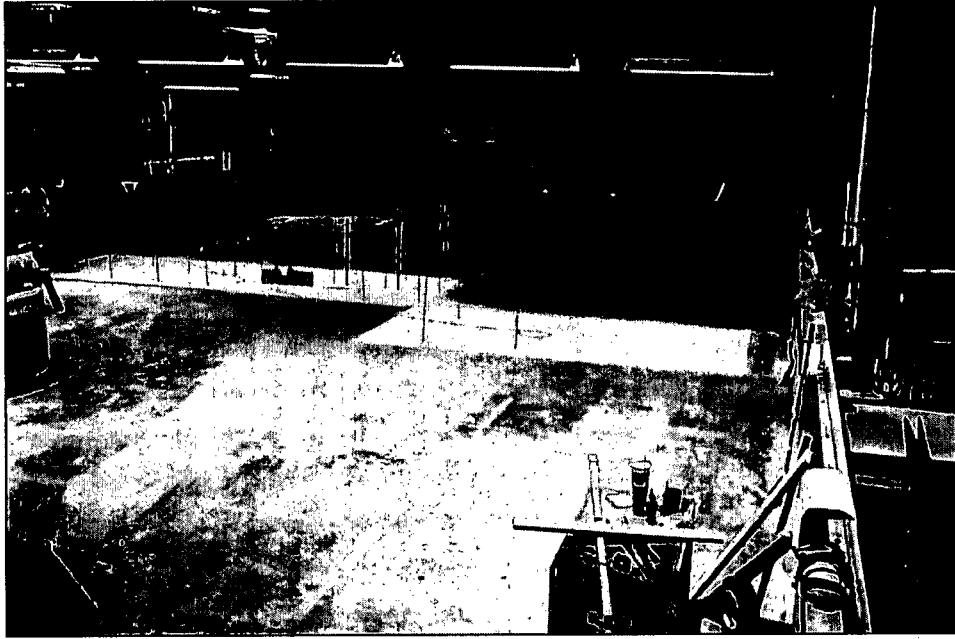
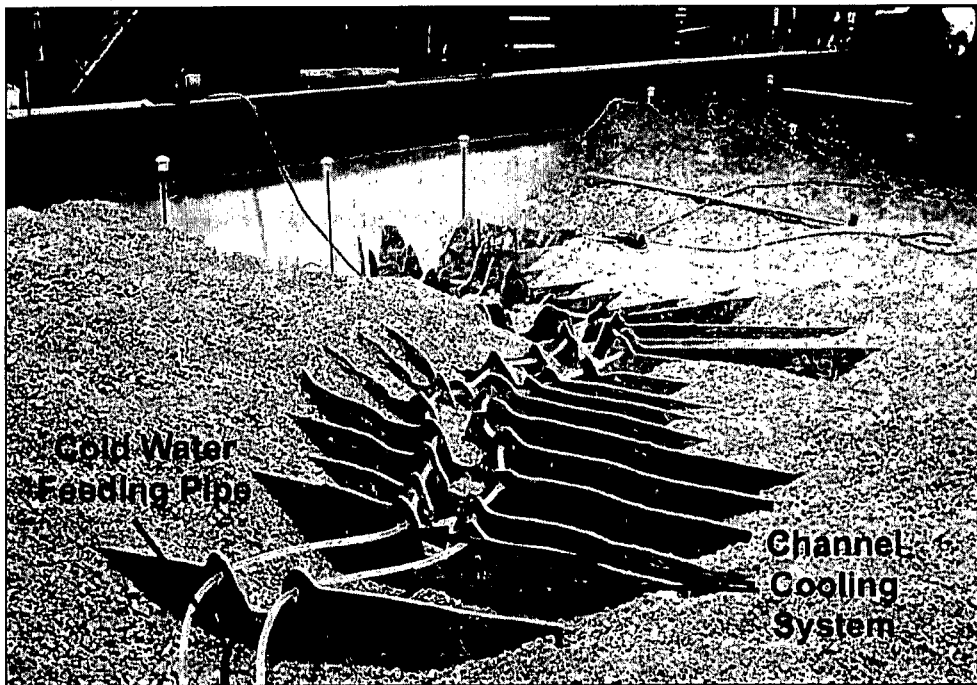


Figure A.4. Positioning of the incised channel templates

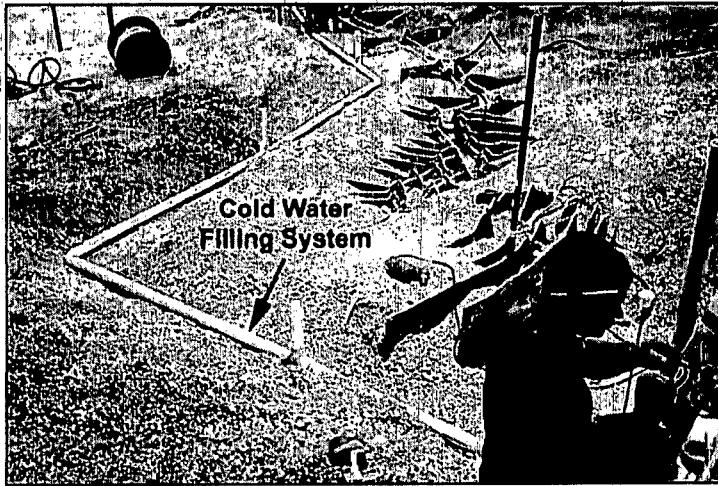


(a)

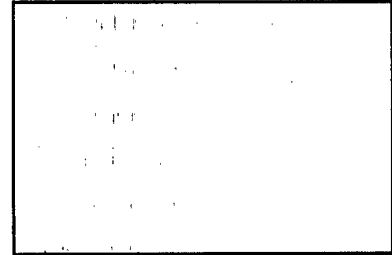


(b)

Figure A.5. Model bathymetry construction: (a) far-field area; (b) channel area near Intake



(a)



(b)

Figure A.6. The cold-water feeding system; (a) the cold-water filling lines  
(b) riser pipes (pop-ups) for water release in the model

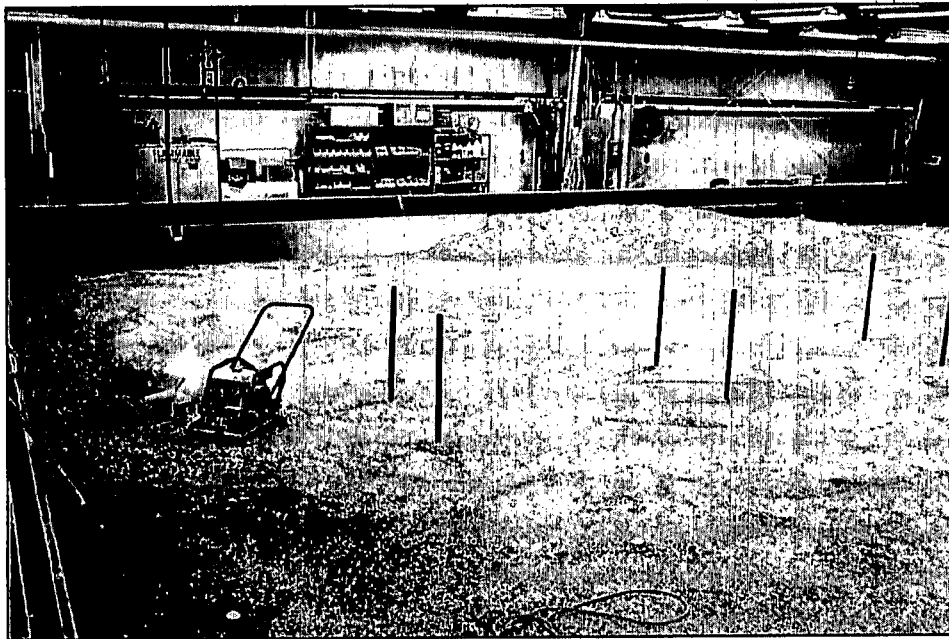
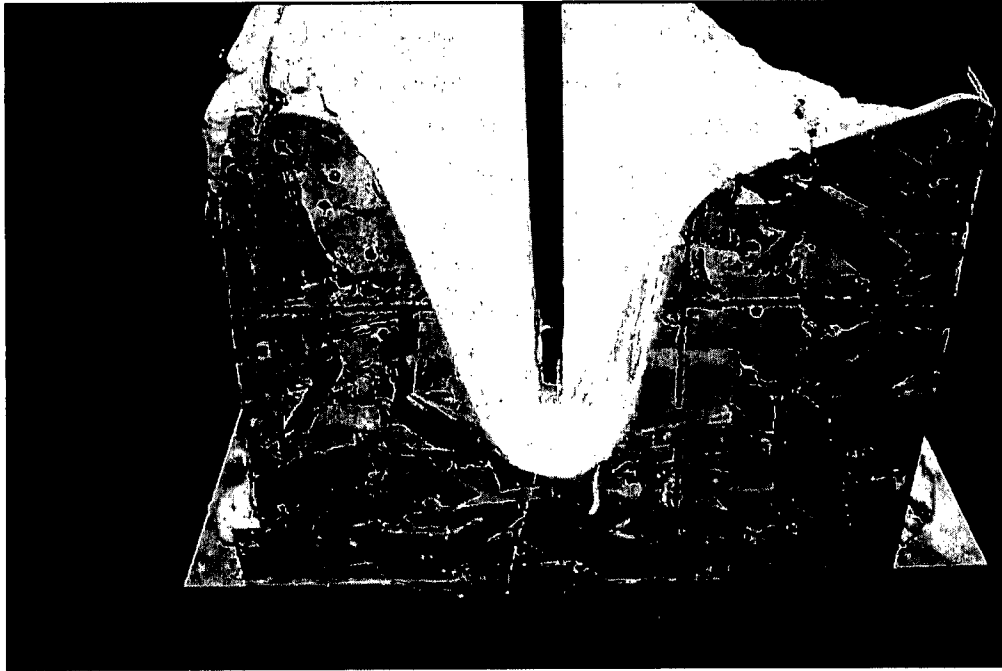
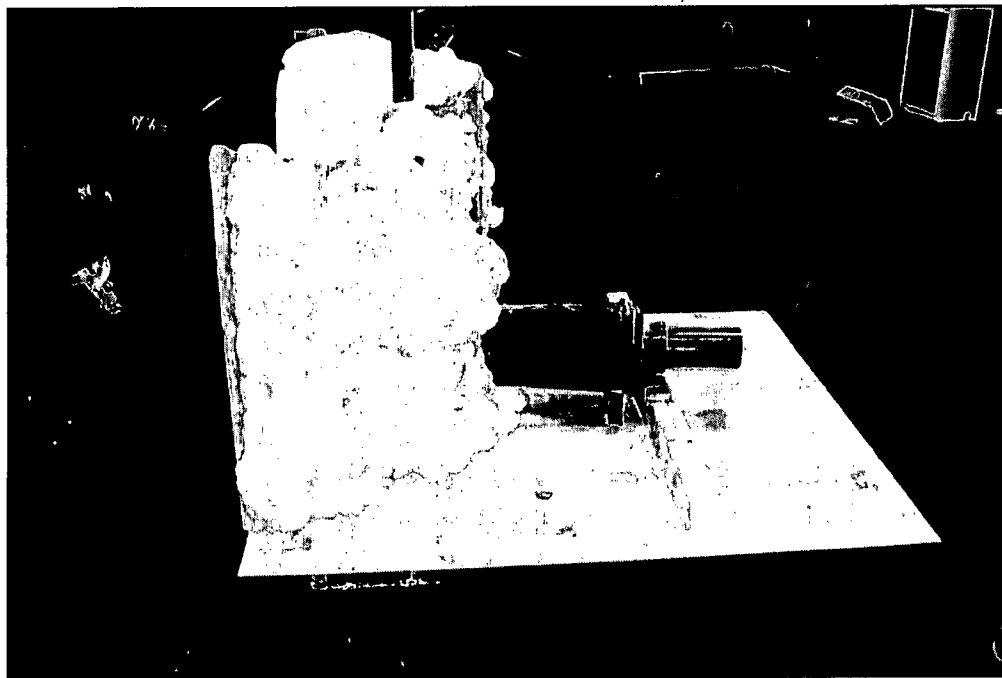


Figure A.7. Compaction of the gravel bed

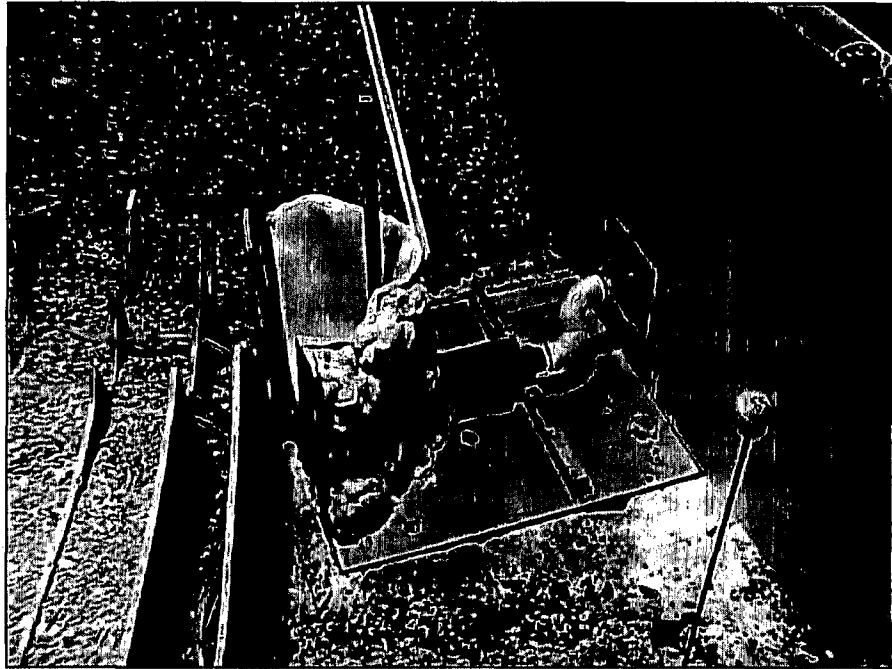


(a)



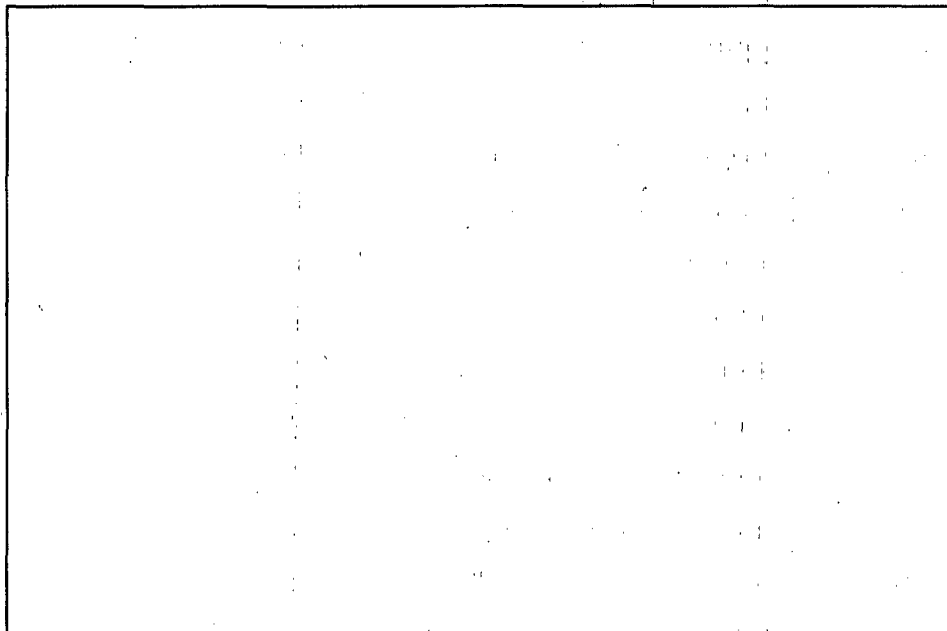
(b)

Figure A.8. Prattville Intake and local bathymetry: (a) view toward the model Intake; (b) side view of the model Intake



(c)

Figure A.8 continued. The Intake positioned in the model

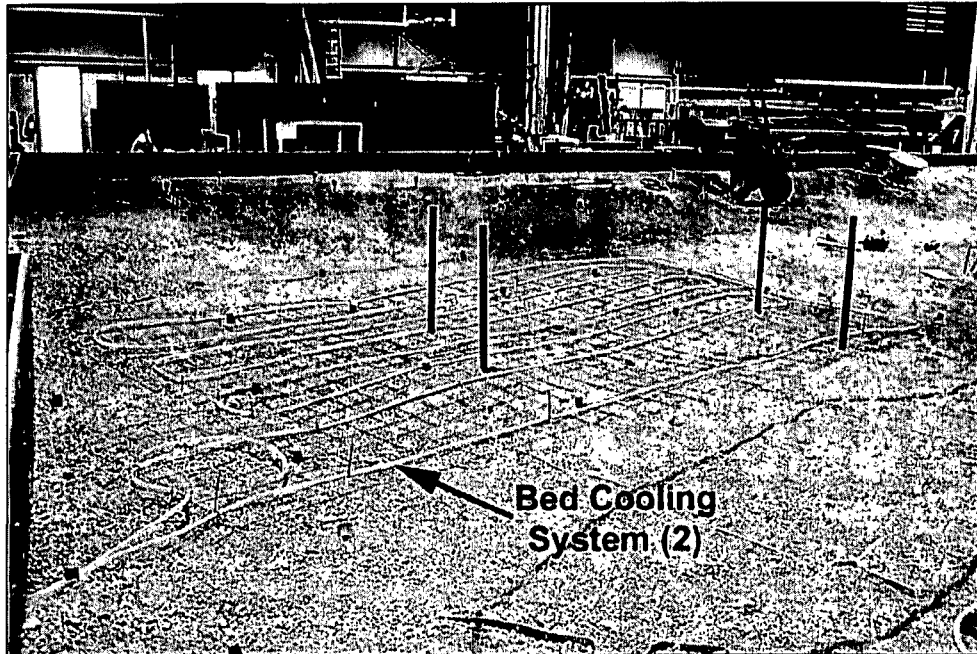


(a)

Figure A.9. Positioning of the cooling coils in the model bed: (a) cooling coils in zone 1

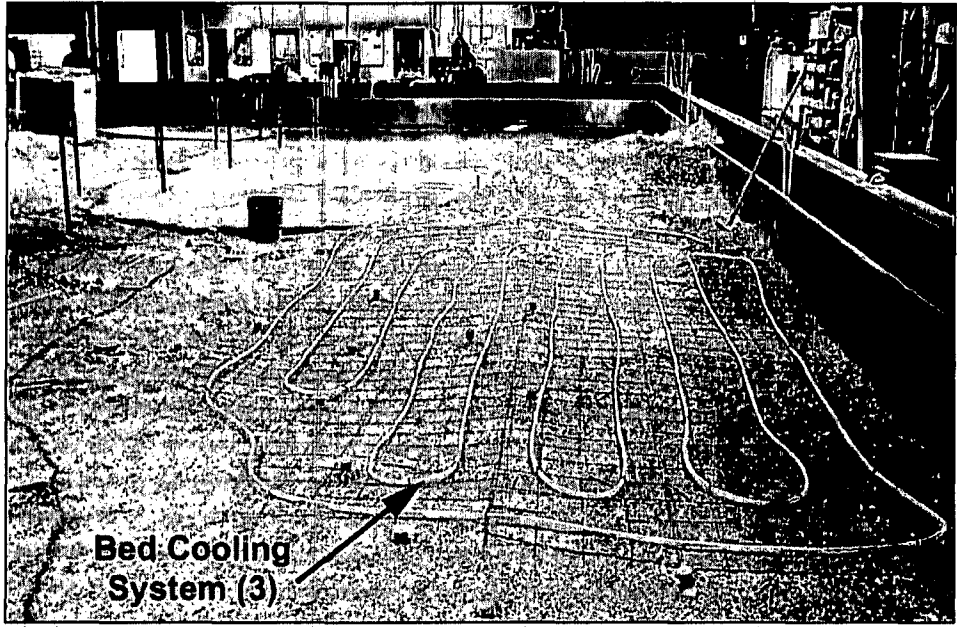


(b)

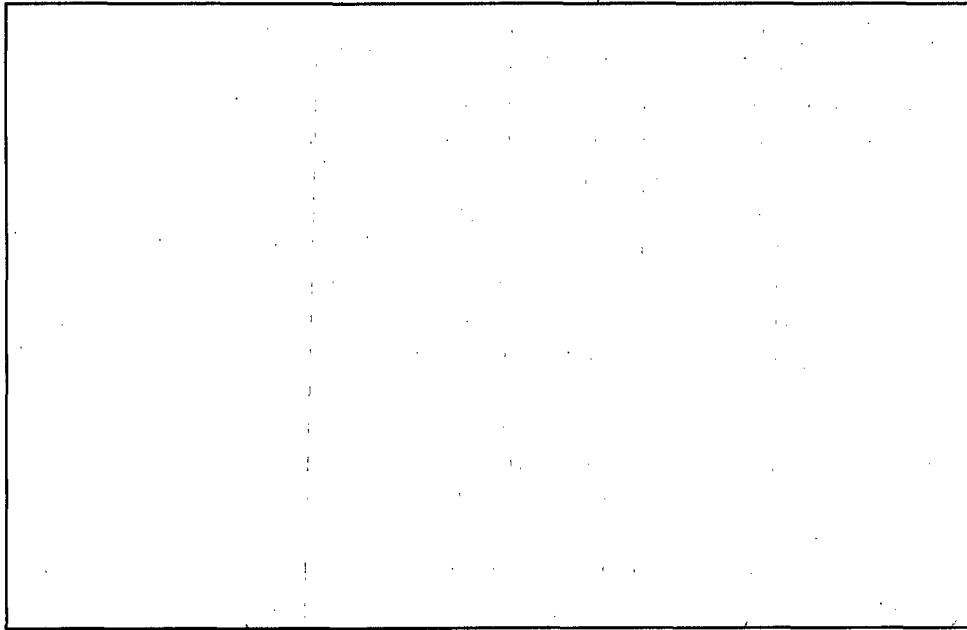


(c)

Figure A.9 continued. (b) construction detail; (c) cooling coils in zone 2



(d)

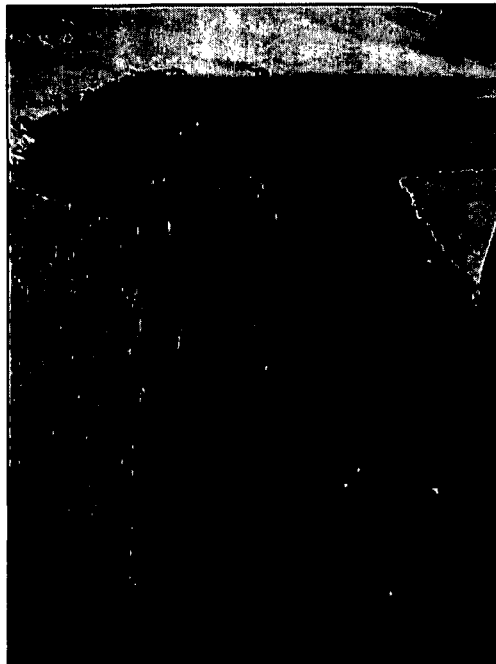


(e)

Figure A.9 continued. (d) cooling coils in zone 3; (e) cooling coils in zones 4 and 5



(a)



(b)

Figure A.10. Construction of the incised channel: (a) "Quikrete" mix layered on a fine gravel bed; (b) close-up of the channel cross-section (note perforations in the channel bed for cold seepage flow)



(c)

Figure A.10 continued. (c) Overall view of the channel area

**APPENDIX B**  
**LISTING OF VIDEO CLIPS**

## CODING FOR THE VISUALIZATION TEST LABELS

**Note on test coding:**

Tests are labeled as a code string separated by dash; e.g., E-08-WL-P1-Q170. The significance of the group in the string is described below:

1. First string group: designates the test objective and configuration.
2. Second string group: designates the month of the year (for setting temperature stratification).
3. Third string group: indicates the if incised channel levees are in place or removed.
4. Fourth string group: designates the test name.
5. The fifth string indicates the discharge used in the visualization test.

**Table B.1: Significance of the string labeling for the tests**

Position in code string				Significance
<b>First group*</b>				
E				Prattville Intake, existing configuration
C#				Prattville Intake & curtains. If a number is associated with the symbol C in the first string group (i.e., 45, 47, 50, etc) it designates curtain's bottom-lip elevation (i.e., EL. 4445ft, EL. 4447ft, EL. 4450ft, respectively)
LHPI				Prattville Intake & long pipe with hooded inlet (BOR design)
SHPI				Prattville Intake & short pipe with hooded inlet
SSHPI				Prattville Intake & shortest pipe with hooded inlet
F				Bottom sill (fence)
D				Prattville Intake & dredged channel
U				Undistorted Intake testbox
D				Distorted Intake testbox
UC				Undistorted Intake testbox & curtain
DC				Distorted Intake testbox & curtain
UH				Undistorted Intake testbox with simplified bathymetry around Prattville Intake
DH				Distorted Intake testbox with simplified bathymetry around Prattville Intake
<b>Second group</b>				
	06			June
	07			July
	08			August
<b>Third group</b>				
		WL		Levees in place
		WOL		Levees removed
<b>Fourth group</b>				
			P#	Production runs #
<b>Fifth group</b>				
			Q#	n X Q discharge

\* C added to the first group designates curtain added to the testbox tests

\*\*B added to the first group designates filled channel in front of the Prattville Intake

Table B.2: List of visualization clips on this DVD

Month	Configuration	Levees	Elevation	n X Q	Project Number	Project Code	Video Clip Length
June	Existing Condition	with		1.70	P17	E-06-WL-P17-Q170	2:44
	Curtain#4	with	4445	1.70	P17	C4(45)-06-WL-P17-Q170	2:35
		without	4445	1.70	P17	C4(45)-06-WOL-P17-Q170	2:35
	Fence	with	4450	1.70	P13	F(50)-06-WL-P13-Q170	2:35
		without	4450	1.70	P14	F(50)-06-WOL-P14-Q170	2:25
	Fence	with	4460	1.70	P13	F(60)-06-WL-P13-Q170	2:30
without		4460	1.70	P14	F(60)-06-WOL-P14-Q170	2:25	
July	Existing Condition	with		1.00	P11	E-07-WL-P11-Q100	2:38
		with		1.70	P11	E-07-WL-P11-Q170	2:28
	Curtain#4	with	4445	1.00	P11	C4(45)-07-WL-P11-Q100	2:26
		without	4445	1.00	P11	C4(45)-07-WOL-P11-Q100	2:43
		with	4445	1.70	P11	C4(45)-07-WL-P11-Q170	2:28
		without	4445	1.70	P11	C4(45)-07-WOL-P11-Q170	2:23
August	Existing Condition	with		0.85	P18	E-08-WL-P18-Q085	3:21
		with		1.70	P18	E-08-WL-P18-Q170	3:14
	Curtain#4	with	4443	0.85	P3	C4(43)-08-WL-P03-Q085	2:52
		without	4443	0.85	P3	C4(43)-08-WOL-P03-Q085	2:45
		with	4443	1.70	P3	C4(43)-08-WL-P03-Q170	2:31
		without	4443	1.70	P3	C4(43)-08-WOL-P03-Q170	2:35
		with	4443	2.23	P3	C4(43)-08-WL-P03-Q223	2:35
		without	4443	2.23	P3	C4(43)-08-WOL-P03-Q223	2:15
	Curtain#4	with	4445	0.85	P18	C4(45)-08-WL-P18-Q085	3:14
		without	4445	0.85	P18	C4(45)-08-WOL-P18-Q085	3:18
		with	4445	1.00	P9	C4(45)-08-WL-P09-Q100	2:35
		without	4445	1.00	P9	C4(45)-08-WOL-P09-Q100	2:45
		with	4445	1.70	P18	C4(45)-08-WL-P18-Q170	2:56
		without	4445	1.70	P18	C4(45)-08-WOL-P18-Q170	3:13
	Curtain#4	with	4447	0.85	P3	C4(47)-08-WL-P03-Q085	2:51
		with	4447	1.70	P3	C4(47)-08-WL-P03-Q170	2:57
		with	4447	2.23	P3	C4(47)-08-WL-P03-Q223	2:56
		with		0.85	P19	LHPI-08-WL-P19-Q085	3:03
Long Hooded Pipe Inlet	without		0.85	P4	LHPI-08-WOL-P04-Q085	2:39	
	with		1.70	P4	LHPI-08-WL-P04-Q170	2:50	
	with		2.23	P19	LHPI-08-WL-P19-Q223	2:39	
	without		2.23	P4	LHPI-08-WOL-P04-Q223	2:50	
Short Hooded Pipe Inlet	with		0.85	P19	SHPI-08-WL-P19-Q085	3:09	
	with		2.23	P19	SHPI-08-WL-P19-Q223	3:00	